ION CHANNELS IN HIGHLY PURIFIED HUMAN PLATELET SURFACE AND INTRACELLULAR MEMBRANES

by

SUSAN DIANE MANNING

A thesis submitted to the University of London

for the degree of

Doctor of Philosophy

in the Faculty of Science

October 1989

National Heart & Lung Institute

Dovehouse Street

LONDON SW3 6LY

Abstract

Highly purified human platelet surface and intracellular membrane vesicles have been separated by a well characterised method involving density gradient sedimentation followed by high-voltage continuous flow electrophoresis. Membrane vesicles have been reconstituted into artificial planar phospholipid bilayers by fusion, facilitating electrophysiological recordings of single channel activity under voltage clamp conditions.

The basic properties of a predominantly anion-selective channel derived from the surface membrane fraction have been investigated. In symmetrical 450mM KCl, this channel has a conductance of ~160pS at -40mV and ~90pS at +40mV. Reversal potential measurements interpreted in terms of the Goldman-Hodgkin-Katz equation indicate a Cl:K permeability of ~4:1 for the channel. The following sequence of relative anion permeabilities (in the presence of K^+) is obtained: $SO_4^{2-} = F^- <$ acetate$^-$ < gluconate$^-$ < $Cl^- < Br^- < I^- < NO_3^- < SCN^-$. Cations as large as TEA^+ are found to be permeant implying that the channel has a large cross-sectional area, at least 37Å^2. Current through the channel is blocked in the presence of HEPES and Tris buffers, and by DIDS, SITS and ATP. The channel shows characteristic bursting behaviour in which comparatively long 'silent' periods alternate with 'active' periods. Lifetime analysis of single channel activity indicates that the channel exhibits at least one open state and at least three closed states. This channel appears to belong to an increasing class of 'anion' channels that also show a degree of cation permeability. As with other members of this class, the physiological role of the platelet surface membrane channel remains to be established.

A subpopulation of the intracellular membrane fraction has been isolated using an oxalate loading density gradient procedure. Fusion of vesicles from this fraction with planar bilayers yields a monovalent cation-selective channel with a conductance of ~300pS in symmetrical 450mM KCl. The open state of the channel appears more noisy at positive voltages than at negative voltages and the time the channel remains in the open state is unaffected by the surrounding calcium concentration. This channel may provide a mechanism for charge compensation during calcium movements into and out of the platelet intracellular membrane, analogous to that found in the sarcoplasmic reticulum of muscle.

Acknowledgements

This project was supervised by Dr. Alan Williams and Professor Neville Crawford. I am indebted to them both for their guidance and encouragement throughout.

I would like to express my gratitude to Kalwant Authi, Beverley Evenden,Nash Hack and Andrew Sankar at the Royal College of Surgeons for their help and advice during the platelet membrane isolation and biochemical characterisation experiments. My thanks also to Klaus Syha for donating platelet membranes prepared on Percoll gradients.

Special thanks are owed to Richard Ashley, Colette Baird and Richard Montgomery (who designed and assembled the bilayer electronics) at the National Heart and Lung Institute for helpful comments and suggestions concerning the single channel experiments.

I also thank the N.H.L.I library staff, especially Janice Hutt, for their assistance in tracking down references.

I acknowledge the Medical Research Council for their financial support.

Finally, but by no means least, I would like to thank all my colleagues and friends at the N.H.L.I. and R.C. of S., my family up North, Mum and Dad Thomas and, most especially Richard, for their continued moral support and encouragement.

TABLE OF CONTENTS

Title page 1

Abstract 2

Acknowledgements 4

Table of Contents 5

List of Figures 11

List of Tables 13

Abbreviations 14

Chapter 1 INTRODUCTION

1.1 GENERAL INTRODUCTION 17

1.2 GENERAL ULTRASTRUCTURAL AND MOLECULAR FEATURES OF THE PLATELET 20

1.2.1 The platelet surface membrane 20

1.2.2 Platelet surface membrane charged groups 23

1.2.3 The platelet intracellular membrane 24

1.2.4 Other platelet intracellular structures 25

1.3 ISOLATION OF PLATELET MEMBRANES 27

1.3.1. Principles of membrane separation by continuous flow electrophoresis 28

1.3.2 Electrophoretic mobility of particles 31

1.4 ION FLUXES ACROSS PLATELET MEMBRANES..... 36

1.4.1 Calcium flux across platelet membranes..... 36

1.4.1a Ca^{2+} mobilisation from intracellular stores on platelet activation..... 40

1.4.1b Ca^{2+} influx on platelet activation..... 42

1.4.2 Na^{+} and K^{+} flux across platelet membranes..... 47

1.5 ION CHANNELS AND THEIR RECONSTITUTION INTO PLANAR BILAYERS..... 50

1.5.1 What are ion channels?..... 50

1.5.2 Ion channel reconstitution into planar bilayers..... 52

1.5.3 Advantages of the planar bilayer technique in single channel recording..... 53

1.5.4 The painted planar bilayer membrane..... 55

1.5.5 Ion channel reconstitution by fusion..... 58

1.5.5a Formation of the pre-fusion state..... 58

1.5.5b Osmotically-driven fusion..... 61

Chapter 2 METHODS

2.1 INTRODUCTION..... 64

2.2 PREPARATION OF HIGHLY PURIFIED PLATELET SURFACE AND INTRACELLULAR MEMBRANES..... 64

2.2.1 Platelet isolation and neuraminidase treatment..... 64

2.2.2 Platelet sonication and separation of mixed membrane fraction..... 66

2.2.3 Membrane separation by continuous flow electrophoresis..... 68

2.2.3a Priming of the electrophoresis unit before use..... 69

2.2.3b Continuous flow electrophoresis running conditions..... 70

2.2.3c Collection of purified platelet membrane fractions..... 71

2.2.4 Isolation of a subpopulation of the intracellular membrane by oxalate loading..... 71

2.2.5 Protein estimation of membrane fractions..... 73

2.3 BIOCHEMICAL CHARACTERISATION OF PLATELET SURFACE AND INTRACELLULAR MEMBRANE FRACTIONS..... 75

2.3.1 SDS-polyacrylamide gel electrophoresis..... 75

2.3.2 NADH-cytochrome *c* reductase enzyme assay..... 76

2.3.3 Assay for calcium uptake by intracellular membrane vesicles..... 77

2.3.4 Ins(1,4,5)P_3-induced release of sequestered calcium from intracellular membrane vesicles..... 78

2.4 PLANAR BILAYER METHODS..... 80

2.4.1 Membrane chamber and electrical equipment..... 80

2.4.2 Procedure for membrane formation..... 84

2.4.3 Incorporation of ion channels by fusion..... 86

2.4.4 Single channel experimental protocol..... 88

2.5 ANALYSIS OF SINGLE CHANNEL DATA..... 91

2.5.1 Conduction properties of channels..... 92

2.5.2 Gating properties of channels..... 94

2.5.2a Aims of analysis..... 95

2.5.2b Event detection by half-amplitude threshold analysis..... 97

2.5.2c Open and closed lifetime distributions..... 99

2.5.2d Fitting of exponentials to distributions..... 100

2.5.2e Determining the number of exponential components..... 104

2.5.2f Correlation between successive closed events..... 105

2.5.2g Measurement of P_o values..... 106

Chapter 3 RESULTS I

BIOCHEMICAL CHARACTERISATION OF PLATELET SURFACE AND INTRACELLULAR MEMBRANE FRACTIONS..... 107

3.1 Introduction..... 108

3.2 SDS-polyacrylamide gel electrophoresis..... 108

3.3 NADH-cytochrome *c* reductase enyzme assay..... 110

3.4 Assay for calcium uptake by intracellular membrane vesicles..... 110

3.5 Ins(1,4,5)P_3-induced release of sequestered calcium from intracellular membrane vesicles..... 113

3.6 Summary..... 115

Chapter 4 RESULTS II

PLATELET SURFACE MEMBRANE CHANNELS..... 116

4.1 Introduction..... 117

4.2 Reconstitution of surface and mixed membrane vesicles into planar bilayers..... 117

CONDUCTION PROPERTIES OF THE SM CHANNEL

4.3 Dependence of single channel conductance on the KCl concentration..... 126

4.4 Single channel rectification 127

4.5 Anion *vs* cation selectivity 129

4.6 Cation conductance 134

4.7 Relative anion permeabilities and conductances 136

4.8 Channel block by DIDS, SITS and ATP 140

4.9 Application of various other agents to the SM channel 143

GATING PROPERTIES OF THE SM CHANNEL

4.10 Probability of the channel being open 145

4.11 Open and closed lifetime analysis 146

4.11a Open lifetime distribution 147

4.11b Closed lifetime distributions 151

4.11c Open and closed lifetimes at various voltages 153

4.11d Lack of correlation between successive closed events 158

FURTHER SINGLE CHANNEL STUDIES ON THE PLATELET SM

4.12 Single channels in agonist-activated platelets 160

4.13 Discussion 163

Chapter 5 RESULTS III

PLATELET INTRACELLULAR MEMBRANE CHANNELS 176

5.1 Introduction 177

5.2 Attempts to reconstitute the IM fraction 177

5.3 Isolation of an IM subpopulation by oxalate loading 179

5.4 Reconstitution of a cation channel from the oxalate loaded IM fraction 179

5.4.1 Conduction properties of the IM channel 180

5.4.2 The probability of the IM channel being open 184

5.4.3 Use of the IM K^+ channel as a 'marker' for fusion 184

5.5 Oxalate loading of the mixed membrane fraction..... 186

5.6 Discussion..... 187

Chapter 6

6.1 Summary..... 194

6.1.1 Platelet surface membrane channels..... 196

6.1.2 Platelet intracellular membrane channels..... 198

Appendix A..... 200

Appendix B..... 201

References..... 202

LIST OF FIGURES

1.1 Diagrammatic representation of a platelet sectioned through equatorial and transverse planes 21

1.2 Continuous flow electrophoresis chamber 29

1.3 Charge characteristics surrounding a negatively charged particle 33

1.4 Ca^{2+} pools and Ca^{2+} transport systems in the platelet 37

1.5 Diagrammatic representation of a working hypothesis for a channel 51

1.6 Formation of a planar lipid bilayer 56

1.7 Diagrammatic representation of the steps in the fusion process 59

2.1 Density gradient sedimentation of platelet mixed membrane fraction 67

2.2 Typical continuous flow electrophoresis profile 72

2.3 Membrane chamber and cup 81

2.4 Bilayer electronics system 83

2.5 Typical waveforms observed during bilayer formation 87

2.6 Half amplitude threshold analysis 98

3.1 SDS polyacrylamide gel of membrane fractions 109

3.2 NADH cytochrome *c* reductase assay 111

3.3 Time course of calcium uptake by intracellular membranes 112

3.4 Time course of the release of sequestered intracellular membrane calcium by $Ins(1,4,5)P_3$ 114

SM channel

4.1 Single channel activity following fusion of SM vesicles..... 119

4.2 Multiple channel recording from the MM fraction..... 121

4.3 Current-voltage relationships in symmetrical 450mM KCl..... 122

4.4 Single channel activity at a range of holding potentials..... 123

4.5 Dependence of single channel conductance (G) on the KCl concentration..... 128

4.6 The effect of HEPES/Tris buffers on single channel current.... 130

4.7 Test for anion/cation selectivity..... 132

4.8 TEA permeation through the channel..... 135

4.9 SO_4^{2-} permeation through the channel..... 137

4.10 Comparison of anion permeabilities..... 138

4.11 Conductances measured at -40mV for various anions..... 141

4.12 The effect of DIDS and SITS on the channel..... 142

4.13 The effect of ATP on the channel..... 144

4.14 Open probability as a function of holding potential..... 146

4.15 25 minute recording of SM channel at -40mV..... 148

4.16 Example of a 'gearshift' change in kinetic state..... 149

4.17 Open lifetime analysis at -40mV..... 150

4.18 Closed lifetime analysis at -40mV..... 152

4.19 Open lifetime τ values at a range of voltages..... 155

4.20 Closed lifetime τ values at a range of voltages..... 156

4.21 Closed lifetime area parameters at a range of voltages..... 157

4.22 Closed lifetime autocorrelation function..... 159

4.23 Single channel activity from MM vesicles prepared from thrombin-stimulated platelets..... 162

IM channel

5.1 Single channel activity following fusion of oxalate loaded IM vesicles..... 181

5.2 Current-voltage relationships in symmetrical KCl solutions..... 182

5.3 Current-voltage relationship in asymmetric KCl solutions..... 183

5.4 Probability of the channel being open..... 185

LIST OF TABLES

1 Comparison of conductance values at -40mV and +40mV..... 124

2 Anion *vs* cation selectivity..... 133

3 Relative anion permeabilities..... 139

ABBREVIATIONS

ADP	adenosine-5'-diphosphate
ATP	adenosine-5'-triphosphate
CFE	continuous flow electrophoresis
EDTA	ethylenediaminetetra-acetic acid
EGTA	ethyleneglycol-bis-(aminoethylether)tetra-acetic acid
DIDS	4,4'-diisothiocyanostilbene-2-2'-disulphonic acid
DTS	dense tubular system
F	the Faraday constant, 96,500 coulombs/mole
gallamine	(1,2,3 Tris[2-triethyl-ammoniumethoxy]benzene)
HEPES	N-2-hydroxyethylpiperazine-N'-2-ethanesulphonic acid
IM	platelet intracellular membrane (= DTS)
$Ins(1,4,5)P_3$	inositol 1,4,5-trisphosphate
$Ins(1,4,5)P_4$	inositol 1,3,4,5-tetrakisphosphate
MM	platelet mixed membrane
NADH	nicotinamide adenine dinucleotide (reduced)
OCS	open canalicular system
PAF	platelet activating factor
p.d.f	probability density function
PE	phosphatidylethanolamine
PRP	platelet rich plasma
PS	phosphatidylserine
pS	picoSiemen
R	the Gas constant, 8.314 joules/degree mol^{-1}
S.D.	sample standard deviation
SDS	sodium dodecyl sulphate

SITS	4-acetamido-4'-isothiocyanotostilbene-2,2'-disulphonic acid
SM	platelet surface membrane
SR	sarcoplasmic reticulum
succinyl choline	2,2'-[(1,4-dioxo-1,4-butanediyl)bis(oxy)] bis[N,N,N-trimethylethylethanaminium]
TEA	tetraethylammonium
Tris	tris(hydroxymethyl)aminomethane

Chapter 1

INTRODUCTION

1.1 GENERAL INTRODUCTION

Platelets represent crucial elements in haemostasis and thrombosis, and are important in the maintenance and integrity of blood vessel walls. Platelets circulate in a resting state and are recruited for functional performance by contact with a 'foreign' surface, such as a damaged vessel wall, or by the action of specific soluble agents functioning as 'activators' (eg. ADP, thrombin, collagen and immune complexes). The activation which follows is mediated by specific reactions at the membrane level leading to the production of intracellular second messengers that transform the initial contact into functional platelet responses. The basic cellular responses are platelet adhesion, shape change, secretion of substances from intracellular granules, and platelet aggregation. It follows from this that the properties of the platelet plasma membrane and of the intracellular organelle membranes and their constituent elements are highly relevant to these functions.

The focus of the experimental work presented in this thesis has been on the ion transporting integral membrane proteins located in the platelet surface membrane and in the intracellular membrane network known as the dense tubular system (DTS). Despite the obvious importance of ion fluxes across platelet membranes, our present understanding of their location, selectivity, rates and magnitudes is somewhat limited. A major reason for this has been the technical difficulties encountered in applying conventional electrophysiological techniques to such small cells (2-4μm diameter). Microelectrode impalement of platelets has not been reported, and only two groups have described the successful patch clamping of platelets to date (Maruyama, 1987; Mahaut-Smith *et al.*, 1989). In these, whole cell currents were measured and some single channel data obtained using the

cell-attached variation (results from these experiments are discussed in section 1.4.1).

The aims of the research presented in this thesis were as follows:

(1) To utilise a well characterised method for separating highly purified platelet surface and intracellular membrane vesicles free from cross contamination using density gradient fractionation and high-voltage continuous flow electrophoresis.

(2) To confirm that the two membrane populations obtained from the separation procedure were correctly fractionated and the intracellular membrane vesicles remained functionally responsive.

(3) To reconstitute the platelet surface and intracellular membrane vesicles into artificial planar phospholipid bilayers by fusion and record single ion channel currents under voltage clamp conditions.

(4) To characterise the ion channels observed in terms of their conduction and gating characteristics.

The introductory chapter discusses various topics of relevance to the experimental approach.

1.2 General ultrastructural and molecular features of the platelet

- with particular emphasis on the composition of the surface and intracellular membranes and the groups that contribute to the net surface charge of the platelet.

1.3 Isolation of platelet membranes

- a brief description of the membrane isolation procedures employed in this experimental work is given, followed by an explanation of the general principles of continuous flow electrophoresis and the factors determining the electrophoretic mobility of particles in an electric field.

1.4 Ion fluxes across platelet membranes

- a brief overview of previous relevant research identifying transport processes of Ca^{2+} and other ions important in platelet homeostasis and activation is presented.

1.5 Ion channels and their reconstitution into planar bilayers

- the nature and function of ion channels in biological membranes is outlined with a discussion of the advantages offered by the planar bilayer technique in single channel recording. Since the success of this technique relies on the ability to form a stable phospholipid bilayer and incorporate ion channels by fusion, the composition and properties of the planar bilayer and the steps involved in the fusion process are discussed.

1.2 GENERAL ULTRASTRUCTURAL AND MOLECULAR FEATURES OF THE PLATELET

The various ultrastructural features of the circulating platelet are illustrated in figure 1.1.

1.2.1 The platelet surface membrane

The platelet surface membrane appears under the electron microscope as a trilaminar structure with a thickness of about 70-90 Å. There are a number of invaginations of the surface membrane into the cytoplasm which form the open canalicular system (OCS). This system significantly increases the surface area of the cell in contact with its aqueous environment and serves as a conduit for uptake of plasma-borne substances as well as a pathway for extrusion of intracellular granule contents upon platelet activation.

The core of the membrane is formed by a lipid bilayer to which peripheral membrane proteins (such as the cytoskeletal proteins) are attached via polar interactions, and which is interrupted to allow hydrophobic interactions with integral membrane proteins. The lipid:protein ratio of the platelet surface membrane is about 0.58 (w/w). Approximately 70% of the total membrane lipid is phospholipid, whilst the remainder consists predominantly of cholesterol plus smaller amounts of glycolipids. Five major phospholipid classes have been identified in human platelets (Marcus *et al.*, 1969; Perret *et al.*, 1979): phosphatidylcholine (38%), phosphatidylethanolamine (27%), sphingomyelin (19%), phosphatidylserine (10%) and phosphatidylinositol (5%). Glucose, mannose, fructose, galactose and hexosamines have all been found in the surface membrane.

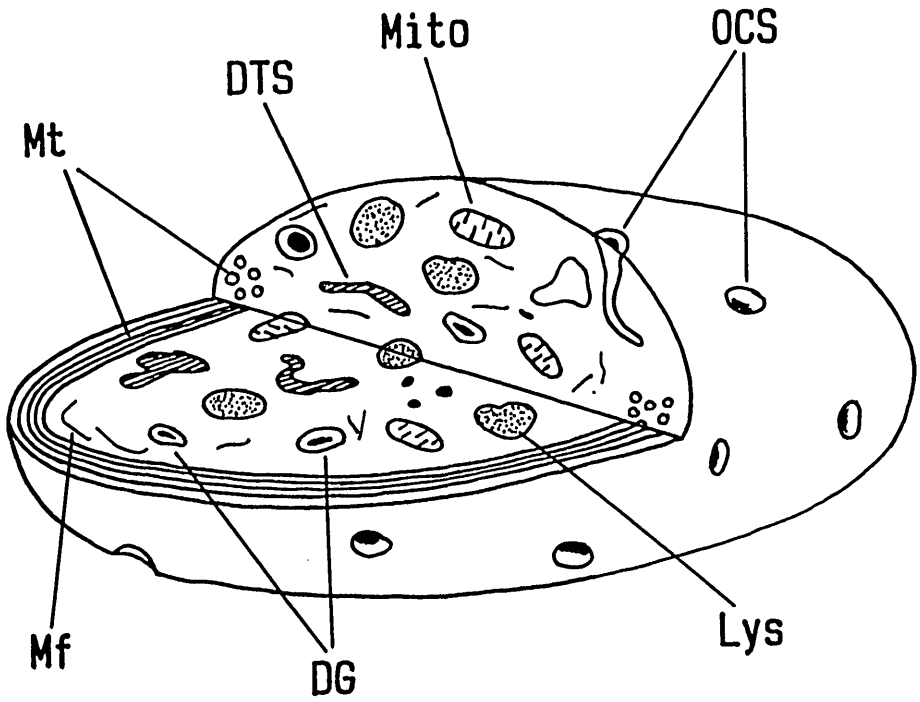


Figure 1.1

Diagrammatic representation of a platelet sectioned through equatorial and transverse planes.

DG, dense granules; **DTS**, dense tubular system; **Lys**, lysosome-like organelles; **Mf**, microfilaments; **Mito**, Mitochondria; **Mt**, microtubules; **OCS**, open canalicular system.

The plasma membrane is associated on the exterior face with an electron-dense 'glycocalyx', representing carbohydrate-rich domains of more than 30 different membrane glycoproteins with the carbohydrate chains exposed to the outside of the cell. Much attention has been paid to these membrane glycoproteins, largely because of their importance in receptor events for a variety of ligands. The most abundant of the glycoproteins are Ib, IIb, IIIa and IV and their functional roles are just beginning to be understood (for review see Clemetson and McGregor, 1987). Progress in this field has been accelerated by the identification of a number of genetic disorders affecting these glycoproteins (Nurden, 1985).

At the cytoplasmic surface, the membrane is linked to certain cytoskeletal proteins that undergo dynamic changes during platelet activation (White, 1971). These involve polymerised actin in the network of filaments that form the membrane/cytoskeletal axis. Interaction between cytoplasmic f-actin and myosin is regulated by the level of phosphorylation of the myosin light chains by a specific myosin light chain kinase which is calmodulin dependent (Adelstein *et al.*, 1975). Actin polymerisation is regulated by a number of proteins, such as gelsolin (Lind *et al.*, 1982) and profilin (Markey *et al.*, 1978), whilst α-actinin has been implicated in the membrane attachment of actin filaments (Sixma *et al.*, 1982). Membrane domain heterogeneity exists since dissociation of the filament network can occur in some regions at the same time as polymeric assembly of actin takes place in other areas.

The platelet surface membrane is also the site of major enzyme activity, such as adenylate cyclase (Menashi *et al.*, 1981), magnesium ATPase (Hack *et al.*, 1986) and phosphodiesterase (Kinoshita *et al.*, 1979).

1.2.2 Platelet surface membrane charged groups

At physiological pH in saline or plasma, platelets exhibit a net negative charge and move more rapidly in an electric field than other formed elements of the blood. The greatest contribution to the platelets' net electronegativity comes from the α-carboxyl groups (pK 2.8) of the sialic acid (N-acetyl neuraminic acid) residues on the surface membrane. (Seaman and Vassar, 1966; Mehrishi, 1973; Tanoue *et al.*, 1982). Treatment of platelets with neuraminidase (which cleaves sialic acid residues) has been shown to reduce both the electrophoretic mobility and charge by about 50%, indicating that these residues are responsible for at least half the surface charge (Holmsen, 1972; Tanoue *et al.*, 1982) [It should be noted that the platelet surface charge, as estimated electrophoretically, is a net charge and does not give information on the distribution of charges on the surface]. Other groups making minor contributions to the platelet negative charge are the carboxyl groups of amino acids, phosphate and sulphate. However, it is uncertain which of these groups belongs to the 'fluffy' layer surrounding the platelet and which to the surface membrane itself.

The treatment of platelets with neuraminidase and consequent reduction in electrophoretic mobility of the surface membrane is the means by which membrane fractions have been separated in the experiments described in this thesis. Following neuraminidase treatment, the less electronegative surface membrane migrates to a position closer to the cathode in the electrophoresis chamber than the more electronegative intracellular membrane. Thus the two membrane fractions can be resolved.

1.2.3 The platelet intracellular membrane

Below the platelet surface membrane and often closely juxtaposed (but not directly in contact) with the OCS, there is a complex of vacuolated membranes, termed by electron microscopists the dense tubular system (DTS). This system is probably derived from the smooth endoplasmic reticulum of the parent megakaryocyte (White, 1972). Both the OCS and the DTS have been proposed to serve functions analogous to the transverse tubules and sarcotubules of the sarcoplasmic reticulum (SR) of muscle cells (White, 1972). Indeed, vesicles derived from the DTS have been shown to accumulate Ca^{2+} as efficiently as the SR of muscle (Kaser-Glanzmann *et al.*, 1978; Menashi *et al.*, 1984; Authi and Crawford, 1985).

The lipid composition of the DTS resembles that of the surface membrane although the cholesterol and sphingomyelin content is much lower. Phosphatidylcholine and phosphatidylinositol are more enriched in the intracellular membrane than in the surface membrane (Lagarde *et al.*, 1982).

The dense tubular system has been shown to contain, amongst others, the enzyme phospholipase A_2 and the sequence of enzymes required for the formation of thromboxane A_2 from liberated arachidonic acid (Gerrard *et al.*, 1976; Lagarde *et al.*, 1981, 1982; Carey *et al.*, 1982). It may also be concerned with some *de novo* synthesis of fatty acids and phospholipids, since it appears to be derived from the megakaryocyte smooth ER. A high activity of the ER marker enzyme antimycin-insensitive NADH cytochrome *c* reductase is also present in the DTS (Menashi *et al.*, 1981) and this enzyme has been used as a marker for the purification of the intracellular membrane in this thesis (see section 2.3.2 and 3.3). Recent studies have shown the presence of a calcium and magnesium ATPase in

the DTS, which is kinetically linked to the uptake of calcium (Hack *et al.*, 1986) and a putative inositol trisphosphate ($Ins(1,4,5)P_3$) receptor associated with release of Ca^{2+} into the cytosolic space when platelets are activated (Authi *et al.*, 1986).

1.2.4 Other platelet intracellular structures

The discoid form of resting platelets is maintained by a circumferential bundle of microtubules located beneath the surface membrane. Together with the micro-filaments of polymerised actin, this microtubule ring contracts during platelet activation (White and Sank, 1984), drawing together the randomly dispersed storage granules to concentrate them into a tightly packed mass. The storage granules contained in the platelet cytoplasm can be divided into 3 sub-classes: α-granules, dense bodies and lysosomal enzyme storage organelles.

The α-granules are the most abundant in human platelets and contain a number of non-enzymatic proteins. These include fibrinogen, ß-thromboglobulin, factors V and XIII, von Willebrand factor, fibronectin, thrombospondin and the heparin-binding protein factor 4. The latter four are important in platelet adhesive phenomena. Platelet-derived growth factor has also been located in α-granules. This cationic protein is capable of eliciting proliferation of arterial smooth muscle cells and fibroblasts in tissue culture (Ross and Vogel, 1978). The lysosomal enzyme storage organelles contain a number of acid hydrolases, such as hyaluronidase, α-N-acetyl-glucosaminidase and ß-glucuronidase (Schmukler and Zieve, 1972). The function of these hydrolases is not certain. The dense bodies contain calcium and low molecular weight compounds such as serotonin, ATP, ADP and pyrophosphate. The ATP and ADP in these granules do not participate in cell metabolism, and are distinguished from the metabolic pool of ATP and ADP

(Holmsen, 1972). Energy requiring functions are regulated by the presence in the cytoplasm of a number of small-sized mitochondria and by active glycolysis in conjunction with glycogen granules which fuel these ATP-producing pathways.

Platelets do not contain a nucleus or any DNA. A small amount of RNA may be present and some ribosomal structures have occasionally been observed. Protein synthesis is almost negligible, and presumably serves no function in platelet physiology.

1.3 ISOLATION OF PLATELET MEMBRANES

Platelets are very labile cells that tend to react almost explosively to exogenous stimuli. During procedures for separating platelets from blood, care is required to prevent stimulation which may initiate the shape change, aggregation and release responses (Sixma and Lips, 1978). Whole platelets are generally isolated by low speed differential centrifugation at room temperature (as described in section 2.2.1). A homogenisation procedure is then required which ideally should disrupt all platelets, keeping intracellular organelles intact and causing minimal damage to the surface membrane. Ultrasonication is the method which has been applied in the preparations described in this thesis. The conditions of time and sonication intensity as devised by Menashi *et al.*, (1981) have been adhered to throughout (see section 2.2.2). Membranes are disrupted non-selectively at high shear forces during sonication and tend to form sealed vesicles, with those from the intracellular membrane (DTS) being somewhat smaller than those from the plasma membrane.

A fraction containing both surface and intracellular membrane vesicles is first separated from other cellular elements by conventional density gradient centrifugation. A mixed membrane fraction is harvested from the low density region of a continuous sorbitol gradient and is clearly separated from denser components such as granules and mitochondria.

To separate purified fractions of surface and intracellular membrane vesicles from the mixed membrane fraction, the procedure followed in this thesis requires prior treatment of the platelets at the whole cell level with neuraminidase. This reduces the electronegativity of the surface membrane (as described in section 1.2.2), allowing good separation of surface and intracellular membranes by high-voltage

continuous flow electrophoresis. The technical procedures are descibed in detail in section 2.2.3. However, an introduction to the general principles of continuous flow electrophoresis and the factors determining the electrophoretic mobility of particles is pertinent here, and follows in sections 1.3.1 and 1.3.2.

1.3.1 Principles of membrane separation by continuous flow electrophoresis

Continuous flow electrophoresis (CFE) enables preparative separation of particles on the basis of their electrophoretic mobility. It provides a complementary separation to rate sedimentation, which separates particles on the basis of size and/or density. CFE is in principle applicable to all classes of substances that differ in electrical charge and migrate in the electric field with different mobilities. CFE has found widespread application in the separation of soluble and insoluble materials such as proteins, nucleic acids, bacteria, viruses, and whole cells, in addition to cell membranes and other subcellular organelles (Hannig, 1969).

The principles of CFE are illustrated in figure 1.2. The separation chamber consists of two parallel glass plates held approximately 0.8mm apart with affiliated pumps, cooling system and power supply (see section 2.2.3). A laminar flowing buffer film passes down the chamber between the glass plates perpendicular to a horizontally applied voltage. The sample to be separated is infused continuously into the flowing buffer film via a port close to the cathodal side of the separation chamber, since most cells or subcellular particles have a net electronegativity. The various components of the sample mixture migrate towards the anode locating at different positions in the chamber according to their electrophoretic mobility.They

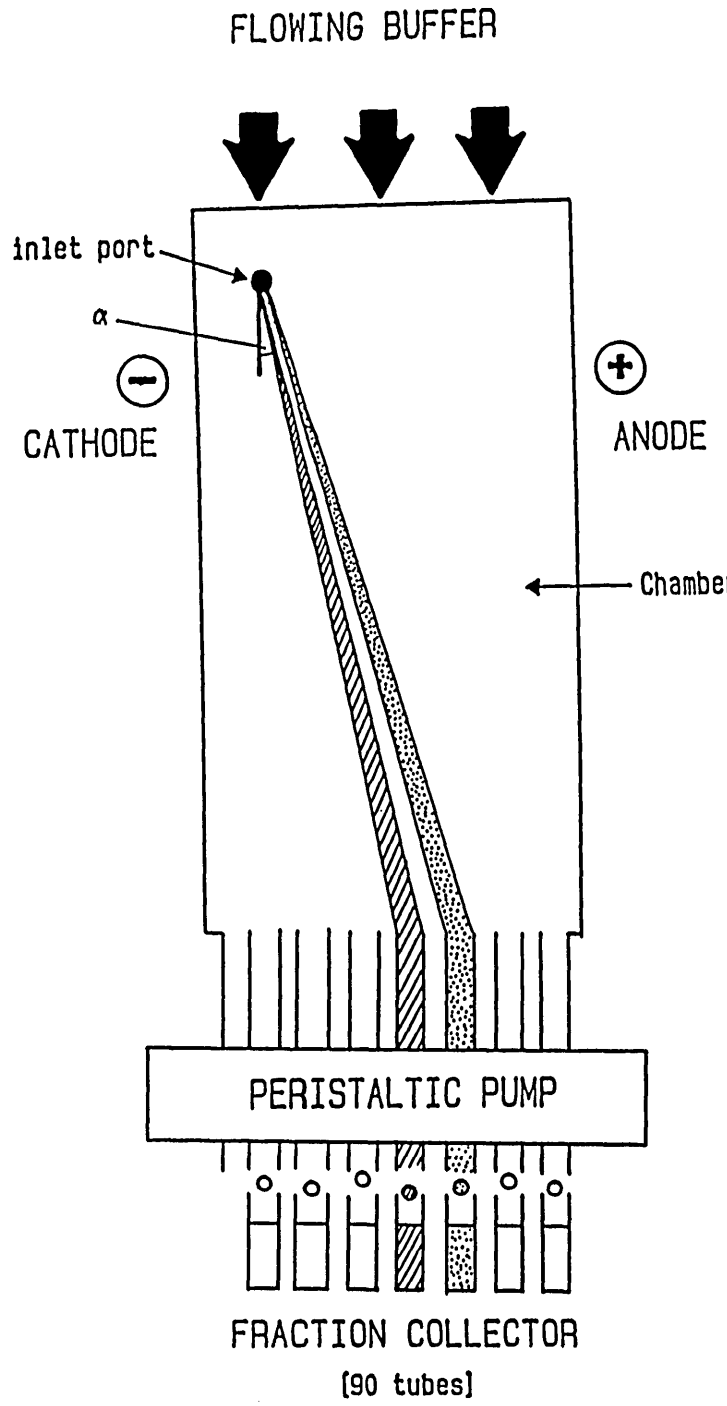


Figure 1.2

Continuous flow electrophoresis chamber

Diagram of the separation chamber used in continuous flow electrophoresis. The sample is introduced into a laminar flowing buffer film on the cathodal side. The components of the sample migrate in the electric field according to their electrophoretic mobility and are collected in fraction tubes at the base of the chamber. (α denotes the angle of deflection - see equation 1).

are collected at the base of the separation chamber where the flowing buffer exits into a fraction collector.

The general laws of electrophoretic migration give the expression for the angle of deflection, α :

$$\tan \alpha = \frac{e.i}{q.k.w} \qquad \text{(equation 1)}$$

where:

e is the electrophoretic mobility of the particle

i is the electric current

q is the cross section of the electrophoresis chamber

k is the specific conductivity of the buffer

w is the streaming velocity of the buffer solution

It is clear from this expression that precautions must be taken to ensure laminar and uniform buffer flow, and that a uniform electric field must be maintained in order to ensure constant running conditions over long periods of time.

For optimum electrophoretic separation of cell organelles a low ionic strength chamber buffer is preferred, but the ionic strength must be greater than that of the particles to be separated (Zeiller *et al.*, 1975). In addition, the buffer should be iso-osmotic with respect to the particles. The chamber buffer chosen by Menashi *et al.*, (1984) has been used in the preparations described in this thesis and consisted of 10mM triethanolamine, 10mM acetic acid, pH 7.2 adjusted to 300mosM by the addition of sorbitol.

The specific CFE running conditions used for the separation of platelet membrane fractions are detailed in section 2.2.3b.

1.3.2 Electrophoretic mobility of particles

If a particle within an electric field is considered in isolation, its electrophoretic mobility (defined as the velocity of the particle divided by the applied electric field) is proportional to the net surface charge as follows:

$$e = \frac{C.D}{K.T} \qquad \text{(equation 2)}$$

where:

e is the electrophoretic mobility of the particle

C is the total net charge of the particle

D is the diffusion constant

K is Boltzmann's constant

T is the absolute temperature

However, since the particle is suspended in an ionic environment, the charged groups on the particle surface attract oppositely charged ions from the surrounding medium. This cloud of ions closely associated with the particle is termed the Stern layer. For a negatively charged particle, this layer consists largely of positively charged ions. Though still electronegative, these ions alter the true surface charge on the particle through electrostatic interactions. A more diffuse and loosely bound layer of ions lies peripheral to the Stern layer and comprises the Gouy-Chapman (or diffuse electrical double) layer. For a negatively charged particle, ions forming part of the Gouy-Chapman layer closest to the Stern layer would be predominantly

negatively charged, and these decrease in number with increasing distance from the particle surface. Complete neutralisation of charge does not occur due to thermal fluctuations. Figure 1.3 summarises the charge characteristics surrounding a negatively charged particle.

In the presence of an electric field, a particle moves in conjunction with its associated 'ion cloud' (the Stern layer and some of the more closely attached ions from the diffuse Gouy-Chapman layer). As a result of this relative movement, a plane of shear develops between the moving particle with its 'ion cloud' and the surrounding bulk solution. The electrostatic potential between a point in the plane of shear and a point in the surrounding medium is referred to as the 'zeta potential'. Since it occurs at the shearing plane, which occurs some distance from the particle surface, the magnitude of the zeta potential may not be as large as the magnitude of the surface potential. The concept of the zeta potential is of fundamental importance in electrophoretic separations and is related to electrophoretic mobility by the **Helmholtz-Smoluchowski** equation:

$$z = \frac{4\pi\eta \cdot e}{\varepsilon D_0} \qquad \text{(equation 3)}$$

where:

z is the zeta potential

η is the coefficent of viscosity ($4\pi\eta$ is the viscosity of the medium)

e is the electrophoretic mobility of the particle

ε is the dielectric constant of water

D_0 is the permittivity of free space

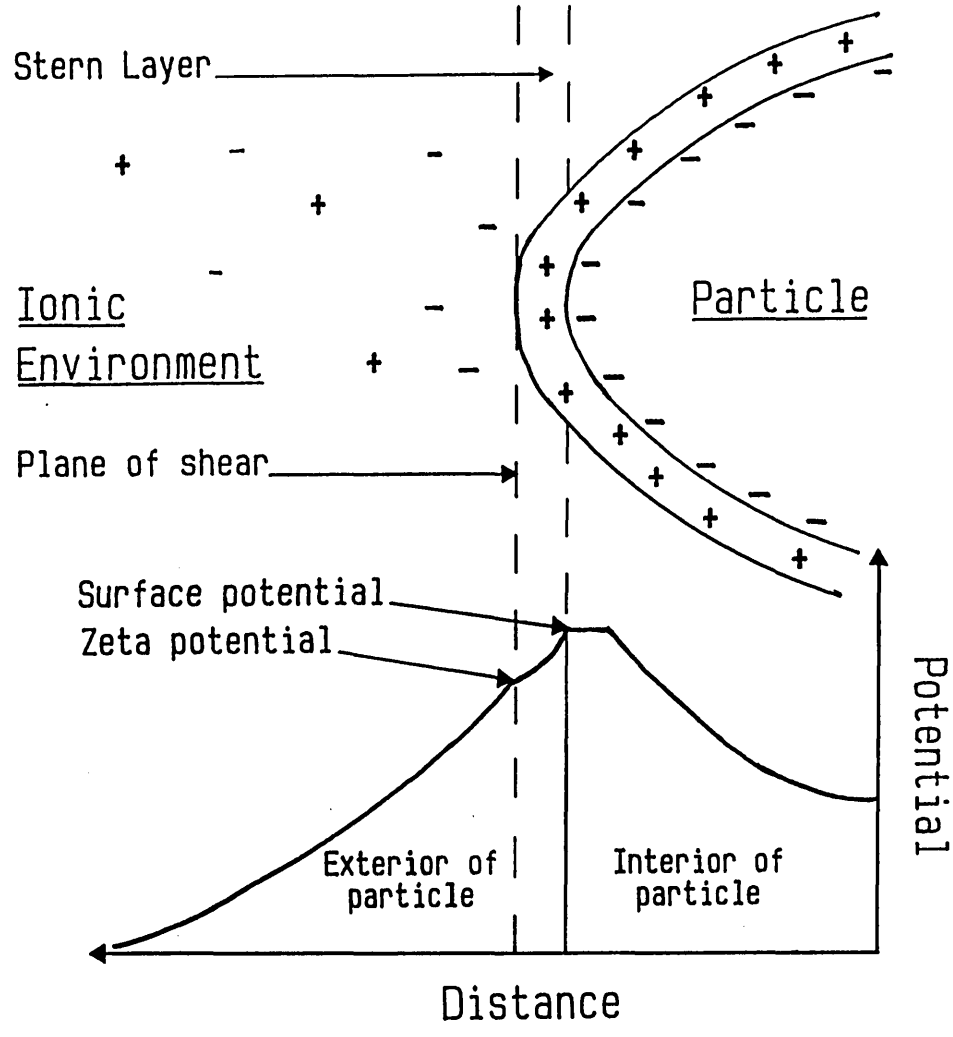


Figure 1.3

Charge characteristics surrounding a negatively charged particle

These theoretical concepts are, however, more appropriate to large and uniformly spherical particles and their application to small, irregularly shaped cells with ruffled or invaginated membrane domains, or membrane vesicles, is at best an approximation. However, the concepts have some merit in discussions of the electrophoretic behaviour of particles in buffers of differing ionic strengths. At physiological or higher ionic strengths, the plane of shear lies close to the particle surface and the 'ion cloud' (or electrokinetic zone) extends for approximately 8 Å. However, at lower ionic strengths, the electrokinetic zone may extend to as much as 15 Å beyond the cell membrane. In the latter case, charged groups lying deeper within the particle (or in surface invaginations, in the case of an irregularly shaped particle) would contribute electrically to the zeta potential. Thus a cell with a ruffled membrane will, at low ionic strengths, behave electrokinetically as though it had a smooth surface.

The concepts summarised by the Helmholtz-Smoluchowski equation are also of assistance in optimising separations by continuous flow electrophoresis. It is known that the separation buffer film has a slower velocity at the edges of the chamber due to the Poisseuille effect. This causes particles nearer to the chamber wall to remain in the chamber for longer and be deflected further than the main stream (Hannig, 1969), leading to a 'band-broadening' effect. There is also an electro-osmotic flow in the opposite direction to the particle movement, due to the difference between the zeta potential of the glass chamber walls and the particles (Strickler and Sacks, 1973). Optimum resolution is achieved if the zeta potential of the separation chamber walls is approximately equal to that of the sample to be separated (Hannig *et al.*, 1975). To facilitate this, the chamber walls can be routinely coated with 3% bovine serum albumin prior to use, to reduce the zeta potential (see section 2.2.3a). Under these conditions, the electro-osmotic effects

and Poisseuille velocity profile effects tend to cancel each other and do not severely affect particle resolution.

1.4 ION FLUXES ACROSS PLATELET MEMBRANES

Transmembrane movement of ions across the various platelet membranes has been studied extensively for Ca^{2+} and much less in the case of Na^+, K^+ or H^+. A comprehensive discussion of the role of Ca^{2+} in platelet responses is beyond the scope of this thesis. Therefore only a brief overview of transport processes of Ca^{2+} and some other ions important in platelet homeostasis and activation will be presented here.

1.4.1 Calcium flux across platelet membranes

The cytosolic free Ca^{2+} concentration ($[Ca^{2+}]_i$) in resting platelets does not exceed 100nM (Rink *et al.*, 1982), whereas the Ca^{2+} concentration in the plasma is 10,000 fold greater (1-2mM). Calcium homeostasis is maintained in unstimulated platelets by limiting the Ca^{2+} influx from the extracellular space, by actively promoting Ca^{2+} efflux, and by sequestering Ca^{2+} within internal storage sites.

Several storage sites for Ca^{2+} exist within the platelet, including the dense tubular system, the amine storage granules and the mitochondria as well as a putative surface membrane-bound calcium pool (Gerrard *et al.*, 1981). A summary of the Ca^{2+} pools and Ca^{2+} transport systems in platelets is shown in figure 1.4.

Various methods exist to measure fluxes, pools and concentrations of Ca^{2+} in stimulated and unstimulated platelets. They include the use of chlortetracycline, quin2, fura-2, indo-1, aequorin or $^{45}Ca^{2+}$.

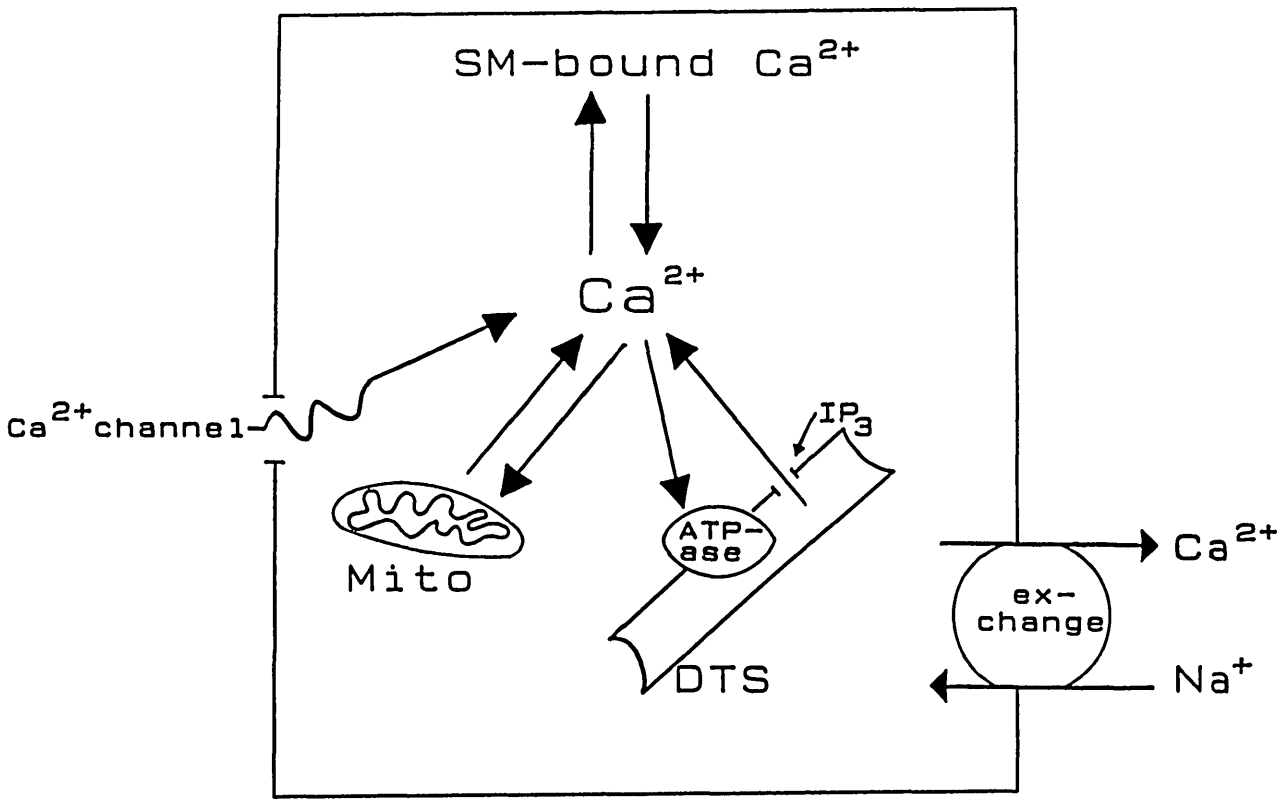


Figure 1.4

Ca^{2+} pools and Ca^{2+} transport systems in the platelet

DTS, dense tubular system; **IP_3**, inositol 1,4,5-trisphosphate; **Mito**, mitochondria; **SM**, surface membrane.

The most popular method currently used for measuring $[Ca^{2+}]_i$ in mammalian cells is the use of the fluorescent probes quin2, fura-2 and indo-1 (Tsien, 1980; Rink *et al.*, 1982; Tsien *et al.*, 1984; Grynkiewicz *et al.*, 1985; Rao *et al.*, 1985; Pollock and Rink, 1986). The ester derivatives of quin2 or fura-2 are membrane permeable and enter intact cells. Cytosolic esterases split off the ester groups and leave the now membrane-impermeable quin2 or fura-2 tetra anion trapped in the cytosol. Increases of $[Ca^{2+}]_i$ are recognised by the chelating dye and indicated by a change in fluorimetric intensity. Quin2 has several limitations (Tsien *et al.*, 1984), one being that, at the concentration required, it may itself act as a Ca^{2+} sink. The limitations are partly overcome by the newer indicators fura-2 and indo-1 (Grynkiewicz *et al.*, 1985).

Another method for assessing $[Ca^{2+}]_i$ is the measurement of the luminescence of the photoprotein aequorin (Johnson *et al.*, 1985; Yamaguchi *et al.*, 1986). Aequorin can be introduced into human platelets, although only a small percentage (<0.05%) of the photoprotein added becomes incorporated and its exact location within platelets is not known. The aequorin signal is assumed to help identify inhomogeneous cytosolic Ca^{2+} pools and local Ca^{2+} fluxes beneath the surface membrane. Estimates of exchangeable Ca^{2+} pools in whole platelets or platelet microsomes are carried out by measuring the distribution of $^{45}Ca^{2+}$. Sizes of surface-bound Ca^{2+} pools and intracellular Ca^{2+} pools and rates of Ca^{2+} exchange into these pools can be measured by this method (Brass and Shattil, 1982; Menashi *et al.*, 1984).

Ca^{2+} efflux from the cytoplasm is mediated in other tissues by a Ca^{2+}-Mg^{2+}ATPase or by a Na^+/Ca^{2+} counter ion exchanger localised in the surface membrane. To date a Ca^{2+} extrusion pump similar to that in the red cell

membrane has not been identified in platelet surface membranes (Steiner and Luscher, 1985; Hack *et al.*, 1986), although a Na^+/Ca^{2+} exchanger has recently been described. Plasma membrane vesicles have been shown to exhibit $^{45}Ca^{2+}$ uptake in exchange for intravesicular Na^+ and Ca^{2+} efflux into an external medium containing NaCl (Rengasamy *et al.*, 1987).

Studies using highly purified intracellular membrane vesicles have confirmed that ATP dependent Ca^{2+} uptake is almost exclusively localised in platelet intracellular membranes (Menashi *et al.*, 1982, 1984; Hack *et al.*, 1986) and appears not to be present in the surface membrane. This Ca^{2+}-sequestering system in the DTS has been well characterised. It is stimulated by Ca^{2+} and ATP and requires the presence of Mg^{2+} (Dean and Sullivan, 1982; Javors *et al.*, 1982; Dean, 1984, 1989; Adunyah and Dean, 1986a,b). The ATPase from human platelets has been purified (Dean, 1984,1988) and is similar in structure and function to the sarcoplasmic reticulum Ca^{2+}ATPase of cardiac and skeletal muscle, transporting two molecules of Ca^{2+} for each molecule of ATP hydrolysed (Dean, 1984,1989).

Platelet intracellular membrane vesicles can also liberate the accumulated Ca^{2+}. The Ca^{2+}-liberation system is different to the Ca^{2+}-uptake system (Enouf *et al.*, 1984; Adunyah and Dean, 1986a) and is regulated by micromolar extravesicular Ca^{2+} concentrations. The second messenger inositol 1,4,5-trisphosphate ($Ins(1,4,5)P_3$) has been shown to mobilise Ca^{2+} from the DTS of saponised platelets and from intracellular membrane vesicles (Adunyah and Dean, 1985; Authi and Crawford, 1985; Brass and Joseph, 1985; O'Rourke *et al.*, 1985, Authi *et al.*, 1986). The exact mechanism of the Ca^{2+}-mobilising effect of $Ins(1,4,5)P_3$ has not been clarified. Since Ca^{2+} release by Ins $(1,4,5)P_3$ does not require ATP (Adunyah and Dean, 1986b; Meyer *et al.*, 1988) and does not display the

temperature-sensitivity expected of an enzymic process (Adunyah and Dean, 1986b), it is thought that Ins(1,4,5)P_3 may activate a Ca^{2+} channel in the DTS through a specific ligand-binding reaction. Extensive efforts have been made in the work carried out for this thesis, to identify this putative Ins(1,4,5)P_3 activated Ca^{2+} channel in highly purified intracellular membrane vesicles (see chapter 5).

There is substantial evidence that $[Ca^{2+}]_i$ rises very rapidly after platelet stimulation by a number of different agents (e.g. Massini and Luscher, 1976; Robblee and Shepro, 1976; Gerrard *et al.*, 1981; Rink *et al.*, 1982; Hallam *et al*, 1984a,b; Hallam and Rink, 1985a; Sage *et al.*, 1989). This Ca^{2+} increase may originate either from the extracellular fluid via surface membrane Ca^{2+} channels, or by release from internal stores (see figure 1.4). The Ca^{2+} sequestered in the amine storage granules does not appear to contribute to this rise in $[Ca^{2+}]_i$, but is released to the extracellular fluid by exocytosis following platelet activation (Murer and Holme, 1970; Steiner and Tateishi, 1974). Furthermore, the decrease in chlortetracycline fluorescence induced by thrombin occurs more rapidly than the secretory response monitored by release of Ca^{2+} (Feinstein, 1980). Although Ca^{2+} release can occur from mitochondria *in vitro*, the conditions required to achieve such release do not appear compatible with participation in events at the cation concentration or time scale involved in platelet activation. Such considerations do not exclude the DTS or the putative plasma membrane Ca^{2+} pool as possible sites from which Ca^{2+} may be mobilised.

1.4.1a Ca^{2+} mobilisation from intracellular stores on platelet activation

In the absence of extracellular Ca^{2+}, the increase of quin2 or fura-2 fluorescence in stimulated platelets reflects a rise in $[Ca^{2+}]_i$ released from the intracellular

stores. Such rises in $[Ca^{2+}]_i$ have been observed on platelet stimulation with a number of agents including thrombin (Rink *et al.*, 1982; Thompson and Scrutton, 1985; Pollock and Rink, 1986), ADP (Fisher *et al.*, 1985; Hallam and Rink, 1985a; Thompson and Scrutton, 1985), PAF (Hallam *et al.*, 1984a), arachidonic acid (Thompson and Scrutton, 1985), vasopressin (Hallam *et al.*, 1984b), ionomycin (Rink *et al.*, 1982) and A23187 (Thompson and Scrutton, 1985). The increase in $[Ca^{2+}]_i$ is rapid and, in most cases, transient. Measuring subsecond time courses of $[Ca^{2+}]_i$ rises by stopped-flow fluorimetry in fura-2 loaded platelets, it was found that thrombin and ADP mobilise intracellular Ca^{2+} with a mean delay time of 0.2-0.3 sec (Sage and Rink, 1986a).

The sites from which Ca^{2+} is released are the DTS and probably the plasma membrane. In many non-excitable cells it now seems that Ins(1,4,5)P_3 is a major trigger for mobilisation of Ca^{2+} sequestered in the endoplasmic reticulum (Berridge and Irvine, 1984). Evidence that Ins(1,4,5)P_3 can release accumulated Ca^{2+} from vesicles prepared from the DTS, as mentioned earlier, suggests that this is one important mechanism in platelets. The cytosolic concentration of Ins(1,4,5)P_3 found in stimulated platelets is between 2 and 10μM (Rittenhouse and Sasson, 1985; Siess, 1985; Dangelmaier *et al.*, 1986). Both the concentration and the rapidity of formation and action support a second messenger role for Ins(1,4,5)P_3 in the release of Ca^{2+} in stimulated platelets. It should be noted, however, that inositol lipid hydrolysis may not be a pre-requisite for elevation of $[Ca^{2+}]_i$, as ADP is an ineffective stimulant to inositol lipid hydrolysis in human platelets, yet evokes an increase in $[Ca^{2+}]_i$ (Fisher *et al* ., 1985).

The increase in $[Ca^{2+}]_i$ upon receptor-activating platelet stimuli is inhibited by substances that increase cAMP production either through receptor-coupled

stimulation of adenylate cyclase (eg.PGE_1, PGD_2), or by direct stimulation of the enzyme (eg. forskolin) (Feinstein *et al.*, 1983; Yamanishi *et al.*, 1983; Sage and Rink, 1985; Thompson and Scrutton, 1985). This is apparently due to interference with the release of internal Ca^{2+} stores and the surface membrane permeability to Ca^{2+}. The inhibition of intracellular Ca^{2+} release can largely be explained by suppression of phosphatidylinositol 4,5-bisphosphate hydrolysis (Feinstein *et al.*, 1983; Imai *et al.*, 1983; Bushfield *et al.*, 1985) and Ins(1,4,5)P_3 production (Watson *et al.*, 1984) by cyclic AMP. In the case of thrombin-induced responses, cyclic AMP may affect G protein/receptor interactions (Knight and Scrutton, 1984), and there is evidence that it prevents receptor-induced dissociation of G-protein subunits (Halenda *et al.*, 1986) and/or binding of thrombin to its receptors (Lerea *et al.*, 1987), thereby preventing activation of phospholipase C and subsequent Ca^{2+} mobilisation. It is possible that cAMP affects $[Ca^{2+}]_i$ by other actions, but these remain unproven.

1.4.1b Ca^{2+} influx on platelet activation

The contribution of Ca^{2+} influx to the rise of $[Ca^{2+}]_i$ can be determined by comparing the increase in $[Ca^{2+}]_i$ in the presence and absence of extracellular Ca^{2+}. The size of the maximal transient rise in $[Ca^{2+}]_i$ on stimulation with thrombin, collagen, ADP, PAF or vasopressin is markedly higher in the presence of external Ca^{2+} than in its absence (Rink *et al.*, 1982; Hallam *et al.*, 1984a,b; Hallam and Rink, 1985a; Rao *et al.*, 1985; Pollock and Rink, 1986; Sage and Rink, 1986a; Jy and Haynes, 1987). In the presence of 1mM Ca^{2+} in the external medium, optimal agonist concentrations raise the $[Ca^{2+}]_i$ from a resting level of 100nM to approximately 1-1.5μM. If the external medium contains <100nM Ca^{2+}, the agonist-stimulated increase in $[Ca^{2+}]_i$ is only 200-300nM as measured with

quin2 (Rink *et al.*, 1982) or 1 μM as measured with fura-2 (Pollock and Rink, 1986). It has been calculated that in platelets stimulated by thrombin, Ca^{2+} influx accounts for >80% of the increase in $[Ca^{2+}]_i$ (Jy and Haynes, 1987). In addition, the elevation of $[Ca^{2+}]_i$ is prolonged in the presence of extracellular Ca^{2+} (Pollock and Rink, 1986). Thus Ca^{2+} influx appears to enhance and prolong the $[Ca^{2+}]_i$ rise. Maximal stimulation of this influx usually occurs within the first 5 secs and then generally decreases rapidly, indicating the presence of mechanisms for the rapid closure of Ca^{2+} channels.

Little is known about the regulation of Ca^{2+} channels in the platelet plasma membrane. Inositol 1,3,4,5-tetrakisphosphate ($Ins(1,3,4,5)P_4$) rapidly produced in stimulated platelets by the action of a specific 3-kinase on $Ins(1,4,5)P_3$ (Connolly *et al.*, 1987) might influence Ca^{2+} influx. $Ins(1,3,4,5)P_4$ has been implicated as a second messenger for the opening of Ca^{2+} channels in sea urchin eggs (Irvine and Moor, 1986). Recently $Ins(1,4,5)P_3$ has been shown to modulate the activity of Ca^{2+} channels from the plasma membrane T-tubules of skeletal muscle (Vilven and Coronado, 1988). $Ins(1,4,5)P_3$ has also been linked to the opening of Ca^{2+} channels in a platelet plasma membrane vesicle fraction (Rengasamy and Feinberg, 1988). Phorbol esters and diacylglycerol evoke a larger aequorin signal in the presence of Ca^{2+} than in its absence (Ware *et al.*, 1985). Protein kinase C activation could thus stimulate plasma membrane Ca^{2+} channels.

The Ca^{2+} influx induced by physiological stimuli is inhibited by elevation of cAMP levels in platelets (Feinstein *et al.*, 1983; Yamanishi *et al.*, 1983) and by prior exposure of platelets to phorbol ester (MacIntyre *et al.*, 1985; Poll and Westwick, 1986). Whereas cAMP inhibits PAF-induced Ca^{2+} release and Ca^{2+} influx in parallel, phorbol esters are found to inhibit the Ca^{2+} influx less than the

Ca^{2+} release (Valone and Johnson, 1987). Therefore protein kinases A and C may control platelet Ca^{2+} channels, either directly or indirectly.

Little is known of the exact mechanism of stimulated Ca^{2+} influx into platelets during activation. Evidence from quin2-loaded cells argues against a role for voltage-gated Ca^{2+} channels (Doyle and Ruegg, 1985). Depolarisation by exposure to K^+-rich solutions does not increase $[Ca^{2+}]_i$ which would be expected if membrane potential alone controlled calcium entry (Hallam and Rink, 1985a). Replacing Na^+ with impermeable cations such as choline does not affect resting $[Ca^{2+}]_i$, nor does it prevent agonist-evoked $[Ca^{2+}]_i$ rises, arguing against Na^+-dependent depolarisation as an important link (Sage and Rink, 1986b). Similar negative results have been obtained with the ionophores valinomycin and gramicidin which respectively hyperpolarise and depolarise the membrane (Hallam and Rink, 1985a).

Measurements of platelet membrane potential with dicarbocyanine fluorescent probes indicate a transmembrane resting potential of 52-60mV, inside negative (MacIntyre and Rink, 1982; Friedhoff and Sonenberg, 1983; Greenberg-Sepersky and Simons, 1984). Only a modest depolarisation (<10mV) is measured on addition of thrombin, PAF or ADP at concentrations that produce substantial $[Ca^{2+}]_i$ transients in standard physiological saline (MacIntyre and Rink, 1982). In Na^+ substituted medium there is a small hyperpolarisation despite which, as mentioned above, $[Ca^{2+}]_i$ transients still occur (Pipili, 1985). Many studies have been made of the effects in platelets of Ca^{2+} channel antagonists that seem to bind to different sites or subgroups of Ca^{2+} channels (eg. diltiazem, verapamil, dihydropyridines). Although high concentrations can inhibit platelet responses, it has been found for thrombin and ADP that the $[Ca^{2+}]_i$ transients are remarkably resistant to these

agents (Doyle and Ruegg, 1985; Hallam and Rink, 1985a). Moreover, where blockade of agonist-induced elevation of $[Ca^{2+}]_i$ by such agents has been observed, the effects can usually be attributed to receptor antagonism (MacIntyre *et al.*, 1985). However, failure to demonstrate that these blockers suppress the increase in $[Ca^{2+}]_i$ is not, by itself, strong evidence against voltage-gated channels, as some types of channel are resistant to these agents.

There is, however, increasing evidence that the platelet surface membrane may possess receptor-operated Ca^{2+} channels. Since the gradient across the membrane *in vivo* is steep, the opening of only a few Ca^{2+} channels may be sufficient to increase the $[Ca^{2+}]_i$ to 1-2μM. Indirect evidence for the existence of such channels has come from stopped-flow fluorimetry studies of quin2 and fura-2 loaded platelets (Rink and Hallam, 1984; Hallam and Rink, 1985b; Sage *et al.*, 1989). The delay in rise of $[Ca^{2+}]_i$ following platelet stimulation with thrombin, vasopressin or PAF, has been found to increase by 50-100ms when Ca^{2+} influx is prevented by chelation of external Ca^{2+} with EGTA or by blockade with extracellular Ni^{2+} (Sage and Rink, 1987), suggesting that an influx of Ca^{2+} precedes the discharge of intracellular Ca^{2+} stores. With ADP acting as the agonist, the difference in time course of $[Ca^{2+}]_i$ rises in the presence and absence of external Ca^{2+} is much more marked than with other agonists. Further experiments using Mn^{2+} as an indicator of bivalent-cation influx in fura-2 loaded platelets have provided additional evidence for receptor-mediated Ca^{2+} entry. Monitoring the fluorescence at dual wavelengths allows the selective study of Mn^{2+} entry without interference to the signal caused by changes in $[Ca^{2+}]_i$. In such studies, ADP has been found to stimulate a rapid (<20ms delay) transient Mn^{2+} influx that clearly precedes internal Ca^{2+} discharge (Sage *et al.*, 1989). The rapidity of this ADP-evoked Mn^{2+} entry is consistent with the suggestion that ADP receptor occupancy is closely coupled to

the opening of plasma membrane Ca^{2+} channels. Thrombin stimulation has been found to evoke a sustained Mn^{2+} entry commencing after the discharge of internal Ca^{2+}, and lasting for many minutes. Thus thrombin and ADP may stimulate Ca^{2+} influx in different ways.

As described above, experiments using fluorescent probes can only provide indirect evidence for the presence of receptor-operated Ca^{2+} channels in the platelet surface membrane. Direct evidence for such channels would be the demonstration of Ca^{2+} currents through single ion channels, in the presence of agonist (Rink, 1988). Such evidence has been difficult to obtain (Rink, 1988), mainly due to the technical difficulties encountered in measuring single channel activity in platelets.

A recent report has identified single channels 30-fold selective for Ba^{2+} (a Ca^{2+} substitute in these experiments) over Na^{+} in a vesicle fraction prepared from thrombin stimulated platelets and reconstituted into planar phospholipid bilayers (Zschauer *et al.*, 1988). The conductance of the channels in symmetrical 150mM Ba^{2+} solutions was ~10pS in the concentration range reported for voltage-gated Ca^{2+} channels studied under similar conditions. The channel open and closing kinetics were not influenced by voltage or by application of 10μM nisolidipine, which is a potent dihydropyridine antagonist of 'L-type' voltage-gated channels. However, the membrane fraction used in these experiments, although certainly containing surface membrane elements, was not highly purified, and it cannot be excluded that the channel activity may have originated from contaminating intracellular membranes. Further comments on this experimental work are made in chapter 4, where attempts to prepare a membrane vesicle fraction from thrombin-stimulated platelets and repeat the experiments are reported.

The first convincing report of agonist-evoked single channel activity in the platelet surface membrane has come from experiments in which platelets have been successfully patch-clamped (Mahaut-Smith *et al.*, 1989). With Ca^{2+}-containing solutions in the patch pipette, and in the absence of ADP, few channel openings (less than 5 per minute) were detected in the platelet membrane patches. After addition of ADP (40μM) to the pipette solution, inward currents of up to 10 channel openings per second were observed at applied voltages (V_p) of -20mV or more positive. Slope conductance at V_p +80mV was approximately 20pS, and channel open probability displayed only weak voltage dependence. Channel activity decayed to control levels within 30 sec-2 min from seal formation, which is consistent with the phasic nature of ADP-dependent $[Ca^{2+}]_i$ elevation. In both control and ADP-stimulated conditions, the current recorded during many individual channel openings often sloped towards the baseline, suggesting that the channel openings in the membrane patch were affecting the potential across the rest of the platelet (Mahaut-Smith, 1989 - personal communication). This implies that platelets normally have a low membrane conductance and that channels were activated only in the membrane patch. These channels may be the pathway by which Ca^{2+} enters the cytosol from the extracellular fluid following stimulation by ADP.

1.4.2 Na^+ and K^+flux across platelet membranes

Unstimulated platelets maintain a large transmembrane gradient of Na^+ and K^+ (Moake *et al.*, 1970), have a negative membrane potential and a K^+-selective membrane permeability (MacIntyre and Rink, 1982; Pipili, 1985) similar to those in most other cells.

During the course of platelet activation, altered fluxes of Na^+ (Feinberg *et al.*, 1977) and K^+ (Buckingham and Maynert, 1964; Zieve *et al.*, 1964) have been reported. Feinberg *et al.* (1977) observed a rapid influx of external Na^+(measured by the use of $^{22}Na^+$) after ADP aggregation which reached a peak at 60 sec and diminished towards control levels at 360 sec. Under the same experimental conditions no change in the level of $^{36}Cl^-$ was observed. Similar observations were made earlier by Born (1970) and by Feinberg *et al.* (1974) who also reported that ADP activation was not accompanied by an increase in platelet volume. Ouabain, which inhibits influx of K^+ into platelets (Gorstein *et al.*, 1967; Cooley and Cohen, 1967), caused a rapid increase in $[Na^+]_i$, probably at the expense of the decrease in $[K^+]_i$. A similar effect was seen with ADP; ie. an increase in $[Na^+]_i$ and a decrease in $[K^+]_i$. Sandler *et al.* (1980) also reported a rise in $[Na^+]_i$ on ADP application and suggested that the nucleotide increases the permeability to Na^+. They extended these studies using other agonists and by blocking the aggregation during ADP stimulation. When platelets were activated by ADP under conditions where the aggregation was inhibited (eg. lack of Ca^{2+} in the external medium), the induction of shape change was followed by a movement of Na^+ into the cell. When the shape change was inhibited (eg. by pretreatment of platelets with PGE_1), the Na^+ uptake was also blocked. As stated previously, ADP also induces an influx of Ca^{2+} (Hallam and Rink, 1985b). Both of these types of influx could depolarise the membrane, but this effect may be partially counterbalanced by an efflux of K^+ via a voltage-gated channel which has been identified in patch-clamped platelets (Maruyama, 1987).

Maruyama (1987) applied whole cell and cell-attached patch clamp variations to unstimulated platelets and identified a voltage and time-dependent K^+ current. On depolarisation the K^+ current was activated with a sigmoid time course, reaching a

peak, followed by inactivation. No inward currents were found when most of the K^+ current was blocked with quinine. At the platelet resting membrane potential, inactivation of the K^+ current was incomplete (approximately 50%) indicating that this current is capable of operating in response to any event which may depolarise the membrane, tending to stabilise the membrane potential. It has been reported that thrombin causes dose-dependent membrane depolarisation (Horne *et al.*, 1981) and a marked net loss of K^+ from platelets (Zieve *et al.*, 1964). This may be explained by cationic influx evoking K^+ efflux, leading to loss of cellular K^+ due to the operation of voltage-gated K^+ current.

The single channel recordings of Maruyama (1987) revealed a voltage gated K^+ channel resembling the delayed rectifier K^+ channel of nerve, muscle and T-lymphocyte (Conti *et al.*, 1975; Conti and Neher, 1980; Fukushima *et al.*, 1984; Cahalan *et al.*, 1985). A conductance of 9pS was measured for the channel with 145mM KCl in the pipette solution, with an estimated 325 channels present per platelet. No reference is made in these experimental findings to the existence of a Cl^- channel in platelets and further reference is made to this in the discussion of single channel experiments carried out on the surface membrane in this thesis (section 4.13).

1.5 ION CHANNELS AND THEIR RECONSTITUTION INTO PLANAR BILAYERS

1.5.1 What are ion channels?

The ion permeability of biological membranes is not a diffuse property of the whole membrane, but is localised in specialised membrane-spanning aqueous 'pores' known as ion channels. This is consistent with the Singer and Nicolson (1972) view that the cell membrane is a mosaic of relatively impermeable lipid bilayer regions into which proteins are inserted. These amphipathic, integral membrane channel proteins form distorted cylinders with a hydrophobic surface facing the lipid and hydrophilic surfaces lining the pore and facing the solutions on the two sides of the membrane.

The primary function of ion channels is to provide a low energy pathway for ions to cross the cell membrane. The channel proteins screen charged permeants from the low dielectric of the membrane lipid, and their pores provide aqueous (or partially hydrated) environments lined with polar residues that can favourably interact with ions to catalyse their transport. A diagrammatic representation of a working hypothesis for a channel is shown in figure 1.5.

Channels may be regarded as membrane enzymes that both catalyse and regulate ion permeation. They are capable of permitting ion transport at very high flux rates across the membrane; in the order of 10^7 ions per second (Latorre and Miller, 1983). The regulatory activity depends upon conformational changes of the protein associated with channel opening and closing (gating properties) and in modulatory effects on the gating and permeation exerted by the environment. As

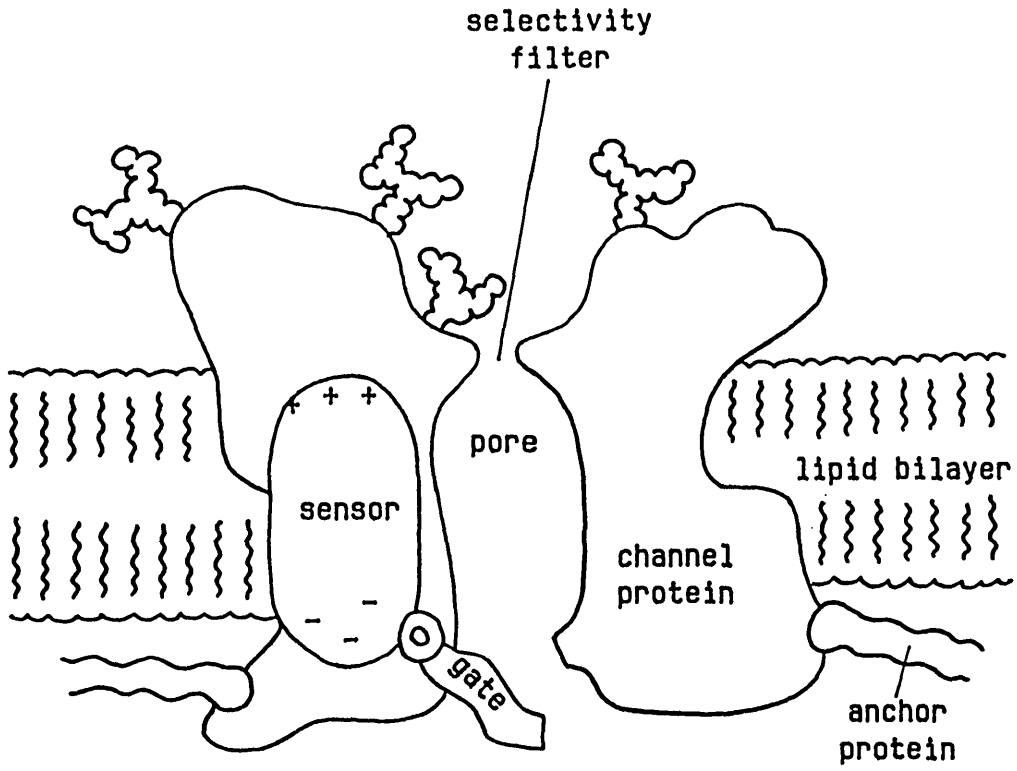


Figure 1.5

Diagrammatic representation of a working hypothesis for a channel

The channel is drawn as a transmembrane macromolecule with a hole through the centre. The external surface of the molecule is glycosylated. When open, the channel forms a water-filled pore extending fully across the membrane. The pore is much wider than an ion over most of its length and may narrow to atomic dimensions only in a short stretch, the selectivity filter. Gating requires a conformational change of the pore that moves a gate into and out of an occluding position. The probability of opening and closing are controlled by a sensor. The functional regions, selectivity filter, gate and sensor are deduced from voltage-clamp experiments but have not yet been charted by structural studies. We have yet to learn how they actually look.

for other biological catalysts, channels are often highly selective for a particular ion species; their catalytic activity saturates at high substrate concentrations (i.e. a maximum transport rate is reached), and they can be competitively inhibited by substrate analogues (ionic blockers of the pore).

Ion channels are found in the membranes of all cell types. Their known physiological functions include establishing and maintaining a resting membrane potential, shaping electrical signals, gating the flow of messenger Ca^{2+} ions, controlling cell volume, and regulating the net flow of ions across epithelial cells of secretory and resorptive tissues.

From the introduction of the high-time-resolution electrical methods of voltage clamping (Hodgkin and Huxley, 1952) to the modern application of patch-recording techniques (Hamill *et al.*, 1981), by which single channel molecules can be observed directly, electrophysiologists have been addressing questions concerning the catalytic mechanisms of these channel proteins, the conformational changes that occur during channel opening and closing, and the gross structures of the protein complexes.

1.5.2 Ion channel reconstitution into planar bilayers

The method of ion channel reconstitution, introduced by Miller and Racker (1976), provides a means by which native membrane channel proteins can be incorporated into a planar bilayer membrane, allowing the measurement of single channel fluctuations. Two methods have been developed to facilitate this transfer of membrane proteins into a planar bilayer. Firstly, they may be fused into the bilayer (Miller, 1978), made either by painting an alkane dispersion of

phospholipid on a hole in a partition (the method employed in experiments described in this thesis), or by folding two air-water interface lipid monolayers over the hole. Alternatively, crude membrane vesicles may be transferred to an air-water interface directly and from there to the end of a patch pipette (Coronado and Latorre, 1983). It is theoretically possible to reconstitute ion channels into planar bilayers from any membrane fraction consisting of ion channel-containing vesicles.

1.5.3 Advantages of the planar bilayer technique in single channel recording

One advantage of reconstitution experiments is the insertion into planar bilayers of vesicles derived from membranes not readily accessible to electrophysiological probes. Thus, for example, channels from the sarcoplasmic reticulum, T-tubule and mitochondrial outer membrane are made accessible to the experimenter (e.g. Miller, 1978; Latorre *et al.*, 1982; Schein *et al.*, 1976). Similarly, as described in this thesis, a channel from the otherwise inaccessible platelet intracellular membrane system, has been made available for investigation by the application of reconstitution techniques.

A second advantage to the reconstitution approach is that it is possible to both simplify and vary the physico-chemical environment of the single channel protein. For example, the planar bilayer technique allows the experimenter to:

(i) control and vary the conducting ions and osmotic conditions of the bathing solutions surrounding the channel protein

(ii) make additions and perfusions on both sides of the membrane during the course of an experiment

(iii) change the lipid composition of the bilayer allowing, for example, examination of the effects of membrane surface charge on the channel behaviour

Finally, reconstitution experiments can also provide an assay system for checking the functional activity of purified channel proteins. For example, the nicotinic acetylcholine receptor has been purified and then reconstituted allowing determination of the minimal functional unit and a detailed characterisation of the behaviour of the purified AChR protein (Tank *et al.*, 1983; Montal *et al.*, 1983).

Probing ion channel behaviour in 'model' bilayer membranes offers the opportunity to investigate questions concerning molecular mechanisms and molecular structure which cannot be answered by studying the channel protein in its complex cellular environment.

A limitation of this model system, however, is that unqualified conclusions about the exact functioning of the protein *in vivo* cannot be made. The behaviour of the channel following reconstitution and its behaviour within its native membrane environment may not be directly comparable. Additionally, the membrane vesicle isolation procedure and the fusion process may preselect for a particular subpopulation of channel proteins. The experimenter must therefore accept that a particular ion channel protein of interest may not necessarily yield itself readily to reconstitution into planar bilayers.

1.5.4 The painted planar bilayer membrane

The success of the ion channel reconstitution studies described in this thesis has depended upon the formation and maintenance of a stable planar phospholipid bilayer. The practical details of bilayer formation and the apparatus required are described in section 2.4. Here an introduction to the composition and properties of the lipid bilayer itself is presented.

In the painted planar bilayer system, a bilayer is formed by spreading a 'forming solution' across a small hole in a hydrophobic partition separating two aqueous phases (Mueller *et al.*, 1962a). The forming solution consists of surface active lipids dispersed in a non-polar solvent such as *n*-decane. The lipid in the solvent tends to form large micelles orientated so as to shield the polar regions of the lipids from the non-polar solvent. Planar bilayers cannot be formed unless these micellar aggregates are present; thus the lipid concentrations used must exceed the critical micelle concentration.

The film created in this way is initially several micrometers thick, but it thins spontaneously to the planar bilayer state (see figure 1.6). The resultant occlusion of the hole is composed of the lipid film surrounded by an annulus, or torus, of the bulk forming solution. These two phases of the system tend towards chemical equilibrium with one another. The lipid film and annulus are, of course, in an aqueous environment, so that the phase behaviour of the lipid-water-hydrocarbon bulk phase determines the state of the bilayer.

The lipid bilayer thins under the influence of various driving forces. The major force initially is the Plateau-Gibbs border suction, which arises from the curvature

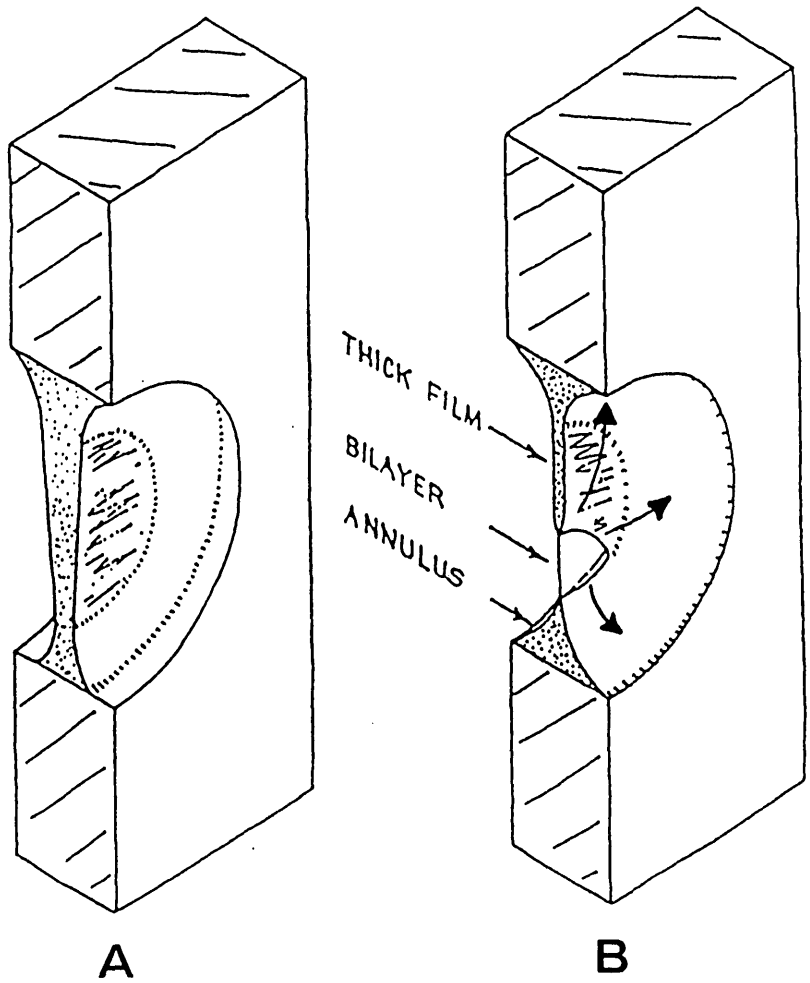


Figure 1.6

Formation of a planar lipid bilayer

The formation of a planar lipid bilayer from lipids dispersed in alkane solvent by the painting method of Mueller *et al.*, (1962a). The lipid dispersion is applied beneath aqueous solution across a hole in a hydrophobic partition (A). Once painted, the bulk solution tends to flow from the thick film into the border causing the film to thin (see arrows, **B**). The bilayer usually forms at the lower margin of the film (**B**) and spreads rapidly over the surface. The resultant structure comprises a lipid bilayer surrounded by an annulus of the bulk forming solution [from White *et al.*, 1976].

of the annulus (note in figure 1.6 and 2.3, the position of the aperture at the centre of a concave section in the cup wall). The bulk solution tends to flow from the flat film into the border, causing the film to thin. As the film approaches a thickness of a few angstroms, a second driving force arises; the London-van der Waals attraction between the aqueous phases separated by the thin film. This is the major force tending to thin the membrane at the equilibrium bilayer thickness. The bilayer usually appears first at the lower margin of the film and spreads rapidly over the surface (White, 1986).

For stability, the London-van der Waals forces must be opposed by another set of forces. When the apposing surfaces of the thicker film meet during thinning, the acyl chains on the lipid tend to interdigitate and exclude any solvent molecules trapped in the film. However, this lipid/solvent 'separation' tends to reduce the entropy of the bilayer and consequently raise the free energy of the system. This gives rise to an opposing force termed the 'steric repulsive' force (White, 1986). The bilayer therefore rests in a local free energy well and stabilises.

The chemical potentials of the lipid and solvent in the bilayer must be equal to the annular bulk phase when the film reaches its local equilibrium. Since the annulus has a mass at least a million times that of the bilayer, the solvent in the bilayer tends to reach equilibrium with the annulus. Therefore there exists an osmotic pressure on the solvent in the annulus tending to drive solvent into the bilayer opposed by the van der Waals force which tends to compress the bilayer (White, 1980). Thus the bilayers' 'equilibrium' is most properly described as an osmotic equilibrium.

Bilayers formed by the painting technique may remain stable for several hours and can withstand perturbation of the surrounding aqueous phases caused either by stirring or by perfusion exchange of the solutions.

1.5.5 Ion channel reconstitution by fusion

Since the first descriptions of the fusion of ion channel-containing vesicles with preformed planar phospholipid bilayers (Miller and Racker, 1976; Miller *et al.*, 1976) many ion channels have been reconstituted using this method (see Hanke, 1986); most usually into decane-containing painted bilayers. Although little is known about the molecular mechanism or physical basis for fusion, a number of conditions have been reported which are an absolute requirement for fusion, or at least increase the probability that fusion occurs.

Two steps have been proposed in the fusion process:

(i) vesicle-planar membrane attachment (the 'pre-fusion' state)

(ii) osmotically driven swelling of the attached vesicles, with subsequent rupture of vesicular and planar membranes in the region of contact leading to fusion.

A diagram depicting the steps in the fusion process is shown in figure 1.7.

1.5.5a Formation of the pre-fusion state

The pre-fusion state consists of a tight adsorption of vesicles to the planar bilayer. This state has been directly observed using fluorescent dye-filled vesicles in a

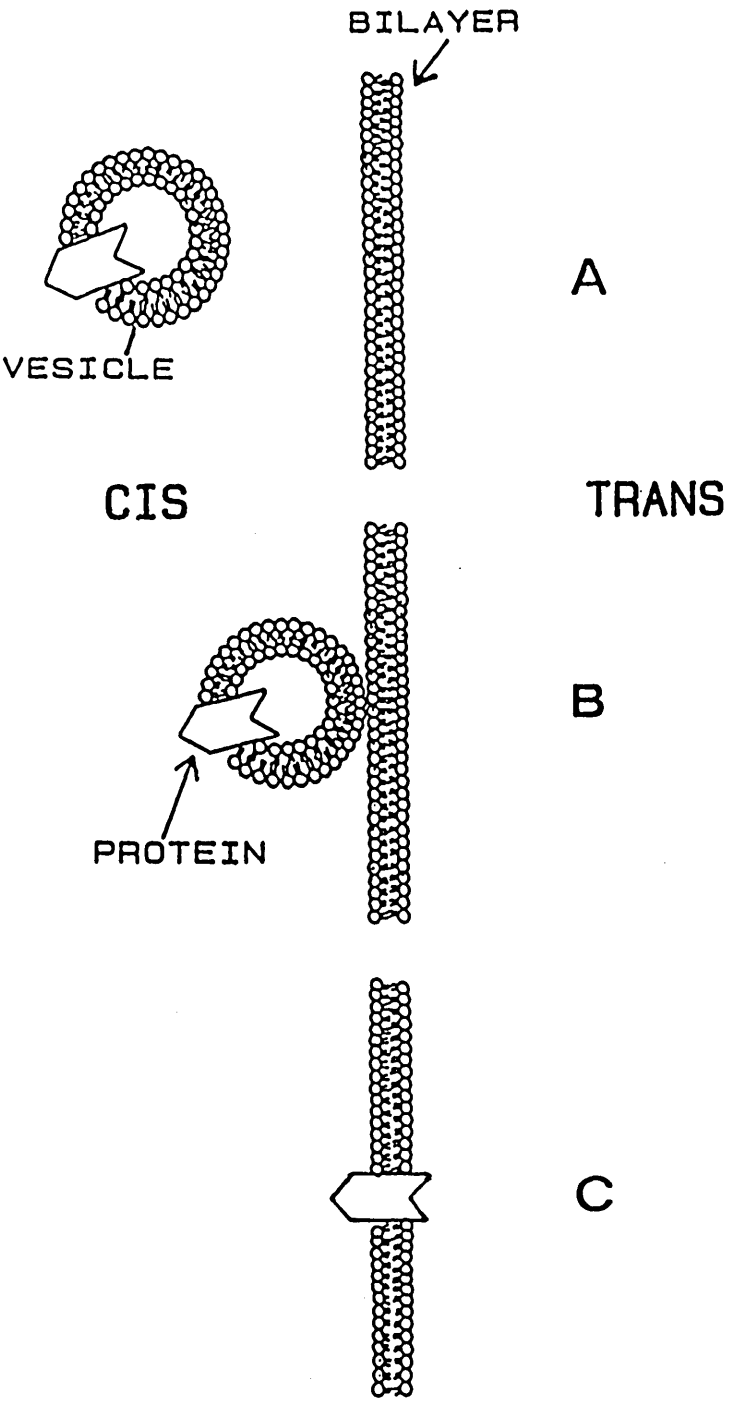


Figure 1.7

Diagrammatic representation of the steps in the fusion process

A: First the vesicle and planar bilayer co-exist well separated.

B: In the pre-fusion state, tight adsorption of the vesicle and bilayer occurs.

C: Fusion occurs and the entire contents of the vesicle membrane, including any channel proteins, are incorporated into the planar bilayer.

video fluorimeter (Niles and Cohen, 1987; Perin and MacDonald, 1989). Calcein-loaded vesicles were allowed to settle on a preformed bilayer and appeared as bright circular profiles on the planar membrane. Vesicles were seen to adsorb directly to the bilayer rather than first attaching to an auxiliary structure, such as the annulus, and then diffusing into the membrane. In bilayers containing anionic phospholipids, the number of vesicles bound in the prefusion state depended on the calcium concentration in the *cis* compartment (the side containing the vesicles). This observation is similar to the findings in previous studies using negatively charged bilayers where the presence of millimolar amounts of calcium in the aqueous solution on the *cis* side was found to increase the probability of fusion (Miller and Racker, 1976; Miller *et al.*, 1976; Miller, 1978; Latorre *et al.*, 1982; Akabas *et al.*, 1984; Cohen *et al.*, 1984).

According to standard models of divalent cation-mediated interactions between phospholipid bilayers (Hauser *et al.*, 1975; Breisblatt and Ohki, 1976; Papahadjopoulos *et al.*, 1977; Portis *et al.*, 1979), each divalent cation bridges two monovalent anionic moieties on the phospholipid head groups of the two opposing monolayers. This divalent cation binding dehydrates the headgroups and leads to a phase separation. The phase boundaries created may be important in forming fusogenic spots when the water between vesicle and bilayer membrane has been removed.

Formation of the pre-fusion state is also assisted by stirring the solution in the vesicle-containing compartment (usually the *cis* chamber). Stirring effectively increases the probability that ion channel containing vesicles are delivered to the planar bilayer and that vesicle-planar membrane contact occurs leading to pre-fusion adhesion.

1.5.5b Osmotically-driven fusion

As described earlier, the addition of calcium to anionic planar bilayers promotes adhesion, but not fusion. The main requirement for fusion (whether bilayers are charged or not) is the establishment of osmotic conditions leading to the swelling of the membrane vesicles (Miller and Racker, 1976; Miller *et al.*, 1976; Cohen *et al.*, 1980; Zimmerberg *et al.*, 1980; Cohen *et al.*, 1982; Akabas *et al.*, 1984; Niles and Cohen, 1987; Cohen *et al.*, 1989; Perin and MacDonald, 1989). Thus the *cis* side (the side containing the vesicles) must be hyperosmotic with respect to the opposite, *trans*, side. It is not the water flow across the planar bilayer membrane *per se*, but rather the net movement of water into the vesicle that is required for fusion. This has been directly demonstrated by Cohen *et al.*, (1982); Akabas *et al.*, (1984) and Niles and Cohen, (1987). In the absence of an osmotic gradient across the planar membrane, fusion could be induced by osmotic swelling of the pre-fusion attached vesicles.

The presence of channels in the vesicle membranes is necessary to allow net swelling of the vesicles. Niles and Cohen (1987) reported that in the absence of the channel-forming antibiotic, nystatin, in their experiments, vesicles did not osmotically rupture either with an osmotic gradient across the bilayer, or with a gradient across the vesicle membrane. When nystatin was added to the *cis* compartment, channels formed in the vesicular membrane, and swelling and fusion were observed.

The ability of the osmoticant (the solute used to establish the osmotic gradient) to promote fusion depends on both its permeability through the bare lipid bilayer as well as its permeability through the channel by which it enters the vesicle interior

(Cohen *et al.*, 1989). In the experiments reported in this thesis, the solution in the *cis* compartment was generally made hyperosmotic by adding KCl. After an initial shrinkage, the ensuing flow of water from the *trans* to *cis* compartments and into the vesicles adhering to the planar membrane causes swelling and the generation of an intravesicular pressure which drives fusion (Niles *et al.*, 1989).

The details of the final step in the fusion process remain to be elucidated. However, it has been suggested that the osmotic entry of water into the vesicles causes some stretching of the vesicular and planar membranes in their region of tight adhesion. On account of the sharp curvature and possible dehydrated state in the area of contact, it seems likely that vesicle rupture may preferentially occur at this point (Akabas *et al.*, 1984).

Chapter 2

METHODS

2.1 INTRODUCTION

The experimental methods used are described in this chapter under the following headings:

2.2 Preparation of highly purified platelet surface and intracellular membranes.

2.3 Biochemical characterisation of platelet surface and intracellular membrane fractions.

2.4 Planar bilayer methods.

2.5 Analysis of single channel data.

The sources of chemicals used in the experimental procedures, unless specified in the text, are listed in Appendix A.

2.2 PREPARATION OF HIGHLY PURIFIED PLATELET SURFACE AND INTRACELLULAR MEMBRANES

The method for preparing highly purified human platelet membrane fractions was essentially as originally reported by Menashi *et al.* (1981) and subsequently modified by Authi and Crawford (1985).

2.2.1 Platelet isolation and neuraminidase treatment.

Human platelets were isolated by a differential-centrifugation procedure from fresh buffy-coat residue packs supplied by the National Blood Transfusion Service Laboratories, Tooting, London SW17 and Brentwood, Essex, UK. Typically 5-8

packs were used in each preparation and laboratory processing commenced within 3-4 hours of blood donation. Polycarbonate tubes, beakers and pipettes were used throughout to prevent platelet contact activation.

The buffy coats were separated into 100ml tubes according to blood group and centrifuged at 200 x g for 20 mins at 25°C and the platelet rich plasma (PRP) retained. The remaining red blood cells were diluted into a large volume of industrial sodium hypochlorite ('chloros', Hays Chemicals Ltd, Leeds) before safe disposal. The PRP was pH adjusted to 6.4 with 0.3M citric acid. The platelets were then sedimented at 1,200 x g for 20 mins at 25°C. The resultant pellet was resuspended in 20mls of 10mM HEPES buffer, pH 6.2, containing 152mM NaCl, 4.17mM KCl, 3mM EDTA. The platelet suspension was equilibrated in a water bath at 37°C for 10 mins before treatment with neuraminidase (*Clostridium perfringens*, Sigma, Grade X, affinity purified). One unit of neuraminidase (i.e. 0.05 unit/ml platelet suspension) was added dropwise whilst mixing and incubation continued at 37°C for a further 20 mins, swirling the suspension occasionally.

Treatment with neuraminidase at the whole cell level lowers the electronegativity of the surface membrane by removal of sialic acid groups. This reduces its electrophoretic mobility and improves the resolution of the two membrane species in the electrophoresis chamber (see section 1.2.2). In preparations where a mixed membrane fraction from cells not treated with neuraminidase was required, the incubation step was omitted and platelets were washed twice as described below prior to sonication.

At the end of the neuraminidase incubation period the suspension was rapidly diluted 1:4 with 10mM HEPES buffer (washing buffer), pH 7.2, containing

152mM NaCl, 4.17mM KCl, 3mM EDTA and centrifuged at 1,200 x g for 1 min at 25^{o}C to remove any remaining red blood cells. The platelets were then washed twice by resuspension in washing buffer followed by centrifugation for 20 mins at 1,200 x g, 25^{o}C, each time.

2.2.2 Platelet sonication and separation of mixed membrane fraction.

From this stage onwards in the preparation, all samples were kept on ice. The final pellet of washed platelets was resuspended in ice-cold 10mM HEPES buffer (sonication buffer), pH 7.2, containing 0.3M sorbitol at a ratio of 4ml buffer/g wet weight of cells (usually 20ml). A protease inhibitor cocktail containing 10μg pepstatin A/ml, 0.2 Units aprotonin/ml and 400μM phenylmethane-sulphonyl fluoride was added to the cell suspension. The sample was then sonicated in 10ml aliquots at setting 6 (at maximum tuning) for 10 secs at 4^{o}C using a Dawes sonicator with a 4mm diameter probe (in a cold room). The sonicates were combined and centrifuged at 2,000 x g for 15 mins at 4^{o}C. The supernatant was removed and kept in a separate tube on ice and the pellet of unbroken cells and large cell fragments was resuspended in 20ml sonication buffer (with protease inhibitors). The sonication and centrifugation steps were carried out three times in all. The resultant supernatants were pooled and layered onto three 40ml linear sorbitol gradients prepared from 1.0 and 3.5M sorbitol solutions, pH 7.2, containing 10mM HEPES and centrifuged at 42,000 x g in a swing out rotor for 90 mins at 4^{o}C.

A mixed membrane (MM) fraction, containing vesicles of both surface and intracellular membrane origin, was located in the low density region of the gradient as shown in figure 2.1. The upper cytosol fraction was carefully removed

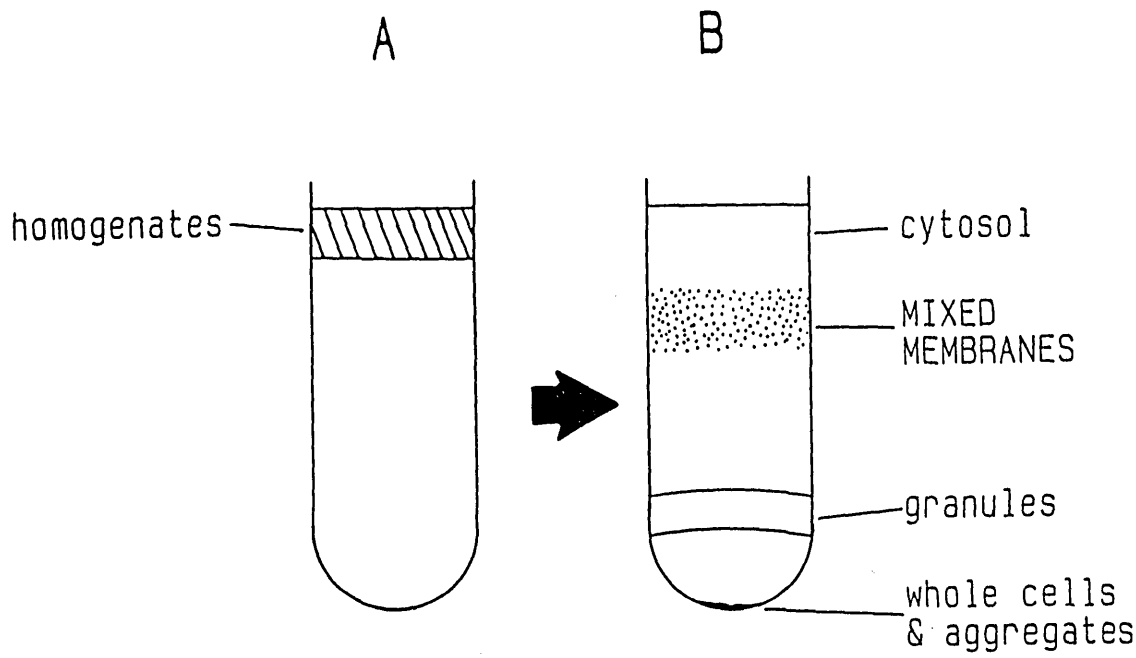


Figure 2.1

Density gradient sedimentation of platelet mixed membrane fraction

The homogenates from the sonication steps are loaded onto a linear sorbitol gradient as shown in A (1-3.5M). Following centrifugation in a swing-out rotor at 42,000 x g for 90 mins at 4^{o}C, a mixed membrane fraction is located in the upper of two discrete particulate zones as shown in B.

and discarded. The MM fraction was then collected and concentrated by centrifugation at 90,000 x g for 80 min at 4^{o}C. Membranes were either (i) resuspended in 0.4M sucrose, 5mM HEPES/Tris, pH 7.2, at a concentration of approximately 1-2 mg protein/ml for subsequent use in reconstitution experiments, or (ii) resuspended in electrophoresis chamber buffer (10mM triethanolamine, 0.4M sorbitol, adjusted first to pH 6.8 with acetic acid and then to pH 7.2 with NaOH) to a concentration of approximately 3-4 mg protein/ml. The latter MM fraction was applied to the continuous flow electrophoresis chamber.

2.2.3 Membrane separation by continuous flow electrophoresis

Membrane separation was carried out using a Bender Hobein Elphor VAP electrophoresis unit (Bender and Hobein, Munich, Germany). Model no.5 was used in the initial membrane preparations followed by the improved model no.22 in later experiments. The latter unit offered superior temperature and electrical stability suitable for the lengthy operating times necessary for improved membrane separation and yield. The general principles of high-voltage continuous flow electrophoresis and a diagram of the apparatus have been presented in section 1.3.1.

The electrophoresis unit consisted of a vertical glass chamber, approximately 60cm high, 10cm wide and 0.8mm deep. The rear plate was silvered and in contact with a cooling system. At the top of the chamber, an inlet port was connected to a reservoir of buffer via a bubble trap. At the base of the unit the buffer/sample streams emerged to give 90 separate fractions. The rate of buffer flow was controlled by a peristaltic pump through which the 90 outlet tubes passed.

On either side of the chamber were two ion-exchange strips (a cation- and anion-exchange resin on the positive and negative sides respectively). Behind these strips were two platinum electrodes. Electrical continuity between the strips and the electrodes was maintained by an electrode buffer (100mM triethanolamine, pH 7.2) which was circulated over and between each electrode from a reservoir via a pump.

The MM sample was transferred to an oscillating syringe at the top of the unit. A second syringe, whose piston could be advanced by a fine-pitched worm gear, was connected to the sample syringe via a column of water and served to inject the sample at a controlled rate into the vertically flowing chamber buffer film through an inlet port on the cathodal side of the chamber.

2.2.3a Priming of the electrophoresis unit before use

The electrophoresis chamber unit was prepared on the day prior to use as follows. A mild detergent solution was infused into the chamber from the base, taking care to exclude any air bubbles. A reservoir of detergent was allowed to run down the chamber under gravity for approximately 15 mins, followed by double distilled water for a further 15 mins. 50mls of 3% (w/v) bovine serum albumin were then infused and the chamber ports clamped shut and left overnight. Two hours prior to use on the following day, the chamber was rinsed by flushing through approximately 5 litres of double distilled water. This was then replaced with electrophoresis chamber buffer (of composition described in section 2.2.2) and fresh electrode buffer introduced into the electrode reservoirs.

2.2.3b Continuous flow electrophoresis running conditions

Once the electrophoresis chamber was primed, the unit was switched on allowing the cooling circuits to stabilise at 6°C. High voltage conditions were then established by slowly increasing the current until 80mA was reached. The initial voltage reading at this current was noted and further readings taken at 10 min intervals until the voltage stabilised. The mixed membrane sample was then introduced into the chamber at a controlled injection rate via the inlet port and the run commenced. The peristaltic pump controlling the chamber buffer flow rate was adjusted to a value slightly faster than the sample injection rate. The following operating conditions were found to be the most appropriate for platelet membrane separation.

Voltage:	1,500 - 1,600V
Current:	80mA
Temperature:	6°C
MM sample injection rate:	2 ml/hour
Chamber buffer flow rate:	2.5 ml/hour/fraction

Fractions were collected at the base of the unit in cooled glass tubes. In the VAP 22 electrophoresis unit, the anode was on the right hand side of the chamber. Accordingly, the higher the fraction number (1-90) in which a particular fraction eluted, the closer its position to the anode, hence the greater its zeta potential.

Typically a run lasted for 6-10 hours depending on the initial volume of MM sample and the maintenance of stable current and temperature conditions during the procedure. A drop in voltage of up to 300V was commonly experienced during

the course of a long electrophoresis run. This introduced no alteration in relative deflection of the membrane sample peaks.

2.2.3c Collection of purified platelet membrane fractions

The absorbance at 280nm of each fraction collected was measured using a spectrophotometer. A typical electrophoresis separation profile is shown in figure 2.2. The more electronegative peak (adjacent to the anode) represents the intracellular membranes (IM) and the less electronegative peak (adjacent to the cathode) represents surface membrane (SM) vesicles (modified by the neuraminidase treatment). The IM and SM fractions were separately pooled and centrifuged at 90,000 x g for 60 mins at $4^{o}C$ onto a cushion of 3.5M sorbitol. The two vesicle fractions were collected and suspended in 0.4M sucrose, 5mM HEPES/Tris, pH 7.2, to a protein concentration of 1-4 mg/ml. Aliquots were either used immediately, in the case of biochemical assays, or 'snap' frozen in liquid nitrogen and stored at $-80^{o}C$ for use in reconstitution experiments.

2.2.4 Isolation of a subpopulation of the intracellular membrane by oxalate loading

Applying the analogy of the platelet IM to the sarcoplasmic reticulum (SR) of muscle, a method to oxalate load and separate a subpopulation of the IM fraction was applied. This was modified from the procedure used by Jones and Cala (1981) and Tomlins *et al.* (1984) to harvest the ryanodine insensitive fraction of cardiac muscle SR.

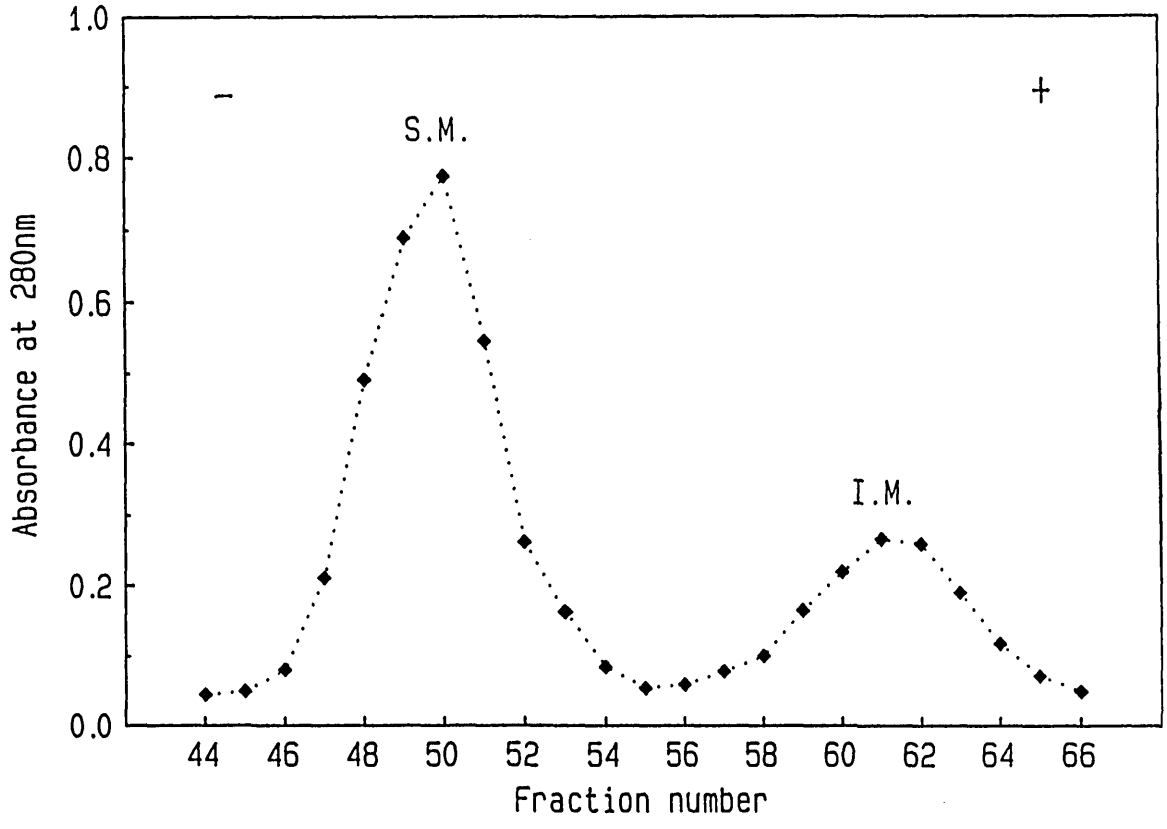


Figure 2.2

Typical continuous flow electrophoresis profile

The absorbance of each fraction at 280nm gives a bimodal distribution. The more electronegative peak represents the intracellular membrane (IM), and the less electronegative peak represents the surface membrane (SM), modified by neuraminidase treatment. For this profile, sample tubes 47-52 (SM) and 58-64 (IM) were separately pooled.

For oxalate loading, the IM vesicles were identified in the continuous flow electrophoresis profile and pooled as described in section 2.2.3. They were then suspended in 30ml of a 'calcium'-oxalate loading medium containing 50mM histidine, 100mM KCl, 65mM $MgCl_2$, 60mM NaATP, 25mM Tris/EGTA, 20mM $CaCl_2$, 5mM Tris/oxalate, pH 7.1. After 5 mins incubation at 37°C, a further 5mM Tris/oxalate was added. The reaction was terminated after a total of 20 mins by placing the mixture on ice. Vesicles were then collected by sedimentation at 105,000 x g for 30 mins. The vesicle pellet was resuspended in 8mls of 0.25M sucrose, 300mM KCl, 50mM NaPPi, 100mM Tris, pH 7.2. The suspension was layered onto 8mls of 1.5M sucrose, 300mM KCl, 50mM NaPPi, 100mM Tris, pH 7.2 and centrifuged in a swing-out rotor at 100,000 x g for 2 hours at 4°C. Unloaded IM located at the 0.25M:1.5M sucrose interface whilst oxalate loaded IM vesicles formed a pellet at the base of the tube. The two fractions were collected and suspended in 0.4M sucrose, 5mM HEPES/Tris, pH 7.2; each to a concentration of approximately 0.5-1.0 mg protein/ml. Aliquots were 'snap' frozen in liquid nitrogen and stored at -80°C for use in reconstitution experiments.

The same oxalate loading method was applied to mixed membrane fractions (untreated with neuraminidase) in an attempt to isolate the same IM subpopulation without use of continuous flow electrophoresis.

2.2.5 Protein estimation of membrane fractions

Protein estimations were carried out using a modification of the method devised by Lowry *et al.*, (1951) as described by Markwell *et al.* (1979).

500μl samples of the membrane fractions were solubilised with 50μl of 1% (w/v) deoxycholic acid and then precipitated with 1ml of 10% (w/v) trichloroacetic acid. Samples were centrifuged at 13,000 rpm for 5 mins in a benchtop Eppendorf centrifuge and the supernatant discarded. Pellets were redissolved in 1ml of a solution of the following composition: 200mM Na_2CO_3, 100mM NaOH, 7mM NaTartrate and 1% (w/v) SDS, to which 1% (v/v) of an aqueous solution of 4% (w/v) $CuSO_4.5H_2O$ had been added immediately prior to use. 100μl of stock Folin and Ciocalteu's phenol reagent was then added and the mixture immediately vortex-mixed. The optical density at 750nm was measured after 30 mins using a spectrophotometer.

For calibration curves, samples of bovine serum albumin were simultaneously assayed as described above (BSA samples of 5, 10, 20, 40 and 50 μg/ml were generally used for calibration purposes). A linear relationship between optical density and protein concentration was found over the range 5-50μg protein/ml. The protein concentration of each platelet membrane sample was estimated from the averge of three dilutions within the limits of the standard curve. Assays were carried out in triplicate at room temperature.

2.3 BIOCHEMICAL CHARACTERISATION OF PLATELET SURFACE AND INTRACELLULAR MEMBRANE FRACTIONS

The purified surface and intracellular membrane fractions prepared by the methods described in section 2.2 have been extensively characterised by Menashi *et al.* (1981), Lagarde *et al.* (1981;1982) and Hack *et al.* (1986) in terms of polypeptide, lipid, phospholipid and enzyme composition.

The purity and functional integrity of membrane vesicles prepared for this experimental work were monitored by the following methods:

1. SDS polyacrylamide gel electrophoresis
2. Antimycin-insensitive NADH cytochrome *c* reductase enzyme assay
3. Assay for Ca^{2+} uptake by IM vesicles
4. Ins(1,4,5)P_3-induced release of sequestered Ca^{2+} from IM vesicles

2.3.1 SDS-polyacrylamide gel electrophoresis

The method used was that described by Laemmli (1970). Membrane samples were solubilised in 0.125M Tris/HCl buffer, pH 6.8, 10% (v/v) ß-mercaptoethanol, 4% (w/v) SDS, 20% (v/v) glycerol, 0.0025% (w/v) bromophenol blue. Denaturing of the sample proteins was achieved by boiling at 100^{o}C for 7 mins.

Gels were prepared using a Bio-Rad Mini PROTEAN II dual slab cell (Bio-Rad, Richmond, CA, USA). Resolving gels of 9% (w/v) and stacking gels of 4.5% (w/v) acrylamide were prepared from a stock solution of 30% (w/v) acrylamide and 0.8% (w/v) of N,N'-*bis*-methylene acrylamide. The stacking gel contained 0.125M

Tris/HCl, pH 6.8 and 0.1% (w/v) SDS, whilst the resolving gel contained 0.38M Tris/HCl, pH 8.8 and 0.1% (w/v) SDS. The gels were polymerised chemically by the addition of 0.001% (v/v) tetramethylethylenediamine (TEMED) and 0.05% (w/v) ammonium persulphate.

The electrode buffer consisted of 0.025M Tris, 0.192M glycine and 0.1% (w/v) SDS, pH 8.3. 7-12μl of the membrane samples and molecular weight standards were transferred into wells prepared in the gels. The following molecular weight markers were used: 94K: phosphorylase b; 67K: bovine serum albumin; 43K: ovalbumin; 30K: carbonic anhydrase. Electrophoresis was carried out with a current of 30mA per gel until the bromophenol blue marker reached the base of the gel (about 40 mins).

The separated proteins were stained and fixed in the gel using a solution of 0.2% (w/v) Coomassie brilliant blue, 45% (v/v) methanol and 15% (v/v) acetic acid [in distilled water] for 30 mins. Destaining was carried out in 10% (v/v) acetic acid and 10% (v/v) methanol [in distilled water] until the gel backgrounds were clear. Gels were generally dried onto filter paper using a commercial gel drier (Model 583, Bio-Rad, Richmond, CA, USA).

2.3.2 NADH-cytochrome *c* reductase enzyme assay

Antimycin-insensitive NADH-cytochrome *c* reductase (EC1.6.99.3) enzyme activity was measured essentially as described by Tolbert (1974). The following reaction mixture was prepared in a spectrophotometer cuvette (final volume 1ml): 0.2M KH_2PO_4 buffer, pH 7.0, 0.08M oxidised cytochrome *c*, 2mM KCN (to inhibit any cytochrome *c* oxidase), 10μl of antimycin A (2mg/ml in ethanol) and the

membrane sample of known protein concentration. After establishing the NADH-independent rate, the reaction was initiated with 0.85mM NADH. The rate of change in optical density of the reaction mixture was followed for 10-15 mins using a UV/VIS SP8-400 spectrophotometer (Pye Unicam Ltd., Cambridge, UK) set at 550nm.

According to the **Beer Lambert Law** describing the absorbance (or optical density), A, of a compound:

$$A = e.c.l \qquad \text{(equation 4)}$$

where:

e is the extinction coefficient of the compound at the particular wavelength of the incident radiation

c is the concentration of the compound

l is the path length the incident radiation travels

Based on an extinction coefficient of 21.1 $mM^{-1}cm^{-1}$ for cytochrome *c* at 550nm (Van Gelder and Slater, 1962) and a path length of 1cm, a change in OD of 1.0 was equivalent to 47.4 nmoles.

Samples of MM, SM and IM of various protein concentrations were assayed.

2.3.3 Assay for calcium uptake by intracellular membrane vesicles

ATP-dependent calcium uptake by IM vesicles was assayed by the method described by Menashi *et al.* (1984). The incubation mixture consisted of: 120mM KCl, 5mM $MgCl_2$, 2mM ATP, 20mM Tris/HCl, pH 7.2 and approximately 1μCi of

$^{45}Ca^{2+}$ (specific activity: 10-40mCi/mg of Ca^{2+}). Ca^{2+} concentrations were controlled by Ca^{2+}-EGTA buffers made up as described by Portzehl *et al.*, (1964) and Durham (1983). At 50μM EGTA, the calculated free Ca^{2+} was 3μM. An aliquot of intracellular membrane vesicle suspension (between 30-50μg membrane protein), was added to the assay mixture (final volume 0.5ml) to start the reaction and incubation commenced at room temperature (21-22^{o}C). Separate control assays were also carried out in the absence of ATP and with surface membrane vesicles. At 3-5 min intervals over 25 mins, 0.45ml of the mixture was removed and rapidly filtered through a Millipore membrane filter, type GS, 0.45μm pore size (presoaked in washing buffer). Three 10ml aliquots of ice-cold washing buffer were then flushed through the filter membrane to wash the vesicles. The washing buffer contained: 120mM KCl, 5mM $MgCl_2$, 20mM Tris/HCl, pH 7.2 and 50μM unlabelled $CaCl_2$. The filters were then air dried, transferred to scintillation vials and 10mls of Scintran Cocktail T scintillant (BDH Chemicals, U.K.) added. Radioactivity was determined in a liquid scintillation counter (Beckman LS 5801; Beckman Instruments, CA, U.S.A) equipped with automatic quench correction.

2.3.4 Ins(1,4,5)P_3-induced release of sequestered calcium from intracellular membrane vesicles

The effect of Ins(1,4,5)P_3 on IM vesicles preloaded with calcium was investigated following the methods of Authi and Crawford (1985).

ATP-dependent $^{45}Ca^{2+}$ loading of IM vesicles was carried out as described above in section 2.3.3. After 20 mins incubation time (i.e. once steady state was established), 10μM Ins(1,4,5)P_3 (Amersham Int. UK.) was added and the reactions stopped at 15 sec, 30 sec, 60 sec and 150 sec intervals by rapid filtration and

washing as described in section 2.3.3. Separate assays were carried out adding the ionophore A23187 (2mM).

2.4 PLANAR BILAYER METHODS

Planar bilayers were formed by the 'painting' technique originally developed by Mueller *et al.* (1962a & b) and described in detail by other workers in the field (Mueller and Rudin, 1969; Miller, 1978,1982a,b; Alvarez, 1986). The advantages of this method for single channel recording, and a theoretical introduction to the formation of planar bilayers and the mechanism of fusion have been described in sections 1.5.3, 1.5.4 and 1.5.5.

2.4.1 Membrane chamber and electrical equipment

A diagrammatic representation of the membrane chamber used for painting bilayers is shown in figure 2.3. It consisted of an acrylic block into which two large intersecting cavities were machined. The diameter of one of the cavities was the exterior diameter of a cup (styrene copolymer or acrylic). A sector of the side wall of the cup was thinned and perforated to give a hole of diameter 0.3 or 0.5mm. This hole was the only connection between the two compartments created when the cup was inserted into the block. The internal volumes of the cup and apposing well shown were 4mls and 5mls respectively. Cups and blocks with reduced internal volumes, as small as 0.5ml, were also available for experiments in which preservation of platelet membrane vesicles and increased probability of fusion were required. The two smaller wells in the block accommodated the electrodes.

Electrical connection of the membrane chamber to the measuring equipment was made using reversible electrodes. Salt bridges connected the solutions in the membrane chambers to the electrode wells and silver chloride-coated silver wire

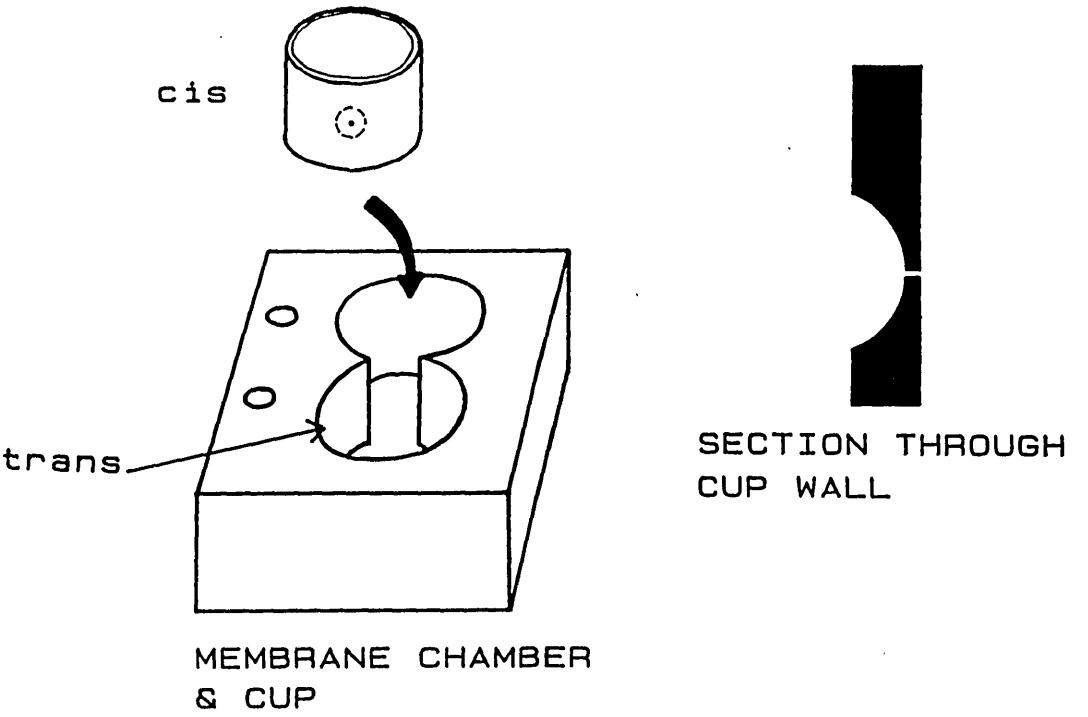


Figure 2.3

Membrane chamber and cup

See text for description.

electrodes connected the wells to the measuring equipment. The salt bridges were prepared by bending glass capillary tubes, of external diameter 1 or 2mm, (Clark Electromedical Instruments, Reading, UK) to an inverted 'U' shape in a Bunsen flame and filled, by suction, with 2% (w/v) agar in 3M KCl. The bridges were trimmed to fit between the electrode well (filled with 3M KCl) and the adjacent membrane chamber. High ionic strength salt bridges were used to minimize liquid-junction potentials in measurements under mixed ion conditions (Cukierman *et al.*, 1985). The silver wire electrodes were coated with AgCl by immersion in household bleach.

The membrane chamber was seated on a lead block to reduce vibration, with a small magnet mounted on a d.c. motor positioned beneath the cup to facilitate stirring of the solution. To eliminate any electrical interference due to a.c. pickup, the membrane chamber/lead block and current measuring circuit were mounted inside an insulating metal box. The box was then placed on an air-cushioned table to prevent floor vibrations interfering with the low-level current measurements.

A schematic diagram of the electronics system is shown in figure 2.4. External voltage commands (V_c) provided by an Amstrad microcomputer (Model CPC 6128) linked to a digital-to-analogue converter, were applied to the cup chamber (designated *cis*), whilst the other chamber (designated *trans*) was held at ground potential. Current through the bilayer was transduced into an analogue voltage signal via an operational amplifier (A1) acting as a current-to-voltage converter. The operational amplifier contained a high precision 10GΩ resistor (R_f) (K & M Electronics, W. Springfield, MA, USA) (Miller, 1982) allowing resolution of current flow in the pA range. The sensitivity of the current-to-voltage converter was 10mV/pA. Basically the negative feedback configuration used routes all the

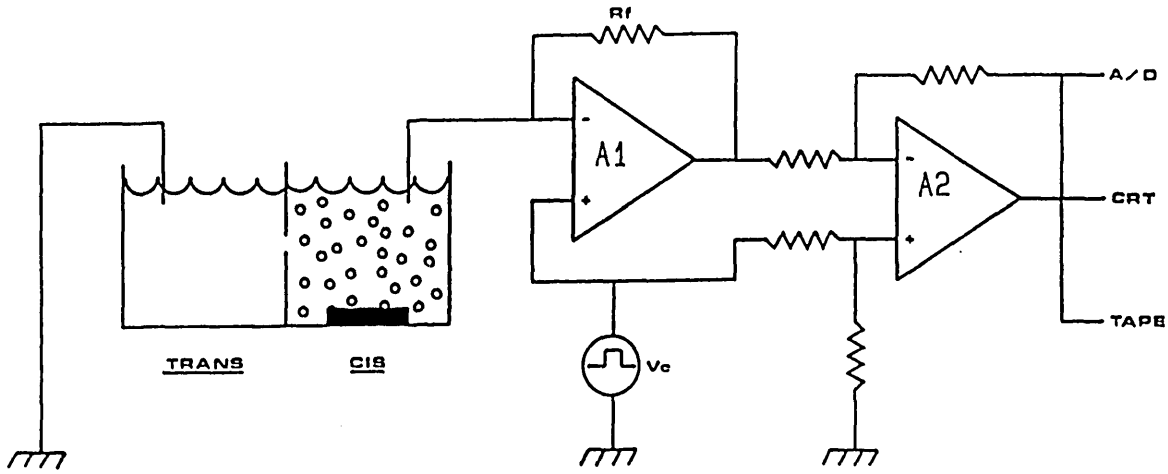


Figure 2.4

Bilayer electronics system

See text for description.

incoming current through the feedback resistor, leaving the potential at the input at ground level. The voltage at the output of the operational amplifier (V_o) is then the current (I_{in}) times the voltage of the feedback resistor (R_f), i.e. $I_{in} = V_o/R_f$. Since the voltage at the input is zero, the voltage across the bilayer membrane is precisely that set up by the microcomputer voltage generator.

The output of the operational amplifier was passed through a second stage differential amplifier (A2) of unitary gain and the clamp voltage subtracted. The signal was filtered as desired using a Krohn-Hite 4 pole Butterworth low pass filter (Krohn-Hite Corp., Avon, MA, USA) before display on an oscilloscope screen (Model 1425, Gould Electronics, Hainault, UK). Unfiltered data were stored on FM tape, using a Racal 4 channel tape recorder (Racal Recorders, Southampton, UK), for subsequent analysis. The time response of the tape recorder was quoted as 2.5 kHz at the recording speed of 3.75 inches/sec routinely used.

The circuit diagram for the second stage amplifier is reproduced in Appendix B with the permission of the designer, R.A.P. Montgomery (National Heart and Lung Institute), who measured the rise time of the head amplifier as ~200μsec.

2.4.2 Procedure for membrane formation

The membrane chamber and cup were soaked, when not in use, in a strong detergent solution. They were rinsed in running water for at least an hour and then dried thoroughly prior to use. Meticulous cleaning of the apparatus was necessary to ensure the formation of stable and durable bilayer membranes. All

aqueous solutions used in bilayer experiments were filtered through Millipore membranes (0.45μm pore size) prior to use.

The membrane 'forming solution' consisted of a dispersion of purified phospholipids in *n*-decane. The phospholipids phosphatidylethanolamine, PE (purified from bovine muscle), and phosphatidylserine, PS (from bovine brain), were supplied by Avanti Polar Lipids, Alabama, USA, and stored at -80^{o}C in chloroform. Bilayers were formed from PE alone or from a 70%/30% or 50%/50% ratio of PE/PS. Stock phospholipids were mixed as required, the chloroform evaporated off under a stream of nitrogen, and then *n*-decane added to give a final phospholipid concentration of 30mM. PS is a negatively charged phospholipid whilst PE is a zwitterion and bilayers consisting of PE alone have no net charge.

At the outset of the experimental protocol a droplet of the 'forming solution' was spread over the aperture in the cup and allowed to dry, thus 'priming' the hole. A painting 'stick' comprising a plastic pipette tip fashioned into a pen nib shape was used for the transfer of phospholipids to the cup. The *cis* and *trans* chambers were then filled with solution; most usually 150mM KCl, 5mM HEPES/Tris, pH 7.2. A further droplet of forming solution was then cast over the hole resulting in a lipid film, probably several micrometers thick, which spontaneously thinned to form a bilayer.

A square wave pulse of ±4mV amplitude was applied to the *cis* chamber during bilayer painting and the signal monitored on the oscilloscope. Occlusion of the hole was detected by the disappearance of the square wave and the appearance of a capacitance spike as the lipid film plugged the hole. Assessment of the thinness of the lipid film was carried out on the basis of the size of the capacitance spike. As

the lipid film thinned, the height of the spike increased to a maximim, characteristic of the size of the hole.

Lipid films which did not appear to thin spontaneously could be induced to do so by applying a large amplitude, high frequency square wave pulse (±120mV at 1kHz) for a few seconds. If this method failed to induce thinning after several repetitions or 'leaky' films were observed, the cup was usually washed and rinsed, reprimed, and the painting process repeated. Typical waveforms observed during bilayer formation are shown in figure 2.5.

2.4.3 Incorporation of ion channels by fusion

The conditions used to incorporate platelet membrane vesicles with the preformed bilayer were based on those reported by others to promote fusion (Miller and Racker, 1976; Hanke, 1986).

Fusion is generally favoured by the presence of negatively charged phospholipids in the bilayer, divalent cations on the side of the bilayer to which membrane vesicles are added (*cis*) and an osmotic gradient across the bilayer with the *cis* side hyperosmotic to the *trans* side. The specific conditions routinely used were as follows: for a negatively charged bilayer (70%/30% or 50%/50%, PE/PS) *cis*: 450mM KCl, 1.0mM $CaCl_2$, 5mM HEPES/Tris, pH 7.2; *trans*: 150mM KCl, 5mM HEPES/Tris, pH 7.2. The osmotic gradient and presence of Ca^{2+} on the *cis* side were established by addition of appropriate volumes of concentrated stock solutions to the chamber once a bilayer was formed. In experiments where neutral bilayers were used, $CaCl_2$ was omitted from the *cis* chamber solution.

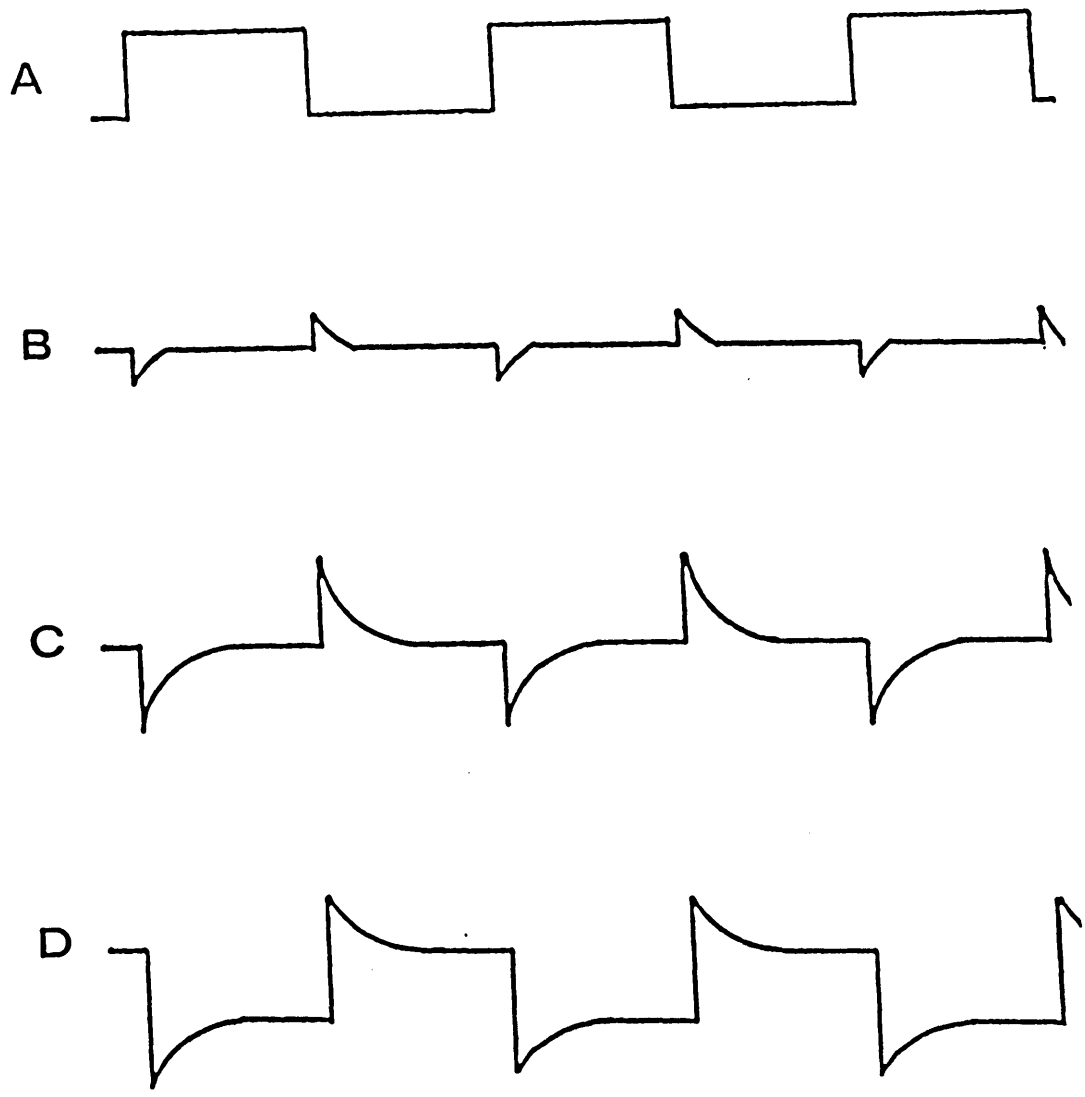


Figure 2.5

Typical waveforms observed during bilayer formation

A: Clamp square wave pulse (±4mV)

B: Capacitance spike due to thick lipid film plugging the hole

C: Bilayer: maximum height of capacitance spike achieved - characteristic of the size of the hole.

D: Leaky film formed

Platelet membrane vesicles were added to the *cis* chamber (usually 5-10μg protein) and mechanically agitated using a small magnetic stirrer. To monitor the occurrence of fusion events a constant potential was applied across the bilayer and the current flow observed. When a vesicle/vesicles containing a channel/channels fused with the bilayer, the current increased in discrete steps. After fusion had occurred, the *cis* chamber was perfused out with the desired solution for the experiment, suppressing further fusion by removing unfused membrane vesicles. Perfusion of the chambers was achieved using a small peristaltic pump set at a flow rate of 25 ml/min, with at least 10 cup volumes exchanged. Flexible plastic tubing attached to the peristaltic pump provided inflow and outlet lines which simultaneously fed the exchange solution into the chamber, and removed fluid out of the chamber so that the volume remained constant. A reed switch located between the input sockets connecting the silver wire electrodes to the amplifier was activated with a magnet during perfusion. This effectively shorted out the chambers preventing any large voltages developing across the bilayer. Bilayers usually withstood chamber perfusion, although breakage at this stage was not uncommon.

In experiments using oxalate loaded intracellular membrane, the perfusate from the *cis* chamber was collected in a centrifuge tube on ice and 'recycled' by pelleting the vesicles and resuspending in 0.4M sucrose, 5mM HEPES/Tris, pH 7.2 in order to conserve membrane (see section 5.4).

2.4.4 Single channel experimental protocol

After platelet membrane fusion, conditions surrounding the reconstituted channel protein were manipulated as required, either by chamber perfusion with a fresh

solution, or by addition of compounds to either the *cis* or the *trans* face. If additions were to be made (after activation of the reed switch) a volume of chamber solution equal to the volume to be added was first removed from the chamber in order to maintain constant solution volume throughout the experiment. When additions were made to the *trans* chamber, the solution was mixed by drawing 200μl into a pipette and then ejecting it back into the chamber. This was repeated several times until adequate mixing was achieved.

In order to characterise the conduction properties of the channels under investigation, single channel currents were recorded at 10mV intervals from -70 to +70mV in a range of symmetrical and asymmetric ionic conditions. In experiments carried out in asymmetric solutions the electrode offset potential was measured in each case once the protocol was completed, in order to correct the measurements (range 1-3mV). These experiments were carried out with either a single channel or multiple channels (2-5) active in the bilayer, though multiple channel fusions were far less frequent.

In experiments designed to investigate the kinetic behaviour of the channels, recordings with only a single channel in the bilayer were required. A single active channel was considered to be present if only one open level was observed:

(i) under conditions where the probability of channel opening was maximised (e.g. for the SM channel, switching from high negative voltage to a high positive voltage [-70 to +60mV]), and

(ii) for the duration of the recording time (> 20 mins).

Steady state recordings at a range of holding potentials were carried out using the following voltage switching protocol. The membrane was held at 0mV for 10 sec and then switched to a given voltage for 5 mins. The voltage was then restored to 0mV for 10 sec prior to each steady state recording at a particular holding potential.

Data were stored on FM tape for subsequent hand or computer-aided analysis. Traces were replayed onto a hot-pen recorder (Ormed MX216) for visual inspection and illustrations.

2.5 ANALYSIS OF SINGLE CHANNEL DATA

Ion channels act as variable-conductance elements that fluctuate in a stochastic fashion from non-conducting, or closed, conformational states, to conducting, or open, conformational states. Single channel records such as those shown in chapters 4 and 5 are essentially the recorded history of these conformational changes for a single macromolecule (or functional complex). It is possible to distinguish two clearly defined levels of current representing the closed state and the open state, which defines the unit conductance of the channel.

To be precise, the single channel record only reveals the rate limiting transitions between open and closed conformations of the channel that occur at the time scale of the recording, i.e. in the range of 10^{-4}-10^{-3} seconds. Conformational events not detected are those which are electrically silent (i.e. involve no change in conductance), or those occurring outside the limiting time response of the recording.

Transitions between open and closed states appear as square wave pulses of current since the actual current relaxation between virtually 0 ions/second (channel closed) to > 10^6 ions/second (channel open) is too fast to measure. An ideal single channel record should consist of a sequence of rectangular pulses of constant amplitude and random duration. In actual experiments, this ideal signal is corrupted by a variety of noise sources and distorted by filtering.

Single channel records provide two types of information used to characterise the channel:

(1) a direct measurement of the conductance value of the open state which relates to the conduction process by which ions interact with and permeate the open channel.

(2) a sampling of resolvable dwell times in the open and closed states which can be related to the gating of the channel.

An examination of conduction and gating properties has been carried out in detail for the channel found in the platelet SM. A less detailed analysis of single channel experiments recorded from a channel found in the platelet IM has also been made.

Experiments in which the conduction properties of these channels were investigated have been analysed by hand from replayed traces. Traces were calibrated by replaying pre-recorded square wave signals of known voltage and frequency for comparison. Channel gating properties were investigated by digitising the data for computer-aided measurements.

2.5.1 Conduction properties of channels

Current-voltage relationships were plotted for channels under a variety of ionic conditions. Where the relationships were ohmic (i.e. linear), regression lines were fitted through the data points. For non-ohmic relationships, curves were 'best' fitted to the data by eye. Reversal potentials were measured to the nearest mV correcting for the electrode offset potential (range 1-3mV) in each case.

The **Nernst equilibrium equation** allows the theoretical prediction of the reversal potential (E) for a single channel ideally selective for a given ion species.

$$E = \frac{R.T}{z.F} \cdot \ln \frac{[C]_{cis}}{[C]_{trans}} \qquad \text{(equation 5)}$$

where R is the gas constant

T is the absolute temperature

z is the valency of the permeant ion

F is the Faraday constant

$[C]_{cis}$ and $[C]_{trans}$ are the bulk concentrations of permeant ion in the *cis* and *trans* solutions

RT/F is 25.2 at 20°C

Thus, in the presence of a 3:1 (*cis*:*trans*) Cl^- concentration gradient, E = +28mV for an ideally selective Cl^- channel. For an ideally selective K^+ channel the sign is reversed, and E = -28mV.

The Nernst equation was not applicable for analysis of the conduction properties of the SM channel where a relatively complex mixture of permeant ions was present. Relative monovalent anion *vs* monovalent cation permeabilities (P_{Cl}/P_K) were therefore calculated to satisfy the following derivation of the **Goldman-Hodgkin-Katz (GHK) voltage equation** (Goldman, 1943; Hodgkin and Katz, 1949).

$$\frac{P_{Cl}}{P_K} = \frac{\{(n.e^{E/k})-1\}}{\{n - e^{E/k}\}} \qquad \text{(equation 6)}$$

where k is RT/F as previously defined

n is the *cis*:*trans* concentration gradient of permeant ions

In experiments comparing the relative permeabilities of various monovalent anions, the anion *vs* anion permeability ratios (P_A/P_{Cl}) were calculated from the following version of the GHK equation which takes into account contributions from K^+, Cl^- and the test monovalent anion, A (from Franciolini and Nonner, 1987).

$$E = \frac{R.T}{F} \cdot \ln \frac{(P_K a_K + P_A a_A)}{(P_K a_K + P_{Cl} a_{Cl})} \qquad \text{(equation 7)}$$

where a_K, a_A and a_{Cl} are the activities of K^+, A^- and Cl^- respectively (activities taken from Robinson and Stokes, 1959).

Divalent *vs* monovalent anion permeability ratios (P_{SO4}/P_{Cl}) were calculated following the same principles, so that

$$\frac{P_{SO4}}{P_{Cl}} = \left[\frac{[Cl]}{4[SO_4]}\right] \cdot \left[\frac{1 + e^{F.E/R.T}}{e^{-F.E/R.T}}\right] \qquad \text{(equation 8)}$$

where [ ] denotes the concentration of the specified anion

2.5.2 Gating properties of channels

Analysis of gating properties has been carried out for the channel identified in the platelet SM which is seen to exhibit only one conductance level. All experiments were carried out with only a **single** active channel in the bilayer (assessed as described in section 2.4.4).

2.5.2a Aims of analysis

The immediate object of the analysis was to extract the underlying signal from the recorded data, i.e. to obtain an idealised version of the experimental record which resembled, as closely as possible, what would have been seen if the experiment had been free of noise and artefacts. The result takes the form of a series of time intervals, each associated with the amplitude of the current during that interval, in the order in which the events actually occurred. Such results will not, of course, be entirely accurate. For example, if a closing event of the channel is too short to measure, not only will its omission from the analysis distort the distribution of closed times, but the open durations on either side of it will be detected as one long open period, so the open time will also be distorted (and *vice versa* for undetected open times).

For detailed studies of channel behaviour, the channel data record should be sufficiently long to register a statistically significant number of events and the sampling rate used in the analysis should be kept high to limit distortions of the fast phases of the signal and minimise the number of events 'missed' during sampling. The following experimental and analytical criteria were applied:

(i) **Data collection**

Single channel records were collected for a minimum of 10 minutes and up to 30 minutes duration for a particular channel under a given set of experimental conditions.

(ii) **Digitisation rate**

A sampling rate of 2.0 kHz was applied in the lifetime analysis (i.e. 2,000 samples taken every second, with an inter-sample period of 500μsec). The criterion for the

choice of sampling rate, as stated, is such that the digitised record, when interpolated, is as close as possible to the original recording (Colquhoun and Sigworth, 1983). For lifetime analysis, digitisation was carried out using an AT based computer system (IntraCel, Cambridge, U.K.).

(iii) **Filtering**

Filtering of the data was required to remove high-frequency noise prior to analysis. Since the events of interest are rectangular, it is undesirable to use a filter with a very sharp roll off, such as a Chebyshev filter, since this type distorts a step input to produce an overshoot and 'ringing' appearance in the band of interest. Thus a 4-pole low pass Butterworth filter was used in RC mode, which gives a comparable response to a Bessel filter. The filter setting was selected at a value high enough to avoid counting an excessive number of noise peaks as channel events, but low enough to catch as many true events as possible.

In practice the filter setting was originally selected by examining a 'noisy' data record to be analysed (subjectively assessed by examining original (unfiltered) data). Knowing the channel size, a value midway between the open and closed state was located. When the channel entered the (long) closed state, the filter setting was adjusted so that the noise was reduced to such a level that no 'false' opening events were detected. A value of 1.0kHz (front panel setting) was found to be appropriate and this was applied to all channel records so that data remained comparable.

2.5.2b Event detection by half-amplitude threshold analysis

The most common procedure for detecting transitions in channel data is the amplitude threshold technique. With this method transitions are assumed to have occurred each time the signal crosses a fixed threshold. (Sachs *et al.*, 1982; Colquhoun and Sigworth, 1983; Cottrell *et al.*, 1983; Sigworth, 1983; Vivaudou *et al.*, 1986). An event detection analysis package, **'Satori'** (IntraCel, Cambridge, U.K.) was used to analyse recordings made from the platelet SM channel. Channel records were sampled at the selected digitisation rate and filter frequency, and the original recording viewed on the computer screen (see figure 2.6). The level of the baseline (closed level) and of the open channel level were located by manually adjusting cursors to pass through the midline of the noise at each level. A transition between the open and closed levels was considered to have taken place when the data signal crossed the 50% threshold (expressed as a percentage between the baseline, 0%, and the channel open position, 100%). Thus in figure 2.6, event x is assessed to represent a closing event, since the 50% threshold is reached, whereas event y is not, since the signal does not reach the threshold. As pointed out by Sachs *et al.* (1982), choosing the threshold at 50% of the channel amplitude is convenient because the time spent above the threshold is then an unbiased estimate of the true duration for long events of either polarity, and can therefore be used to estimate both open and closed times.

However, events such as y in figure 2.6 (which may well represent a channel closing event) never reach the threshold and are 'missed' from the analysis. Thus a 'dead time' (t_{min}) is introduced by this technique, and events shorter than t_{min} are undetected. The exact value of t_{min} for the analytical system used for the SM

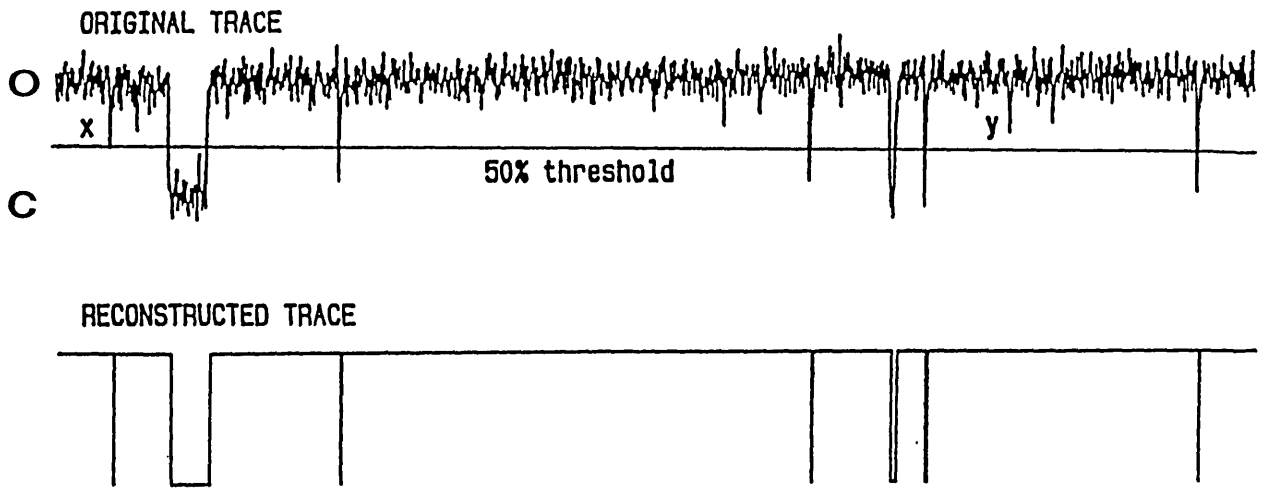


Figure 2.6

Half-amplitude threshold analysis

Original data and reconstructed single channel record assessed using half-amplitude threshold analysis. Data were filtered at 1kHz and digitised at 2kHz using the 'Satori' package (IntraCel, Cambridge, U.K.). Event x represents a channel closing event since the 50% threshold is reached, whereas event y does not reach the threshold and so does not appear as a closing event on the reconstructed trace.

channel was measured experimentally by the following method (cf. Colquhoun and Sigworth, 1983).

With the filter at 1kHz (front panel setting), a square wave pulse from a signal generator was relayed through the filter onto an oscilloscope screen. Starting at a low signal frequency, f, (e.g. 100Hz) the square wave was observed and the amplitude, A_0, measured. The signal frequency was then increased until a value, f_m, was reached where the amplitude was exactly $A_0/2$. $1/f_m$ then gave the t_{min} for the filter at 1kHz. Using this method a t_{min} value of 1.6msec was measured for the filter used in the analysis. Thus using the half-amplitude threshold analysis only events >1.6msec were resolved.

A t_{max} was introduced into the analysis by the limiting memory size of the 'Satori' computer programme. Sampling at a digitisation rate of 2kHz, a tape read of 64 seconds was possible. For the platelet SM channel, closed events lasting >64 secs were observed in most recordings. These events were therefore necessarily excluded from the analysis.

2.5.2c Open and closed lifetime distributions

A typical 'Satori' session measuring open and closed lifetimes involved the following steps:

(1) Data were acquired at 2kHz digitisation rate, filtering at 1kHz (front panel setting) in 64 second 'chunks'.

(2) A typical, clearly resolved opening event was located in the raw data record and cursors used to manually locate the open and closed levels. The programme then 'learnt' these levels and set a threshold at 50% of the amplitude.

(3) Each event in the single channel record was then assessed for half-amplitude threshold crossing. The programme then reconstructed the channel recording producing an idealised representation of the channel current signal (see figure 2.6). The computer operator was then requested to decide whether the reconstructed fit was adequate or not. If acceptable, the duration of open and closed events in the reconstructed trace were measured and stored in separate open and closed lifetime files. Any drift in the baseline was corrected by adjusting the cursor positions, relocating the open and closed levels and 'relearning' the revised positions. Close inspection of all the events included in the analysis was necessary to detect both baseline drift and possible artefacts (Colquhoun, 1988).

(4) Sequential 64sec 'chunks' of data were analysed from the channel record until at least 10 minutes of recorded data, or $\geq$ 4,000 events (up to 8,000, which was the limiting number of events which could be accommodated by the fitting programme).

(5) Channel open and closed lifetimes were then grouped into (non-cumulative) histograms for display on linear scales [frequency per bin *vs* measured duration].

2.5.2d Fitting of exponentials to distributions

Data collected as described above consisted of sets of open and closed lifetimes. Since lifetimes are random variables, their behaviour must be described by

probability distributions. The term 'random' used in this context means that the probability that an open channel will close is constant, regardless of what has gone before (i.e. regardless of how long the channel has already been open). Thus the system is 'memoryless' (Markovian), and the future events depend on the present state of the system, and not on its past history. A detailed discussion of the characteristics of random lifetimes is presented by Colquhoun and Hawkes (1983).

Individual lifetimes (either open or closed times) may be fitted to an exponential probability density function (p.d.f). For a simple exponential distribution for an interval of duration t, the p.d.f is given by:

$$f(t) = \tau^{-1}.\exp(-t/\tau) \qquad \text{(for } t>0\text{)} \qquad \text{(equation 9)}$$

where: τ is the mean of the distribution (or the time constant of the curve)
(the initial constant in the equation, τ^{-1}, ensures that the p.d.f has unit area)

The p.d.f is clearly not itself a probability; it is a function such that the area under the curve between any specified time values is the probability of observing a lifetime between those values.

The p.d.f for a distribution that has the form of the sum of (for example) k exponentials is given by:

$$f(t) = \sum_{j=1}^{k} a_j.\tau_j^{-1}.\exp(-t/\tau_j) \qquad \text{(equation 10)}$$

where: τ_j are the time constants ($1/\tau_j$ being the corresponding apparent closing or opening rates)

a_1 to a_k are the relative areas under each of the components

The sum of the areas adds up to unity, and they are roughly proportional to the number of events in each component.

As stated in section 2.5.2c, lifetimes lasting <1.6msec and >64,000msec were to be excluded from the analysis. A correction for these 'missed events' was therefore necessary (Colquhoun and Sigworth, 1983; Milne *et al.*, 1989). Thus:

$$f(t) = \frac{\sum_{j=1}^{k} a_j.\tau_j^{-1}.\exp(-t/\tau_j)}{P(t_{min} < t < t_{max})} \qquad \text{(equation 11)}$$

where the denominator is simply the probability that an observation with the distribution of the numerator lies between t_{min} (the minimum resolvable lifetime) and t_{max} (the maximum period of observation). i.e.

$$P(t_{min} < t < t_{max}) = \sum_{j=1}^{k} a_j[\exp(-t/\tau_j) - \exp(-t_{max}/\tau_j)] \qquad \text{(equation 12)}$$

An estimate of the true number of events (N), including those shorter than t_{min} or longer than t_{max}, can be obtained from the observed number,n, such that:

$$N = \frac{n}{P(t_{min} < t < t_{max})} \qquad \text{(equation 13)}$$

The problem in fitting probability density functions is how to find the values for the parameters (i.e. the time constants, τ_1, τ_2....., and the relative areas a_1, a_2....) which 'best fit' the experimental data. The method of **maximum likelihood** is

considered preferable to other criteria for 'best fit' (Colquhoun and Sigworth, 1983; Horn and Lange, 1983). This method optimises the values for areas and time constants such that the probability (likelihood) of obtaining the observed set of data is maximised.

For example, for a given set of measurements (e.g. closed times), t_1, t_2..., t_n. If these observations are independent of one another, then the probability (density) of making all n observations is proportional to the product of the separate probability densities for each observation. This gives the likelihood of a particular set of parameters. So:

$$Lik = f(t_1).\ f(t_2)....\ f(t_n) \qquad \text{(equation 14)}$$

where f is the conditional p.d.f defined in equation 11.

In practice, the optimisation programme used (the 'Efit' companion programme to 'Satori') worked with the log-likelihood, L, which, from equation 14, is given by:

$$L = \log(Lik) = \sum_{i=1}^{n} \log f(t_i) \qquad \text{(equation 15)}$$

A typical 'Efit' session proceeded as follows:

(1) Open and closed lifetime files collected as described in section 2.5.2c were 'stripped' of events shorter than t_{min} (1.6msec).

(2) For a trial set of values of the parameters (areas and time constants) supplied by the computer operator, the programme calculated the probability that

each observed interval duration was drawn from the distribution described by equation 11. The logarithms of the probabilities for each interval were then added to obtain the log(Lik) estimate for the trial parameters.

(3) This entire process was repeated until parameters (τ and a) which made the value for L (equation 15) as large as possible were found.

(4) The following parameters were displayed. e.g. for a double exponential fit: τ_1, τ_2, a_1, a_2 (see equation 11), N (see equation 13) and -L (see equation 15). P.d.fs were then fitted to the lifetime histograms using the calculated parameters.

2.5.2e Determining the number of exponential components

A likelihood ratio test (Horn and Lange, 1983; Labarca *et al.*, 1985; Blatz and Magleby, 1986) was used to determine the number of significant exponential components required to fit the distribution of open and closed lifetimes. Comparisons of fits with different numbers of exponentials were made from the ratio of the maximum likelihoods. Twice the natural logarithm of the ratio of the likelihoods is distributed as χ^2, with degrees of freedom equal to the difference in the number of independent parameters in the two compared distributions. For example, to determine whether 3 exponentials fitted the closed time data for the SM channel significantly better than 2, the difference between the natural log of the maximum likelihood estimates for fits with 2 and 3 exponentials was multiplied by 2, giving the χ^2 value. This value was then used with a χ^2 table to determine the value of P using 2 degrees of freedom. Only when the likelihood ratio test gave a probability of <0.05 (5% significance level) for the fit with one

fewer exponentials were the parameters obtained from a curve fit taken as significant.

The number of significant exponentials determined by the likelihood ratio test agreed with the number that was obtained by visual inspection of fits with different numbers of exponentials to the data (see example in section 4.11b).

2.5.2f Correlation between successive closed events

Correlation functions provide information on the minimum number of ways in which open and closed states communicate (Labarca *et al.*, 1985; Kerry *et al.*, 1987) and are important in defining the gating kinetics of multistate channels.

The autocorrelation coefficient for the k'th closing along, r_k, was estimated from the original observations, y_i (i = 1,2,3.....N; mean y'), as:

$$r_k = \frac{\sum_{i=1}^{n-k} (y_i - y')(y_{i+k} - y')}{\sum_{i=1}^{n} (y_i - y')^2} \qquad \text{(equation 16)}$$

The confidence limits for r_k, outside which correlation was considered significant, were set at ± 0.05 (± twice the approximate standard error of the estimate in the case of white noise) as described by Labarca *et al.* (1985).

The measurement of significant correlation between successive dwell times (open or closed) in single channel recordings suggests more than one isomerisation pathway linking the states.

2.5.2g Measurement of P_0 values

The probability of channels being in the open, conducting, state (P_0) was estimated from the **IPOCH** (Vivaudou *et al.*, 1986) sampling programme run on a PDP-11/73 microcomputer (Indec, Sunnyvale, CA, U.S.A.). Continuous channel recordings containing a **single** ion channel were sampled at either 500Hz (SM channel) or 1kHz (IM channel) [low pass filter frequencies were set at 250Hz or 500Hz accordingly]. The digitisation rate was limited by the memory size of the programme. For example, for measurements on the SM channel the rate was set to 500Hz in order to accommodate analysis of four minutes recording time. Thus some of the short closing events were missed in the sampling. However, this was a necessary 'trade-off' in order to measure a large number of openings.

Applying the 50% amplitude threshold criterion (see section 2.5.2b), steady state amplitude histograms were constructed. Integration of amplitude histograms gave an estimation of P_0 values.

Chapter 3

RESULTS I

BIOCHEMICAL CHARACTERISATION OF PLATELET SURFACE AND INTRACELLULAR MEMBRANE FRACTIONS

3.1 Introduction

A prerequisite for the single channel experiments described in this thesis was the preparation of native platelet membrane vesicles of well defined origin. The protocol followed for the preparation of the surface and intracellular membranes (see section 2.2) was expected to yield highly purified membrane fractions free from cross-contamination as described by Menashi *et al.* (1981) and Authi and Crawford (1985). It was considered prudent to ensure that the membrane vesicles prepared for the experiments presented in this thesis were of comparable purity and functional integrity to those described by the original workers characterising the preparation.

This chapter contains the results obtained using membrane fractions from several different human platelet preparations subjected to the biochemical assays described in section 2.3.

3.2 SDS-polyacrylamide gel electrophoresis

The protein profiles obtained with mixed membranes and the surface and intracellular membrane fractions from a typical continuous flow electrophoresis separation are shown in figure 3.1.

The mixed membrane fraction is shown to contain at least 30 discrete polypeptide bands under the experimental conditions applied. The protein band co-migrating with the 43,000 molecular weight standard is identified as actin. Another prominent band has mobility characteristics corresponding to the heavy chain of myosin (M_r=200,000). Although a 200,000 molecular weight marker was not

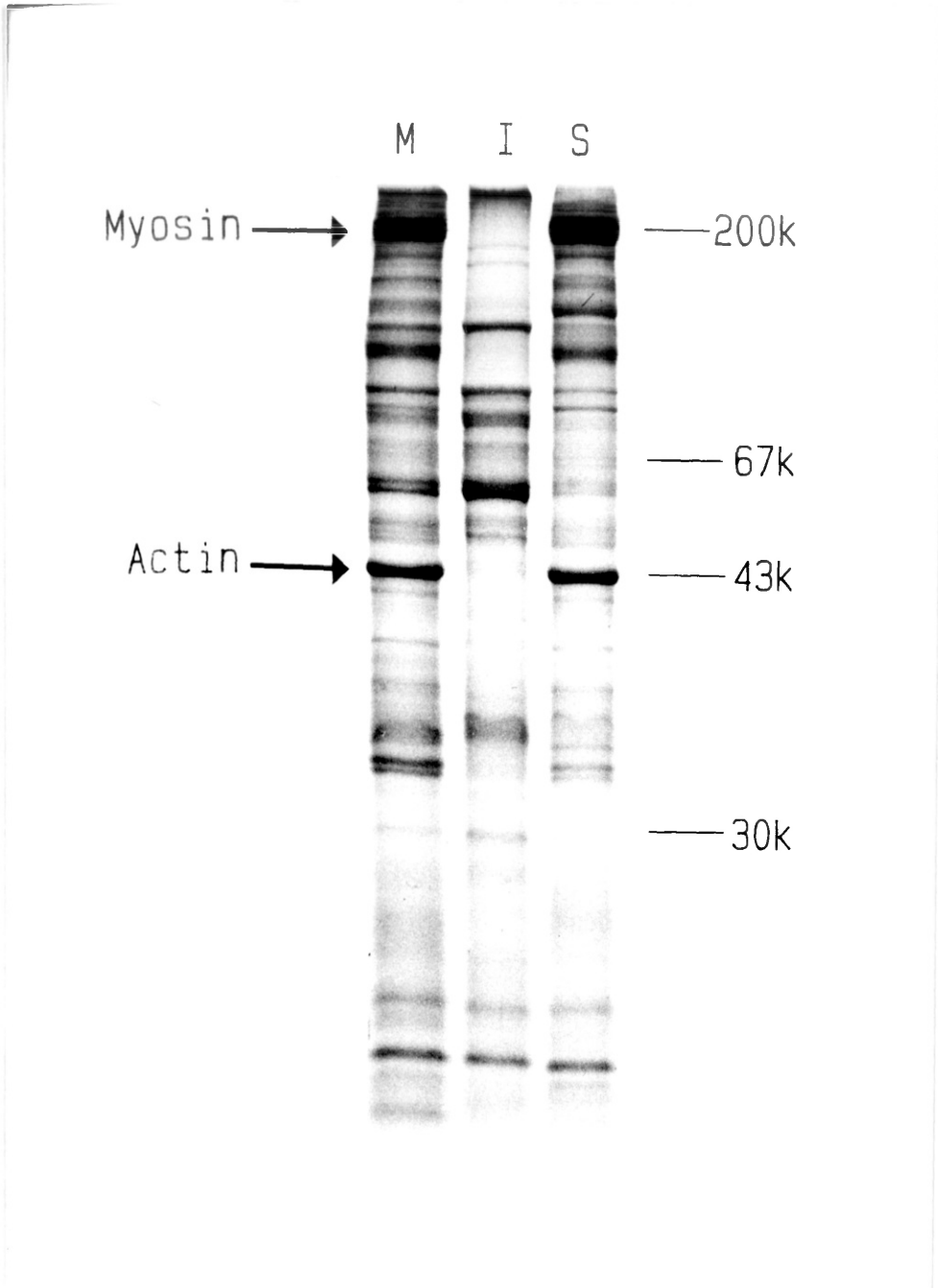


Figure 3.1

SDS-polyacrylamide gel of membrane fractions

SDS polyacrylamide gel (9%) separation of platelet membrane fractions from a human platelet preparation. **M**, mixed membrane; **S**, surface membrane; **I**, intracellular membrane. The gel was prepared as described in section 2.3.1.

applied to the gels, the position of this band is distinctive on comparison with similar gels carried out following membrane preparation by the same methods (see Menashi *et al.*, 1981) and is marked in the figure. Both of these proteins are also found in the surface membrane fraction.

The most significant difference between the membrane fractions is the complete absence of the two contractile proteins in the intracellualar membrane fraction.

3.3 NADH-cytochrome *c* reductase enzyme assay

Figure 3.2 summarises the results of antimycin-insensitive NADH-cytochrome *c* reductase enzyme activity in membrane fractions from four separate preparations. An almost exclusive enrichment of this enzyme is found in the intracellular membrane fraction with little or no activity detected in the surface membrane fraction. Enrichment ratios from 3.2 to 9.2 are calculated for intracellular membranes with respect to the mixed membrane fraction from the same platelet preparation.

3.4 Assay for calcium uptake by intracellular membrane vesicles

Both the surface and intracellular membrane fractions were investigated for their capacity to sequester Ca^{2+} by an ATP-dependent mechanism. Figure 3.3 shows the results of $^{45}Ca^{2+}$ accumulation by vesicles from the IM in the presence and absence of ATP, and by SM vesicles in the presence of ATP (all in the presence of 3μM external free Ca^{2+}). Calcium uptake is found to be exclusively confined to the intracellular membrane. The process is clearly ATP dependent, since in the absence of ATP from the incubation medium, values for IM Ca^{2+} uptake

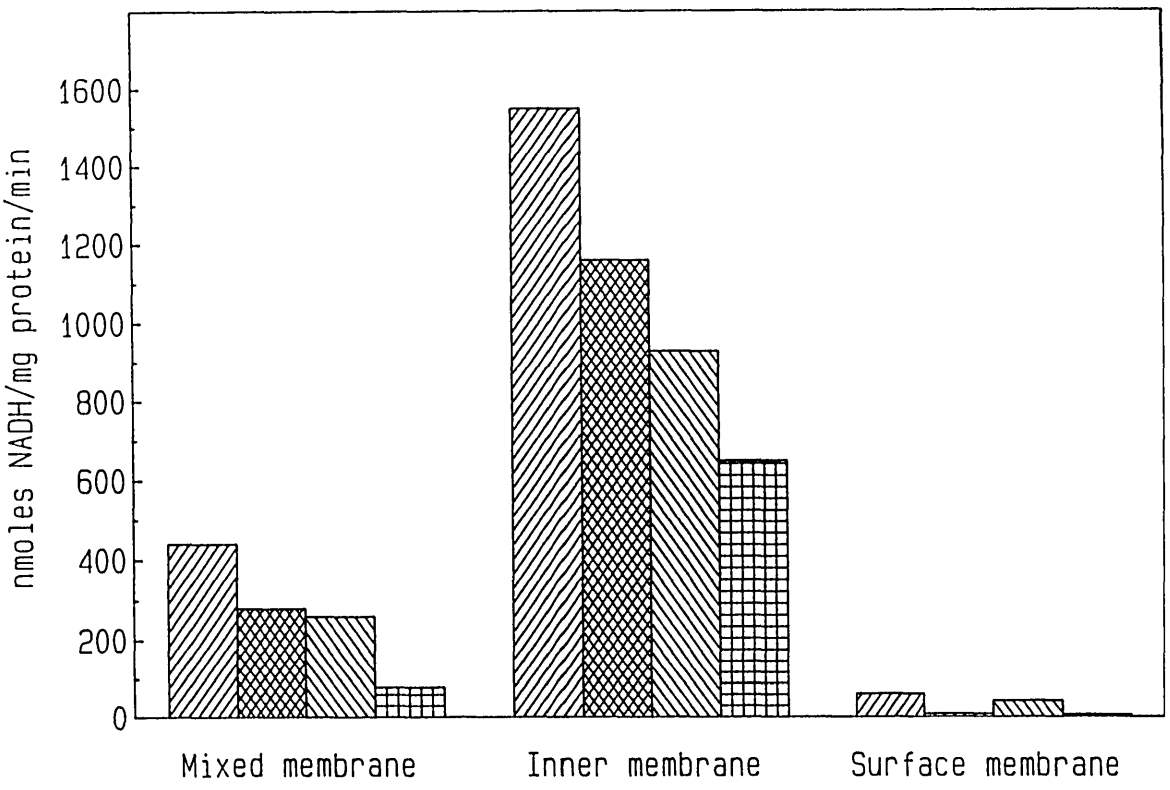


Figure 3.2

NADH cytochrome *c* reductase assay

Antimycin-insensitive NADH cytochrome *c* reductase enzyme activity in the mixed, surface and intracellular membrane fractions isolated from four different human platelet preparations (represented by the different shading of the columns). Assays were carried out as described in section 2.3.2.

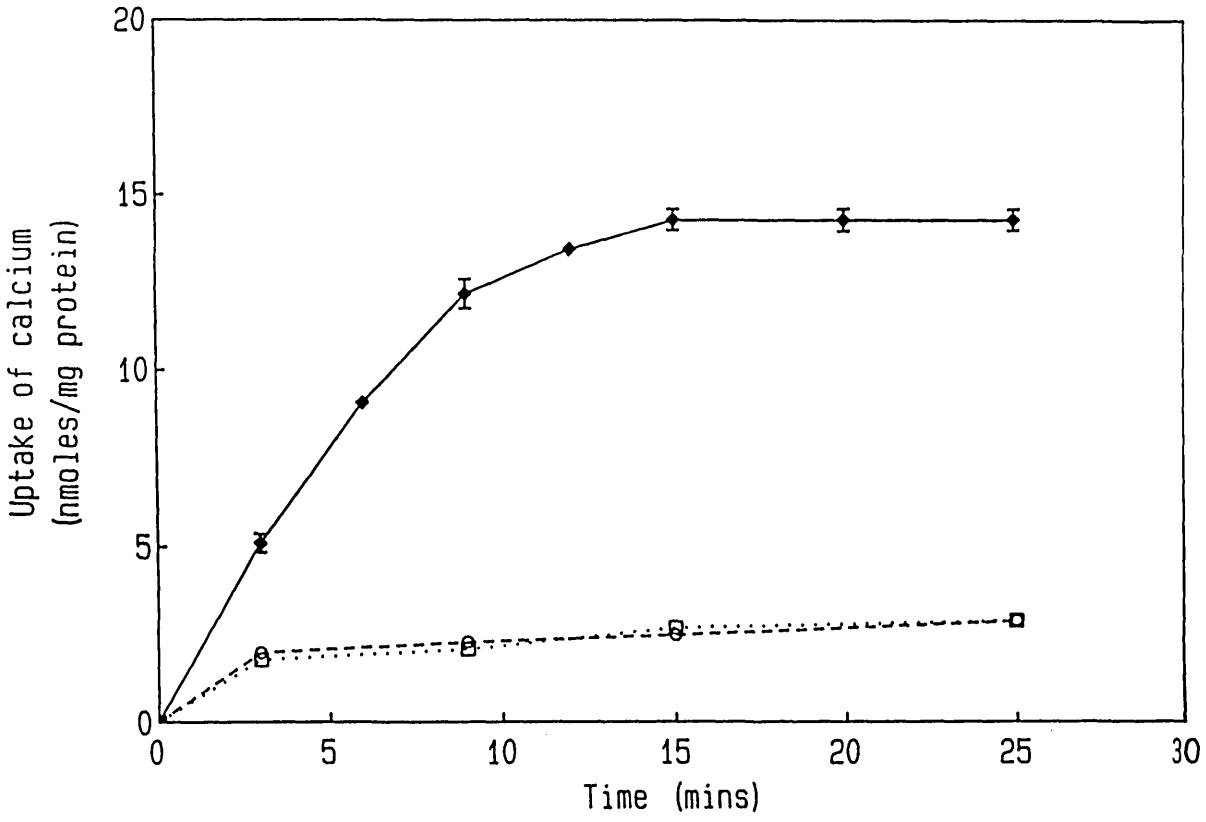


Figure 3.3

Time course of calcium uptake by intracellular membranes

$^{45}Ca^{2+}$ accumulation by vesicles from the intracellular membrane in the presence (♦) and absence (O) of ATP (2mM); and by SM vesicles (□) in the presence of ATP. Uptake proceeded at room temperature in the presence of 3μM external free Ca^{2+} and was stopped at the times shown by rapid filtration and washing as described in section 2.3.3. Vertical bars represent S.D. (n=3).

coincided with those for the SM vesicles. Uptake by SM vesicles represents approximately 20% of the rates recorded for intracellular membranes from the same platelet population. Uptake of Ca^{2+} into intracellular membrane vesicles is fairly rapid with a steady state concentration reached within the vesicles at 10-15 mins.

When the calcium ionophore A23187 (2mM) is added to the incubation mixture after a steady state level has been reached (i.e. after 20 mins), the sequestered Ca^{2+} is rapidly and almost totally released from the vesicles (see figure 3.4). Over 50% of the stored Ca^{2+} is liberated within the first 30 sec and more than 90% within 4 mins. The presence of A23187 destroys the vectoral properties of the Ca^{2+} pump in the IM vesicles, and the finding that most of the accumulated Ca^{2+} is liberated indicates that binding of Ca^{2+} to the vesicle membranes accounts for only a very small proportion of the stored Ca^{2+}.

3.5 Ins (1,4,5)P_3-induced release of sequestered calcium from IM vesicles

Events following the addition of 10μM Ins(1,4,5)P_3 to the intracellular membrane vesicles (time t=1 in figure) preloaded for 20 mins with $^{45}Ca^{2+}$ are shown in figure 3.4. 30% of the sequestered Ca^{2+} is released during the first 15 sec after Ins(1,4,5)P_3 addition to the incubation medium. This is followed by a rapid reuptake of the Ca^{2+}, with full restoration to the former steady state values 60 sec after the release event. This reaccumulation phenomenon was observed by Authi and Crawford (1985) and has also been reported by other workers (Streb *et al.*, 1983; Dawson and Irvine, 1984; O'Rourke *et al.*, 1985). Authi and Crawford (1985) observed that a second application of Ins(1,4,5)P_3 to the IM after the vesicles had returned to steady state conditions produced a release almost identical with that

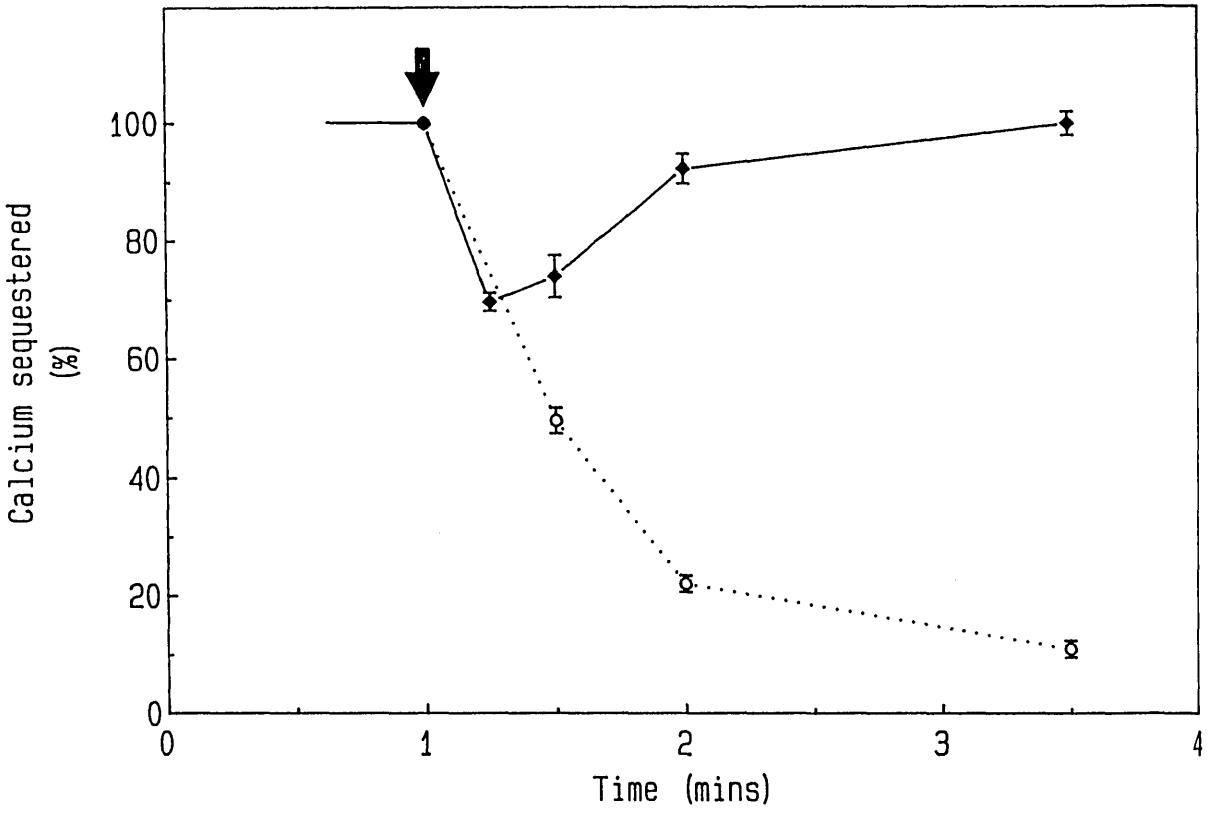


Figure 3.4

Time course of the release of sequestered intracellular membrane calcium by Ins(1,4,5) P_3

$^{45}Ca^{2+}$ uptake in the presence of 3μM Ca^{2+} was allowed to proceed until steady state was reached after 20 mins, at which time (time t=1 on graph) 10μM Ins(1,4,5)P_3 (◆) or 2mM A23187 (O) was added [indicated by arrow]. Reactions were stopped at the times indicated by rapid filtration through a 0.45μm filter as described in section 2.3.4. Vertical bars represent S.D. (n=3). '100% Ca^{2+}' in the membranes represented 14.2 ± 0.32 nmol/mg of protein, the steady state values reached in the presence of 3μM external Ca^{2+} (see figure 3.3).

elicited by the first application of $Ins(1,4,5)P_3$. The membranes are therefore not desensitised by $Ins(1,4,5)P_3$ addition, and the refilling of the vesicles with Ca^{2+} during the reuptake phase is probably related to $Ins(1,4,5)P_3$ degradation.

3.6 Summary

The results presented in this chapter clearly indicate that highly purified platelet surface and intracellular membrane vesicle fractions were successfully isolated using the protocol descibed in section 2.2. The following observations agree with those of the original workers characterising the membrane fractions prepared using this protocol (see Menashi *et al.*, 1981; 1982; 1984; Authi and Crawford, 1985).

(1) The presence of the contractile proteins actin and myosin in the SM fraction and their absence from the IM fraction.

(2) The enrichment of the endoplasmic reticulum marker NADH cytochrome *c* reductase in the IM fraction.

(3) The demonstration that IM vesicles sequester Ca^{2+} in the presence of MgATP whilst SM vesicles do not.

(4) The demonstration that $Ins(1,4,5)P_3$, when added to calcium-loaded IM vesicles, causes a rapid release of Ca^{2+} followed by reuptake within 1 min, whilst the ionophore A23187 liberates Ca^{2+} irreversibly.

The observations in (3) and (4) indicate that most of the vesicles in the IM fraction are likely to be orientated such that the inside of the vesicle corresponds to the inside of the DTS. No information is available concerning the orientation of the SM vesicles.

Chapter 4

RESULTS II

PLATELET SURFACE MEMBRANE CHANNELS

4.1 Introduction

This chapter details the results of single channel experiments carried out on the highly purified platelet surface membrane fraction. Fusion of vesicles from this fraction with a planar phospholipid bilayer in the presence of KCl solutions yields a predominantly anion-selective channel with characteristic bursting behaviour. The initial identification of this channel was communicated to the Physiological Society (Semba and Williams, 1986).

A detailed characterisation of the conduction properties of this channel has been carried out. Some of the results presented in this section have been published (Manning and Williams, 1989a,b). Reprints of these publications are attached at the back of this volume. Computer-aided analysis of the gating characteristics of this channel has also been carried out.

The results of experiments designed to identify possible agonist-activated Ca^{2+} channels in the surface membrane vesicle fraction are presented in section 4.12.

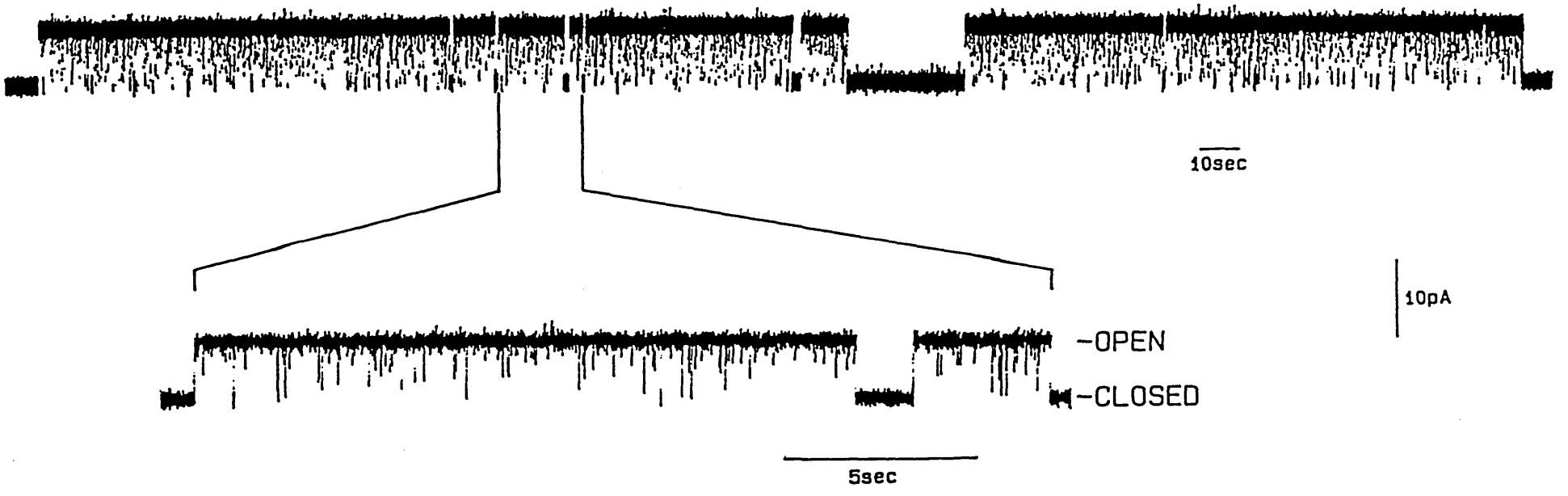
4.2 Reconstitution of surface and mixed membrane vesicles into planar bilayers

Planar phospholipid bilayers comprising 70% PE/30% PS were formed in 150mM KCl, 5mM HEPES/Tris, pH 7.2 and platelet membrane vesicles from the surface membrane (SM) were added to the *cis* chamber to a final protein concentration of approximately 10μg per ml. Creation of an osmotic gradient (3:1, *cis:trans*) and addition of 1mM $CaCl_2$ (*cis*), as described in section 2.4.3, resulted in fusion of channel-containing vesicles, usually within 20 mins. The solutions in the *cis* and

trans chambers were then either exchanged (by perfusion) with the desired experimental solutions, or an appropriate volume of stock 3M KCl solution added to achieve the required KCl concentration. Fusion with neutral bilayers (100% PE) was more difficult to achieve; channels were often not incorporated after 1hour following addition of vesicles to the *cis* chamber, despite increasing the osmotic gradient to 9:1 (*cis:trans*). All data presented concerning the SM channel was therefore recorded from channels reconstituted into charged bilayers (70% PE/30% PS).

Fusion of vesicles from the SM fraction under the conditions described yields a channel with distinctive 'bursting' behaviour. Fusion of vesicles from the intracellular membrane fraction does not yield this channel (see section 5.4). Figure 4.1 shows a representative recording following reconstitution of a channel from the SM. The channel is bathed in symmetrical 450mM KCl, 5mM HEPES/Tris, pH 7.2, and held at -40mV. The lower trace in the figure shows single channel fluctuations in more detail at a higher time resolution. The channel exhibits characteristic bursting behaviour in which comparatively long 'silent' periods alternate with 'active' periods.

A possible criticism levelled at experiments studying the biophysical characteristics of this channel (identified from a membrane vesicle fraction obtained following a lengthy preparative procedure) would be the potential detrimental effect of the preparation on the single channel protein. It was considered possible that exposure of the surface membrane to neuraminidase treatment and high-voltage continuous flow electrophoresis might have altered the channel protein leading to alterations in its conduction properties. This problem was addressed by measuring the


10sec
10pA
-OPEN
-CLOSED
5sec

conductance characteristics of channels fused from the following membrane fractions:

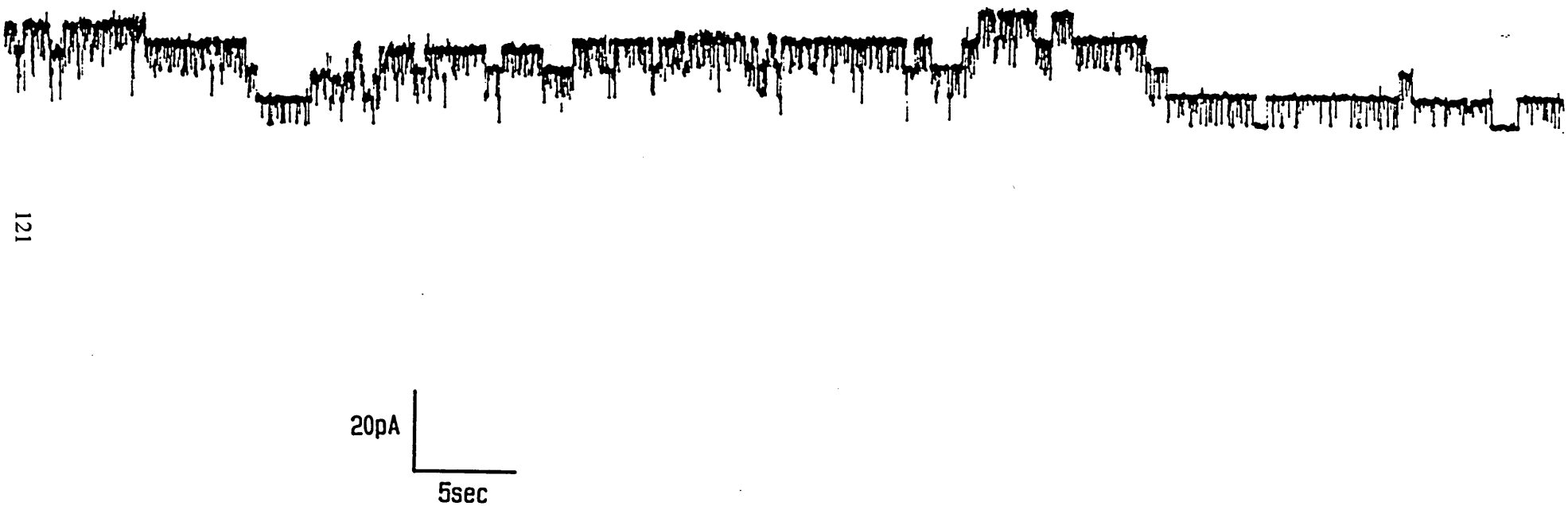
A: mixed membrane treated with neuraminidase

B: mixed membrane, untreated with neuraminidase

C: surface membrane, treated with neuraminidase and subjected to CFE

Channels appear qualitatively similar in behaviour whether vesicles from fractions A, B or C are used. Figure 4.2 shows a recording of (at least) 5 channels observed following fusion of MM vesicles untreated with neuraminidase. The ionic and voltage conditions are the same as those in figure 4.1. Multiple channel fusions of this type were fairly rare occurrences (<10% of all fusion events under the conditions described yielded $\geq$ 2 channels) regardless of the membrane fraction and were **not** a particular characteristic of fusions of non-neuraminidase treated MM vesicles. Comparing figures 4.1 and 4.2 illustrates that there are no obvious differences in channel activity (e.g. no appearance of substates or obvious changes in gating) following neuraminidase treatment and exposure of the vesicles to high-voltage CFE.

Current-voltage relationships in symmetrical 450mM KCl, 5mM HEPES/Tris, pH 7.2 were measured for channels from the 3 membrane vesicle sources, A, B or C. Graphs of these relationships are illustrated in figure 4.3. An example of single channel recordings from one such experiment (membrane source C) at a range of holding potentials is shown in figure 4.4. For A, B and C the current-voltage relationships (figure 4.3) are non-linear and channel current is said to rectify, with less current flowing at positive than at negative holding potentials. Visual examination of the data indicates no obvious differences in the three curves.


20pA
5sec

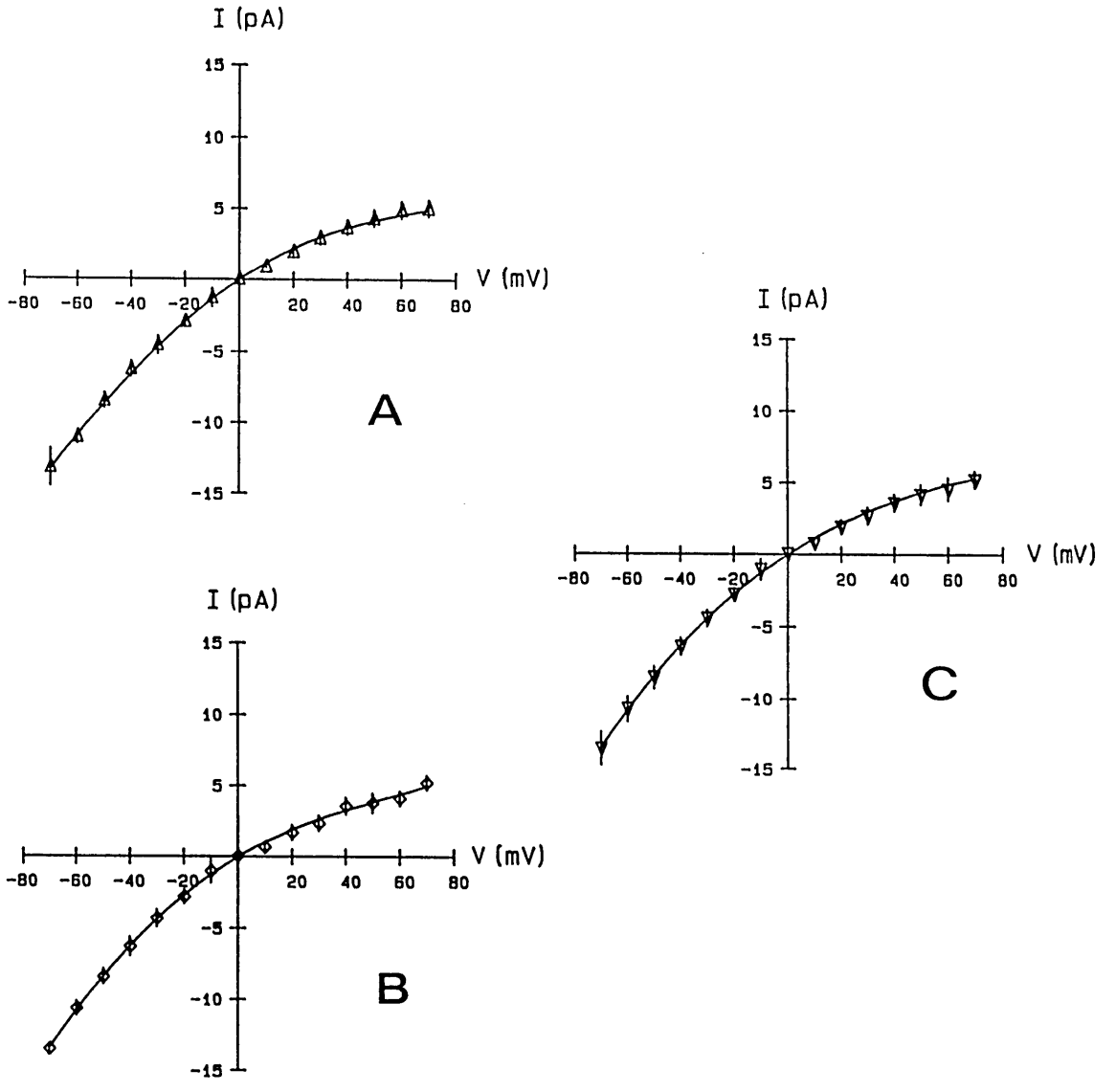


Figure 4.3

Current-voltage relationships in symmetrical 450mM KCl

Single channel current-voltage relationships in symmetrical 450mM KCl, 5mM HEPES/Tris, pH 7.2 for channels fused from the following membrane vesicle populations. **A**: mixed membrane treated with neuraminidase; **B**: mixed membrane, untreated; **C**: surface membrane. Each point represents the mean ± S.D. of measurements from 12 (**A** and **C**) or 6 (**B**) separate channel recordings. Curves fitted to the data points have no theoretical significance.

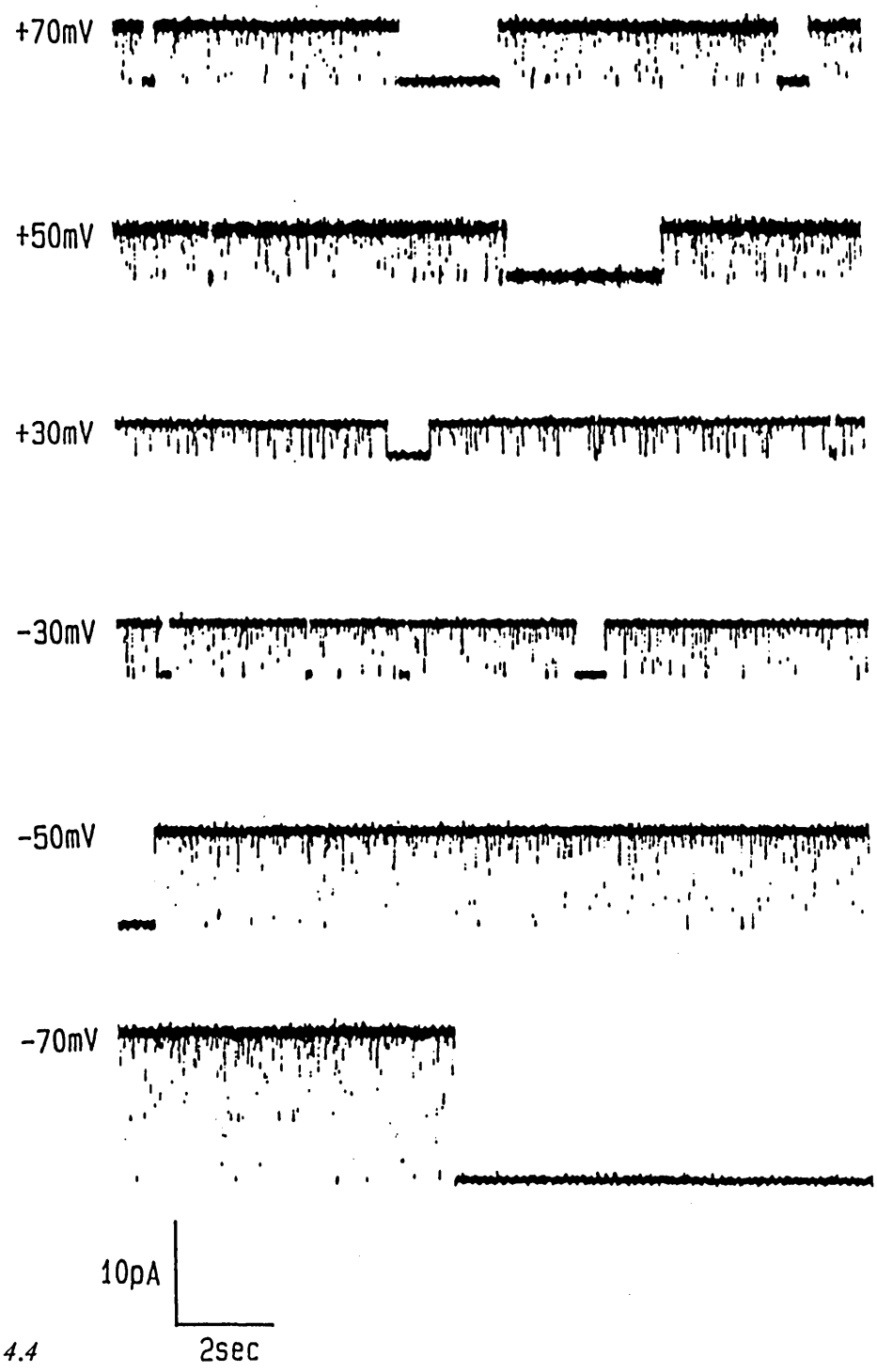


Figure 4.4

Single channel activity at a range of holding potentials

Channel fluctuations from the SM channel at the holding potentials indicated on the left, in symmetrical 450mM KCl, 5mM HEPES/Tris, pH 7.2. The recordings are shown low pass filtered at 250Hz. Traces at negative holding potentials have been inverted so that all channel openings are shown as upwards deflections.

Membrane fraction	G at -40mV (pS)	G at +40mV (pS)	n
MM (A)	160.1 ± 11	91.4 ± 14	12
MM (B)	158.3 ± 17	88.5 ± 15	6
SM (C)	161.0 ± 16	92.5 ± 16	12

Table 1

Comparison of conductance values at -40mV and +40mV

Mean conductance values, G, (± standard deviation) at -40mV and +40mV in symmetrical 450mM KCl measured from the experiments illustrated in figure 4.3 for channels from the following membrane sources:

A: Mixed membrane treated with neuraminidase

B: Mixed membrane untreated with neuraminidase

C: Surface membrane treated with neuraminidase and subjected to CFE

Conductance values at -40mV and +40mV from these experiments are summarised in table 1. It is obvious from the data that there is no significant difference in conductance values from channels of origin A, B or C, as previously defined.

In symmetrical 450mM KCl, a single channel conductance for the channel of ~160pS is obtained at -40mV and a conductance of ~90pS at +40mV.

From these results it is surmised that:

(i) the channel protein exhibiting the single channel activity observed in these experiments originates from the platelet surface membrane.

(ii) its conduction properties are preserved following neuraminidase treatment and membrane purification by high voltage continuous flow electrophoresis.

Further support for these statements was obtained from experiments carried out on a fraction of human platelet plasma membranes prepared by separation on alkaline Percoll gradients by Dr. K. Syha according to the method described by Fauvel *et al.* (1986) (and kindly donated for these experiments). This membrane separation procedure relies on the effect of pH on the apparent density of intracellular membranes. A channel identified following fusion of plasma membrane vesicles prepared by this method had a single channel conductance of 160.8 ± 19pS at -40mV and 89.6 ± 8pS at +40mV (mean ± S.D., n=3 channels) in symmetrical 450mM KCl, 5mM HEPES/Tris, pH 7.2 (*data not shown*). These values are similar to those obtained in the experiments summarised in table 1. The channel from the Percoll preparation also displayed qualitatively similar gating behaviour to the channels illustrated in figures 4.1 and 4.2. However, various other small channels

were also incorporated into the bilayer from this membrane fraction and bilayers often broke immediately following addition of vesicles to the *cis* chamber. Bilayer breakage may have been due to the presence of Percoll silica particles remaining in the vesicle fraction. The origin of the small channels (not observed following fusion of SM vesicles prepared by CFE) is uncertain, although they may arise from contaminating membrane of intra-platelet origin (e.g. mitochondria, dense granules etc).

Nevertheless, identification of a similar channel to the one described in this section from an alternative membrane preparation is further corroboration that the neuraminidase treatment and high-voltage CFE method applied has not altered the channel protein; at least as far as can be ascertained from the conduction measurements described.

In subsequent experiments channels were fused either from the MM (neuraminidase treated) or SM vesicle fraction (prepared by CFE). No distinction is made between the two vesicle sources and the term SM channel is used throughout.

CONDUCTION PROPERTIES OF THE SM CHANNEL

4.3 Dependence of single channel conductance on the KCl concentration

The dependence of the single channel conductance on the surrounding bulk KCl concentration was investigated. Current-voltage relationships were measured for the channel in a range of symmetrical KCl solutions from 50mM to 3000mM (all buffered with 5mM HEPES/Tris to pH 7.2). In all cases the relationships were

found to be non-linear (i.e. rectification was apparent; cf. figure 4.3). Mean conductance values (± S.D.) at -40mV at a given KCl concentration are shown in figure 4.5. The data could be fitted with a simple Michaelis-Menten type saturation curve, where;

$$G = \frac{G_{max}}{1 + (K_d/[Cl^-])} \qquad \text{(equation 17)}$$

where: K_d is the dissociation constant for Cl^-

G_{max} is the maximum conductance

The values of K_d and G_{max} were obtained from an 'Enzfitter' computer programme (Elsevier, BIOSOFT, Cambridge, U.K.) which used the method of least squares to find suitable best-fit values for K_d and G_{max} which minimised the reduced χ^2 value.

For the data shown in figure 4.5, half maximal conductance is achieved at a concentration of 1008mM KCl, and the curve saturates at a conductance of 503pS.

4.4 Single channel rectification

It was considered possible that the single channel rectification observed in current-voltage relationships might be caused by assymetric block by the buffering compounds, HEPES and Tris, in the solutions. The effect of altering the concentration of HEPES and Tris on the single channel activity was therefore investigated.

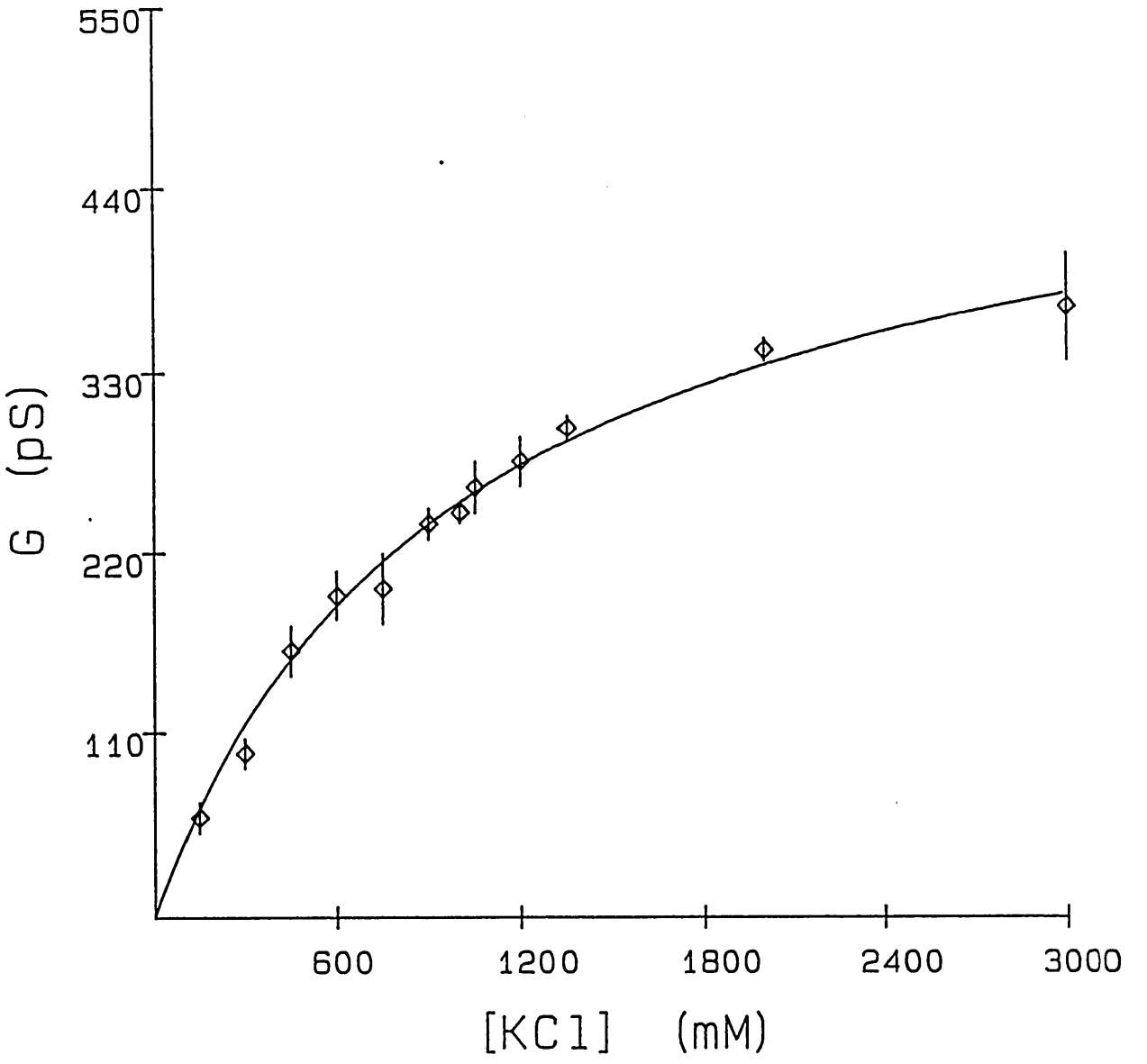


Figure 4.5

Dependence of single channel conductance (G) on the KCl concentration

All conductance values (pS) were measured at -40mV and points represent the mean ± S.D. of 4 to 12 separate determinations at each KCl concentration. The curve was drawn according to equation 17 (see text), where G_{max} = 503pS and K_d = 1008mM.

Figure 4.6A shows the current-voltage relationship for the SM channel exposed to symmetrical 450mM KCl buffered with either:

(i) 0.5mM HEPES/KOH, pH 7.2 ('**reduced HEPES**'),

(ii) 5mM HEPES/KOH, pH 7.2 ('**no Tris**'), or

(iii) 5mM HEPES/Tris, pH 7.2 ('**standard**' conditions)

In the absence of Tris, rectification appears slightly less than that obtained in 'standard' conditions (the HEPES concentration being the same in both cases). However, when the concentration of HEPES buffer is reduced tenfold, from 5 to 0.5 mM, current at positive holding potentials increases significantly and rectification is considerably reduced. In figure 4.6B, the mean conductance (G) measured at each holding potential under 'reduced HEPES' conditions is taken as $G_{0.app}$. The ratio $G/G_{0.app}$ is plotted with G values from either 'no Tris' conditions or 'standard' conditions. In both of these conditions the HEPES concentration is the same (5mM), and in both cases blocking of single channel conductance is apparent. The degree of block is seen to increase as the holding potential is made more positive. With the added presence of Tris buffer ('standard conditions'), the apparent block is increased.

4.5 Anion *vs* cation selectivity

Experiments were carried out in asymmetric KCl solutions to determine the anion *vs* cation selectivity of the channel. Reversal potential measurements determined in the presence of a KCl gradient across the bilayer demonstrated that although the channel is preferentially selective for Cl^-, K^+ is also permeant.

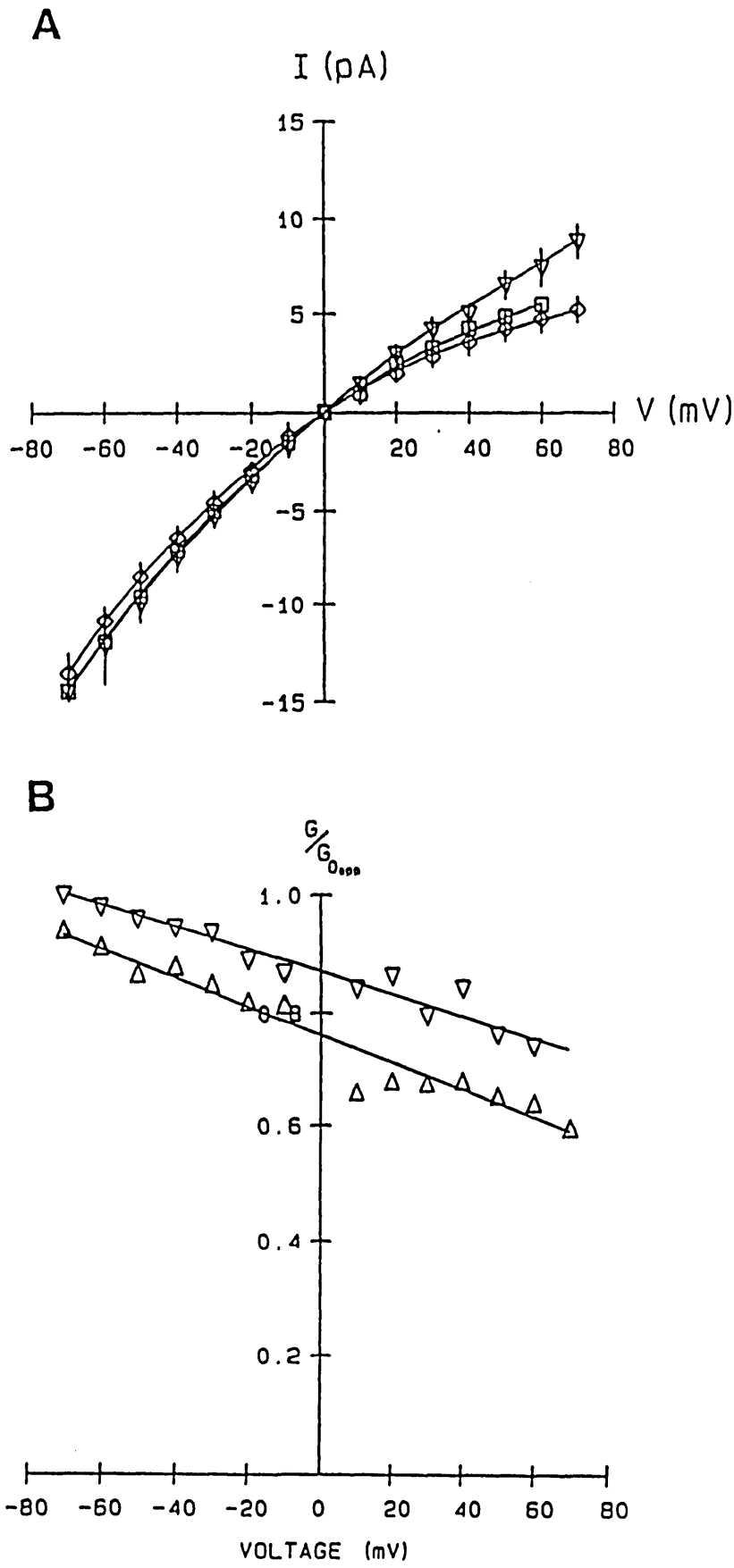

A
I (pA)
15
10
5
-5
-10
-15
V (mV)
-80
-60
-40
-20
20
40
60
80
B
G/G0
1.0
0.6
0.4
0.2
-80
-60
-40
-20
0
20
40
60
80
VOLTAGE (mV)

Figure 4.7 (Δ) shows the single channel current flow over a range of holding potentials from -70mV to +70mV with a 3:1 KCl gradient across the bilayer (*cis*, 450mM KCl, 5mM HEPES/Tris, pH 7.2: *trans*, 150mM KCl, 5mM HEPES/Tris, pH 7.2). The measured reversal potential, +16mV, deviates from that calculated from the Nernst equation (equation 5, section 2.5.1) for an ideally anion-selective channel under these conditions (i.e. +28mV). This deviation from the Nernst potential does not vary significantly in size upon reversing the gradient across the bilayer. Figure 4.7 (∇) shows the single channel current-voltage relationship with a 1:3 KCl gradient (150mM KCl *cis*: 450mM KCl *trans*). The channel appears to show no significant asymmetry in cation/anion discrimination.

Experiments carried out with an increased KCl gradient of 5:1 (750mM KCl *cis*: 150mM KCl *trans*) are also shown in figure 4.7. There is a shift in the measured reversal potential to +22mV. Under these conditions, the Nernst equation predicts a reversal potential of +41mV for an ideally Cl^- selective channel.

The results of these reversal potential measurements are summarised in table 2. Anion/cation selectivity ratios are calculated from an appropriate version of the GHK equation (equation 6, section 2.5.1). They indicate that the channel is over 4 times more permeable to Cl^- than K^+. The current measured in these experiments is therefore the resultant of the net movement of both Cl^- and K^+ through the channel.

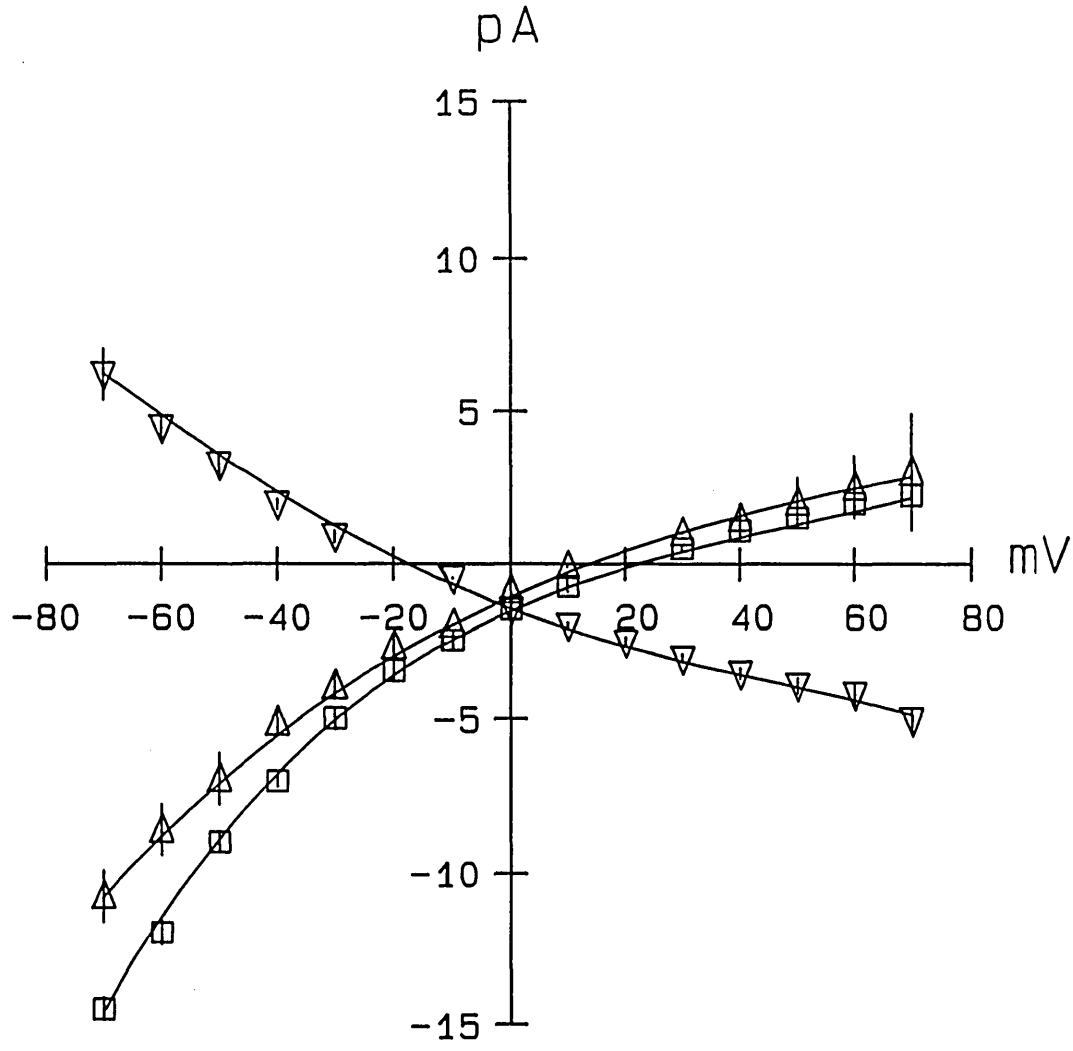


Figure 4.7

Test for anion/cation selectivity

Single channel current-voltage relationships under the following conditions: [KCl] *cis* : [KCl] *trans* - (Δ) 450:150 mM; (▽) 150:450 mM; (□)750:150 mM. All solutions were buffered with 5mM HEPES/Tris to pH 7.2. Each point represents the mean ± S.D. for 3 to 10 separate determinations under each experimental condition. Curves fitted to the data points have no theoretical significance. A summary of the measured reversal potentials and calculated anion/cation selectivity ratios for these experiments is given in table 2.

cis (mM KCl)	*trans* (mM KCl)	E (mV)	number of expt.	P_{Cl}/P_K
450	150	+16	(10)	4.2
150	450	-17	(3)	4.7
750	150	+22	(8)	4.2

Table 2

Anion *vs* cation selectivity

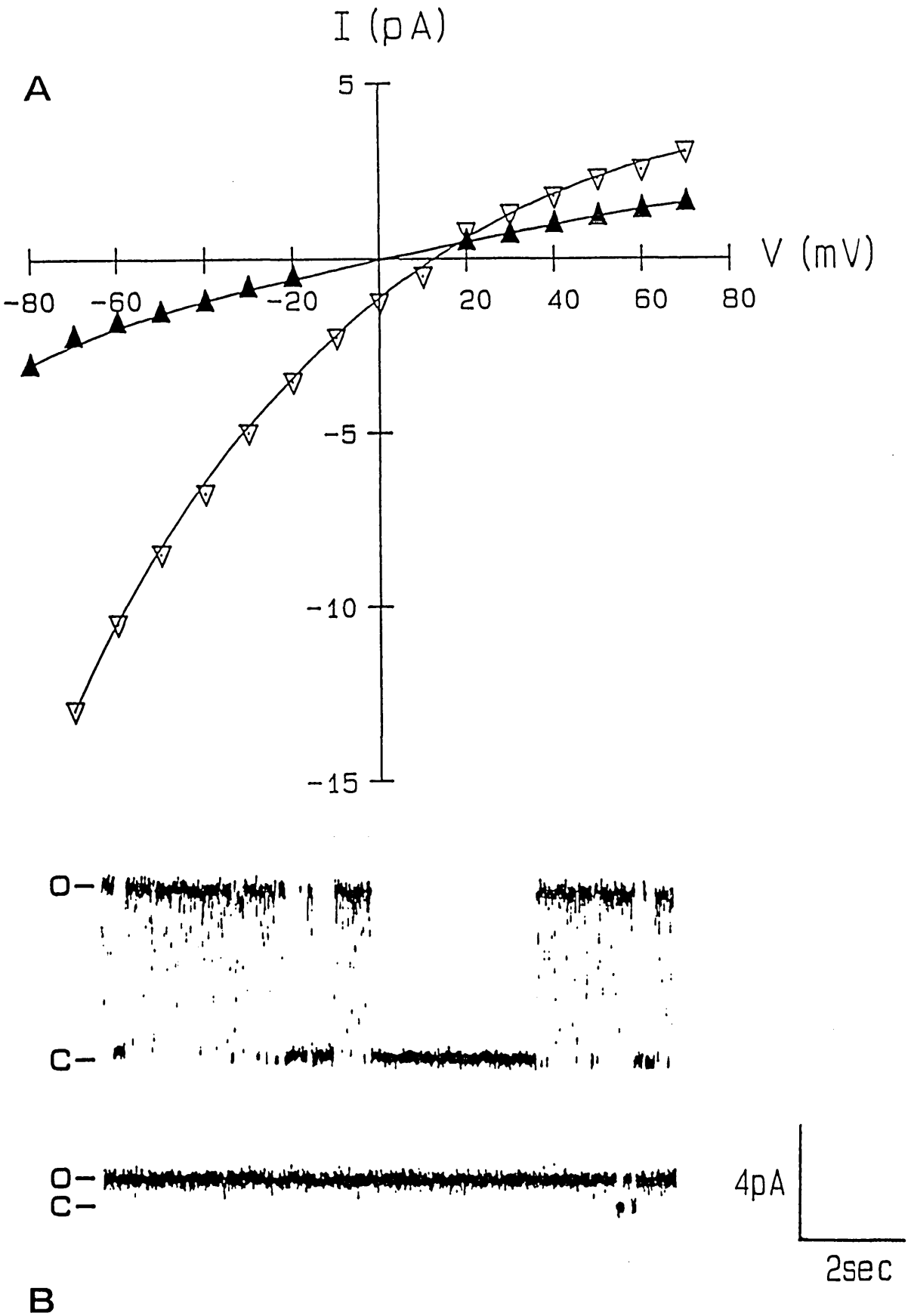
Summary of experiments carried out in asymmetric KCl solutions buffered with 5mM HEPES/Tris to pH 7.2 as shown in figure 4.7. Reversal potentials (E) are measured to the nearest mV. Ratios P_{Cl}/P_K are calculated from equation 6, section 2.5.1.

4.6 Cation conductance

An inert, nonpermeant cation was sought to allow measurement of the current carried by anions alone. An obvious candidate, tetraethylammonium, TEA^+, was tested, but found to be permeant. Figure 4.8A shows the current-voltage relationships with a 3:1 KBr and a 3:1 TEABr gradient across the bilayer (*cis*, 450mM KBr: *trans*, 150mM KBr or *cis*, 450mM TEABr: *trans*, 150mM TEABr). From the reversal potential measurement in asymmetric KBr (+13mV), the P_{Br}/P_K ratio is calculated as 3.0 (equation 6, section 2.5.1). Thus, under these conditions Br^- is 3 times more permeant than K^+.

In asymmetric TEABr, there is less apparent rectification in single channel current and the current reverses at 0mV. This indicates that under these conditions TEA^+ and Br^- are equally permeant. The single channel records shown in figure 4.8B illustrate an alteration in gating observed in asymmetric TEABr solutions compared with that observed in KBr. In TEABr, the channel remains predominantly in the open state with only occasional brief closures.

Experiments were also attempted in asymmetric succinyl choline-Cl, gallamine-Cl, and choline-Cl. Channels were initially fused in standard KCl solutions as described in section 4.2, and then the *cis* and *trans* chambers perfused out with the test solutions (100mM in each case buffered with 5mM HEPES/Tris to pH 7.2). In the presence of succinyl choline and gallamine solutions difficulties were experienced with repeated breakage of bilayers on perfusion. In two experiments where choline-Cl was successfully exchanged into the chambers by perfusion and a 3:1 gradient established (300mM *cis*:100mM *trans*), choline appeared to be permeant through the channel. However, the single channel records in these


I (pA)
A
5
V (mV)
-80
-60
-20
20
40
60
80
-5
-10
-15
O
C
O
C
4pA
2sec
B

experiments were extremely noisy making quantitative measurements difficult (*data not shown*).

4.7 Relative anion permeabilities and conductances

The possibility that a divalent anion, such as SO_4^{2-}, might be impermeant was investigated. Figure 4.9 shows the current-voltage relationship for channels bathed in 225mM K_2SO_4 *cis*: 450mM KCl *trans*. Under these conditions the current reverses at -21mV and the permeability ratio P_{SO4}/P_{Cl} is 0.32 (equation 8, section 2.5.1).

The relative anion permeabilities of various monovalent anions compared to Cl^- were estimated from reversal potential measurements with 450mM KCl in the *trans* chamber and either 450mM KF, KBr, KI, KNO_3, KSCN, K-acetate or K-gluconate in the *cis* chamber. Channels were fused in asymmetric KCl solutions (750mM KCl *cis*: 450mM KCl *trans* and then the KCl in the *cis* chamber substituted with the test solution by exchange perfusion. All solutions were buffered to pH 7.2 with 5mM HEPES/Tris. Figure 4.10 shows six of the current-voltage curves obtained from these experiments. As shown in graph A of the figure, when Cl^- in the *cis* chamber was substituted by F^-, the intersection of the current-voltage curve was shifted to a negative potential (-20mV), indicating that F^- is less permeant than Cl^-. The reversal potentials for Br^- and SCN^- are found to be positive (+10mV and +20mV respectively), indicating that these ions are accepted by the channel in preference to Cl^-. In graph B of figure 4.10, it can be seen that gluconate ions are less permeant and NO_3^- and I^- are more permeant than Cl^-.

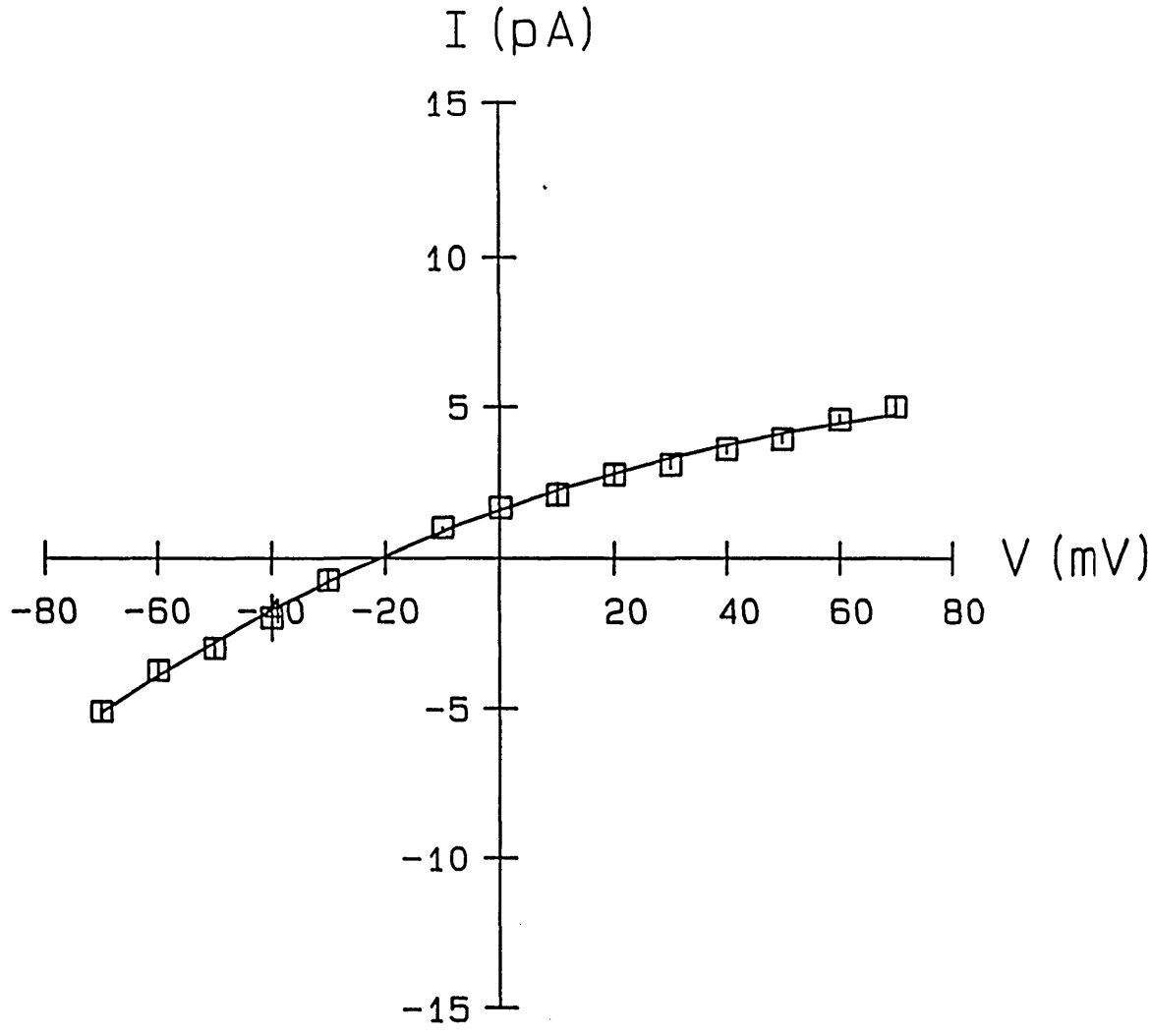
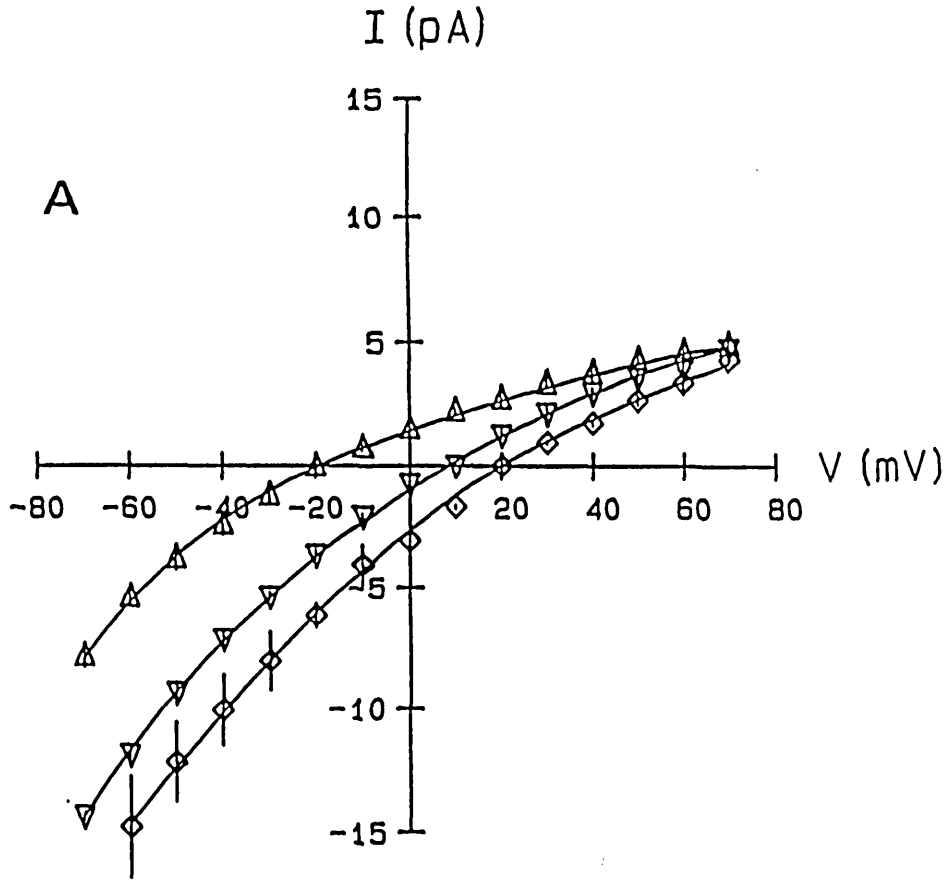
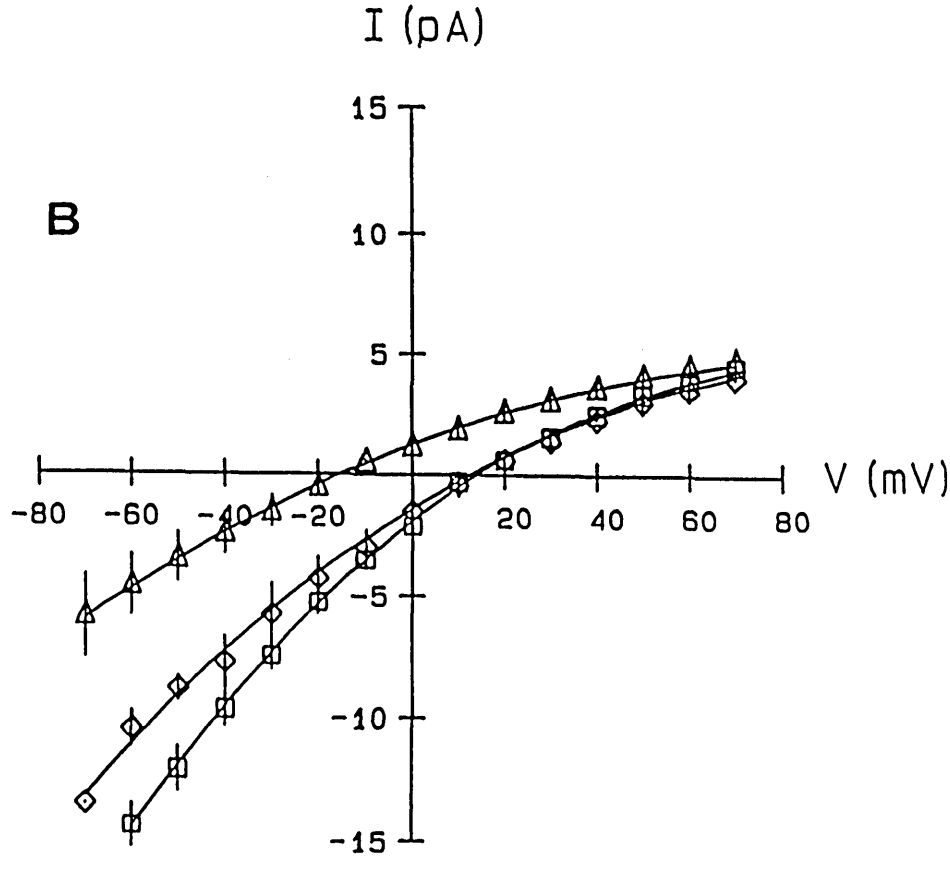


Figure 4.9

SO_4^{2-} permeation through the channel

Single channel current-voltage relationship with 225mM K_2SO_4 in the *cis* chamber and 450mM KCl in the *trans* chamber (both solutions buffered with 5mM HEPES/Tris to pH 7.2). Each point represents the mean current ± S.D. for measurements from 3 separate channels. The curve fitted to the data points has no theoretical significance.


I (pA)
A
15
10
5
-5
-10
-15
V (mV)
-80
-60
-40
-20
20
40
60
80


I (pA)
B
15
10
5
-5
-10
-15
V (mV)
-80
-60
-40
-20
20
40
60
80

Test anion A	E (mV)	number of expt.	P_A/P_{Cl}
SULPHATE	-21	3	0.32
FLUORIDE	-20	8	0.32
ACETATE	-17	5	0.35
GLUCONATE	-16	10	-*
CHLORIDE	0	--	1.00
BROMIDE	+10	7	1.58
IODIDE	+13	4	1.76
NITRATE	+14	8	2.23
THIOCYANATE	+20	5	2.48

* No activity value was available for gluconate

Table 3

Relative anion permeabilities

Reversal potential shifts, E, to the nearest mV, are expressed with respect to control KCl solutions. In all experiments the *trans* chamber contained 450mM KCl; the *cis* chamber contained the K salt of the test anion, A, at the same concentration (450mM), except for sulphate (225mM). Permeability ratios, P_A/P_{Cl} are calculated from appropriate versions of the GHK equation as detailed in section 2.5.1 (equation 7 or 8). P_K/P_{Cl} is taken as 0.23 (mean value, see table 2) and is considered to be independent of the anion.

Table 3 summarises the data from the anion permeability experiments in terms of permeability ratios (calculated from equation 7 or 8, section 2.5.1, as appropriate). The sequence of relative anion permeabilities (in the presence of K^+) is as follows:

$$SO_4^{2-} = F^- < \text{acetate}^- < \text{gluconate}^- < Cl^- < Br^- < I^- < NO_3^- < SCN^-$$

The conductance at -40mV of the above anions (except acetate and sulphate) was determined in a separate series of experiments. Channel activity was recorded in symmetrical 450mM KA (where A is the test anion), 5mM HEPES/Tris, pH 7.2. Results are summarised in the chart in figure 4.11. Among the monovalent anions investigated, nitrate has the highest conductance (198 ± 10pS, n=4) and gluconate the lowest (47 ± 4pS, n=3) (mean ± S.D.).

4.8 Channel block by DIDS, SITS and ATP

Agents which have been used as inhibitors of Cl^- transport proteins were applied to the SM channel; namely DIDS and SITS (Cabantchik and Rothstein, 1972;1974; Russel and Brodwick, 1979; Miller and White, 1984; Nelson *et al*, 1984; Hanrahan *et al.*, 1985) and zinc (Woodbury and Miles, 1973; Franciolini and Nonner, 1987).

Figure 4.12 shows current fluctuations from channels at holding potentials of -40mV and +40mV, recorded after symmetrical application of 100μM DIDS or SITS (in the presence of 450mM KCl, 5mM HEPES/Tris, pH 7.2 *cis* and *trans*). Openings at all positive voltages (+10 to +70mV) are poorly resolved, and at negative voltages (-10 to -70mV) openings are noisy and burst durations appear to be shortened. At both positive and negative holding potentials the single channel

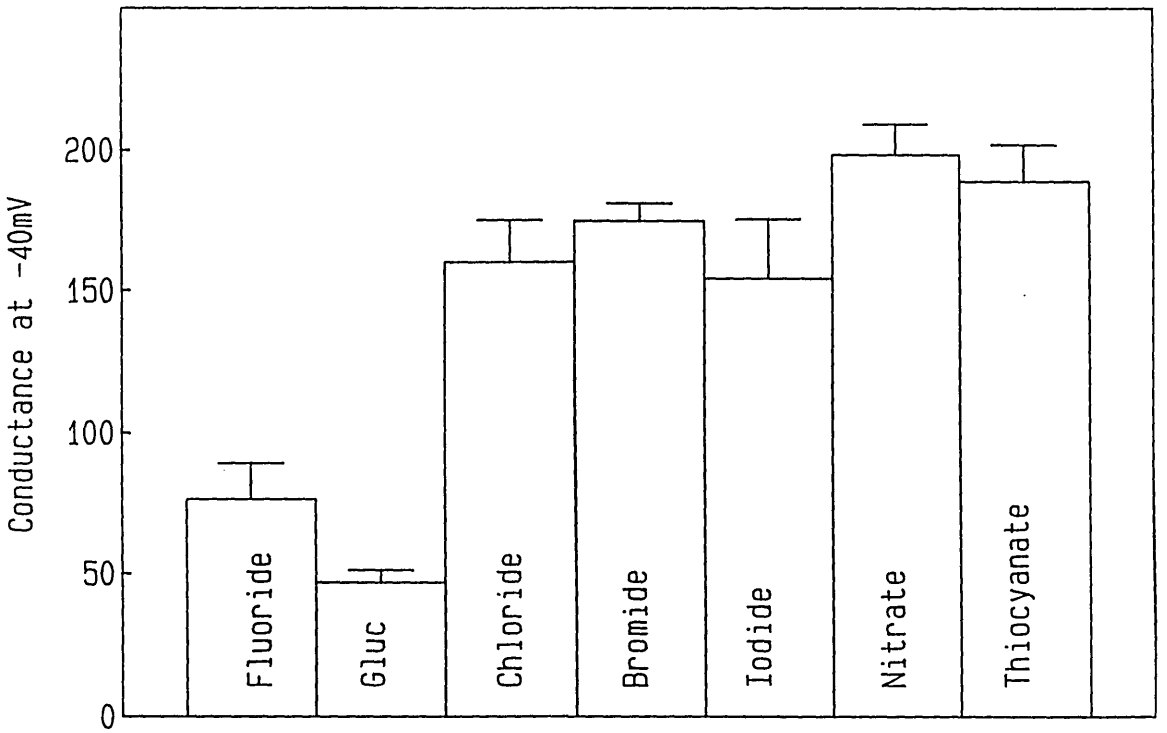


Figure 4.11

Conductances measured at -40mV for various anions

Single channel conductance at -40mV for channels bathed in a symmetrical 450mM solution of the K^+ salt of the anion under test. All solutions were buffered with 5mM HEPES/Tris to pH 7.2. Mean conductance values (from 3-12 experiments) and S.D. bars are shown.

[Gluc = gluconate]

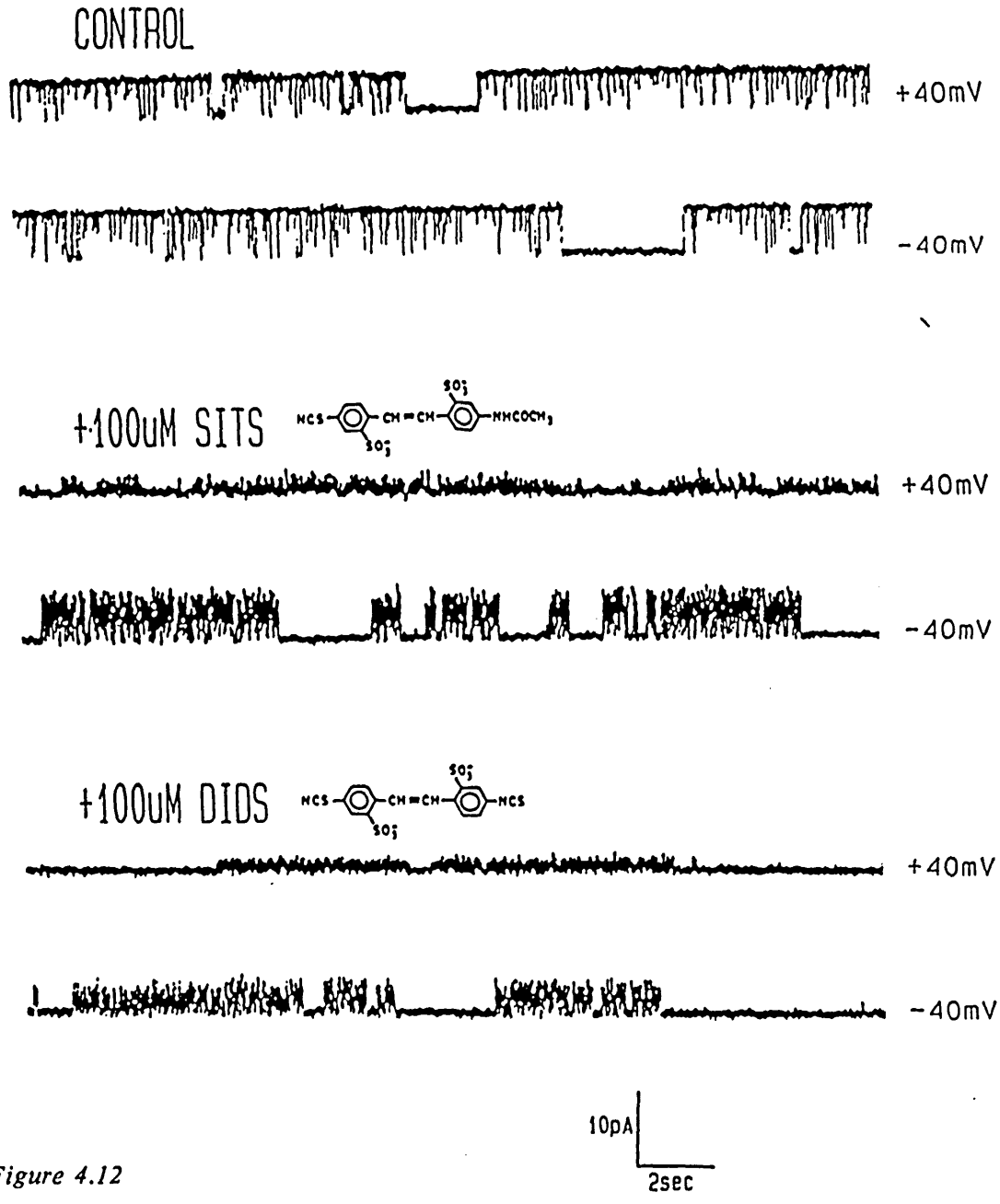


Figure 4.12

The effect of DIDS and SITS on the SM channel

All recordings were made in symmetrical 450mM KCl, 5mM HEPES/Tris, pH 7.2, with 100μM SITS or 100μM DIDS added symmetrically as shown. Current traces are shown low pass filtered at 150Hz at +40 and -40mV. Traces at negative holding potentials have been inverted so that all channel openings are shown as upwards deflections.

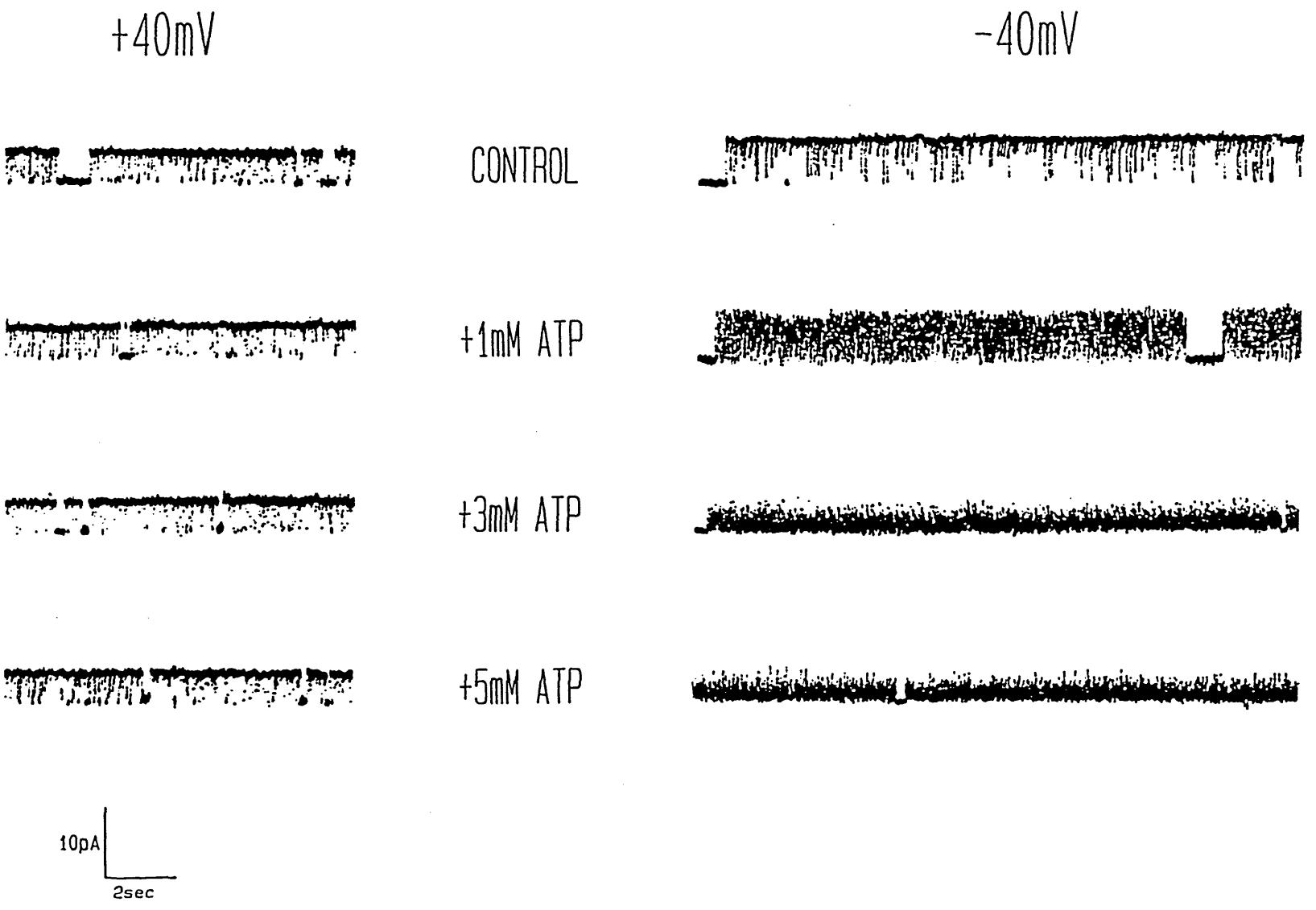
conductance is reduced. The addition of up to 2mM zinc symmetrically has no effect on the activity of the SM channel.

The action of ATP on the channel was also investigated. Figure 4.13 shows the effect of 1, 3 and 5mM ATP added to both the *cis* and *trans* faces of a SM channel. In this case the rapid flickering block is seen only at negative holding potentials (-10 to -70mV) and appears to increase as the ATP concentration is raised. No effect is seen at positive potentials (+10 to +70mV). Thus ATP appears to be effective only from the *cis* face of the channel. The ATP blocking effect is reversed when ATP is removed by perfusion (*data not shown*).

It was found that the blocking effects of SITS, DIDS and ATP were not observed in all applications to the SM channel. In some cases, no effect on single channel activity was found, despite increasing the concentration of agent up to 10mM. The blocking effect of SITS was observed in five out of eight applications; DIDS, three out of six, and ATP, seven out of 10 applications to the channel. A flickery block from the *cis* face of the channel, similar to the block by ATP, was also observed in three out of five applications of 1mM ADP to the channel. However, in all other conduction properties measured (e.g. conductance and selectivity) channels that are sensitive or insensitive to these agents are indistinguishable.

4.9 Application of various other agents to the channel

A number of other agents known to be important in platelet responses or anion channel regulation were applied to the SM channel.


+40mV
-40mV
CONTROL
+1mM ATP
+3mM ATP
+5mM ATP
10pA
2sec

Channels were recorded in 'control' conditions of symmetrical 450mM KCl, 5mM HEPES/Tris, pH 7.2 and the agent added first to the *cis* chamber alone and then also to the *trans* chamber (giving symmetrical conditions). Channel activity was studied over a range of holding potentials for at least 5 minutes following agent application. The following agents are found to have no measurable effect on the activity of the SM channel: Ca^{2+} (up to 5mM) or EGTA (10mM); thrombin (0.5U/ml); PAF (20ng/ml); and $Ins(1,4,5)P_3$ (10μM).

GATING PROPERTIES OF THE SM CHANNEL

4.10 Probability of the channel being open

The probability of the SM channel being in the open state, P_0, was estimated by integrating steady state amplitude histograms as described in section 2.5.2g.

For channels bathed in symmetrical 450mM KCl, 5mM HEPES/Tris, pH 7.2, the first four minutes of data immediately following switching to a given holding potential from 0mV were analysed. In order to allow for possible variation in the proportion of time spent in the open state between channels, results (figure 4.14) are normalised to the P_0 at -40mV for each individual channel (hence values >1.0 are possible).

Data in figure 4.14 quantify visual observations from experiments carried out on this channel, i.e. channel open probability is voltage dependent and at high negative holding potentials ($\geq$ -60mV) the channel tends to close down.

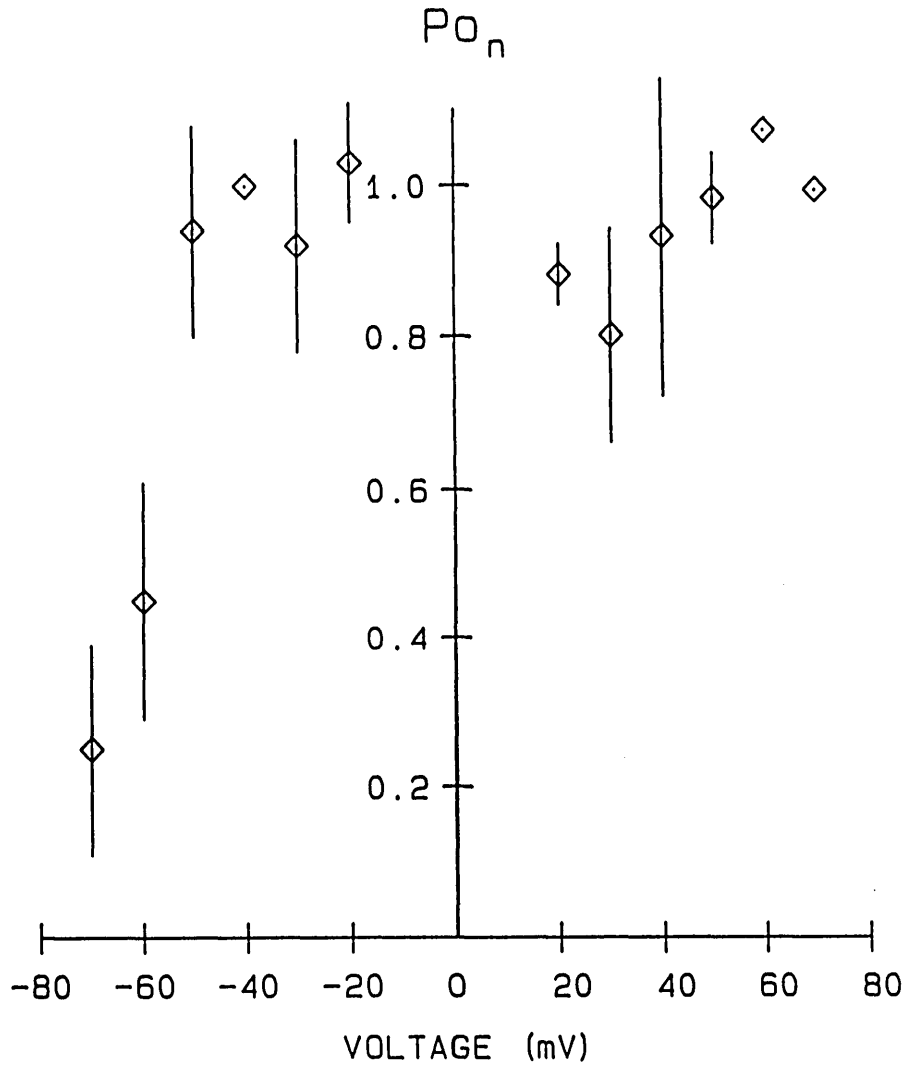


Figure 4.14

Open probability as a function of holding potential

P_{0n}, the probability of opening at a given holding potential normalised to the P_0 at -40mV for each individual channel plotted against the applied holding potential. Mean P_{0n} values are shown ± S.D. (n=10 channels). Channels are bathed in symmetrical 450mM KCl, 5mM HEPES/Tris, pH 7.2. Continuous 4 minute recordings at each voltage were low pass filtered at 250Hz, sampled at 500Hz and P_0 values estimated by integrating amplitude histograms as described in section 2.5.2g.

4.11 Open and closed lifetime analysis

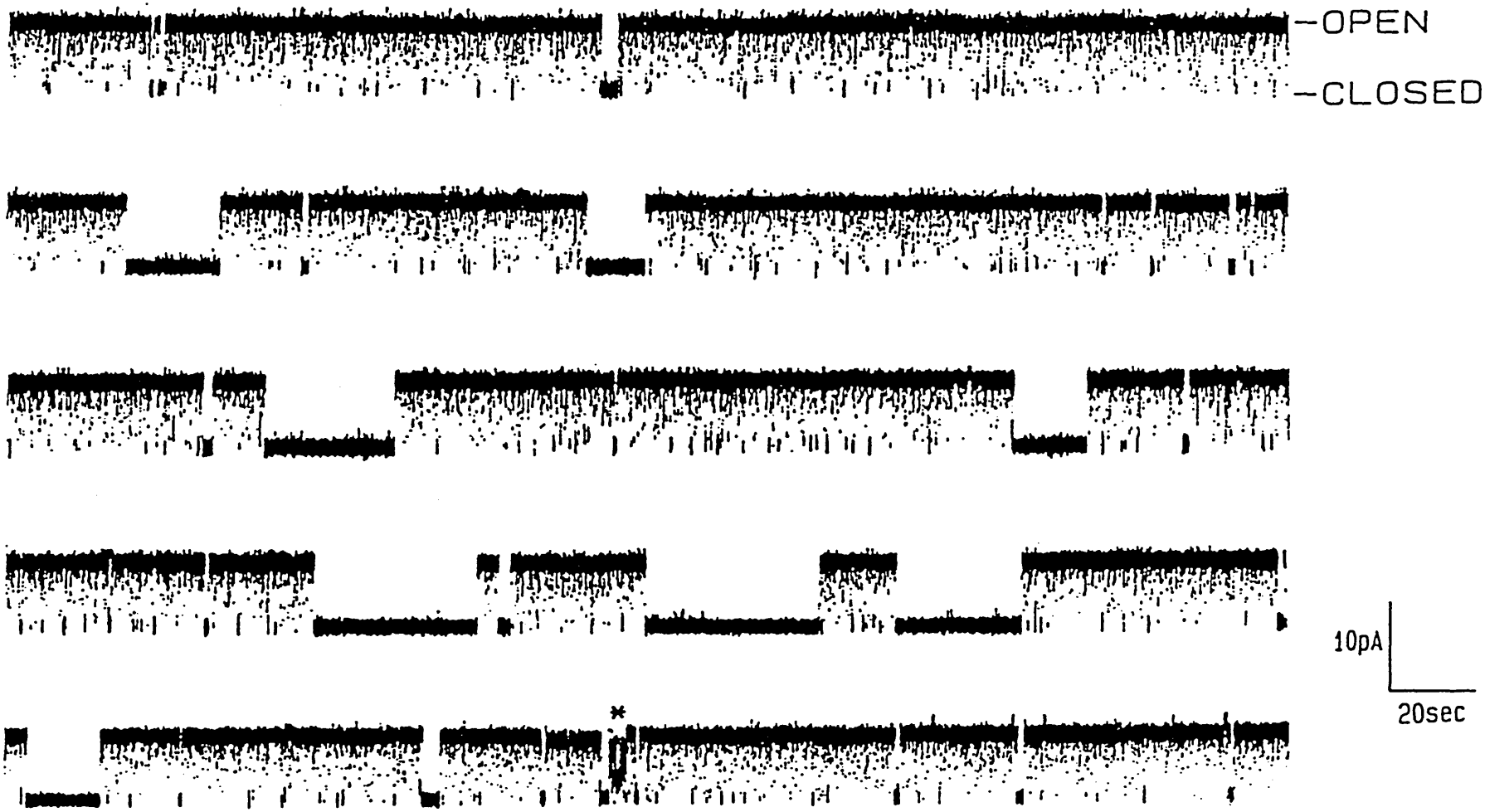
Channel data suitable for lifetime analysis were selected to meet the requirements described in section 2.5.2, i.e. a single active channel in the bilayer, $\geq$ 10mins steady state recording time and low signal/noise ratio.

An example of data recorded at -40mV and used for lifetime analysis is shown in figure 4.15. The starred section of data in the figure indicates an example of a sudden change in kinetic state or 'gearshift' occurrence. These spontaneous variations in opening probability of the channel are found to occur fairly infrequently in channel recordings. Nevertheless they were excluded from the lifetime analysis (though, given the frequency of occurrence, their inclusion would probably not have altered the results). A clearer example of this phenomenon on an expanded timescale is illustrated in figure 4.16. The vertical arrows mark the abrupt changes in open probability of the channel.

Open and closed lifetime analysis was carried out on channels bathed in symmetrical 450mM KCl, 5mM HEPES/Tris, pH 7.2 at the following voltages: +30mV, +40mV, -40mV, -50mV. The following sections (4.11a and b) detail an example of the analysis for the channel illustrated in figure 4.15.

4.11a Open lifetime distribution

Graph A in figure 4.17 shows all the open lifetimes accumulated from the original channel data grouped into a non-cumulative histogram. A total of 7982 events are detected by half-amplitude threshold analysis for this channel. The histogram in B shows the data 'stripped' of open intervals outside the t_{min}-t_{max} range (i.e.


OPEN
CLOSED
10pA
20sec

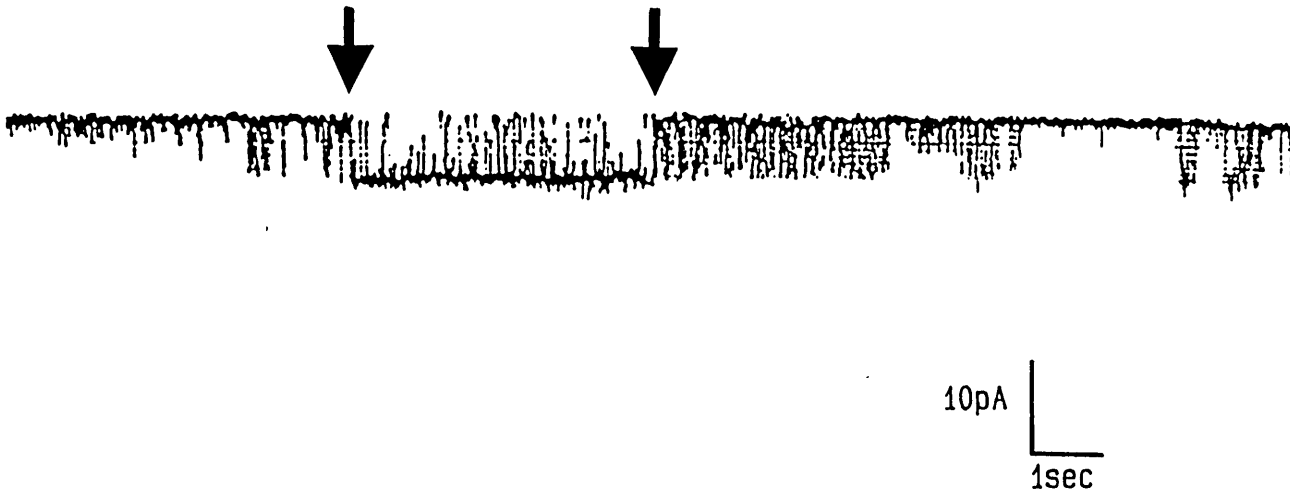
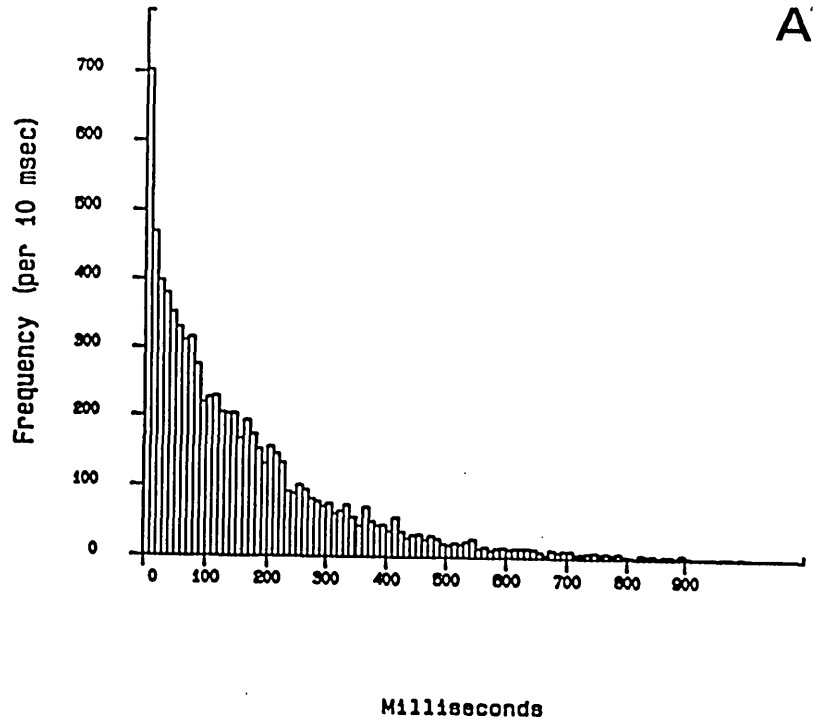
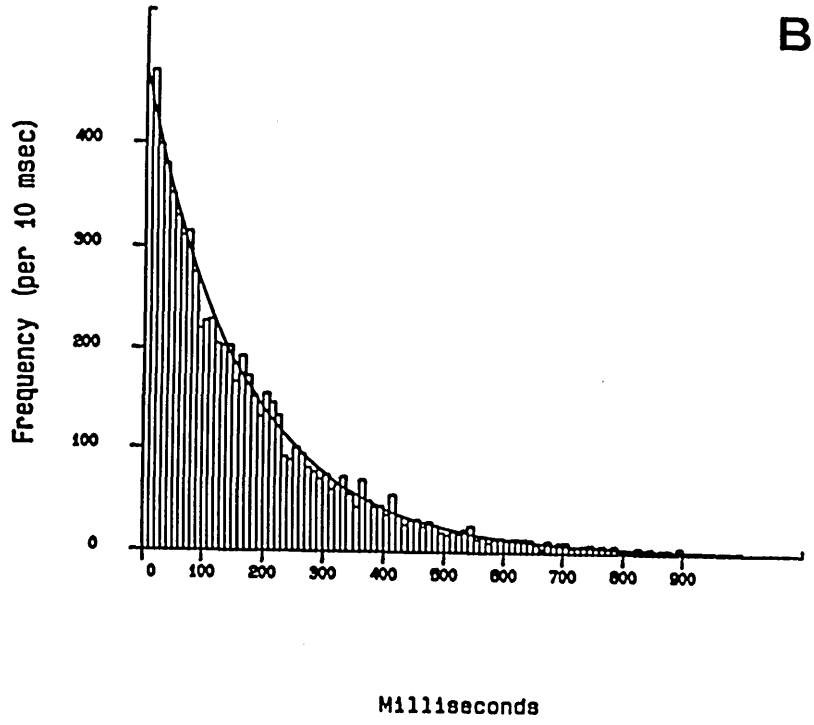


Figure 4.16

Example of a 'gearshift' change in kinetic state

Single channel activity illustrating a 'sudden change in kinetic state' (marked by vertical arrows). The channel is bathed in symmetrical 450mM KCl, 5mM HEPES/Tris, pH 7.2, held at -40mV, and is shown low pass filtered at 150Hz. Upwards deflections represent channel openings.


A
Frequency (per 10 msec)
700
600
500
400
300
200
100
0
0
100
200
300
400
500
600
700
800
900
Milliseconds


B
Frequency (per 10 msec)
400
300
200
100
0
0
100
200
300
400
500
600
700
800
900
Milliseconds

1.6msec < t < 64,000msec). 243 events (~3%) are excluded from the analysis to meet these criteria. Lifetime data are fitted to a p.d.f with a single exponential component by the method of maximum likelihood including the missed events correction as described in section 2.5.2d. A value of 7814 is calculated for N, the corrected number of events. The open lifetime data are best fitted with a single exponential with the following p.d.f;

$f(t)=(1/165.63)exp(-t/165.63)$ (time constant in msec).

A double exponential fitted to the same data gives an equal value for the log(Lik) (-ln(Lik)=47282) to that obtained fitting the single exponential. Thus a single exponential p.d.f. is sufficient to describe the open lifetime distribution.

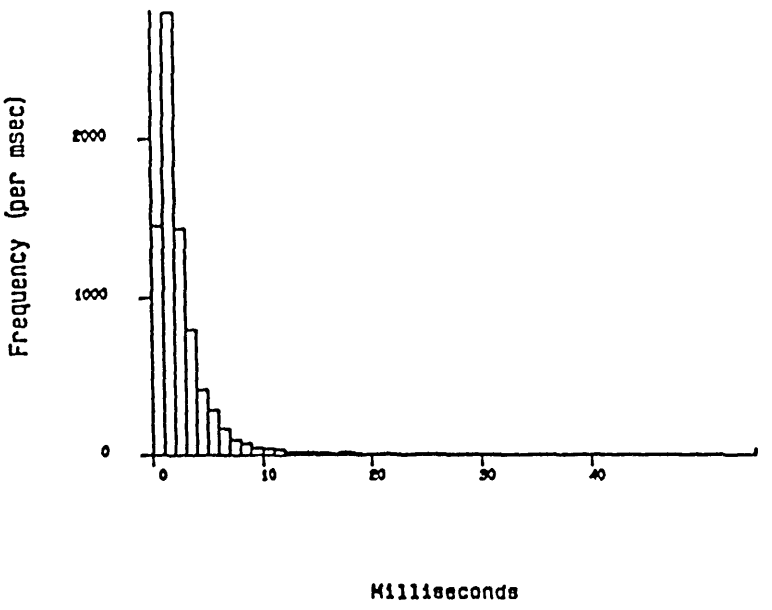
4.11b Closed lifetime distribution

Figure 4.18 shows the closed lifetime analysis for the same channel as 4.11a. In graph A, the lifetime histogram for the original data is shown. 8002 closed events are detected by half-amplitude threshold analysis. Histograms in B and C are of the 'stripped' data (1.6msec < t < 64,000msec) fitted to p.d.fs with two (B) or three (C) exponential components. In this case 4249 events (~53%) in the original data fall outside the t_{min}-t_{max} range.

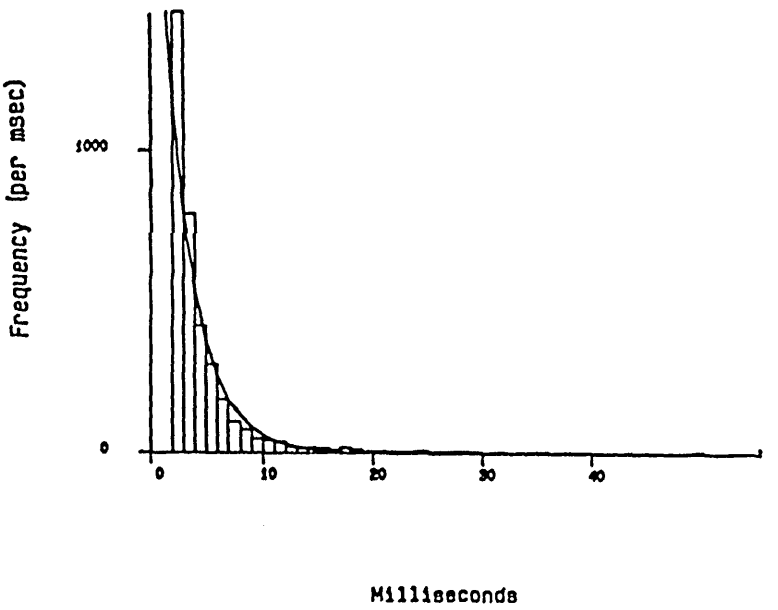
The p.d.fs in B and C (figure 4.18) are as follows [N= corrected number of events]:

B: $f(t)=0.97(1/2.64)exp(-t/2.64) + 0.03(1/1125.69)exp(-t/1125.69)$ [N=6721];

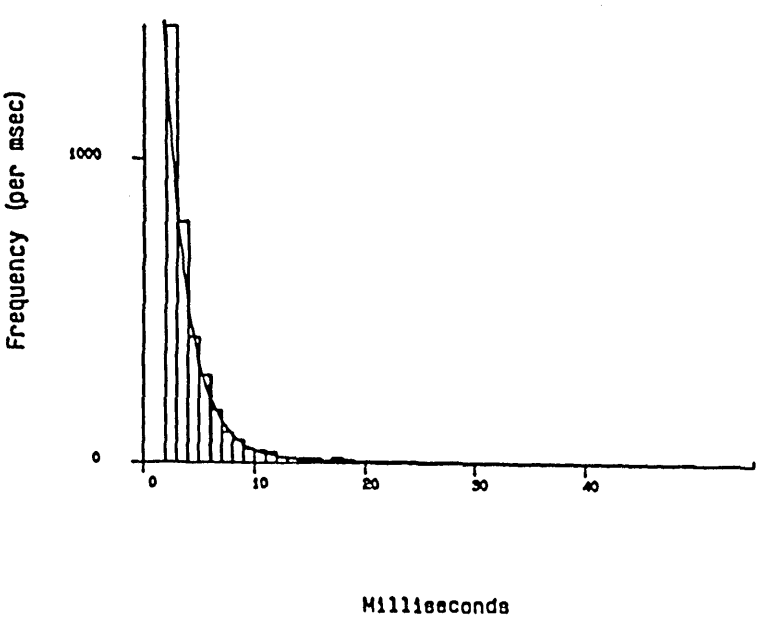
A


Frequency (per msec)
2000
1000
0
0
10
20
30
40
Milliseconds

B


Frequency (per msec)
1000
0
0
10
20
30
40
Milliseconds

C


Frequency (per msec)
1000
0
0
10
20
30
40
Milliseconds

C:$f(t)=0.95(1/2.18)exp(-t/2.18)+0.04(1/31.28)exp(-t/31.28)+0.01(1/2216.31)exp(-t/2216.31)$ [N=7424]

In both cases the time constants are quoted in msec. The -ln(Lik) values for the fits in B and C are 9191 and 8892 respectively. Comparison of these gives a P value >0.05 using the likelihood ratio test (see section 2.5.2e). Thus the closed time data are better fitted by 3 exponentials as shown in graph C. (Visual inspection of the fits in B and C supports the findings of the likelihood ratio test).

4.11c Open and closed lifetimes at various voltages

Lifetime analysis was carried out for the SM channel at various holding potentials to assess the effect of voltage on the gating characteristics.

For open lifetime analysis, 4.33 ± 3.3% of events (mean ± S.D., n=23 channels) were excluded to meet the t_{min}-t_{max} criteria; whereas 55.4 ± 5.6% of closed events (mean ± S.D., n=23) were 'stripped' from the original data. Open lifetime distributions in each case were fitted to a p.d.f with a single exponential component, whilst closed lifetimes were best fitted to a p.d.f consisting of the sum of three exponential components. The number of exponential components were determined by the application of the likelihood ratio test (see section 2.5.2e) and by visual inspection of fits with different number of exponentials to the data.

Figure 4.19 shows mean values (± S.D.) for the open lifetime time constant as a function of the applied holding potential. Lifetime analysis was carried out for 4 to 9 separate recordings at each voltage. Figures 4.20 and 4.21 show the kinetic parameters (τ_1, τ_2, τ_3, a_1, a_2, a_3) from fits to channel closed times for the same

data. To test the significance of group differences, (the four groups being the measurements at the four applied voltages) analysis of variance was carried out on the data for each kinetic parameter. P values in all cases for each parameter were >0.05 and were therefore not considered to be statistically significant. This suggests that there is no variation between parameter values at different voltages that cannot be accounted for by variation at a single applied voltage.

The three closed states identified for the SM channel have time constants of 2.92 ± 0.1msec, 48.94 ± 10.6msec and 1916.91 ± 70.2msec (mean values ± S.D. for all 23 measurements shown in figure 4.20). Of all the closed events detected, 90.36 ± 3.23% (mean ± S.D., n=23) are to the short lifetime distribution. The longer lasting closures comprise a relatively small, but significant, proportion of events. Less than 2% of closings are to the longest lifetime distribution detected by the analysis.

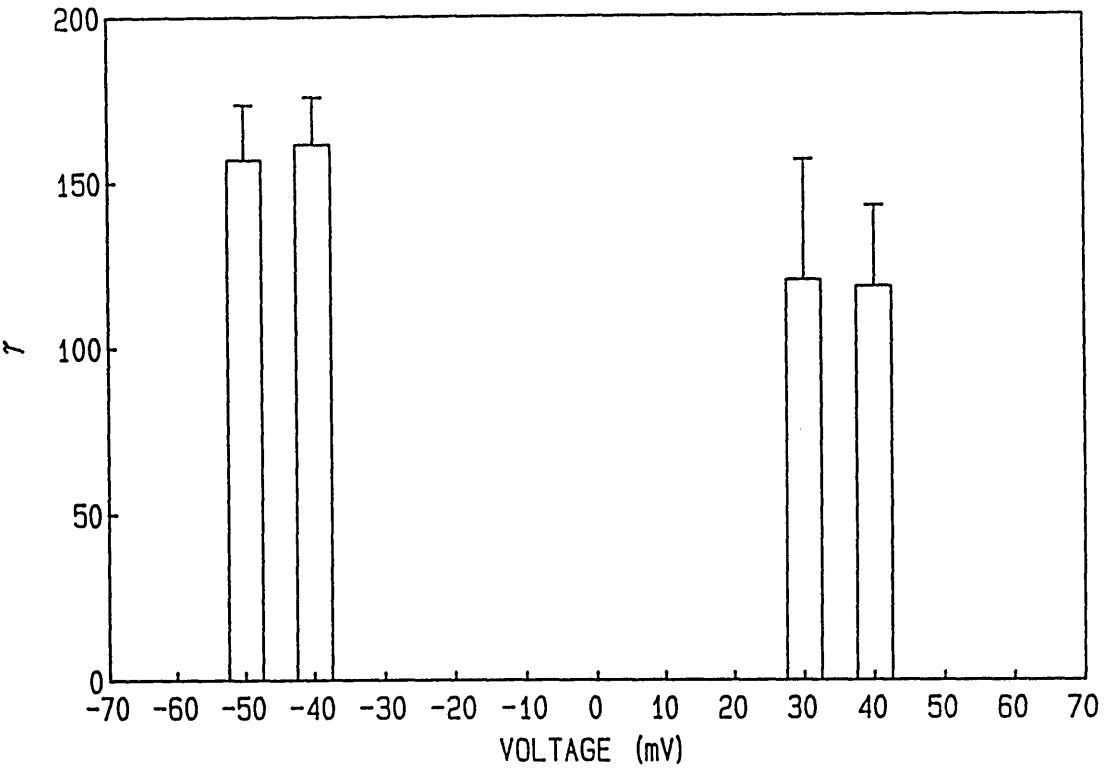
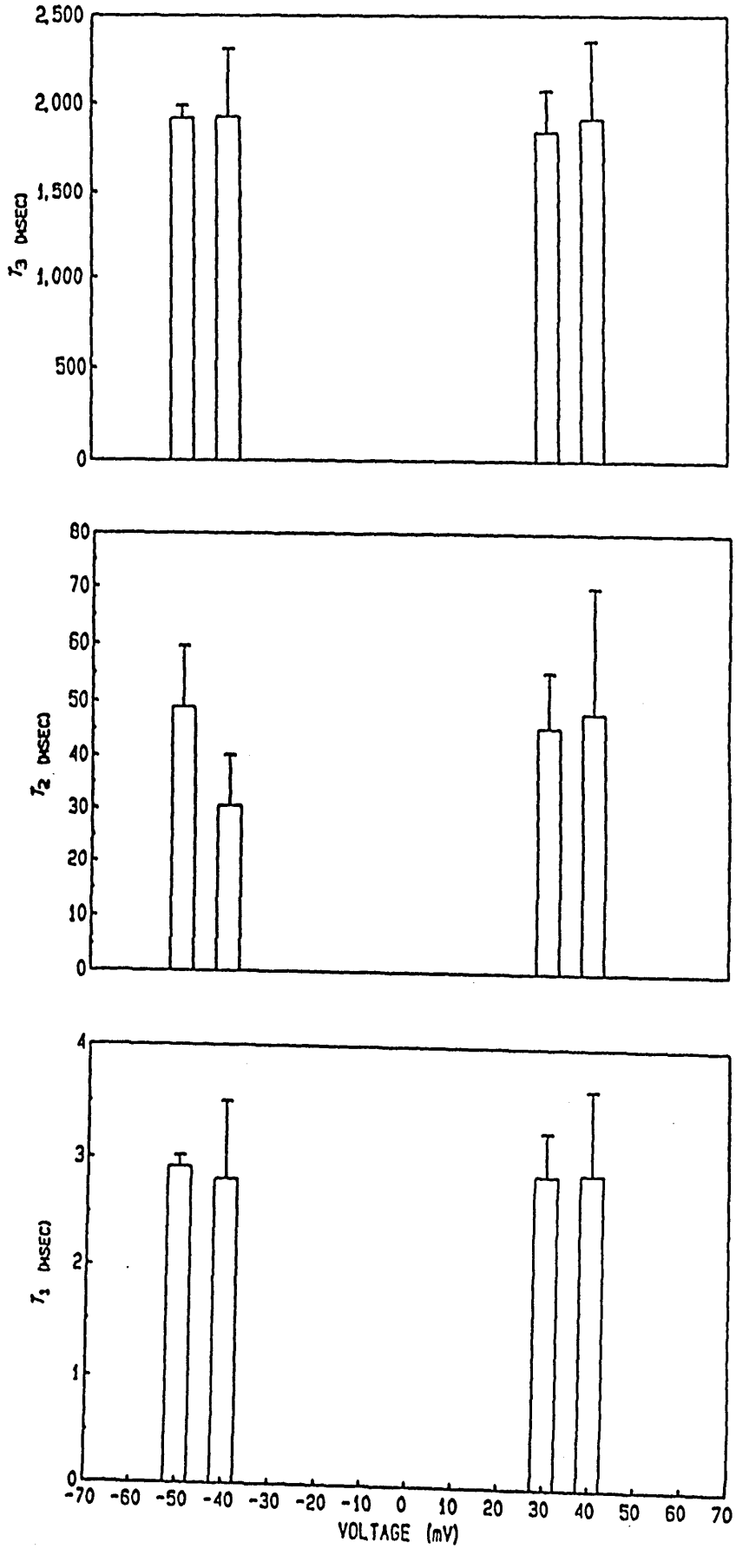


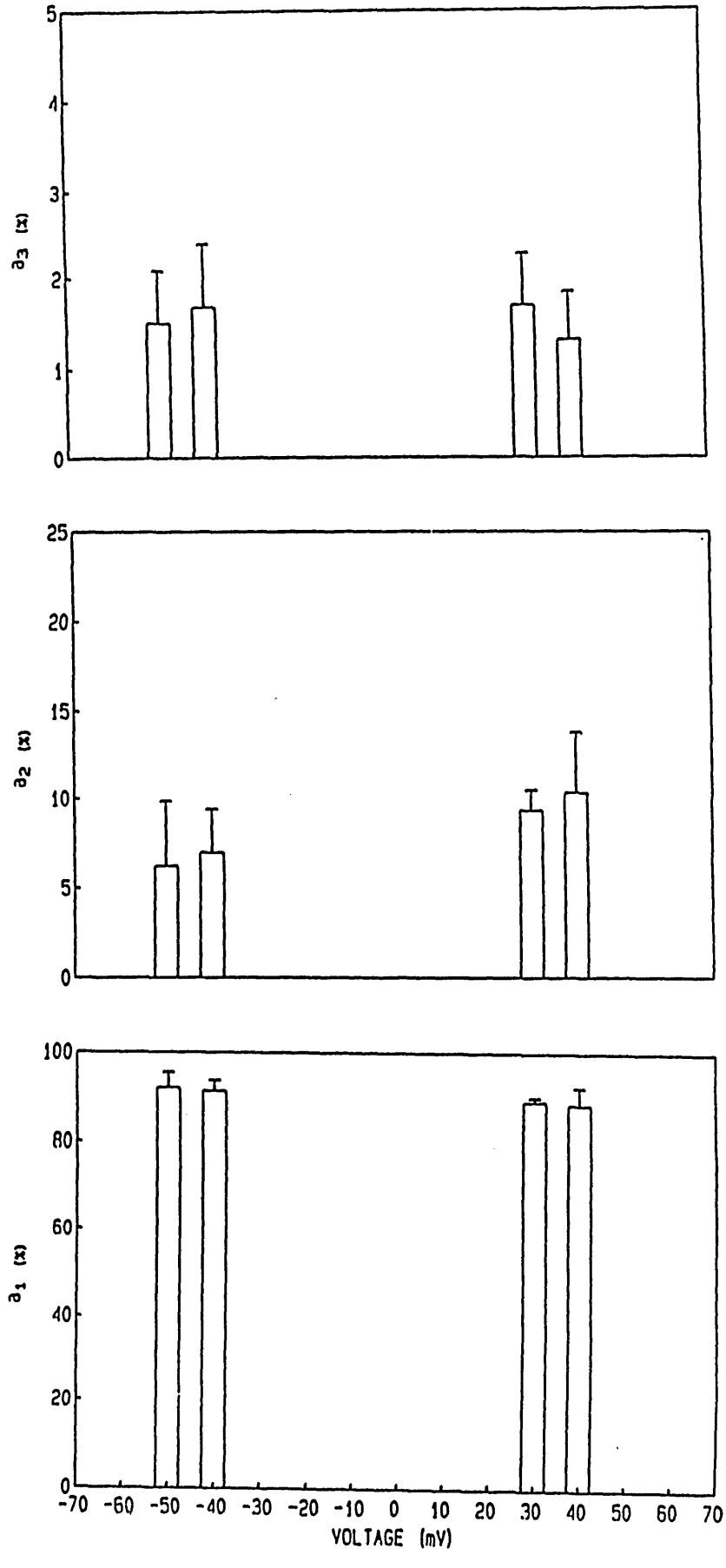
Figure 4.19

Open lifetime τ values at a range of voltages

Mean values for τ (in msec ± S.D.) at four applied voltages. The number of channels analysed were as follows: +30mV (n=4); +40mV (n=6); -40mV (n=9); -50mV (n=4). All channels were bathed in symmetrical 450mM KCl, 5mM HEPES/Tris, pH 7.2.

Lifetime analysis was carried out as described in section 2.5.2 (see example in section 4.11a).


2,500
2,000
1,500
1,000
500
0
τ_3 (MSEC)
80
70
60
50
40
30
20
10
0
τ_2 (MSEC)
4
3
2
1
0
τ_1 (MSEC)
-70 -60 -50 -40 -30 -20 -10 0 10 20 30 40 50 60 70
VOLTAGE (mV)


5
4
3
2
1
0
a3 (%)
25
20
15
10
5
0
a2 (%)
100
80
60
40
20
0
a1 (%)
-70 -60 -50 -40 -30 -20 -10 0 10 20 30 40 50 60 70
VOLTAGE (mV)

4.11d Lack of correlation between successive closed events

Autocorrelation analysis was carried out on the sequential closed lifetime files collected by half amplitude threshold analysis as described in section 2.5.2f, in order to investigate possible connectivity between closed states.

Figure 4.22 illustrates a typical example of the autocorrelation function for up to every 20th closing, calculated for over 2,000 successive closing events. All values at lag>1 lie between the 95% confidence limits for zero correlation, indicating that there is no significant correlation between successive closing events.

From this analysis there is clearly no evidence for the presence of more than one isomerisation pathway linking the closed states.

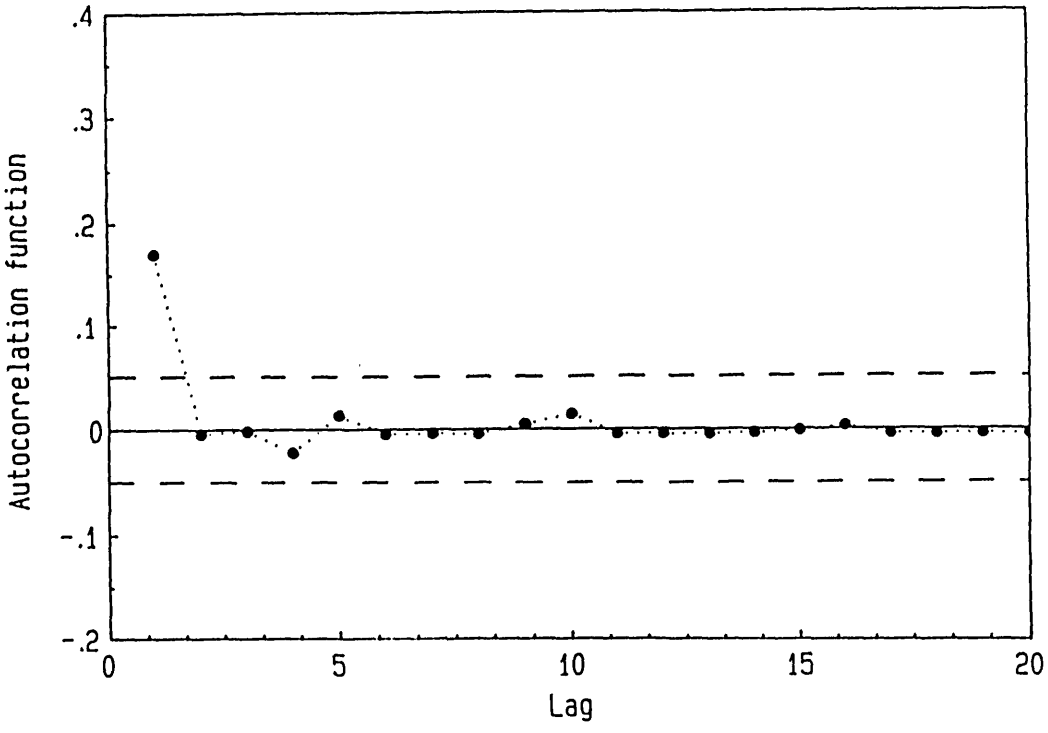


Figure 4.22

Closed lifetime autocorrelation function

Autocorrelation function for up to every 20th closing (lag 1 to 20) for 2020 successive closings of a typical SM channel. The 95% confidence limits for the absence of correlation are shown as dashed lines (these represent twice the approximate error of the estimate in the case of white noise).

FURTHER SINGLE CHANNEL STUDIES ON THE PLATELET SM

4.12 Single channels in agonist-activated platelets

Experiments were carried out to attempt to monitor agonist induced Ca^{2+} channel activity in the platelet SM fraction. SM vesicles were fused with charged bilayers (70% PE/30% PS) in KCl solutions as described in section 2.4.3 and activity from the SM anion channel used as a marker for vesicle fusion. Following fusion, the *cis* chamber was perfused with a solution composed of 1mM EGTA, 250mM HEPES/Tris, pH 7.4. The *trans* chamber was then perfused with a solution composed of 250mM HEPES adjusted to pH 7.4 with $Ca(OH)_2$. The agonist agents ADP (1mM) or thrombin (0.5U/ml) or the second messenger $Ins(1,4,5)P_3$ (10μM) were then added to the *trans* chamber solution. Alternatively, the *cis* and *trans* chamber perfusion solutions were reversed and the agent added to the *cis* chamber.

No evidence was obtained from these experiments for currents due to Ca^{2+} movement through SM receptor or second messenger operated channels.

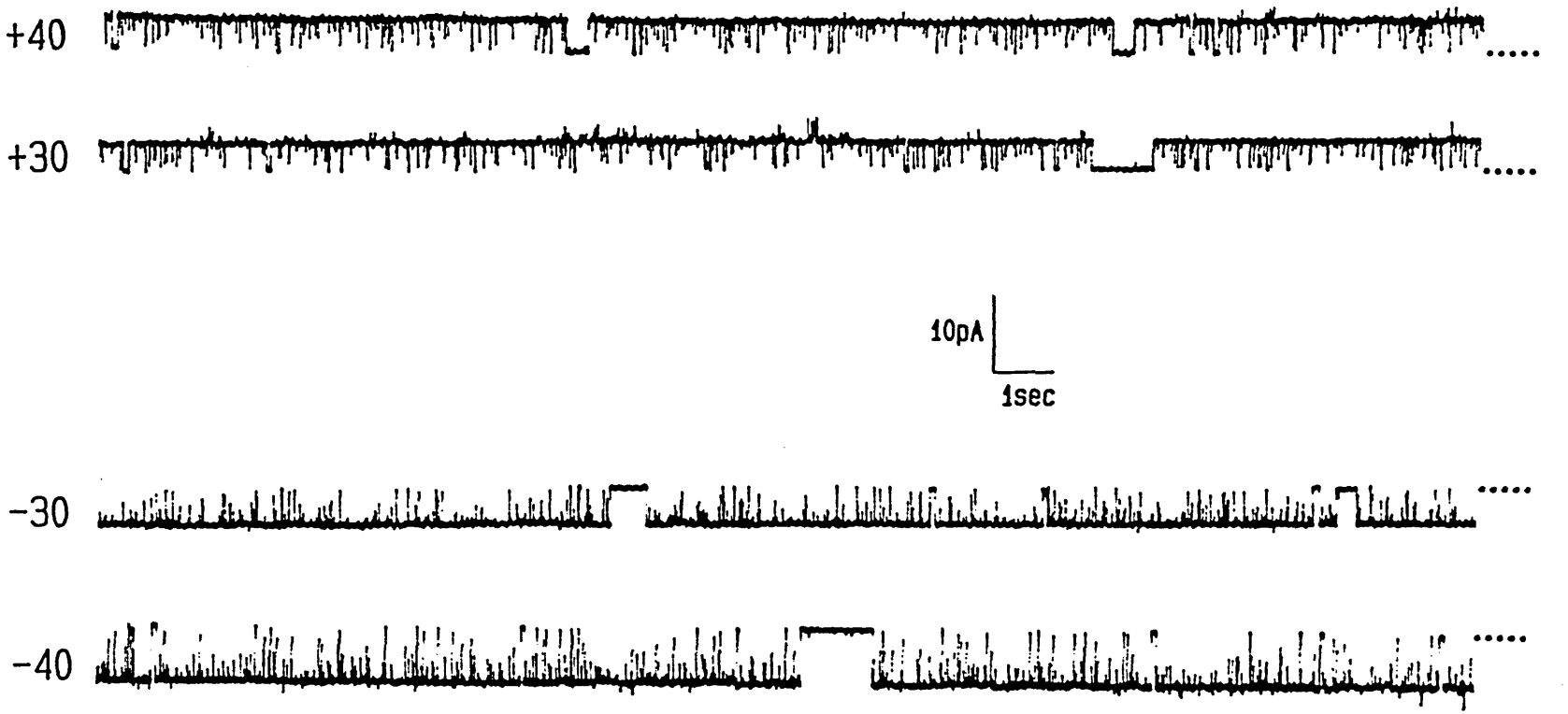
Zschauer *et al.* (1988) also report no Ca^{2+} channel activity in planar bilayers from a platelet membrane vesicle fraction containing surface membrane elements. However, they recorded Ba^{2+} currents following fusion of vesicles prepared from platelets pre-treated with thrombin (as mentioned in section 1.4.1b).

A thrombin-stimulated platelet mixed membrane preparation was carried out in order to try to repeat the findings of Zschauer *et al* (1988). Half of the platelets isolated from 5 buffy-coat residue packs were treated at the whole cell level with thrombin (0.2U/ml for 2 mins at room temperature) and half left untreated

('control' fraction). Thrombin treatment was carried out at the preparation stage where neuraminidase was usually applied to the platelets. 'Control' and stimulated platelets were then washed, subjected to sonication and the homogenates applied to two separate continuous sorbitol gradients as described in section 2.2.2. The MM fraction from the stimulated platelets was less dense and the pellet at the base of the tube considerably larger than those obtained for the 'control' MM (unquantified observation). Presumably the sonication procedure failed to break up some of the platelet aggregates arising as a result of the thrombin stimulation step.

Vesicles from the 'control' and thrombin pre-treated MM fractions were fused with charged bilayers (70% PE/30% PS) in $BaCl_2$ solutions as described by Zschauer *et al.* (1988). Bilayers were initially painted over 0.5mm diameter holes and later over 0.3mm holes for improved resolution. The following fusion conditions were applied: *cis*; 300mM $BaCl_2$, 5mM HEPES/Tris, pH 7.0: *trans*; 100mM $BaCl_2$, 5mM HEPES/Tris, pH 7.0. Single channel activity was observed from both control and agonist treated membrane fractions. Although full current-voltage relationships were not recorded, current appeared to reverse at positive potentials indicating that in both cases the charge carrying species was predominantly Cl^- and not Ba^{2+}. Fusion of the thrombin pre-treated MM vesicles in KCl solutions confirmed the identification of the predominantly anion selective channel described in this chapter. Figure 4.23 shows representative recordings of the SM anion channel observed following fusion of MM vesicles prepared from platelets pre-treated with thrombin. The conductance characteristics of the channel are unaffected by the treatment.

The 10pS Ba^{2+} channel described by Zschauer *et al* (1988) was not identified in these experiments.


+40
+30
10pA
1sec
-30
-40

4.13 Discussion

This chapter reports the basic characterisation of a predominantly anion-selective channel found in the surface membrane of human platelets. The majority of fusion events incorporate a single active channel into the bilayer. Using the criterion of the direction of rectification of the current-voltage relationship in symmetrical KCl solutions, it is found that approximately 98% of insertions result in the channel being orientated in the same direction in the bilayer. No information is available concerning the initial orientation of SM vesicles following membrane separation and purification.

Channel activity occurs in characteristic bursts of openings often lasting several tens of seconds. Bursts are separated by long closed periods, and closed intervals between bursts lasting >5mins have been recorded.

Good evidence has been obtained that the channel protein has not been altered by the membrane preparation protocol applied. Channels with qualitatively similar gating characteristics and quantitatively indistinguishable conductances in KCl solutions have been identified in a mixed membrane fraction (not treated with neuraminidase or subjected to CFE) as well as a plasma membrane fraction prepared by an alternative (and much shorter) method.

Single channel rectification

Single channel current rectification is observed under all ionic conditions applied to the SM channel, with more current flowing at negative holding potentials. This behaviour was investigated by examining whether the presence of HEPES or Tris

in the solutions was related to the degree of rectification (figure 4.6). It has been demonstrated by others that some anionic buffering compounds (including HEPES) may block chloride channels when applied in mM concentrations, e.g. in cultured *Drosophila* neurones (Yamamoto and Suzuki, 1987) and vascular smooth muscle cells (Soejima and Kokubun, 1988). Tris is also known to compete for cationic binding sites in *Aplysia* neurones (Ascher *et al.*, 1978).

From the results in figure 4.6 it is surmised that the rectification observed in experiments on the platelet SM channel is caused, for the most part, by the asymmetric blocking of current flow. HEPES blocks in a voltage-dependent manner, mainly from the *trans* face of the channel (i.e. at positive voltages). Tris buffer also appears to block current flow through the channel, though to a lesser degree and presumably mainly from the *cis* face.

Conductance and selectivity

The SM channel has a relatively high conductance: ~160pS in symmetrical 450mM KCl at -40mV. With increasing KCl concentration, the single channel conductance increases to a saturating value of ~500pS. The conductance-concentration relationship follows a simple rectangular hyperbola expected for Michaelis-Menten kinetics (figure 4.5). There is no deviation from this relationship at a conductance of three times the half-maximal conductance (~1000mM). Behaviour of this type is typically, but not exclusively, found in channels that can be occupied by a single ion at a time (Lauger, 1973), and suggests the presence of a saturatable binding site within the channel. This is unlike the situation in VDAC, a large conductance non-selective channel in the mitochondrial outer membrane, where no saturation

of conductance occurs at up to 4M KCl (Colombini, 1986) and ions move through the channel under electrostatic influences rather than via ion-binding sites.

Reversal potential measurements in asymmetric KCl solutions indicate that both K^+ and Cl^- permeate the channel (figure 4.7). Several other 'anion' channels have been shown to exhibit similar significant cation permeabilities. Blatz and Magleby (1985) found a small conductance anion channel in myotubules with a Cl:K permeability ratio of 5:1. Franciolini and Nonner (1987) measured a Cl:Na permeability ratio of 5:1 for a channel in hippocampal neurones. Woll *et al.* (1987) report an estimated Cl:Na ratio of 3.5:1 for a high conductance channel in skeletal muscle. These ratios are of similar magnitude to the Cl:K ratio of over 4:1 observed for the platelet SM channel (table 2).

The mechanism of ion permeation through ion channels of this type may be complex. Franciolini and Nonner (1987) have presented the only attempt to describe a possible mechanism for cation and anion conduction. They postulate that anions and cations interact whilst passing through the hippocampal neuronal channel, and that cations will pass only when a permeant anion is present. This mechanism was tested in their experiments by replacing Cl^- with SO_4^{2-} (which is impermeant in the neuronal channel), and observing no cation current through the channel. It is not possible to postulate this sort of mechanism in the platelet SM channel from the results obtained, since all anions tested so far have been permeant, including SO_4^{2-} (figure 4.9).

Cations as large as TEA^+ also pass through the platelet SM channel (figure 4.8), implying that the channel has a very large cross sectional area, at least 37 $Å^2$ (Coronado and Miller, 1982). TEA^+ is found to be as permeant as Br^- from

experiments in asymmetric TEABr (figure 4.8A), although single channel conductance is considerably lower than in the presence of the same asymmetric concentrations of KBr. In TEABr solutions, the duration of channel openings is markedly increased (figure 4.8B). A similar situation has been reported for Cs^+ conductance in the skeletal muscle sarcoplasmic reticulum K^+ channel (Cukierman *et al.*, 1985). Cs^+ is found to have a low conductance, a comparable permeability to K^+ and maintains the channel in the open state. This is interpreted to be due to Cs^+ binding more tightly within the channel than K^+.

Reversal potential measurements indicate that the relative permeability sequence for halide anions in the SM channel (table 3) is $F^-<Cl^-<Br^-<I^-$. This corresponds to sequence I of Eisenman's (1965) seven halide anion sequences (Diamond and Wright, 1969). In this sequence halide permeability increases with decreasing hydration enthalpy of the ion and with the crystal radius (Edwards, 1982). The same sequence has been observed in Cl^- channels from the Schwann cell (Gray *et al.*, 1984), vascular smooth muscle (Soejima and Kokubun, 1988) and pulmonary epithelial cells (Schneider *et al.*, 1985). The platelet SM channel is also permeant to the divalent anion, SO_4^{2-}, as well as to large anion molecules such as acetate and gluconate, which are commonly used for impermeant anion replacement in Cl^- channels of various tissues (Edwards, 1982). The Cl^- channel in Schwann cells has also been shown to be permeant to SO_4^{2-} and acetate (Gray *et al.*, 1984). Chloride channels permeant to large organic anions have been reported in several tissues. For example, in cat cortical neurones (Kelly *et al.*, 1969) the Cl^- channel admits anions as large as chloroacetate, propionate and glutamate. Kelly *et al.* (1969) estimated that the diameter of the selectivity filter of the neuronal channel is about 5-8Å, which gives a cross sectional area of about 20-50$Å^2$. The estimation of at least 37$Å^2$ for the platelet SM channel lies between these values. The relative

permeability sequence for all anions tested is approximately within the range of sequences described as lyotrophic (see Dani *et al.*, 1983). Lyotrophic adsorption is characterised by interaction of the anion with an electric charge or dipole and neighbouring hydrophobic groups.

Channel block by DIDS, SITS and ATP

In addition to asymmetric block of the SM channel by HEPES acting from the *trans* face, a reduction in single channel current has also been observed by other agents previously reported to block anion channels. The reactive disulphonic acid stilbenes (DIDS and SITS) are found to act from both sides of the channel when applied symmetrically (figure 4.12). These agents are known to block various other Cl^- channels including the low conductance channels of *Torpedo* electroplax and rabbit urinary bladder (Miller and White, 1984; Hanrahan *et al.*, 1985), and the large conductance channels of A6 epithelial cells and urinary bladder (Nelson *et al.*, 1984; Hanrahan *et al.*, 1985). Block in the platelet SM channel is characterised by a series of small noisy openings at positive voltages and shortened bursts containing rapid flickering events at negative voltages. This behaviour is unlike the reported action of these agents on other anion channels; for example, DIDS is seen to eliminate all channel openings in the *Torpedo* electroplax and rabbit urinary bladder channels (Miller and White, 1984; Hanrahan *et al.*, 1985).

Zinc has been shown to block Cl^- currents in other preparations (Woodbury and Miles, 1973; Franciolini and Nonner, 1987; Woll *et al.*, 1987). However, the SM channel is unaffected by the presence of up to 2mM zinc appled to both *cis* and *trans* solutions.

The effect of ATP on the channel was investigated since Maruyama (1987) applied mM ATP to his pipette solutions whilst patch clamping whole platelets to improve seal formation in the cell-attached configuration. No reference is made in the Maruyama paper to a Cl^- channel, and the possibility was considered that it may have been blocked in his experiments. ATP has recently been reported to induce a flickery channel block in a non-selective channel in neonatal rat central neurones (Ashford *et al.*, 1988). The effect of ATP on the SM channel (figure 4.13) is evident only at negative voltages when fast flickering events are observed. No effect of ATP is seen at positive voltages. Thus ATP appears to be blocking from the *cis* face of the channel with the degree of block increasing as the ATP concentration is increased. A similar blocking effect is observed with ADP applied symmetrically to the channel. This suggests that ATP and ADP may be acting as large impermeant anions, but only from one face of the channel. The presence of 3mM ATP, together with the lower anion concentrations applied by Maruyama (1987) may explain the absence of the channel reported here from his patch recordings. If this is the case, it would imply that the *trans* side of the SM channel would face the platelet cytosol. However, not all reconstituted SM channels showed the same response to ATP, so the reason for the absence of Cl^- currents in cell-attached platelet recordings in anionic solutions remains unclear.

Mahaut-Smith (Cambridge, U.K.) has recently recorded single Cl^- currents in human platelets using the whole-cell configuration of the patch clamp. These channels were not observed using cell-attached patch recordings (the same mode used by Maruyama, 1987), though no ATP was present in the pipette solution. An increased number of Cl^- channels appear with time, together with a steady increase in the channel open probability, though clear reversal potentials have not yet been measured (Mahaut-Smith, 1989 - personal communication). Thus the

absence of Cl^- channels in the cell-attached patch recordings of platelets reported by Maruyama (1987) may not be due to ATP block of the channel, but to other influences of the method of recording.

The effect of other agents on single channel activity

Various agents were applied to the SM channel to investigate possible regulatory mechanisms. In a number of tissues an increase in intracellular Ca^{2+} concentration causes the activation of Cl^- channels (Miledi, 1982; Bader *et al.*, 1982; Marty *et al.*, 1984; Owen *et al.*, 1984; Mayer, 1985). However, in experiments carried out on the platelet SM channel, neither the addition of symmetrical mM Ca^{2+} nor its chelation with EGTA altered the single channel activity.

The activity of the SM channel is also unaffected by the platelet activators thrombin and PAF, and no effect of $Ins(1,4,5)P_3$ is found when agents were added to either (or both) the *cis* and *trans* faces.

Gating characteristics of the channel

The activity of the SM channel is found to be strongly dependent on the applied voltage. The channel is active between +70mV and -60mV with high open probabilities, but at more negative voltages the channel enters an apparently 'inactivated' state. When switching holding potential from 0mV to -70mV, for example, the channel is initially open and remains so for several seconds before closing down [c.f. figure 4.4] for as long as recording is continued (i.e. up to 15 mins). Activity is then only resumed by switching to a more positive holding potential. A similar voltage dependence is exhibited for the anion channel in

amphibian skeletal muscle (Woll and Neumcke, 1987). This skeletal channel, like the platelet channel, is shut for most of the time at voltages more negative than -60mV, but remains open at depolarised potentials up to at least 60mV.

The voltage dependence observed in the platelet SM channel differs significantly from that reported for large-conductance anion channels of A6 epithelial cells (Nelson *et al.*, 1984), rat myotubes, Schwann cell or alveolar cells (Blatz and Magleby, 1983; Gray *et al.*, 1984; Bevan *et al.*, 1985; Schneider *et al.*, 1985), mouse macrophages and chicken myotubes (Schwarze and Kolb., 1984) and the voltage dependent anion channel of mitochondria (Schein *et al.*, 1976). All of these channels are predominantly open near 0mV, but tend to close with 20 to 30mV deviations on either side of 0mV.

A feature of anion channels described in a variety of tissues is that sub-conductance states are common (Miller, 1982a; Tank *et al.*, 1982; Nelson *et al.*, 1984; Schwarze and Kolb., 1984; Hanrahan *et al.*, 1985; Kolb *et al.*, 1985; Krouse *et al.*, 1986; Bormann *et al.*, 87; Woll *et al.*, 1987; Rousseau, 1989). Substates may be true stable states of a channel with different total conductance or they might be conditions of extremely rapid gating between fully open and closed states whose fractional open time determines the apparent conductance measured using a recording system of limited bandwidth. However they arise, substates require that the channel has several open states, and suggest that these anion channels have different components (helices, domains, subunits or cochannels) that pack in several alternative ways to form the conducting pathway.

However, the platelet SM does not exhibit any substates of conductance. In addition, lifetime analysis carried out on steady state recordings of the channel at

four voltages indicate that the channel only exhibits one open state under the conditions applied (figure 4.19). There is no significant difference between the time constants of the open state at the voltages tested. The mean τ for all 23 measurements is ~140 msec.

A number of closed states have been identified in statistical terms for the SM channel. The closed lifetime distribution is best fitted to a p.d.f consisting of the sum of three exponential components, indicating the presence of three closed states.

More accurately, the channel is said to exhibit 'at least' one open and three closed states, since the estimate of the number of states is a **minimum estimate** for the following reasons:

(1) The finite resolution of the channel detection system (i.e. bilayer amplifier plus 50% threshold discriminator) sets an overall dead time. Any channel closed (or open) events with briefer mean lifetimes are unlikely to be detected. Therefore the present description of single channel kinetics deals only with duration states with mean lifetimes greater than the dead time of 1.6msec.

(2) The limiting size of 64 seconds for the 'Efit' memory when sampling at 2kHz necessitated the exclusion from the analysis of closed events $\geq$ 64 secs. As stated earlier, closed events longer than this have been recorded for the SM channel. However, if inclusion of these events in the analysis had been possible it is unlikely that a fourth exponential component would be added to the closed time p.d.f since such a statistically small number of events would be detected.

None of the kinetic parameters associated with the closed state show significant voltage dependence in the voltage range studied. Over 90% of all the closed events detected are to the short lifetime distribution which has a time constant of ~3msec. These are the rapid flickers within a burst. The longer lasting closures comprise a relatively small, (though significant) proportion of events, with less than 2% of all closing events being to the longest lifetime distribution.

A linear gating scheme with only a single pathway linking the closed states and the open state (e.g. C-C-C-O, C-C-O-C) is consistent with the lack of correlation found between successive dwell times in the closed state (figure 4.22).

An assumption of lifetime analysis at steady state is that the probability of the various channel conformations is constant during the length of the record. This appears to be so for the SM channel during the majority of recording periods. However, the channel does exhibit occasional spontaneous variations seen as a 'sudden change in kinetic state' (figure 4.16) [these were omitted from lifetime analysis]. Examples of similar non-stationary single channel activity appear in the literature and are termed 'gearshift' occurrences. They are exhibited by the glutamate-activated channel of locust muscle in cell patches (Patlak *et al.*, 1979) and the Ca^{2+} activated K^+ channel (Moczydlowski and Latorre, 1983) and batrachotoxin-activated Na^+ channel (Moczydlowski *et al.*, 1984) in planar bilayers. At present, no publications have attempted a systematic study of the frequency of 'gearshift' occurrences, so few conclusions can be drawn about this phenomenon. It is possible that they may represent very slow conformational changes affecting gating that are superimposed on the characteristic rapid processes (Moczydlowski, 1986).

Putative agonist-activated Ca^{2+} channels in the platelet surface membrane

As mentioned in the introductory chapter (section 1.4.1b), there is increasing evidence that the platelet surface membrane may possess receptor-operated Ca^{2+} channels. Most of this evidence, however, is indirect and has come from experiments using fluorescent probes. Single channel recordings of agonist-evoked divalent cation currents from the platelet surface membrane are required to provide direct evidence for such channels.

The highly purified surface membrane fraction prepared in this thesis was considered ideal 'starting material' to attempt to reconstitute the putative agonist-activated Ca^{2+} channels. Fusion of vesicles in these experiments was monitored using the SM anion channel as a marker. The conditions in the *cis* and *trans* chambers were then altered to establish a Ca^{2+} gradient across the bilayer. The addition of ADP, thrombin or $Ins(1,4,5)P_3$ did not induce Ca^{2+} currents in these experiments. The second messenger was added to the chambers in some of these experiments since Ca^{2+} channels regulated by $Ins(1,4,5)P_3$ have been identified in lymphocytes (Kuno and Gardner, 1987), mast cells (Penner *et al.*, 1988) and skeletal muscle T-tubules (Vilven and Coronado., 1988). It was considered possible that such Ca^{2+} currents were too small to be resolved in the bilayer system since many Ca^{2+} channels have conductances in the range ~5 to ~25pS (for about 100mM Ba^{2+} ions; Nelson, 1986). Also the density of Ca^{2+} channels in the vesicle preparation may be low giving a low probability for their successful reconstitution in these experiments. However, despite numerous attempts, applying conditions to maximise the probability of observing Ca^{2+} currents, no recordings of putative agonist-activated Ca^{2+} channels were made.

Subsequent to these experiments, a report has been published identifying ADP-evoked Ca^{2+} channel activity in patch clamped platelets (Mahaut-Smith *et al.*, 1989). A single channel conductance of ~20pS is measured and activity in membrane patches decays to control levels within 30sec-2min from seal formation, which is consistent with the phasic nature of the rise in platelet intracellular Ca^{2+} following activation by ADP.

Data presented by Zschauer *et al.* (1988) have demonstrated single Ba^{2+}-selective channels obtained by incorporating membrane vesicles from thrombin-stimulated platelets into planar bilayers. Two points may be raised in criticism of the authors' claim for the identification of receptor-operated Ca^{2+} channels.

(1) It is not clear from the experiments described whether the channels studied are derived from the plasma membrane. The preparation consisted of subjecting thrombin pre-treated platelets to freeze-thawing and high speed differential centrifugation. The yield of platelet membranes certainly contain surface membrane elements, since adenylate cyclase and calmodulin-dependent Ca^{2+}ATPase activities are present, but it cannot be excluded that the channel activity may have originated from contaminating intracellular membranes.

(2) No direct link between agonist-receptor interaction and channel openings has been demonstrated. The authors merely report the absence of this channel in membrane fractions prepared from unstimulated platelets and its presence in membranes prepared from thrombin-stimulated platelets.

Direct evidence for thrombin-stimulated channels would be the demonstration of Ca^{2+} or Ba^{2+} currents through ion channels (from a surface membrane fraction of well defined origin) in the presence of thrombin in bilayer experiments.

The claim by Zschauer *et al.* (1988) that a 'true' receptor-operated Ca^{2+} channel in the platelet surface membrane has been identified in their experiments is therefore considered rather premature. Similar criticisms have been levelled at this report by Petersen in correspondence published in Nature (Petersen, 1988).

A membrane preparation from thrombin-stimulated platelets was carried out using the procedures routinely applied to prepare mixed membranes in this thesis. Preliminary experiments using this thrombin-stimulated MM fraction did not yield the channel described by Zschauer *et al.* (1988). Activity from the predominantly anion-selective SM channel, however, was recorded in KCl solutions and its conductance properties found to be unaffected by the thrombin treatment.

Chapter 5

RESULTS III

PLATELET INTRACELLULAR MEMBRANE CHANNELS

5.1 Introduction

This chapter contains details of experiments carried out on the highly purified intracellular membrane fraction of the human platelet.

Experiments designed to reconstitute single channels into planar bilayers from the IM fraction collected following CFE proved particularly difficult for a number of reasons, which are discussed in section 5.6.

A subpopulation of the IM was harvested following the application of an oxalate loading procedure modified from protocols previously used to collect the ryanodine insensitive fraction of cardiac muscle sarcoplasmic reticulum. Vesicles from this IM subpopulation have been incorporated into planar bilayers and single channel activity recorded from a monovalent cation-selective channel.

5.2 Attempts to reconstitute the IM fraction

Attempts were made to fuse vesicles from the purified IM fraction collected following CFE as described in section 2.2.3. The following conditions were applied using charged planar bilayers (70% PE/30% PS or 50% PE/50% PS) and adding IM to the *cis* chamber to a final protein concentration of approximately 10 μg per ml.

(i) 3:1 *cis:trans* KCl gradient. 450mM KCl, 1.0mM $CaCl_2$, 5mM HEPES/Tris, pH 7.2: 150mM KCl, 5mM HEPES/Tris, pH 7.2

(ii) 3:1 *cis:trans* $BaCl_2$ gradient. 300mM $BaCl_2$, 5mM HEPES/Tris, pH 7.2: 100mM $BaCl_2$, 5mM HEPES/Tris, pH 7.2

(iii) 3:1 *cis:trans* $CaCl_2$ gradient. 300mM $CaCl_2$, 5mM HEPES/Tris, pH 7.2: 100mM $CaCl_2$, 5mM HEPES/Tris, pH 7.2

In many of these experiments, in order to maximise the probability of fusion occurring, small chamber volume *cis* cups (0.5ml) were used. The hole in these cups was 0.3mm in diameter, reducing the bilayer size and thus improving the resolution (since Ca^{2+} channel currents may be small).

In each case, when no single channel activity was observed, the gradient across the bilayer was increased to 9:1 by addition of aliquots of the appropriate 1M or 3M stock solution (i.e. KCl, $BaCl_2$ or $CaCl_2$) to the *cis* chamber. In Ba^{2+} (ii) and Ca^{2+} (iii) solutions Ins(1,4,5)P_3 was also added (5-10μM), first to the *trans* chamber and then, in addition, to the *cis* chamber solution. Under these conditions stirring of the *cis* chamber solution was continued for up to 1 hour, or as long as bilayers remained stable. The condition of the bilayer was monitored at frequent intervals during this time by applying a ±4mV square wave pulse and assessing the size of the capacitance spike as described in section 2.4.2. Thickening of the lipid film occasionally occurred during this time. If re-thinning could not be induced by application of a large amplitude pulse (±120mV) or the light 'brushing' of the painting 'stick' over the hole, the experiment was terminated and the procedure repeated (washing and rinsing the cup as necessary).

No channel activity was observed under the conditions described, despite dozens of attempts using IM vesicles from 14 separate platelet membrane preparations. Possible explanations for the absence of channel activity in these experiments are discussed in section 5.6.

5.3 Isolation of an IM subpopulation by oxalate loading

Applying the analogy of the platelet DTS to the SR of muscle cells (see section 1.2.3), a method to oxalate load and separate a subpopulation of the IM fraction containing Ca^{2+} pumps was applied. This was modified from the procedures used by Jones and Cala (1981) and Tomlins *et al.* (1984) to isolate the ryanodine insensitive fraction of cardiac muscle SR (see section 2.2.4).

Protein estimations carried out on six oxalate loaded membrane preparations have revealed that approximately 1/10th of the IM (collected by high-voltage CFE) loads with oxalate using this method. For example; from a membrane preparation (5 blood packs) in which ~600μg of protein was collected in the IM fraction following CFE, the yield of oxalate-loaded membrane was ~60μg of protein. Resuspension of this membrane (in 0.4M sucrose, 5mM HEPES/Tris, pH 7.2) at a protein concentration of 1mg/ml gave 60μl of 'starting material' for bilayer experiments. For a 0.5ml volume *cis* chamber, 5μl aliquots are added per experiment to give a final protein concentration of 10μg protein/ml. Thus the 'starting material' from this preparation provided sufficient aliquots for only 12 experiments. The difficulties experienced in obtaining data from this membrane fraction were therefore primarily due to the low yield of 'starting material'.

5.4 Reconstitution of a cation channel from the oxalate-loaded IM fraction

Vesicles from the oxalate loaded IM fraction were successfully fused with neutral bilayers (100%PE) formed over a 0.3mm diameter hole revealing a monovalent cation-selective channel. Fusion conditions were as follows: *cis*: 450mM KCl, 5mM HEPES/Tris, pH 7.2, *trans*: 150mM KCl, 5mM HEPES/Tris, pH 7.2. Following

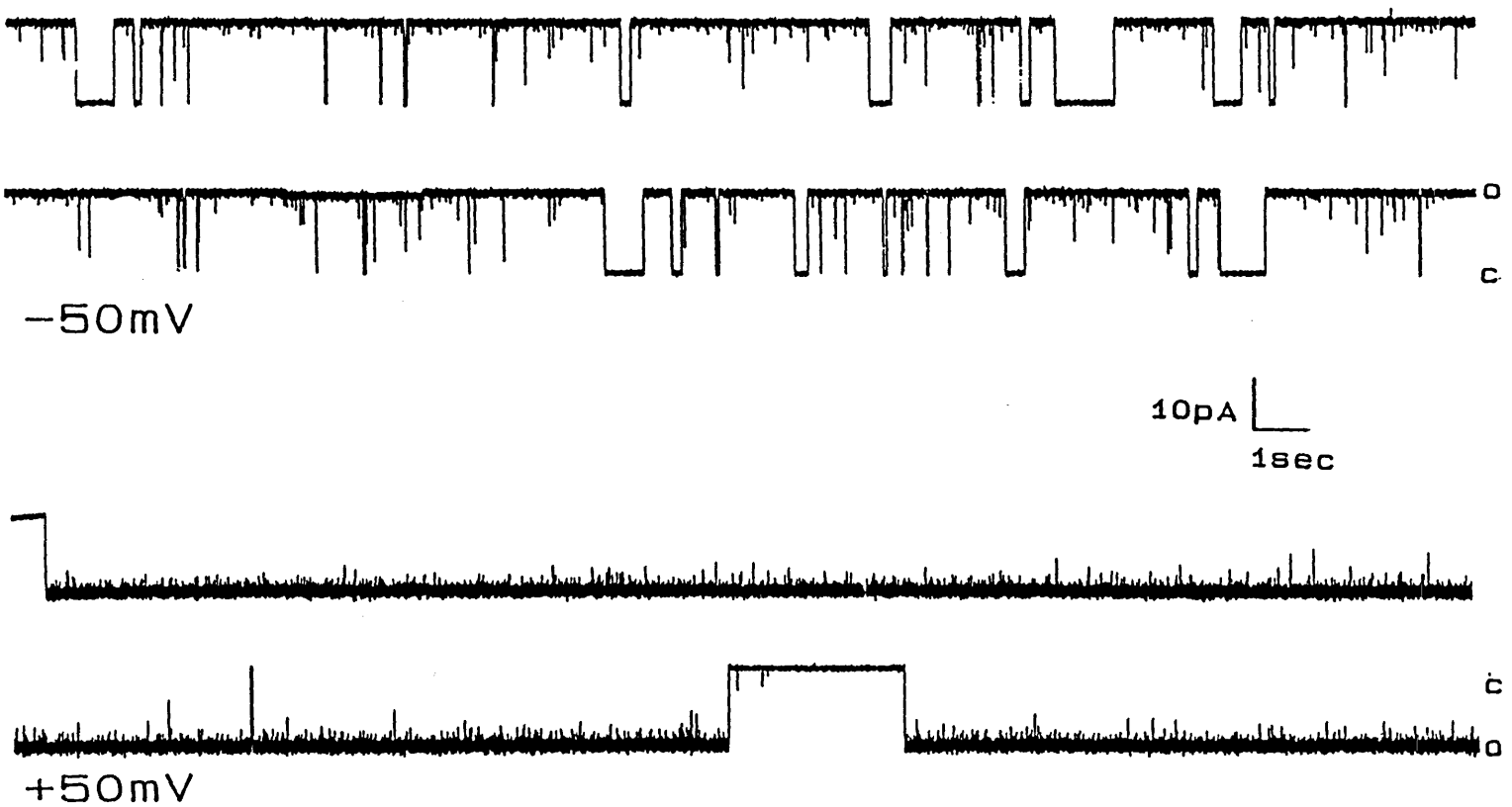
fusion, unfused vesicles were perfused out into a centrifuge tube on ice. These were then 'recycled' by pelleting the vesicles (centrifuging at 90,000 x g for 30 mins at $4^{o}C$) and resuspending them in 0.4M sucrose, 5mM HEPES/Tris, pH 7.2 in order to conserve the membrane.

5.4.1 Conduction properties of the IM channel

Figure 5.1 shows representative samples of single channel currents at -50mV and +50mV recorded in symmetrical 450mM KCl, 5mM HEPES/Tris, pH 7.2. From visual inspection of this channel record (and see figure 5.3A), it is clear that the single channel conductance is independent of the applied voltage (i.e. no rectification in current is seen). At positive holding potentials the open state appears more noisy than at negative holding potentials and few clear closing events are observed. The 'noisiness' of the open state may be due to very rapid flickering events occurring which have not been resolved in these recordings.

The current-voltage relationships for the channel in symmetrical 450mM KCl and 150mM KCl (both buffered to pH 7.2 with 5mM HEPES/Tris) are shown in figure 5.2. In both conditions there is an apparent linear relationship between single channel current and holding potential over the range ±70mV. The mean conductances (± S.D) in the presence of symmetrical 450mM and 150mM KCl are 299.7 ± 21.1pS and 217.3 ± 9.4pS respectively. These values are calculated from measured currents in the 4 different channels in the range ± 70mV.

A measurement of the reversal potential in asymmetric KCl solutions is shown in figure 5.3. With a 3:1 KCl gradient across the bilayer (*cis*, 450mM KCl: *trans*, 150mM KCl), the voltage at which no net current flows is found to be -24mV.


O
C
−50mV
10pA
1sec
C
O
+50mV

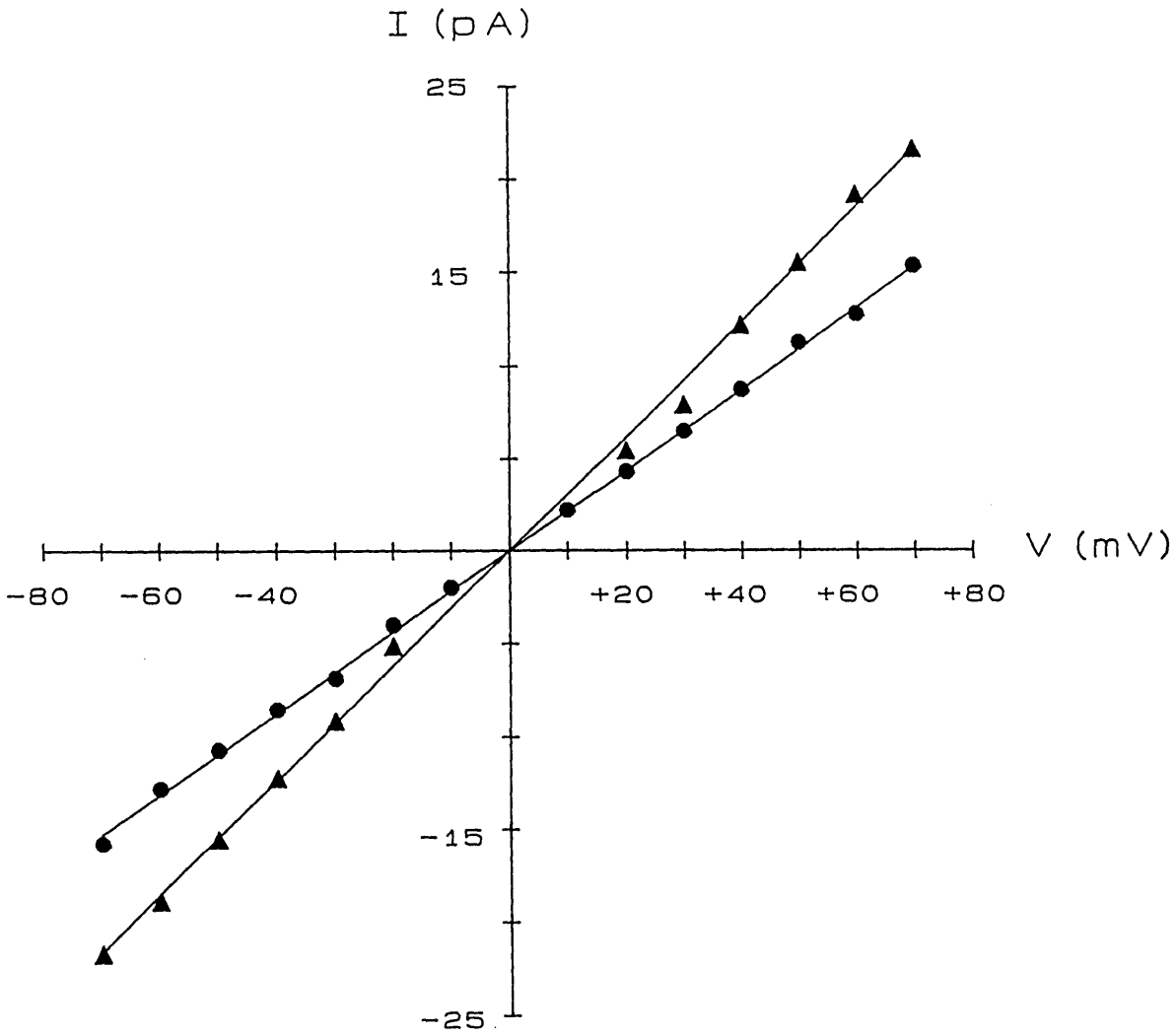


Figure 5.2

Current-voltage relationships in symmetrical KCl solutions

Single channel current-voltage relationships for channels bathed in symmetrical 450mM KCl (▲) and 150mM KCl (●), 5mM HEPES/Tris, pH 7.2. In both cases points are mean values (± S.D., n=4). Error bars are smaller than the symbols. Lines were drawn by least squares regression.

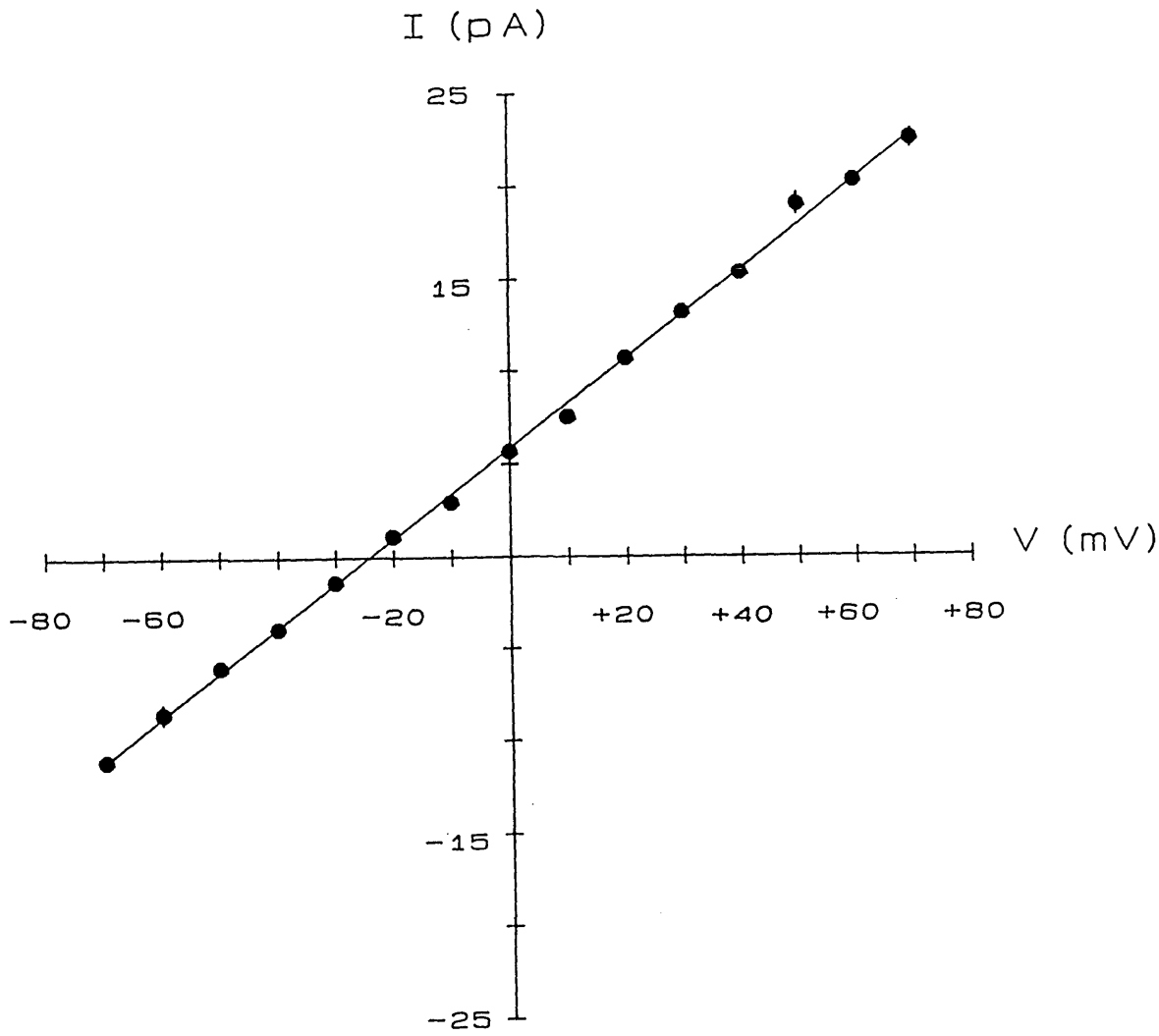


Figure 5.3

Current-voltage relationship in asymmetric KCl solutions

Single channel current-voltage relationship with a 3:1 KCl gradient across the bilayer (*cis*: 450mM KCl: *trans*: 150mM KCl (buffered in both cases with 5mM HEPES/Tris to pH 7.2). Points are mean values (± S.D., n=5) and error bars smaller than the symbols are not shown. The fitted regression line gives a reversal potential of -24mV.

This is in close agreement with the reversal potential calculated from the Nernst equation (equation 5, section 2.5.1) for an ideally monovalent cation-selective channel under these conditions (-28mV).

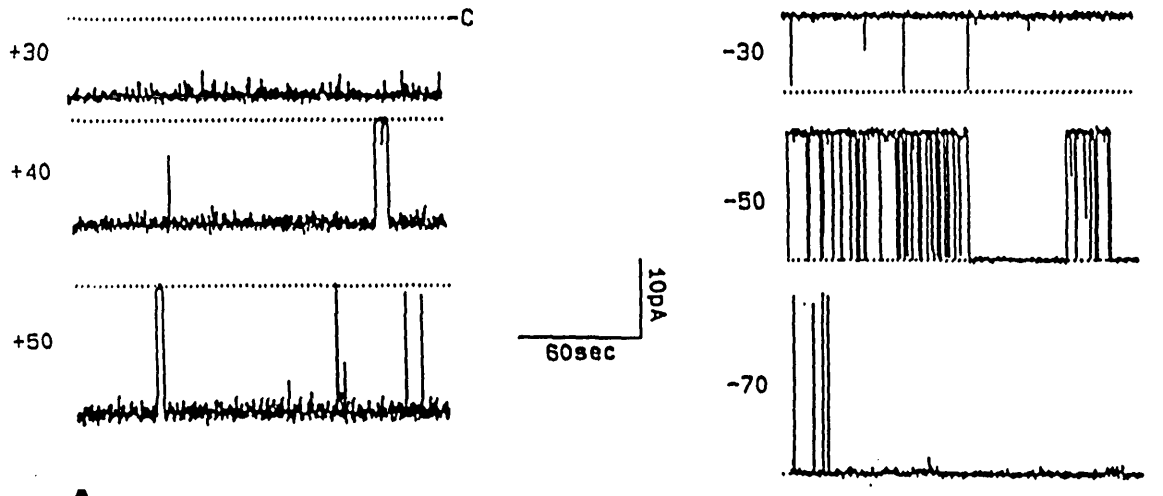
5.4.2 The probability of the IM channel being open

Figure 5.4B shows a plot of P_0, the probability of the channel being in the open state, as a function of the applied holding potential. P_0 values were estimated by integrating steady state amplitude histograms as described in section 2.5.2g for the channel illustrated in figure 5.4A. At voltages from -40mV to +60mV, the channel remains mainly in the open, conducting, state with only occasional closures observed. As the holding potential is made more negative the channel tends to close down until at -70mV very few openings occur.

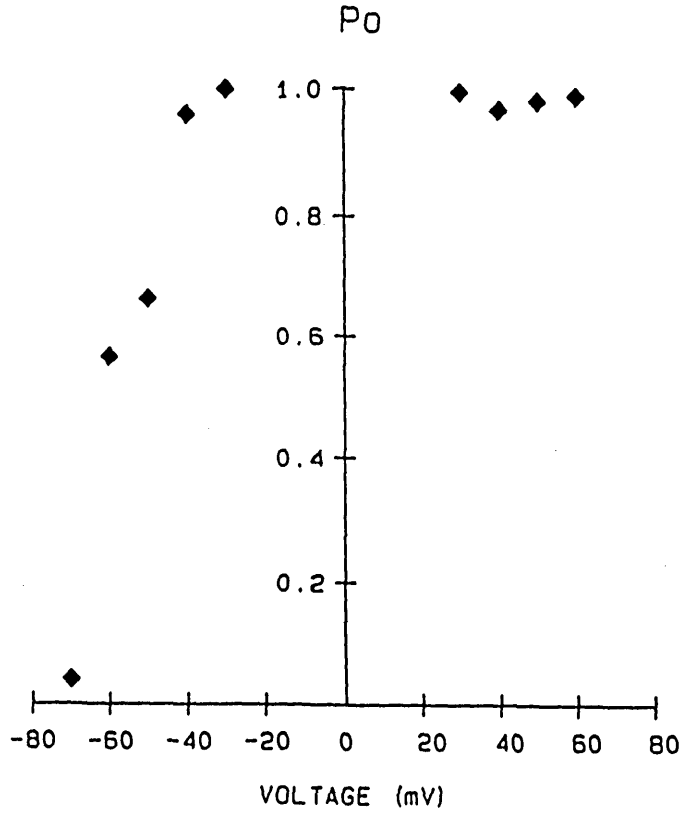
The time the channel remains in the open state is found to be unaffected by the calcium concentration in the bathing solutions. The addition of up to 100mM $CaCl_2$ or 1mM EGTA to both *cis* and *trans* chamber solutions with the channel bathed in symmetrical 450mM KCl, 5mM HEPES/Tris, pH 7.2 produces no effect on single channel activity.

5.4.3 Use of the IM K^+ channel as a 'marker' for fusion

The identification of the monovalent cation-selective channel as described above provided a 'marker' for fusion of the IM vesicles. Similar experiments using vesicles from the IM which did not load with oxalate (collected from the 0.25M:1.5M sucrose interface on the gradient, see section 2.2.4) have provided no evidence for activity from the K^+ channel.


-C
+30
+40
+50
-30
-50
-70
10pA
60sec

A


Po
1.0
0.8
0.6
0.4
0.2
-80
-60
-40
-20
0
20
40
60
80
VOLTAGE (mV)

B

Once fusion of the K^+ channel from the oxalate loaded IM was achieved, the conditions in the *cis* and *trans* chambers were altered, by exchange perfusion, to those favouring Ca^{2+} channel activity. Thus, in 26 experiments, the *cis* chamber was perfused with a solution composed of 1mM EGTA, 250mM HEPES/Tris, pH 7.4. The *trans* chamber was then perfused with a solution composed of 250mM HEPES adjusted to pH 7.4 with $Ca(OH)_2$ (leaving the Ca^{2+} on the *trans* side of the bilayer as the only small ion present in the system). Ins(1,4,5)P_3 (5-10μM) was then added to the *cis* chamber and the solution mixed thoroughly. Bilayer currents were then monitored at a range of holding potentials. In 5 experiments the *cis* and *trans* chamber perfusion solutions were reversed and Ins(1,4,5)P_3 added to the *trans* chamber. In all 31 experiments no channel openings were observed under the conditions described.

5.5 Oxalate loading of the mixed membrane fraction

The same oxalate loading method used to isolate the IM subpopulation was also applied to the MM fraction (untreated with neuraminidase). This procedure was carried out in order to attempt to isolate the same IM subpopulation with the omission of the CFE step. Under these conditions, a much larger pellet of oxalate loaded membrane was obtained (unquantified observation) than that found when oxalate loading the purified IM fraction.

Fusion of vesicles from the oxalate loaded MM fraction with both charged and uncharged bilayers (70% PE/30% PS or 100% PE) in KCl solutions yielded the SM channel described in chapter 4. These observations were corroborated by the appearance of actin and myosin on SDS polyacrylamide gels of this membrane

fraction. A purified IM vesicle fraction clearly cannot be isolated by oxalate loading the MM fraction.

5.6 Discussion

As described in chapter 3, the highly purified platelet intracellular membrane fraction prepared by CFE has been shown to accumulate Ca^{2+} in the presence of ATP and release pre-loaded Ca^{2+} following the application of $Ins(1,4,5)P_3$. The latter process is thought to be induced by $Ins(1,4,5)P_3$ binding to receptors linked to Ca^{2+} channels in the IM. The primary aim of experiments carried out on the IM fraction was therefore to attempt to identify individual $Ins(1,4,5)P_3$-sensitive Ca^{2+} channels by reconstitution into planar bilayers.

However, attempts to fuse purified IM vesicles identified from the CFE profile under a range of conditions proved unsuccessful. The following explanations for the difficulties encountered were considered.

(1) vesicles from the IM fraction **were not fusing** with the planar bilayer, despite the application of conditions designed to maximise the probability of fusion occurring (i.e. large *cis:trans* osmotic gradient, divalent cations in the *cis* compartment in the presence of negatively charged phospholipids in the bilayer, and efficient stirring of the *cis* chamber solution in order to deliver vesicles to the planar bilayer).

(2) vesicles **were fusing** with the bilayer, but these contained **no channel proteins.** This explanation seems unlikely in view of the observations of Niles and Cohen (1987) (see section 1.5.5b) that the presence of channels

through which the osmoticant is permeant, is necessary in the vesicle membrane to allow net swelling and vesicle fusion.

(3) the low density of channel proteins in the IM vesicle fraction was such that the probability of ion channel-containing vesicles fusing with the bilayer was extremely low.

(4) channel-containing vesicles were fusing with the bilayer, but channels were inactivated so that single channel activity was not observed.

(5) channel currents were too small to be resolved.

Since the occurrence of fusion in the bilayer experiments described in this thesis was monitored only by the appearance of activity from reconstituted channel proteins, the possibility of (1) and (2) (obviously) could not be tested. The possibility of (4) seemed unlikely since application of Ins(1,4,5)P_3 (5-10μM) in experiments carried out in barium and calcium did not induce single channel activity. Bilayer conductance was unchanged throughout and appeared as if no channels were present.

The most likely explanations for the lack of success in these reconstitution experiments were considered to be either (3) or (5), see above. The possibility of isolating a subpopulation of the IM containing Ca^{2+} pumps (and also the putative Ins(1,4,5)P_3-activated Ca^{2+} channel) was investigated.

Single channel experiments using oxalate loaded IM vesicles

A subpopulation of the IM containing Ca^{2+} pumps has been isolated by the application of an oxalate loading procedure. Vesicles from this fraction fuse with uncharged bilayers in KCl solutions. A channel is obtained which is ideally selective for K^+ over Cl^- (figure 5.3) with a single channel conductance of ~300pS in symmetrical 450mM KCl (figure 5.2). The open probability of this channel is influenced by the applied voltage (figure 5.4), but is unaffected by the surrounding Ca^{2+} concentration. The presence of Ca^{2+} in the solutions does not alter the current-voltage relationship for the channel in KCl, nor are Ca^{2+} currents through the channel observed when K^+ solutions are exchanged for Ca^{2+} solutions. Thus Ca^{2+} ions do not permeate the K^+ channel, nor does their presence regulate channel gating.

Muscle sarcoplasmic reticulum is also known to contain monovalent cation-selective channels. Single K^+ channels have been extensively studied after the incorporation of SR vesicles into planar bilayers (Coronado and Miller, 1979; 1980; 1982; Coronado *et al.*, 1980; Labarca *et al.*, 1980; Labarca and Miller, 1981; Miller, 1982b; Tomlins *et al.*, 1984; Cukierman *et al.*, 1985; Gray *et al.*, 1985; Hill *et al.*, 1989), and patch clamp measurements have been made from reconstituted liposomes (Tomlins and Williams, 1986) and skinned muscle fibers (Stein *et al.*, 1989; Tang *et al.*, 1989).

The single channel activity displayed by the platelet IM cation channel is qualitatively similar to that observed when native cardiac and skeletal muscle SR K^+ channels are reconstituted into planar bilayers or liposomes. The single channel conductance of these channels is generally large (in the range ~150-300pS); indeed

they have been termed 'maxi' K^+ channels (Latorre and Miller, 1983), and they are generally highly selective and voltage dependent. Further characterisation of the platelet IM K^+ channel in terms of conduction and blocking characteristics is required in order to present a more detailed comparison of its properties to other endoplasmic reticulum K^+ channels.

The K^+ channels identified in muscle SR are believed to act as charge compensators for the release of Ca^{2+} which causes muscle activation (Miller *et al.*, 1984). It is possible that the monovalent cation channel identified in the platelet IM may also act as a charge compensator for Ins(1,4,5)P_3 induced Ca^{2+} release on platelet activation. This contention is supported by evidence from groups working with other tissues. Muallem *et al.*, (1985) first indicated a relationship between Ca^{2+} and K^+ transport systems in rough endoplasmic reticulum from hepatocytes. They demonstrated that the Ca^{2+} conductance activated by Ins(1,4,5)P_3 requires an opposite flow of K^+ as a counter-ion. Shah and Pant (1988) found that Ins(1,4,5)P_3 induced Ca^{2+} release in microsomal fractions from rat brain was insensitive to a variety of Ca^{2+} channel blockers, but was inhibited by K^+ channel blockers such as tetraethylammonium (TEA) chloride. This again suggests that Ins(1,4,5)P_3 induced Ca^{2+} release requires an opposite flow of K^+ ions and blockade of the K^+ movement underlies the inhibition of Ca^{2+} release by TEA in their experiments.

Similar experiments to those devised by Shah and Pant (1988) have been carried out using the purified platelet IM vesicle fraction. IM vesicles identified following CFE have been incubated in KCl medium in the presence of ATP and $^{45}Ca^{2+}$ at room temperature for 15 mins. After steady state Ca^{2+} uptake was reached, TEA (3mM) was added and the mixture incubated for a further 15 mins. Ins(1,4,5)P_3

(10μM) was then applied and the Ca^{2+} release measured as described in section 2.3.3. These experiments have so far produced inconclusive results (B. Evenden, 1989- preliminary observations). Single channel experiments demonstrating TEA blockade of the platelet IM K^+ channel, together with the conclusive block of Ins(1,4,5)P_3 induced Ca^{2+} release in vesicle ion flux experiments, would provide good evidence to support a physiological role for the K^+ channel as a charge compensator in the platelet IM.

The K^+ channel as a marker for IM fusion

Extensive characterisation of the platelet IM monovalent cation channel has proved difficult due to the low yield of oxalate loaded IM vesicles obtained. This channel was mainly used as a 'marker' for fusion of the IM. Once the K^+ channel was identified in the bilayer, the conditions surrounding the membrane were altered to those favouring Ca^{2+} channel activity.

Ion flux experiments have indicated that most of the IM vesicles prepared by CFE are 'right-side-out' since they can be loaded with Ca^{2+} in the presence of ATP; i.e. the outside of the vesicle corresponds to the platelet cytosol and the inside of the vesicle to the lumen of the DTS. Similarly the oxalate loaded subpopulation of the IM consists of vesicles with the 'correct' orientation, since the Ca^{2+} pump must be functional in order for the isolation method to proceed. Fusion of oxalate loaded vesicles with planar bilayers in KCl solutions was therefore assumed to yield K^+ channels orientated such that the *cis* chamber represented the cytoplasmic side of the DTS. Thus, once fusion of the IM was established, conditions were altered to give a Ca^{2+} gradient from *trans* to *cis*. Ins(1,4,5)P_3 was then added to the *cis* chamber solution and bilayer currents monitored for channel openings

indicating divalent cation movement from the *trans* to the *cis* chamber. The *cis:trans* conditions were reversed in 2 experiments in order to rule out the possibility that Ca^{2+} channels had fused with the bilayer in the opposite orientation. Ins(1,4,5)P_3 induced channel activity was not observed in any of these experiments.

Ca^{2+} channels activated by Ins(1,4,5)P_3 have been successfully identified in vascular smooth muscle SR vesicles following reconstitution into planar bilayers (Ehrlich and Watras, 1988). SR vesicles (pre-tested in an assay for Ins(1,4,5)P_3-induced Ca^{2+} release) were incorporated into bilayers using a Cl^- channel as a marker for fusion. Following fusion, chamber conditions were altered to give a large *trans:cis* Ca^{2+} gradient. In the presence of Ins(1,4,5)P_3 (1-5μM *cis*) Ca^{2+} channels have been identified with a conductance of ~10pS which do not appear to be voltage-dependent. Heparin, which has been shown to bind to an Ins(1,4,5)P_3 receptor found in the cerebellum (Supattapone *et al.*, 1988) and to inhibit tension development in saponin-permeabilised smooth muscle (Kobayashi *et al.*, 1988) was found to reduce Ins(1,4,5)P_3 induced Ca^{2+} release from aortic SR and inhibit Ca^{2+} channel currents in bilayers when added to the *cis* chamber.

The experimental rationale applied by Ehrlich and Watras (1988) was essentially the same as that used in the experiments described in this chapter, i.e.

(i) initial test for Ins(1,4,5)P_3 induced Ca^{2+} release from the membrane vesicle fraction of interest.

(ii) the identification of a channel used as a 'marker' for fusion of the membrane fraction.

(iii) subsequent alteration of recording solutions, following vesicle fusion, to establish conditions favouring Ca^{2+} channel activity.

However, whereas an $Ins(1,4,5)P_3$ gated Ca^{2+} channel has been identified in the SR of vascular smooth muscle, experiments carried out on the platelet IM as described in this chapter, have not, to date, been so fruitful.

The main difficulty with experiments using the platelet IM fraction, as stated previously, has been the low yield of 'starting material'. In two preparations the oxalate loading procedure was applied to the MM fraction in attempts to separate the IM fraction containing Ca^{2+} pumps without the use of CFE. However, vesicles separated in this way are found to contain the predominantly anion selective channel known to originate in the SM. This suggests the possibility that some direct contact may exist between the DTS and SM in the platelet, analogous to the structural relationship between the junctional SR and transverse tubules in muscle. Membrane separation by CFE may exclude such vesicles (containing both IM and SM elements) since only selected fractionation tubes along the CFE profile are pooled (see figure 2.2).

Future experiments searching for evidence of single channel activity from an $Ins(1,4,5)P_3$ regulated Ca^{2+} channel in the platelet must therefore continue to utilise the highly purified IM fraction prepared by high-voltage CFE and loaded with oxalate.

Chapter 6

SUMMARY

6.1 Summary

This thesis contains the first biophysical characterisations of ion channel proteins in purified human platelet surface and intracellular membranes.

The project has brought together two well developed procedures to facilitate single channel recordings from ion channels located in the two highly purifed membrane fractions.

(a) high-voltage continuous flow electrophoresis, which allows the differential isolation of highly purified platelet surface and intracellular membrane vesicles free from cross-contamination, and

(b) a method for fusion of the vesicles with artificial planar phopholipid bilayers allowing electrophysiological recordings of ion channel activity under voltage clamp conditions.

Investigations so far have concerned the detailed characterisation of a predominantly anion-selective channel from the platelet surface membrane, and the identification of a monovalent cation-selective channel from the intracellular membrane. Experiments designed to identify divalent cation currents through agonist-activated channels in the platelet surface membrane and Ins(1,4,5)P_3-gated channels in the intracellular membrane have also been attempted.

6.1.1 Platelet surface membrane channels

A predominantly anion selective channel is observed following fusion of vesicles from the platelet surface membrane. Channels with consistent and comparable conduction characteristics are also found in the mixed membrane fraction (both treated with neuraminidase or left untreated). The membrane purification procedure therefore does not appear to alter the conduction properties of the single channel protein.

Experiments have been carried out to probe the conduction behaviour of this channel. Reversal potential measurements determined in the presence of KCl gradients show that although the channel is preferentially selective for Cl^-, it also has a permeability to K^+. A partial cation permeability of this type is also exhibited by other 'anion' channels in a variety of tissues. Cations as large as tetraethylammonium (TEA^+) are found to permeate the platelet SM channel, implying a minimum cross-sectional area for the conduction pathway of at least $37Å^2$.

The channel accepts all of the halides as well as a number of other anions. A sequence of relative anion permeabilities comparing various anions to Cl^- has been measured. The channel appears to select between anions according to their interaction with electric charges or dipoles and neighbouring hydrophobic groups within the channel.

Current through the SM channel has been shown to be blocked by HEPES and Tris buffers and, in most cases, by DIDS and SITS, which are known inhibitors of Cl^- transport proteins. ATP and ADP also induce an asymmetric block of single

channel current and may be acting as large impermeant anions from one face of the channel.

The stochastic properties of this channel have also been investigated to obtain information about possible gating mechanisms which underlie channel opening and closing. The distribution of open channel intervals can be described by a single expontential, whilst the distribution of closed intervals is best described by the sum of three exponential components. Thus a minimum transition model is proposed with (at least) one open state and (at least) two closed states. A linear kinetic scheme most likely describes the gating properties of this channel since no correlation has been found between successive closed events.

The nature of the characterisation experiments applied to this channel has required the application of relatively extreme physicochemical conditions on the channel protein and hence inferences concerning its possible physiological function are difficult to make. The application of various agents known to be important in platelet responses (e.g. thrombin, PAF, $Ins(1,4,5)P_3$) have not, so far, shed any further light on a possible physiological role for this channel.

Ionic conditions surrounding fused SM vesicles have been manipulated to attempt to monitor agonist induced Ca^{2+} channel activity in the surface membrane. Although indirect evidence from other workers in the field using fluorescent probes suggests the presence of such channels in platelets, no single channel evidence from the bilayer experiments reported in this thesis has been obtained. The recent publication of ADP-evoked Ca^{2+} channel currents in patch clamped platelets (Mahaut-Smith *et al.*, 1989) suggests that the patch technique may prove a more suitable method for investigation of the properties of these channels.

6.1.2 Platelet intracellular membrane channels

The platelet intracellular membrane is inaccessible to patch pipettes and so single channel recordings from this membrane are only possible following incorporation of membrane vesicles into planar bilayers. A great deal of effort has therefore been devoted to the reconstitution of channel proteins from this membrane fraction. Difficulties in accruing single channel data have mainly been due to the low yield of membrane prepared. Fusion of vesicles containing a monovalent cation-selective channel have only been observed from a subpopulation of the intracellular membrane separated by an oxalate loading procedure. This K^+ channel may provide a mechanism for charge compensation during calcium movements into and out of the platelet intracellular membrane, analogous to that found in the sarcoplasmic reticulum of muscle.

Although the IM vesicles prepared for these experiments have been shown to release pre-loaded Ca^{2+} on application of $Ins(1,4,5)P_3$, the putative channel responsible has so far eluded reconstitution in bilayer experiments.

APPENDICES & REFERENCES

APPENDIX A

Sources of chemicals used in experiments (unless specified in the text)

All reagents were of analytical grade where possible and solutions were prepared in Analar water (BDH) or Millipore distilled water

Aldrich Chemical Company Ltd., U.K.

DIDS

BDH Chemicals Ltd., U.K.

acetic acid, acrylamide, agar, ammonium persulphate, $BaCl_2$, bromophenol blue, $CaCl_2$, $Ca(OH)_2$, chloroform, cholineCl, Ciocalteu's phenol reagent, citric acid, $CuSO_4$, deoxycholic acid, EDTA, EGTA, ethanol, Folin, glycerol, glycine, HCl, HEPES, histidine, Kacetate, KBr, KCl, KCN, KF, Kgluconate, KH_2PO_4, KI, KOH, KNO_3, Koxalate, KSCN, K_2SO_4, ß-mercaptoethanol, methanol, $MgCl_2$, NaCl, Na_2CO_3, NaOH, NaPPi, Natartrate, SDS, sorbitol, sucrose, TEABr, TEMED, trichloroacetic acid, triethanolamine, Tris, $ZnCl_2$

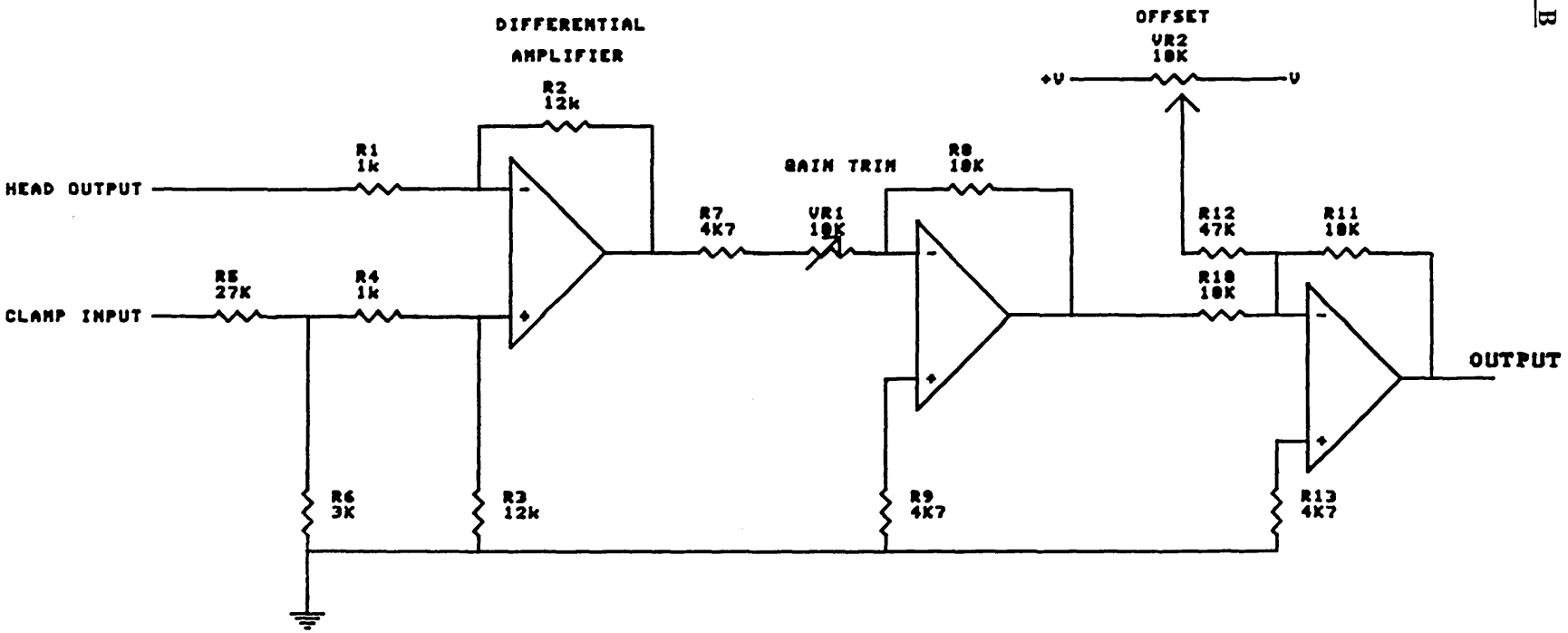
Calbiochem Ltd., U.K.

A23187

Sigma Chemical Company Ltd., U.K.

ADP, antimycin A, aprotonin, ATP, bovine serum albumin, cytochrome *c*, Coomassie blue, *n*-decane, gallamine-Cl, NADH, PAF, pepstatin A, phenyl-methane-sulphonyl fluoride, SITS, succinylcholine-Cl, thrombin

SECOND STAGE AMPLIFIER



NOTE

1) ALL AMPLIFIERS TYPE TL071
2) ALL AMPLIFIERS DECOUPLED BY 0.1uF
   CERAMIC CAPACITORS AT POWER TERMINALS

REFERENCES

Adelstein, R.S., Conti, M.A., Daniel, T.L. and Anderson, W. Jr. 1975. The interaction of platelet actin, myosin and myosin light chain kinase. *In*: Biochemistry and pharmacology of platelets. Ciba Foundation Symposium **35**. Elsevier-Excerpta Medica, North Holland. pp 101-119

Adunyah, S.E. and Dean, W.L. 1985. Inositol trisphosphate-induced Ca^{2+} release from human platelet membranes. *Biochem. Biophys. Res. Commun.* **128**: 1274-1280

Adunyah, S.E. and Dean, W.L. 1986a. Ca^{2+} transport in human platelet membranes. Kinetics of active transport and passive release. *J. Biol. Chem.* **261**: 3122-3127

Adunyah, S.E. and Dean, W.L. 1986b. Effects of sulfhydryl reagents and other inhibitors on Ca^{2+} transport and inositol trisphosphate-induced Ca^{2+} release from human platelet membranes. *J. Biol. Chem.* **261**: 13071-13075

Akabas, M.H., Cohen, F.S. and Finkelstein, A. 1984. Separation of the osmotically driven fusion event from vesicle-planar membrane attachment in a model system for exocytosis. *J. Cell Biol.***98**: 1063-1071

Alvarez, O. 1986. How to set up a bilayer system. *In*: Ion Channel Reconstitution. Ed: Miller, C. Plenum Press New York. pp 115-129

Ascher, P., Marty, A. and Neild, T.O. 1978. Lifetime and elementary conductance of the channels mediating the excitatory effects of acetylcholine in *Aplysia* neurones. *J. Physiol. (London).* **278**: 177-206

Ashford, M.L.J., Sturgess, N.C., Trout, N.J., Gardner, N.J. and Hales, C.N. 1988. Adenosine-5'-triphosphate-sensitive ion channels in neonatal rat cultured central neurones. *Pflugers Arch.* **412**: 297-304

Authi, K.S. and Crawford, N. 1985. Inositol 1,4,5-trisphosphate-induced release of sequestered Ca^{2+} from highly purified human platelet intracellular membranes. *Biochem. J.* **230**: 247-253

Authi, K.S., Evenden, B.J. and Crawford, N. 1986. Metabolic and functional consequences of introducing inositol 1,4,5-trisphosphate into saponin-permeabilized human platelets. *Biochem. J.* **233**: 709-718

Bader, C.R., Bertrand, D. and Schwartz, E.A. 1982. Voltage-activated and calcium-activated currents studied in solitary rod inner segments from the salamander retina. *J. Physiol. (London)* **331**: 253-284

Berridge, M.J. and Irvine, R.F. 1984. Inositol trisphosphate, a novel second messenger in cellular signal transduction. *Nature.* **312**: 315-321

Bevan, S., Chiu, S.Y., Gray, P.T.A. and Ritchie, J.M. 1985. The presence of voltage-gated sodium, potassium and chloride channels in rat cultured astrocytes. *Proc. R. Soc. (London)* **B225**: 299-313

Blatz, A.L. and Magleby, K.L. 1983. Single voltage-dependent chloride selective channels of large conductance in cultured rat muscle. *Biophys. J.* **43**: 237-241

Blatz, L.A. and Magleby, K.L. 1985. Single chloride-selective channels active at resting membrane potentials in cultured rat skeletal muscle. *Biophys. J.* **47**: 119-123

Blatz, L.A. and Magleby, K.L. 1986. Quantitative description of three modes of activity of fast chloride channels from rat skeletal muscle. *J. Physiol. (London).* **378**: 141-174

Bormann, J., Hamill, O.P. and Sakmann,B. 1987. Mechanism of anion permeation through channels gated by glycine and α-aminobutyric acid in mouse cultured spinal neurones. *J. Physiol. (London)* **385**: 243-286

Born, G.V.R. 1970. Observations on the change in shape of blood platelets brought about by adenosine diphosphate. *J. Physiol. (London)* **290**: 487-511

Brass, L.F. and Joseph, S.K. 1985. A role for inositol triphosphate in intracellular Ca^{2+} mobilization and granule secretion in platelets. *J. Biol. Chem.* **260**: 15172-15179

Brass, L.F. and Shattil, S.J. 1982. Changes in surface-bound and exchangeable calcium during platelet activation. *J. Biol. Chem.* **257**: 14000-14005

Breisblatt, W. and Ohki, S. 1976. Fusion in phospholipid spherical membranes. II Effect of cholesterol, divalent ions and pH. *J. Membr. Biol.* **29**: 127-146

Buckingham, S. and Maynert, E.W. 1964. The release of 5-hydroxytryptamine, potassium and amino acids from platelets. *J. Pharmacol. Exp. Ther.* **143**: 332-339

Bushfield, M., McNicol, A. amd MacIntyre, D.E. 1985. Inhibition of platelet activating factor-induced human platelet activation by prostaglandin D_2. Differential sensitivity of platelet transduction processes and functional responses to inhibition by cyclic AMP. *Biochem. J.* **232**: 267-271

Cabantchik, Z.I. and Rothstein, A. 1972. The nature of the membrane sites controlling anion permeability of human red blood cells as determined by studies with disulphonic stilbene derivatives. *J. Membr. Biol.* **10**: 311-330

Cabantchik. Z.I. and Rothstein, A. 1974. Membrane proteins related to anion permeability of human red blood cells. I. Localization of disulphonic stilbene binding sites in proteins involved in permeation. *J. Membr. Biol.* **15**: 207-226

Cahalan, M.D., Chandy, K.G., DeCoursey, T.E. and Gupta, S. 1985. A voltage-gated potassium channel in human T lymphocytes. *J. Physiol. (London)* **358**: 197-237

Carey, F., Menashi, S. and Crawford, N. 1982. Localisation of cyclooxygenase and thromboxane synthetase in human platelet intracellular membranes. *Biochem. J.* **204**: 847-851

Clemetson, K.J. and McGregor, J.L. 1987. Characterisation of platelet membrane glycoproteins. *In:* Platelets in Biology and Pathology III. Ed: MacIntyre and Gordon. Elsevier Science Publishers. pp. 1-36

Cohen, F.S., Akabas, M.H. and Finkelstein, A. 1982. Osmotic swelling of phospholipid vesicles causes them to fuse with a planar phospholipid bilayer membrane. *Science* **217**: 458-460

Cohen, F.S., Akabas, M.H., Zimmerberg, J. and Finkelstein, A. 1984. Parameters affecting the fusion of unilamellar phospholipid vesicles with planar bilayer membranes. *J. Cell. Biol.* **98**: 1054-1062

Cohen, F.S., Niles, W.D. and Akabas, M.H. 1989. Fusion of phospholipid vesicles with a planar membrane depends on the membrane permeability of the solute used to create the osmotic pressure. *J. Gen. Physiol.* **93**: 201-210

Cohen, F.S., Zimmerberg, J. and Finkelstein, A. 1980. Fusion of phospholipid vesicles with planar phospholipid bilayer membranes. II Incorporation of a vesicular membrane marker into the planar membrane. *J. Gen. Physiol.* **75**: 251-270

Colombini, M. 1986. Voltage gating in VDAC. Towards a molecular mechanism. *In:* Ion Channel Reconstitution. Ed: Miller, C. Plenum Press, New York. pp 533-550

Colquhoun, D. 1988. Single channel analysis costs time. *Trends Pharmacol. Sci.* **9**: 157-158

Colquhoun, D. and Hawkes, A.G. 1983. The principles of the stochastic interpretation of ion channel mechanisms. *In:* Single channel recording. Eds: Sakmann, B. and Neher, E. Plenum Press, New York. pp 135-174

Colquhoun, D. and Sigworth, F.J. 1983. Fitting and statistical analysis of single channel records. *In*: Single channel recording. Eds: Sakmann, B. and Neher, E. Plenum Press, New York. pp 191-263

Connolly, T.M., Bansal, V.S., Bross, T.E., Irvine, R.F. amd Majerus, P.W. 1987. The metabolism of tris and tetraphosphates of inositol by 5-phosphomonoesterase and 3-kinase enzymes. *J. Biol. Chem.* **262**: 2146-2149

Conti, F., Defelice, L.J. and Wanke, E. 1975. Potassium and sodium ion current noise in the membrane of the squid giant axon. *J. Physiol. (London)* **248**: 45-82

Conti, F. and Neher, E. 1980. Single channel recordings of K^+ currents in squid giant axon. *Nature* **285**: 140-143

Cooley, M.H. and Cohen, P. 1967. Potassium transport in human blood platelets. *J. Lab. Clin. Med.* **70**: 69-79

Coronado, R. and Latorre, R. 1983. Phospholipid bilayers made from monolayers on patch-clamp pipettes. *Biophys. J.* **43**: 231-236

Coronado, R. and Miller, C. 1979. Voltage-dependent caesium blockade of a cation channel from fragmented sarcoplasmic reticulum. *Nature.* **280**: 807-810

Coronado, R. and Miller, C. 1980. Decamethonium and hexamethonium block K^+ channels of sarcoplasmic reticulum. *Nature.* **288**: 495-497

Coronado, R. and Miller, C. 1982. Conductance and block by organic cations in a K^+- selective channel from sarcoplasmic reticulum incorporated into planar phospholipid bilayers. *J. Gen. Physiol.* **79**: 529-547

Coronado, R., Rosenberg, R.L. and Miller, C. 1980. Ionic selectivity, saturation and block in a K^+-selective channel from sarcoplasmic reticulum. *J. Gen. Physiol.* **76**: 425-446

Cottrell, G.A., Duff, D.A. and Lambert, J.J. 1983. An inexpensive microcomputer system for analysis of single channel currents. *J. Neurosci. Methods* **9**: 259-267

Cukierman, S., Yellen, G. and Miller, C. 1985. The K^+ channel of sarcoplasmic reticulum. A new look at Cs^+ blockade. *Biophys. J.* **48**: 477-484

Dangelmaier, C.A., Daniel, J.L. and Smith, J.B. 1986. Determination of basal and stimulated levels of inositol triphosphate in [^{32}P]orthophosphate-labelled platelets. *Anal. Biochem.* **154**: 414-419

Dani, J.A., Sanchez, J.A. and Hille, B. 1983. Lyotrophic anions. Na channel gating and Ca electrode response. *J. Gen. Physiol.* **81**: 255-281

Dawson, A.P. and Irvine, R.F. 1984. Inositol (1,4,5) trisphosphate-promoted Ca^{2+} release from microsomal fractions of rat liver. *Biochem. Biophys. Res. Commun.* **120**: 858-864

Dean, W.L. 1984. Purification and reconstitution of a Ca^{2+} pump from human platelets. *J. Biol. Chem.* **259**: 7343-7348

Dean, W.L. 1988. Isolation and reconstitution of a Ca^{2+} pump from human and porcine platelets. *Methods Enzymol.* **157**: 351-360

Dean, W.L. 1989. Structure, function and subcellular localisation of a human platelet Ca^{2+}ATPase. *Cell Calcium.* **10**: 289-297

Dean, W.L. and Sullivan, D.M. 1982. Structural and functional properties of a Ca^{2+}-ATPase from human platelets. *J. Biol. Chem.* **257**: 14390-14394

Detwiler, T.L., Caro, I.F. and Fienman, R.D. 1978. Evidence that calcium regulates platelet function. *Thromb. Haemostas.* **40**: 207-211

Diamond, J.M. and Wright, E.M. 1969. Biological membranes: The physical basis of ion and nonelectrolyte selectivity. *Ann. Rev. Physiol.* **31**: 581-646

Doyle, V.M. and Ruegg, U.T. 1985. Lack of evidence for voltage dependent calcium channels on platelets. *Biochem. Biophys. Res. Commun.* **127**: 161-167

Durham, A.C.H. 1983. A survey of readily available chelators for buffering calcium ion concentration in physiological solutions. *Cell Calcium.* **4**: 33-46

Edwards, C. 1982. The selectivity of ion channels in nerve and muscle. *Neuroscience* **7**: 1335-1366

Ehrlich, B.E. and Watras, J. 1988. Inositol 1,4,5-trisphosphate activates a channel from smooth muscle sarcoplasmic reticulum. *Nature* **336**: 583-586

Eisenman, G. 1965. Some elementary factors involved in specific ion permeation. *Proc XXIII Int. Cong. Phys. Sci.* 87: 489-506

Enouf, J., Bredoux, R. and Levy-Toledano, S. 1984. Characterisation of calcium liberation from a human platelet membrane fraction. *Biochim. Biophys. Acta.* 772: 251-258

Fauvel, J., Chap, H., Roques, V., Levy-Toledano, S. and Douste-Blazy, L. 1986. Biochemical characterisation of plasma membranes and intracellular membranes isolated from human platelets using Percoll gradients. *Biochim. Biophys. Acta* 856: 155-164

Feinberg, H., Michel, H. and Born, G.V.R. 1974. Determination of the fluid volume of platelets by their separation through silicon oil. *J. Lab. Clin. Med.* 84: 926-934

Feinberg, H., Sandler, W.C., Scorer, M., Le Breton, G.C., Grossman, B. and Born, G.V.R. 1977. Movement of sodium into human platelets induced by ADP. *Biochim. Biophys. Acta.* 470: 317-324

Feinstein, M.B. 1980. Release of intracellular membrane-bound calcium precedes the onset of stimulus-induced exocytosis in platelets. *Biochem. Biophys. Res. Commun.* 93: 593-600

Feinstein, M.B., Egan, J.J., Sha'afi, R.I. and White, J. 1983. The cytoplasmic concentration of free calcium in platelets is controlled by stimulators of cyclic AMP production (PGD_2, PGE_1, forskolin). *Biochem. Biophys. Res. Commun.* **113**: 598-604

Fisher, G.J., Bakshian, S. and Baldassare, J.J. 1985. Activation of human platelets by ADP causes a rapid rise in cytosolic free calcium without hydrolysis of phosphatidylinositol-4,5-bisphosphate. *Biochem. Biophys. Res. Commun.* **129**: 958-964

Franciolini, F. and Nonner, W. 1987. Anion and cation permeability of a chloride channel in rat hippocampal neurones. *J. Gen. Physiol.* **90**: 453-478

Friedhoff, L.T. and Sonenberg, M. 1983. The membrane potential of human platelets. *Blood.* **61**: 180-185

Fukushima, Y., Hagiwara, S. and Henkart, M. 1984. Potassium current in clonal cytotoxic lymphocytes from the mouse. *J. Physiol. (London)* **351**: 645-656

Gerrard, J.M., Peterson, D.A. and White, J.G. 1981. Calcium mobilisation. *In*: Platelets in Biology and Pathology. Ed: Gordon, J.L. Elsevier, Amsterdam. pp 407-436

Gerrard, J.M., White, J.G. and Rao, G.H.R. 1976. Localisation of platelet prostaglandin production in the platelet dense tubular system. *Am. J.Pathol.* **83**: 283-298

Goldman, D.E. 1943. Potential, impedance and rectification in membranes. *J. Gen. Physiol.* 27: 37-60

Gorstein, F., Carrol, H.J. and Puszkin, E. 1967. Electrolyte concentrations, potassium flux kinetics and the metabolic dependence of potassium transport in human platelets. *J. Lab. Clin. Med.* 70: 92-103

Gray, P.T.A., Bevan, S. & Ritchie, J.M. 1984. High conductance anion-selective channels in rat cultured Schwann cells. *Proc. R.Soc. London.* B221: 395-409

Gray, M.A., Montgomery, R.A.P. and Williams, A.J. 1985. Asymmetric block of a monovalent cation-selective channel of rabbit cardiac sarcoplasmic reticulum by succinyl choline. *J. Membr. Biol.* 88: 85-95

Greenberg-Seperksy, S.M. and Simons, E.R. 1984. Cation gradient dependence of the steps in thrombin stimulation of human platelets. *J. Biol. Chem.* 295: 1502-1508

Grynkiewicz, G., Poenie, M. and Tsien, R.Y. 1985. A new generation of Ca^{2+} indicators with greatly improved fluorescent properties. *J. Biol. Chem.* 260: 3440-3450

Hack, N., Croset. M. and Crawford, N. 1986. Studies on the bivalent-cation-activated ATPase activities of highly purified human platelet surface and intracellular membranes. *Biochem. J.* 233: 661-668

Halenda, S.P., Volpi, M., Zavoico, G.B., Sha'afi, R.I. and Feinstein, M.B. 1986. Effects of thrombin, phorbol myristate acetate and prostaglandin D_2 on 40-41 kDa protein that is ADP ribosylated by pertussis toxin in platelets. *FEBS Lett.* **204**: 341-346

Hallam, T.J. and Rink, T.J. 1985a. Responses to adenosine diphosphate in human platelets loaded with the fluorescent calcium indicator quin 2. *J. Physiol.* (London) **368**: 131-146

Hallam, T.J. and Rink, T.J. 1985b. Agonists stimulate divalent cation channels in the plasma membrane of human platelets. *FEBS Lett.* **186**: 175-179

Hallam, T.J., Sanchez, A. and Rink, T.J. 1984a. Stimulus-response coupling in human platelets. Changes evoked by platelet-activating factor in cytoplasmic free calcium monitored with the fluorescent calcium indicator quin 2. *Biochem. J.* **218**: 819-827

Hallam, T.J., Thompson, N.T., Scrutton, M.C. and Rink, T.J. 1984b. The role of cytoplasmic free calcium in the responses of quin2-loaded human platelets to vasopressin. *Biochem. J.* **221**: 897-901

Hamill, O.P., Marty, A., Neher, E., Sakmann, B. and Sigworth, F.J. 1981. Improved patch-clamp techniques for high resolution current recording from cells and cell free membrane patches. *Pflugers Arch.* **391**: 85-100

Hanke, W. 1986. Incorporation of ion channels by fusion. *In:* Ion Channel Reconstitution. Ed: Miller, C. Plenum Press, New York

Hannig, K. 1969. The application of free-flow electrophoresis to the separation of macromolecules and particles of biological importance. *In:* Modern Separation Methods of Macromolecules and Particles. Vol. I. Ed: Gerritsen, T. John Wiley and Sons Inc., New York. pp 45-69

Hannig, K., Wirth, H., Meyer, B-H. and Zeiller, K. 1975. Free-flow electrophoresis. I. Theoretical and experimental investigations of the influence of mechanical and electrokinetic variables on the efficiency of the method. *Hoppe-Seylers Z. Physiol. Chem.* **356**: 1209-1223

Hanrahan, J.W., Alles, W.P. and Lewis, S.A. 1985. Single anion-selective channels in basolateral membrane of a mammalian tight epithelium. *Proc. Natl. Acad. Sci. USA.* **82**: 7791-7795

Hauser, H., Phillips, M.C. and Barratt, M.D. 1975. Differences in the interaction of inorganic and organic (hydrophobic) cations with phosphatidylserine membranes. *Biophys. Acta* **413**: 341-353

Hill, J.A., Coronado, R. and Strauss, H.C. 1989. Potassium channel of cardiac sarcoplasmic reticulum is a multi-ion channel. *Biophys. J.* **55**: 35-46

Hodgkin, A.L. and Huxley, A.F. 1952. A quantitative description of membrane current and its application to conduction and excitation in nerve. *J. Physiol. (London)* **117**: 500-544

Hodgkin, A.L. and Katz, B. 1949. The effect of sodium ions on the activity of the giant axon of the squid. *J. Physiol (London)* **108**: 37-77

Holmsen, H. 1972. The platelet: its membrane, physiology and biochemistry. *Clin. Haematol.* 1: 235-266

Horn, R. and Lange, K. 1983. Estimating kinetic constants from single channel data. *Biophys. J.* 43: 207-223

Horne, W.C., Norman, N.E., Schwartz, D.B. and Simons, E.R. 1981. Changes in cytoplasmic pH and in membrane potential in thrombin-stimulated human platelets. *Eur. J. Biochem.* 120: 295-302

Imai, A., Hattori, H., Takahashi, M. and Nozawa, Y. 1983. Evidence that cyclic AMP may regulate Ca^{2+} mobilisation and phospholipases in thrombin-stimulated human platelets. *Biochem. Biophys. Res. Commun.* 112: 693-700

Irvine, R.F. and Moor, R.M. 1986. Micro-injection of inositol 1,3,4,5-tetrakisphosphate activates sea urchin eggs by a mechanism dependent on external Ca^{2+}. *Biochem. J.* 240: 917-920

Javors, M.A., Bowden, C.L. and Ross, D.H. 1982. Kinetic characterisation and substrate requirement for the Ca^{2+} uptake system in platelet membranes. *Biochim. Biophys. Acta.* 691: 220-226

Johnson, P.C., Ware, J.A., Cliveden, P.B., Smith, M., Dvorak, A.M. and Salzman, E.W. 1985. Measurement of ionized calcium in blood platelets with the photoprotein aequorin. Comparison with quin2. *J. Biol. Chem.* 260: 2069-2076

Jones, L.R. and Cala, S.E. 1981. Biochemical evidence for functional heterogeneity of cardiac sarcoplasmic reticulum vesicles. *J. Biol. Chem.* **256**: 11809-11818

Jy, W. and Haynes, D.H. 1987. Thrombin-induced calcium movements in platelet activation. *Biochim. Biophys. Acta.* **929**: 88-102

Kaser-Glanzmann, R., Jakabova, M., George, J.N. and Luscher, E.F. 1978. Further characterisation of calcium-accumulating vesicles from human blood platelets. *Biochim. Biophys. Acta.* **512**: 1-12

Kelly, J.S., Krnjevic, K., Morris, M.E. and Yim, G.K.W. 1969. Anionic permeability of neurones. *Exp. Brain. Res.* 7: 11-31

Kerry, C.J., Kits, K.S., Ramsey, R.L., Sansom, M.S.P. and Usherwood, P.N.R 1987. Single channel kinetics of a glutamate receptor. *Biophys. J.* **51**: 137-144

Kinoshita, T., Nachman, R.L. and Minick, R. 1979. Isolation of human platelet plasma membranes with polylysine beads. *J. Cell. Biol.* **82**: 688-696

Knight, D.E. and Scrutton, M.C. 1984. Cyclic nucleotides control a system which regulates Ca^{2+} sensitivity of platelet secretion. *Nature* **309**: 66-68

Kobayashi, S. Somiyo. A.V. and Somiyo, A.P. 1988. Heparin inhibits the inositol 1,4,5-trisphosphate-dependent, but not the independent, calcium release induced by guanine nucleotide in vascular smooth muscle. *Biochem. Biophys. Res. Commun.* **153**: 625-631

Kolb, H-A., Brown, C.D.A. and Murer, H. 1985. Identification of a voltage-dependent anion channel in the apical membrane of a Cl^- secretory epithelium (MDCK). *Pflugers Arch.* **403**: 262-265

Krouse, M.E., Schneider, G.T. and Gage, P.W. 1986. A large anion-selective channel has seven conductance levels. *Nature* **319**: 58-60

Kuno, M. and Gardner, P. 1987. Ion channels activated by inositol 1,4,5-trisphosphate in plasma membrane of human T-lymphocytes. *Nature* **326**: 301-304

Labarca, P., Coronado, R. and Miller, C. 1980. Thermodynamic and kinetic studies of the gating behaviour of a K^+-selective channel from the sarcoplasmic reticulum membrane. *J. Gen. Physiol.* **76**: 397-424

Labarca, P. and Miller, C. 1981. A K^+-selective, three-state channel from fragmented sarcoplasmic reticulum of frog leg muscle. *J. Membr. Biol.* **61**: 31-38

Labarca, P., Rice, J.A., Fredkin, D.R. and Montal, M. 1985. Kinetic analysis of channel gating. Application to the cholinergic receptor channel and the chloride channel from *Torpedo californica. Biophys. J.* **47**: 469-478

Laemmli, U.K. 1970. Cleavage of structural proteins during the assembly of the head of bacteriophage T4. *Nature.* **227**: 680-685

Lagarde, M., Guichardant, M., Menashi, S. and Crawford, N. 1982. The phospholipid and fatty acid composition of human platelet surface and intracellular membranes isolated by high voltage free flow electrophoresis. *J. Biol. Chem.* **257**: 3100-3104

Lagarde, M., Menashi, S. and Crawford, N. 1981. Localisation of phospholipase A_2 and diglyceride lipase activities in human platelet intracellular membranes. *FEBS Lett.* **124**: 23-26

Latorre, R. and Miller, C. 1983. Conduction and selectivity in potassium channels. *J. Membr. Biol.* **71**: 11-30

Latorre, R., Vergara, C. and Hidalgo, C. 1982. Reconstitution in planar lipid bilayers of a calcium dependent potassium channel from transverse tubule membranes isolated from rabbit skeletal muscle. *Proc. Natl. Acad. Sci. USA.* **79**: 805-809

Lauger, P. 1973. Ion transport through pores: a rate-theory analysis. *Biochim. Biophys. Acta.* **311**: 423-441

Lerea, K.M., Glomset, J.A. and Krebs, E.G. 1987. Agents that elevate cAMP levels in platelets decrease thrombin binding. *J. Biol. Chem.* **262**: 282-288

Lind, S.E., Yin, H.L. and Stossel, T.P. 1982. Human platelets contain gelsolin; a regulator of actin filament length. *J. Clin. Invest.* **69**: 1384-1387

Lowry, O.H., Rosebrough, N.J., Farr, A.L. and Randall, R.J. 1951. Protein measurement with the folin phenol reagent. *J. Biol. Chem.* **193**: 265-275

MacIntyre, D.E., McNicol, A. and Drummond, A.H. 1985. Tumor-promoting phorbol esters inhibit agonist-induced phosphatidate formation and Ca^{2+} flux in human platelets. *FEBS Lett.* **180**: 160-164

MacIntyre, D.E. and Rink, T.J. 1982. The role of platelet membrane potential in the initiation of platelet aggregation. *Thromb. Haemostas.* **47**: 22-26

MacIntyre, D.E., Shaw, A.M., Bushfield, M., MacMillan, L.J., McNicol, A. and Pollock, W.K. 1985. Endogenous and pharmacological mechanisms for the regulation of human platelet cytosolic free Ca^{2+}. *Nouv. Rev. Fr. Hematol.* **27**: 285-292

Mahaut-Smith, M.P., Rink, T.J. and Sage, S.O. 1989. Single channels in human platelets activated by ADP. *J Physiol. (London)* **415**: 24P

Manning, S.D. and Williams, A.J. 1989a. Ion discrimination in a predominantly anion-selective channel from human platelet surface membrane. *J. Physiol. (London).* **410**: 88P

Manning, S.D. and Williams, A.J. 1989b. Conduction and blocking properties of a predominantly anion-selective channel from human platelet surface membrane reconstituted into planar phospholipid bilayers. *J. Membr. Biol.* **109**: 113-122

Marcus, A.J., Ullman, H.L. and Safier, L.B. 1969. Lipid composition of subcellular particles of human blood platelets. *J. Lipid Res.* **10**: 108-114

Markey, F., Lindberg, U. and Eriksson, L. 1978. Human platelets contain profilin, a potential regulator of actin polymerisability. *FEBS Lett.* **88**: 75-79

Markwell, M.A., Haas, S.M., Bieber, L.L. and Tolbert, N.E. 1979. A modification of the Lowry procedure to simplify protein determination in membrane and lipoprotein samples. *Anal. Biochem.* **87**: 206-210

Marty, A., Tan, Y.P. and Trautmann, A. 1984. Three types of calcium-dependent channel in rat lacrimal glands. *J. Physiol. (London)* **357**: 293-325

Maruyama, Y. 1987. A patch-clamp study of mammalian platelets and their voltage-gated potassium current. *J. Physiol. (London).* **391**: 467-485

Massini, P. and Luscher, E.F. 1976. On the significance of the influx of calcium into stimulated human blood platelets. *Biochim. Biophys. Acta.* **436**: 652-663

Mayer, M.L. 1985. A calcium-activated chloride current generates the after-potential of rat sensory neurones in culture. *J. Physiol. (London)* **364**: 217-239

Mehrishi, J.N. 1973. Topochemistry of the surface of some human blood elements. *Bibl. Anat.* **11**: 260-271.

Menashi, S., Authi, K.S., Carey, F. and Crawford, N. 1984. Characterisation of the calcium-sequestering process associated with human platelet intracellular membranes isolated by free-flow electrophoresis. *Biochem. J.* **222**: 413-417

Menashi, S., Davis, C. and Crawford, N. 1982. Calcium uptake associated with an intracellular membrane fraction prepared from human blood platelets by high-voltage free flow electrophoresis. *FEBS Lett.* **140**: 298-302

Menashi, S., Weintroub, H. and Crawford, N. 1981. Characterisation of human platelet surface and intracellular membranes isolated by free-flow electrophoresis. *J. Biol. Chem.* **256**: 4095-4101

Meyer, T., Holowka, D. and Stryer, L. 1988. Highly cooperative opening of calcium channels by inositol 1,4,5-trisphosphate. *Science* **240**: 653-655

Miledi, R. 1982. A calcium-dependent transient outward current in Xenopus laevis oocytes. *Proc. R. Soc. (London)* **215**: 491-497

Miller, C. 1978. Voltage-gated cation conductance channel from fragmented sarcoplasmic reticulum: steady state electrical properties, *J. Membr. Biol.* **40**: 1-23

Miller, C. 1982a. Open-state substructure of single chloride channels from *Torpedo* electroplax. *Phil. Trans. R. Soc. London.* **B299**: 401-411

Miller, C. 1982b. Bis-quaternary ammonium blockers as structural probes of the sarcoplasmic reticulum K^+ channel. *J. Gen. Physiol.* **79**: 869-891

Miller, C., Arvan, P., Telford, J.N. and Racker, E. 1976. Calcium-induced fusion of proteoliposomes: effect of transmembrane osmotic gradient. *J. Membr. Biol.* **30**: 271-282

Miller, C., Bell, J.E. and Garcia, A.M. 1984. The potassium channel of sarcoplasmic reticulum. *In*: Ion Channels: Molecular and Physiological Aspects. *Current Topics in Membranes and Transport.* **21**: 99-132

Miller, C. and Racker, R. 1976. Calcium induced fusion of fragmented sarcoplasmic reticulum with artificial planar bilayers. *J. Membr. Biol.* **30**: 283-300

Miller. C. and White, M.M. 1984. Dimeric structure of single chloride channels from *Torpedo* electroplax. *Proc. Natl. Acad. Sci. USA.* **81**: 2772-2775

Milne, R.K., Yeo, G.F., Madsen, B.W. and Edeson, R.O. 1989. Estimation of single channel kinetic parameters from data subject to limited time resolution. *Biophys. J.* **55**: 673-676

Moake, J.L., Ahmed, K., Bachus, H.R. and Gutfreund, D.E. 1970. Reversal by adenosine of ADP inhibition of platelet (Na-K)-ATPase. *Biochim. Biophys. Acta.* **211**: 337-344

Moczydlowski, E. 1986. Single channel enzymology. *In*: Ion Channel Reconstitution. Ed: Miller, C. Plenum Press, New York. pp 75-113

Moczydlowski, E., Garber, S.S. and Miller, C. 1984. Batrachotoxin-activated Na^+ channels in planar lipid bilayers: competition of tetrodotoxin block by Na^+. *J. Gen. Physiol.* **84**: 665-686

Moczydlowski, E. and Latorre, R. 1983. Gating kinetics of Ca-activated K-channels from rat muscle incorporated into planar lipid bilayers: Evidence for two voltage-dependent Ca^{2+} binding reactions. *J. Gen. Physiol.* **82**: 511-542

Montal, M., Suarez-Isla, B., Wan, K. and Lindstrom, J. 1983. Single-channel recordings from purified acetylcholine receptors reconstituted in bilayers formed at the tip of patch pipettes. *Biochemistry* **22**: 2319-2323

Muallem, S., Schoeffield, M., Pandol, S. and Sachs, G. 1985. Inositol trisphosphate modification of ion transport in rough endoplasmic reticulum. *Proc. Natl. Acad. Sci. USA.* **82**: 4433-4437

Mueller, P. and Rudin, D.O. 1969. Bimolecular lipid membranes. Techniques of formation, study of electrical properties and induction of ionic gating phenomena. *In:* Laboratory Techniques in Membrane Biophysics. Ed: Passow, H. and Stampfli, R. Springer-Verlag, Berlin pp 141-156

Mueller, P. Rudin, D.O., Tien, H.T. and Wescott, W.C. 1962a. Reconstitution of cell membrane structure *in vitro* and its transformation into an excitable system. *Nature.* **194**: 979-980

Mueller, P., Rudin, D.O. Tien, H.T. and Wescott, W.C. 1962b. Reconstitution of excitable cell membrane structure *in vitro. Circulation* **26**: 1167-1171

Murer, E.H. and Holme, R. 1970. A study of the release of calcium from human blood platelets and its inhibition by metabolic inhibitors, N-ethylmaleimide and aspirin. *Biochim. Biophys. Acta* **222**: 197-205

Nelson, M.T. 1986. Calcium channels. *In*: Ion Channel Reconstitution. Ed: Miller C. Plenum Press, New York. pp 507-522

Nelson, D.J., Tang, J.M. and Palmer, L.G. 1984. Single channel recordings of apical membrane chloride conductance in A6 epithelial cells. *J. Membr. Biol.* **80**: 81-89

Niles, W.D. and Cohen, F.S. 1987. Video fluorescence microscopy studies of phospholipid vesicle fusion with a planar phospholipid membrane. Nature of membrane-membrane interactions and detection of release of contents. *J. Gen. Physiol.* **90**: 703-735

Niles, W.D., Cohen, F.S. and Finkelstein, A. 1989. Hydrostatic pressures developed by osmotically swelling vesicles bound to planar membranes. *J. Gen. Physiol.* **93**: 211-244

Nurden, A.T. 1985. Glycoprotein defects responsible for abnormal platelet function in inherited platelet disorders. *In*: Platelet membrane glycoproteins. Ed: George, J.N., Nurden, A.T. and Phillips, D.R. Plenum Press, New York. pp 357-392

O'Rourke, F.A., Halenda, S.P., Zavoico, G.B. and Feinstein, M.B. 1985. Inositol 1,4,5-trisphosphate releases Ca^{2+} from a Ca^{2+}-transporting membrane vesicle fraction derived from human platelets. *J. Biol. Chem.* **260**: 956-962

Owen, D.A., Segal, M., Barker, J.L. 1984. A Ca-dependent Cl^- conductance in cultured spinal cord neurones. *Nature* **311**: 567-570

Papahadjopoulos, D., Vail, W.J., Newton, G., Nir, S.M., Jacobson, K., Poste, G. and Lazo, R. 1977. Studies on membrane fusion. III The role of calcium induced phase changes. *Biochim. Biophys. Acta.* **465**: 579-598

Patlak, J.B., Gration, K.A.F. and Usherwood, P.N.R. 1979. Single glutamate-activated channels in locust muscle. *Nature.* **278**: 643-645

Penner, R., Matthews, G. and Neher, E. 1988. Regulation of calcium influx by second messengers in rat mast cells. *Nature* **334**: 499-504

Perin, M.S. and MacDonald, R.C. 1989. Fusion of synaptic vesicle membranes with planar bilayer membranes. *Biophys. J.* **55**: 973-986

Perret, B., Chap, H.J. and Douste-Blazy, L. 1979. Asymmetric distribution of arachidonic acid in the plasma membrane of human platelets. A determination using purified phospholipases and a rapid method for membrane isolation. *Biochim. Biophys. Acta* **556**: 434-446

Petersen, O.H. 1988. Calcium channels. *Nature* **336**: 528

Pipili, E. 1985. Platelet membrane potential: simultaneous measurement of $diSc_{3(5)}$ fluorescence and optical density. *Thromb. Haemostas.* **54**: 645-649

Poll, C. and Westwick, J. 1986. Phorbol esters modulate thrombin-operated calcium mobilisation and dense granule release in human platelets. *Biochim. Biophys. Acta.* **886**: 434-440

Pollock, W.K. and Rink, T.J. 1986. Thrombin and ionomycin can raise platelet cytosolic Ca^{2+} to micromolar levels by discharge of internal Ca^{2+} stores: studies using fura-2. *Biochem. Biophys. Res. Commun.* **139**: 308-314

Portis, A., Newton, C., Pangbourn, W. and Papahadjopoulous, D. 1979. Studies on the mechanism of membrane fusion: evidence for an intermembrane Ca^{2+}-phospholipid complex, synergism with Mg^{2+}, and inhibition by spectrin. *Biochemistry* **18**: 780-790

Portzehl, H., Caldwell, P.C. and Ruegg, J.C. 1964. The dependence of contraction and relaxation of muscle fibres from the crab *Maia Squinado* on the internal concentration of free calcium ions. *Biochim. Biophys. Acta.* **79**: 581-591

Rao, G.H., Peller, J.D. and White, J.G. 1985. Measurement of ionized calcium in blood platelets with a new generation calcium indicator. *Biochem. Biophys. Res. Commun.* **132**: 652-657

Rengasamy, A. and Feinberg, H. 1988. Inositol 1,4,5-trisphosphate-induced calcium release from platelet plasma membrane vesicles. *Biochem. Biophys. Res. Commun.* **150**: 1021-1026

Rengasamy, A., Soura, S. and Feinberg, H. 1987. Platelet Ca^{2+} homeostasis: Na^{+}-Ca^{2+} exchange in plasma membrane vesicles. *Thromb. Haemostas.* **57**: 337-340

Rink, T.J. 1988. A real receptor-operated calcium channel? *Nature* **334**: 649-650

Rink, T.J. and Hallam, T.J. 1984. What turns platelets on? *Trends Biochem. Sci.* **9**: 215-219

Rink, T.J., Smith S.W. and Tsien, R.Y. 1982. Cytoplasmic free Ca^{2+} in human platelets: Ca^{2+} thresholds and Ca-independent activation for shape-change and secretion. *FEBS. Lett.* **148**: 21-26

Rittenhouse, S.E. and Sasson, J.P. 1985. Mass changes in myoinositol trisphosphate in human platelets stimulated by thrombin. Inhibitory effects of phorbol ester. *J. Biol. Chem.* **260**: 8657-8660

Robblee, L.S. and Shepro, D. 1976. The effect of external calcium and lanthanum on platelet calcium content and on the release reaction. *Biochim. Biophys. Acta.* **436**: 448-459

Robinson, R.A. and Stokes, R.H. 1959. Electrolyte Solutions. (2nd ed.). Butterworth, London. pp 491-500

Ross, R. and Vogel, A. 1978. The platelet-derived growth factor. *Cell* **14**: 203-210

Rousseau., E. 1989. Single chloride-selective channel from cardiac sarcoplasmic reticulum studied in planar lipid bilayers. *J. Membr. Biol.* **110**: 39-47

Russell, J.M. and Brodwick, M.S. 1979. Properties of chloride transport in barnacle fibres. *J. Gen. Physiol.* **73**: 343-368

Sachs, F. 1983. Automated analysis of single channel records. *In*: Single channel recording. Eds: Sakmann, B. and Neher, E. Plenum Press, New York. pp 265-285

Sachs, F., Neil, J. and Barkakati, N. 1982. The automated analysis of data from single ionic channels. *Pflugers Arch.* **395**: 331-340

Sage, S.O., Merritt, J.E., Hallam, T.J. and Rink, T.J. 1989. Receptor-mediated calcium entry in fura-2-loaded human platelets stimulated with ADP and thrombin. Dual wavelength studies with Mn^{2+}. *Biochem. J.* **258**: 923-926

Sage, S.O. and Rink, T.J. 1985. Inhibition by forskolin of cytosolic calcium rise, shape change and aggregation in quin2-loaded human platelets. *FEBS Lett.* **188**: 135-140

Sage, S.O. and Rink, T.J. 1986a. Kinetic differences between thrombin-induced and ADP-induced calcium influx and release from internal stores in fura-2-loaded human platelets. *Biochem. Biophys. Res. Commun.* **136**: 1124-1129

Sage, S.O. and Rink, T.J. 1986b. Effects of ionic substitution on $[Ca^{2+}]_i$ rises evoked by thrombin and PAF in human platelets. *Eur. J. Pharmacol.* **128**: 99-107

Sage, S.O. and Rink, T.J. 1987. The kinetics of changes in intracellular calcium concentration in fura-2-loaded human platelets. *J. Biol. Chem.* **262**: 16364-16369

Sandler, W.C., Le Breton, G.C. and Feinberg, H. 1980. Movement of sodium into human platelets. *Biochim. Biophys. Acta.* **600**: 448-455

Schein, S., Colombini, M. and Finkelstein, A. 1976. Reconstitution in planar lipid bilayers of a voltage-dependent anion-selective channel obtained from *Paramecium* mitochondria. *J. Membr. Biol.* 30: 99-120

Schneider, G.T., Cook, D.I., Gage, P.W. and Young, J.A. 1985. Voltage sensitive, high conductance chloride channels in the luminal membrane of cultured pulmonary alveolar (type II) cells. *Pflugers Arch.* **404**: 354-357

Schmukler, M. and Zieve, P.D. 1972. The effect of glucose feeding on fatty acid synthesis in human platelets. *J. Lab. Clin. Med.* **80**: 231-235

Schwarze, W. and Kolb, H-A. 1984. Voltage dependent kinetics of an anionic channel of large unit conductance in macrophages and myotube membranes. *Pflugers Arch.* **402**: 281-291

Seaman, G.V.F. and Vassar, P.S. 1966. Changes in the electrokinetic properties of platelets during their aggregation. *Arch. Biochem. Biophys*: **117**: 10-17

Semba, C. and Williams, A.J. 1986. Chloride channels in highly purified human platelet surface membranes. *J. Physiol. (London).* **373**: 86P

Shah, J. and Pant, H.C. 1988. Potassium-channel blockers inhibit inositol trisphosphate-induced calcium release in the microsomal fractions isolated from the rat brain. *Biochem. J.* **250**: 617-620

Siess, W. 1985. Evidence for the formation of inositol 4-monophosphate in stimulated human platelets. *FEBS Lett.* **185**: 151-156

Sigworth, F.J. 1983. An example of analysis. *In*: Single channel recording. Eds: Sakmann, B. and Neher, E. Plenum Press, New York. pp 301-321

Singer, S.J. and Nicolson, G.L. 1972. The fluid mosaic model of the structure of cell membranes. *Science* **175**: 720-731

Sixma, J.J. and Lips, J.P.M. 1978. Isolation of platelet membranes. A Review. *Thrombos. Haemostas.* **39**: 328-337

Sixma, J.J., Schiphorst, M.E., Verhoeckx, C. and Jockusch, B.M. 1982. Peripheral and integral proteins of human blood platelet membranes. Alpha-actinin is not identical to glycoprotein III. *Biochim. Biophys. Acta.* **704**: 333-344

Soejima, M. and Kokubun, S. 1988. Single anion selective channel and its ion selectivity in the vascular smooth muscle cell. *Pflugers Arch.* **411**: 304-311

Stein, P.G., Nelson, T.E. and Palade, P.T. 1989. Mammalian sarcoplasmic reticulum K^+ channels recorded in skinned fibers. *Biophys. J.* **55**: 480a

Steiner, B. and Luscher, E.F. 1985. Evidence that the platelet plasma membrane does not contain a (Ca^{2+} + Mg^{2+})-dependent ATPase. *Biochim. Biophys. Acta.* **818**: 299-309

Steiner, M. and Tateishi, T. 1974. Distribution and transport of calcium in human platelets. *Biochim. Biophys. Acta.* **367**: 232-246

Streb, H., Irvine, R.F., Berridge, M.J. and Schulz, I. 1983. Release of Ca^{2+} from a nonmitochondrial intracellular store in pancreatic acinar cells by inositol 1,4,5-trisphosphate. *Nature* **306**: 67-69

Strickler, A. and Sacks, T. 1973. Continuous free-film electrophoresis: the crescent phenomenon. *Prep. Biochem.* **3**: 269-277

Supattapone, S., Worley, P.F., Baraban, J.M. and Snyder, S.H. 1988. Solubilisation, purification and characterisation of an inositol trisphosphate receptor. *J. Biol. Chem.* **263**: 1530-1534

Tang, J.M., Wang, J. and Eisenberg, R.S. 1989. K^+-selective channel from sarcoplasmic reticulum of split lobster muscle fibers. *J. Gen. Physiol.* **94**: 261-278

Tank, D.W., Huganir, R.L., Greengard, P. and Webb, W.W. 1983. Patch-recorded single-channel currents of the purified and reconstituted *Torpedo* acetylcholine receptor. *Proc. Natl. Acad. Sci. USA.* **80**: 5129-5133

Tank, D.W., Miller, C. and Webb, W.W. 1982. Isolated-patch recording from liposomes containing functionally reconstituted chloride channels from *Torpedo* electroplax. *Proc. Natl. Acad. Sci. USA.* **79**: 7749-7753

Tanoue, K., Jung, S.M., Isohisa, I., Yamamoto, N and Yamazaki, H. 1982. The role of surface charge in platelet function. *Acta Haematol. Jpn.* **45**: 1391-1400

Thompson, N.T. and Scrutton, M.C. 1985. Intracellular calcium fluxes in human platelets. *Eur. J. Biochem.* **147**: 421-427

Tolbert, N.E. 1974. Isolation of subcellular organelles of metabolism on isopycnic sucrose gradients. *Methods Enzymol.* **31**: 734-746

Tomlins, B., and Williams, A.J. 1986. Solubilisation and reconstitution of the rabbit skeletal muscle sarcoplasmic reticulum K^+ channel into liposomes suitable for patch clamp studies. *Pflugers Archiv.* **407**: 341-347

Tomlins, B., Williams, A.J. and Montgomery, R.A.P. 1984. The characterisation of a monovalent cation-selective channel of mammalian cardiac muscle sarcoplasmic reticulum. *J. Membr. Biol.* **80**: 191-199

Tsien, R.Y. 1980. New calcium indicators and buffers with high selectivity against magnesium and protons: design, synthesis and properties of prototype structures. *Biochemistry.* **19**: 2396-2404

Tsien, R.Y., Pozzan, T. and Rink, T.J. 1984. Measuring and manipulating cytosolic Ca^{2+} with trapped indicators. *Trends Biochem. Sci.* **9**: 263-266

Valone, F.H. and Johnson, B. 1987. Modulation of platelet-activating factor-induced calcium influx and intracellular calcium release in platelets by phorbol esters. *Biochem. J.* **247**: 669-674

Van Gelder, B.F. and Slater, E.C. 1962. The extinction coefficient of cytochrome c. *Biochim. Biophys. Acta.* **58**: 593-595

Vilven, J. and Coronado, R. 1988. Opening of dihydropyridine calcium channels in skeletal muscle membranes by inositol trisphosphate. *Nature* **336**: 587-589

Vivaudou, M.B., Singer, J.J. and Walsh Jr., J.V. 1986. An automated technique for analysis of current transitions in multilevel single channel recordings. *Pflugers Arch.* **407**: 355-364

Ware, J.A., Johnson, P.C., Smith, M. and Salzman, E.W. 1985. Aequorin detects increased cytoplasmic calcium in platelets stimulated with phorbol ester or diacylglycerol. *Biochem. Biophys. Res. Commun.* **133**: 98-104

Watson, S.P., McConnell, R.T. and Lapetina, E.G. 1984. The rapid formation of inositol phosphates in human platelets by thrombin is inhibited by prostacyclin. *J. Biol. Chem.* **259**: 13199-13203

White, J.G. 1971. Platelet morphology. *In*: The Circulating Platelet. Ed: Johnson, S.A. Academic Press, New York. pp 45-121

White, J. G. 1972. Interaction of membrane systems in blood platelets. *Am. J. Pathol.* **66**: 295-312

White, S.H. 1980. How electric fields modify alkane solubility in lipid bilayers. *Science* **207**: 1075-1077

White, S.H. 1986. The physical nature of planar bilayer membranes. *In*: Ion Channel Reconstitution. Ed: Miller, C. Plenum Press New York. pp. 3-35

White, S.H., Petersen, D.C., Simon, S. and Yafuso, M. 1976. Formation of planar bilayer membranes from lipid monolayers. *Biophs. J.* **16**: 481-489

White, J.G. and Sank, J.J. 1984. Microtubule coils in spread blood platelets. *Blood* 64: 470-478

Woll, K.H., Leibowitz, M.D., Neumcke, B. and Hille, B. 1987. A high-conductance anion channel in adult amphibian skeletal muscle. *Pflugers Arch.* 410: 632-640

Woll, K.H. and Neumcke, B. 1987. Conductance properties and voltage dependence of an anion channel in amphibian skeletal muscle. *Pflugers Arch.* 410: 641-647

Woodbury, J. W. and Miles, P.R. 1973. Anion conductance of frog muscle membranes: one channel, two kinds of pH dependence. *J. Gen. Physiol.* 62: 324-353

Yamaguchi, A., Suzuki, H., Tanoue, K. and Yamasaki, H. 1986. Simple method of aequorin loading into platelets using dimethyl sulfoxide. *Thromb. Res.* 44: 165-174

Yamamoto, D. and Suzuki, N. 1987. Blockage of chloride channels by HEPES buffer. *Proc. R. Soc. London.* B230: 93-100.

Yamanishi, J., Kawahara, Y. and Fukuzaki, H. 1983. Effect of cyclic AMP on cytoplasmic free calcium in human platelets stimulated by thrombin: direct measurement with quin2. *Thromb. Res.* 32: 183-188

Zeiller, K., Loser, R., Pascher, G. and Hannig, K. 1975. Free-flow electrophoresis. II. Analysis of the method with respect to preparative cell separation. *Hoppe-Seylers Z. Physiol. Chem.* **356**: 1225-1244.

Zieve, P.D., Gamble, J.L. and Jackson, D.P. 1964. Effects of thrombin on the potassium and ATP content of platelets. *J. Clin. Invest.* **43**: 2063-2069

Zimmerberg, J., Cohen, F.S. and Finkelstein, A. 1980. Fusion of phospholipid vesicles with planar phospholipid bilayer membranes. I. Discharge of vesicular contents across the planar membrane. *J. Gen. Physiol.* **75**: 241-250

Zschauer, A., van Breemen, C., Buhler, F.R. and Nelson, M.T. 1988. Calcium channels in thrombin-activated human platelet membrane. *Nature.* **334**: 703-705

[*From the Proceedings of the Physiological Society*, 4–5 *November* 1988
Journal of Physiology, **410**, 88*P*, 1989]

Ion discrimination in a predominantly anion-selective channel from human platelet surface membrane

By S. D. Manning and A. J. Williams. *Department of Cardiac Medicine, Cardiothoracic Institute, University of London, Dovehouse Street, London SW3 6LY, and Department of Biochemistry, Hunterian Institute, Royal College of Surgeons, Lincoln's Inn Fields, London WC2A 3PN*

We have recorded single-channel currents from a predominantly anion-selective channel derived from highly purified human platelet surface membrane (Semba & Williams, 1986). This channel has been reconstituted into planar phospholipid bilayers (70% phosphatidylethanolamine, 30% phosphatidylserine) by fusion and recorded under voltage-clamp conditions.

Reversal potential measurements determined in the presence of asymmetric KCl solutions show that, although the channel is preferentially selective for Cl^-, K^+ is also permeant. With a 3:1 or 5:1 KCl gradient across the bilayer (450:150 or 750:150 mM-KCl; all solutions buffered to pH 7·2 with 5 mM-HEPES/Tris) the measured reversal potentials were +16 and +22 mV respectively. These are consistent with a Cl:K selectivity ratio of 4:1. Reversing the concentration gradient across the bilayer (150:450 mM-KCl) does not alter the selectivity ratio, indicating that the channel shows no asymmetry in Cl:K discrimination. Cations as large as tetraethylammonium permeate the channel. Significant monovalent cation permeabilities have been reported for several other predominantly anion-selective channels (Blatz & Magleby, 1985; Franciolini & Nonner, 1987; Woll *et al.* 1987).

The relative permeabilities of various anions compared to Cl^- were estimated from reversal potential measurements with 450 mM-KCl on one side of the bilayer and the K^+ salt of the test anion, A, at the same concentration, on the other. The order of relative anion permeabilities (in the presence of K^+) is $F^- < Cl^- < Br^- < I^- < NO_3^- < SCN^-$, with the following permeability ratios (P_A/P_{Cl}): F^-, 0·32; Cl^-, 1·00; Br^-, 1·58; I^-, 1·76; NO_3^-, 2·23; SCN^-, 2·48, calculated according to the Goldman–Hodgkin–Katz equation.

This work was supported by grants from the MRC and the British Heart Foundation. We thank Professor N. Crawford for helpful advice.

REFERENCES

Blatz, L. A. & Magleby, K. L. (1985). *Biophys. J.* **47**, 119–123.
Franciolini, F. & Nonner, W. (1987). *J. gen. Physiol.* **90**, 453–478.
Semba, C. & Williams, A. J. (1986). *J. Physiol.* **373**, 86*P*.
Woll, K. H., Leibowitz, M. D., Neumcke, B. & Hille, B. (1987). *Pflügers Arch.* **410**, 632–640.

J. Membrane Biol. 109, 113–122 (1989)

The Journal of
Membrane Biology
© Springer-Verlag New York Inc. 1989

Conduction and Blocking Properties of a Predominantly Anion-Selective Channel from Human Platelet Surface Membrane Reconstituted into Planar Phospholipid Bilayers

S.D. Manning†‡ and A.J. Williams†

†Department of Cardiac Medicine, National Heart and Lung Institute, University of London, London SW3 6LY, and ‡Department of Biochemistry, The Hunterian Institute, Royal College of Surgeons of England, London WC2A 3PN, United Kingdom

Summary. We have investigated the basic properties of a predominantly anion-selective channel derived from highly purified human platelet surface membrane. Single channels have been reconstituted into planar phospholipid bilayers by fusion of membrane vesicles and recorded under voltage-clamp conditions.

The channel is found to have the following properties: (i) Channel activity occurs in bursts of openings separated by long closed periods. (ii) The current-voltage relationship is nonlinear. Channel current is seen to rectify, with less current flowing at positive than at negative voltages. Rectification may be due to asymmetric block by HEPES/Tris buffers. In 450 mM KCl, 5 mM HEPES/Tris, pH 7.2, the single channel conductance at −40 mV is ~160 pS and at +40 mV is ~90 pS. (iii) The conductance-concentration relationship follows a simple saturation curve. Half maximal conductance is achieved at a concentration of ~1000 mM KCl, and the curve saturates at a conductance of ~500 pS. (iv) Reversal potentials interpreted in terms of the Goldman-Hodgkin-Katz equation indicate a Cl : K permeability ratio of 4 : 1. (v) The channel accepts all of the halides as well as a number of other anions. The following sequence of relative anion permeabilities (in the presence of K^+) is obtained: $F^- < \text{acetate}^- < \text{gluconate}^- < Cl^- < Br^- < I^- < NO_3^- < SCN^-$. (vi) Cations as large as TEA^+ are permeant. (vii) Current through the channel is blocked in the presence of DIDS, SITS and ATP, but not by Zn^{2+}.

Key Words platelet surface membrane · lipid bilayer · anion channel · ion selectivity · block

Introduction

It is well established that anion and cation fluxes across platelet membranes play an important role in maintaining homeostasis and in the triggering of metabolic and functional responses initiated by agonists and other platelet activating agents. Despite the obvious importance of these fluxes in platelets, our present understanding of their location, selectivity, rates and magnitudes is somewhat limited. A major reason for this has been the technical difficulties encountered in applying conventional electrophysiological techniques to such small cells (2–4 μm diameter). Microelectrode impalement of platelets has not been reported, and only one paper describing the successful patch clamping of platelets has been published to date (Maruyama, 1987). In this, whole cell currents were measured and some single channel data obtained using the cell-attached variation. A voltage-gated K^+ channel with a conductance of 9 pS was resolved.

Our approach to the study of ion channels in human platelets utilizes a well-characterized method for separating highly purified surface and intracellular membrane vesicles free from cross contamination using continuous flow electrophoresis (Menashi, Weintroub & Crawford, 1981). In this paper we report the reconstitution of a predominantly anion-selective channel from the surface membrane into preformed planar phospholipid bilayers and the basic characterization of its conduction and blocking properties.

The initial identification of this channel was communicated to the Physiological Society (Semba & Williams, 1986).

Materials and Methods

Preparation of Platelet Membranes

The method for preparing highly purified human platelet membranes essentially followed the procedures reported by Menashi et al. (1981). Human platelets were isolated by a differential-centrifugation procedure from fresh buffy-coat residue packs supplied by the Blood Transfusion Service Laboratories, Tooting, London SW17, UK. Laboratory processing commenced within 3–4 hr of blood donation.

The buffy coats were centrifuged at 200 × *g* for 20 min, and the platelet-rich plasma (PRP) was collected and pH adjusted to 6.4 using citric acid. The platelets were then sedimented at 1,200 × *g* for 20 min, resuspended in 10 mM HEPES[1] buffer, pH 6.2, containing 152 mM NaCl, 4.17 mM KCl, 3 mM EDTA, and incubated at 37°C for 5 min. The suspension was then treated with neuraminidase (Sigma Grade X, affinity purified) at a concentration of 0.05 unit/ml for 20 min at 37°C. Treatment with neuraminidase at the whole cell level lowered the electronegativity of the surface membrane by removal of sialic acid groups, thus reducing its electrophoretic mobility. At the end of the incubation period the suspension was rapidly diluted 1:4 with 10 mM HEPES buffer (washing buffer), pH 7.2, containing 152 mM NaCl, 4.17 mM KCl, 3 mM EDTA and centrifuged at 1,200 × *g* for 15 min. The platelets were washed twice by resuspension in the washing buffer and finally resuspended in ice-cold 10 mM HEPES buffer (sonication buffer), pH 7.2, containing 0.3 M sorbitol at a ratio of 4 ml buffer/g wet wt of cells. A protease-inhibitor cocktail containing 5 μg pepstatin A/ml, 10 μg soybean Trypsin inhibitor/ml and 400 μM phenylmethane-sulfonyl fluoride was added to the cell suspension. The sample was then sonicated at setting 6 for 10 sec at 4°C using a Dawe sonicator with a 4 mm diameter probe. The sonicate was centrifuged at 2,000 × *g* for 10 min at 4°C, the supernatant retained on ice and the pellet resuspended in sonication buffer. The sonication and centrifugation steps were carried out three times in all. The resultant supernatants were combined and layered onto a linear sorbitol gradient prepared from 1.0 and 3.5 M sorbitol solutions, pH 7.2, containing 10 mM HEPES and centrifuged at 42,000 × *g* for 90 min at 4°C. A mixed membrane (MM) fraction, containing both surface and intracellular membrane vesicles, was located in the low-density region of the gradient. The fraction was removed and concentrated by centrifugation at 90,000 × *g* for 80 min at 4°C. Membranes were either (i) resuspended in 0.4 M sucrose, 5 mM HEPES, pH 7.2, at a concentration of approximately 1–2 mg protein/ml for subsequent use in reconstitution experiments, or (ii) resuspended in electrophoresis chamber buffer (10 mM triethanolamine, 0.4 M sorbitol, adjusted to pH 6.8 with acetic acid and then to pH 7.2 with NaOH) to a concentration of approximately 3–4 mg protein/ml. The latter MM fraction was applied to the chamber of a Bender Hobein VAP22 continuous-flow electrophoresis unit operating at 160 V/cm, 80 mA with buffer flow conditions as described by Menashi et al. (1981). Two vesicle subpopulations were resolved; the more electronegative fraction represented intracellular membranes (IM), and the least electronegative peak represented surface membrane (SM) vesicles (modified by neuraminidase treatment). Separately pooled IM and SM fractions were centrifuged at 90,000 × *g* for 1 hr at 4°C and resuspended in 0.4 M sucrose, 5 mM HEPES, pH 7.2, to a protein concentration of 1–2 mg/ml.

In the experiments reported here vesicles from the mixed membrane (MM) (both neuraminidase treated and untreated) and surface membrane (SM) fractions were used. Aliquots were frozen in liquid nitrogen and stored at −80°C.

[1] *Abbreviations:* HEPES, N-2-hydroxyethylpiperasine-N′-2-ethanesulfonic acid; EDTA, ethylenediaminetetra-acetic acid; Tris, tris(hydroxymethyl)aminomethane; TEA, tetraethylammonium; DIDS, 4,4′-diisothiocyanostilbene-2-2′-disulfonic acid; SITS, 4-acetamido-4′-isothiocyanotostilbene-2,2′-disulfonic acid.

Measurement of Single-Channel Activity in Planar Phospholipid Bilayers

Planar bilayers were formed by the 'painting' technique of Mueller and Rudin (1969) using suspensions of 30 mM phospholipid (70% phosphatidylethanolamine, 30% phosphatidylserine, supplied by Avanti Polar Lipids, Birmingham, AL) in decane. A bilayer was formed over a 0.5 mm diameter hole separating two chambers containing aqueous solutions. Electrical connection was made to the chamber solutions via 2% agar glass bridges containing 3 M KCl, and Ag/AgCl electrodes. High ionic strength salt bridges were used to minimize errors in the measurement of reversal potentials under mixed ion conditions (Cukierman, Yellen & Miller, 1985). Platelet membrane vesicles were always added to the chamber, designated *cis*, which could be clamped at a range of holding potentials. The other chamber, *trans*, was held at ground potential. The clamp voltage was provided by a microcomputer linked to a digital-to-analog converter. The current-to-voltage converter for measuring current through the bilayer used a feedback resistor of 10 GΩ (Miller, 1982). The current signal was displayed on an oscilloscope and stored on FM tape for subsequent analysis. The channel traces shown as illustrations (Figs. 1, 2*A*, 7*B*, 8, and 9) were obtained by replaying recorded data onto a hot-pen recorder (Ormed MX216).

Platelet membrane vesicles were incorporated into preformed planar bilayers by fusion. The conditions applied during these experiments were those generally reported by others to promote membrane vesicle fusion (Hanke, 1986), in particular, the presence of negatively charged phospholipids in the bilayer (phosphatidylserine was used throughout), an osmotic gradient across the bilayer and the presence of divalent cations in the *cis* chamber (to which membrane vesicles were added). Fusion conditions were as follows: *cis*—450 mM KCl, 1.0 mM $CaCl_2$, 5 mM HEPES/Tris, pH 7.2; *trans*—150 mM KCl, 5 mM HEPES/Tris, pH 7.2. All solutions used in the experiments reported here were filtered through Millipore membranes (0.45 μm pore size) prior to use. The *cis* chamber solution was mechanically agitated with a magnetic stirrer to increase the rate of fusion of vesicles with the bilayer. 5–10 μl of platelet MM or SM vesicle suspension were added to the *cis* chamber, and fusion usually occurred within 5–10 min. Unfused vesicles were perfused out using a peristaltic pump and ionic conditions in the two chambers altered as required. All experiments were carried out at room temperature (~22°C).

Current-voltage relationships were constructed by applying potentials at 10 mV intervals from +70 to −70 mV. For those experiments carried out in asymmetric solutions reversal potentials (E_{rev}) were measured to the nearest mV, correcting for electrode offset potential (range 1–3 mV) in each case. Anion/cation (P_{Cl}/P_K) selectivity ratios and anion/anion (P_A/P_{Cl}) permeability ratios were calculated according to the Goldman-Hodgkin-Katz (GHK) voltage equation.

Results

Channel Reconstitution into Planar Bilayers

A predominantly anion-selective channel is observed following fusion of vesicles from the mixed membrane fraction (either neuraminidase treated or

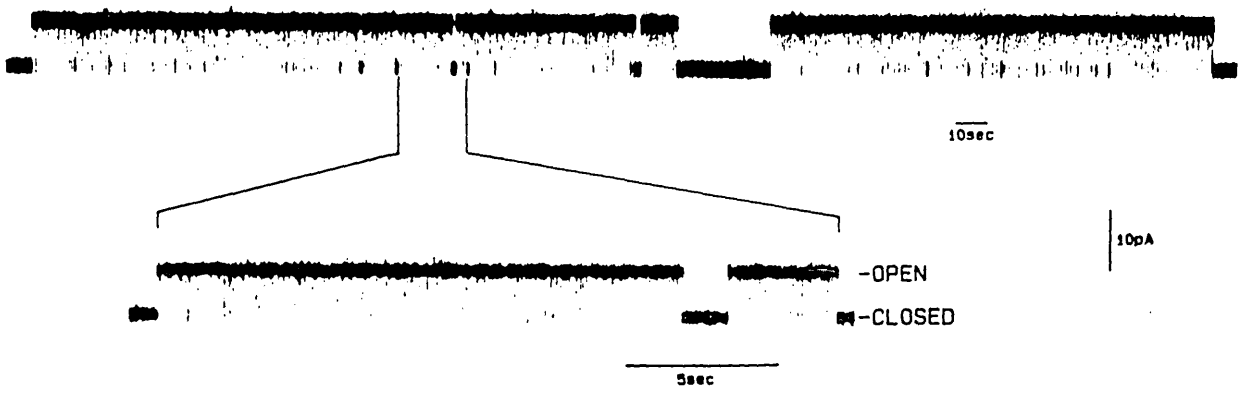


Fig. 1. A single channel from platelet surface membrane reconstituted into a planar phospholipid bilayer as described in Materials and Methods. The recording was made at −40 mV in symmetrical 450 mM KCl, 5 mM HEPES/Tris, pH 7.2, and is shown low-pass filtered at 500 Hz. An upwards deflection represents the channel opening. An expanded time scale trace is displayed (lower trace) to show the rapid closing events in more detail (note the different time calibrations for the two traces)

untreated) and the surface membrane fraction. Fusion of vesicles from the inner membrane fraction does not yield the channel. As far as we can ascertain from our experiments, the channel exhibits both qualitatively and quantitatively comparable characteristics when either MM or SM fractions are used. From this we surmise that (i) the channel protein originates from the platelet surface membrane and (ii) its properties are preserved following neuraminidase treatment and membrane purification by high voltage continuous-flow electrophoresis. The term SM channel is used throughout.

Figures 1 and 2*A* show representative recordings following incorporation of the SM channel into a planar phospholipid bilayer. Channels are bathed in symmetrical 450 mM KCl, 5 mM HEPES/Tris, pH 7.2, and recorded at the holding potentials indicated. The lower trace in Fig. 1 shows channel fluctuations in more detail at higher time resolution. The channel shows characteristic bursting behavior in which comparatively long 'silent' periods alternate with 'active' periods.

Figure 2*B* shows the relationship between single-channel current and holding potential over the range ± 70 mV in symmetrical 150 and 450 mM KCl solutions (buffered with 5 mM HEPES/Tris to pH 7.2). The current-voltage relationship is nonlinear. Channel current is seen to rectify with less current flowing at positive than negative holding potentials. In symmetrical 450 mM KCl a conductance of 159.4 ± 20 pS (mean ± SD, n = 12) is obtained at −40 mV and a conductance of 92.6 ± 19.7 pS (mean ± SD, n = 12) at +40 mV.

The dependence of the single channel conductance on the salt concentration is shown in Fig. 3. Each point represents the mean conductance (± SD, n = 4 to 12 determinations) at −40 mV at a given KCl concentration. The data could be fitted with a simple Michaelis-Menten type saturation curve. Half-maximal conductance is achieved at a concentration of 1008 mM KCl, and the curve saturates at a conductance of 503 pS.

Single Channel Rectification

The effect of the buffering compounds (HEPES and Tris) on the degree of single channel rectification was investigated. Figure 4*A* shows the current-voltage relationship for the SM channel exposed to symmetrical 450 mM KCl buffered with either 5 mM HEPES/Tris, pH 7.2 ('standard' conditions), 0.5 mM HEPES/KOH, pH 7.2 ('reduced HEPES') or 5 mM HEPES/KOH, pH 7.2 ('no Tris'). In the absence of Tris, rectification appears slightly less than that obtained in 'standard' conditions (the HEPES concentration being the same in both cases). However, when the concentration of HEPES buffer is reduced tenfold, from 5 to 0.5 mM, current at positive holding potentials increases significantly and rectification is considerably reduced. In Fig. 4*B*, the mean conductance (G) measured at each holding potential under 'reduced HEPES' conditions is taken as $G_{O_{app}}$. The ratio $G/G_{O_{app}}$ is plotted with G values from either 'no Tris' conditions (▽) or 'standard' conditions (△). In both of these conditions the HEPES concentration is the same (5 mM), and in both cases blocking of single channel conductance is apparent. The degree of block is seen to increase as the holding potential is made more positive. With

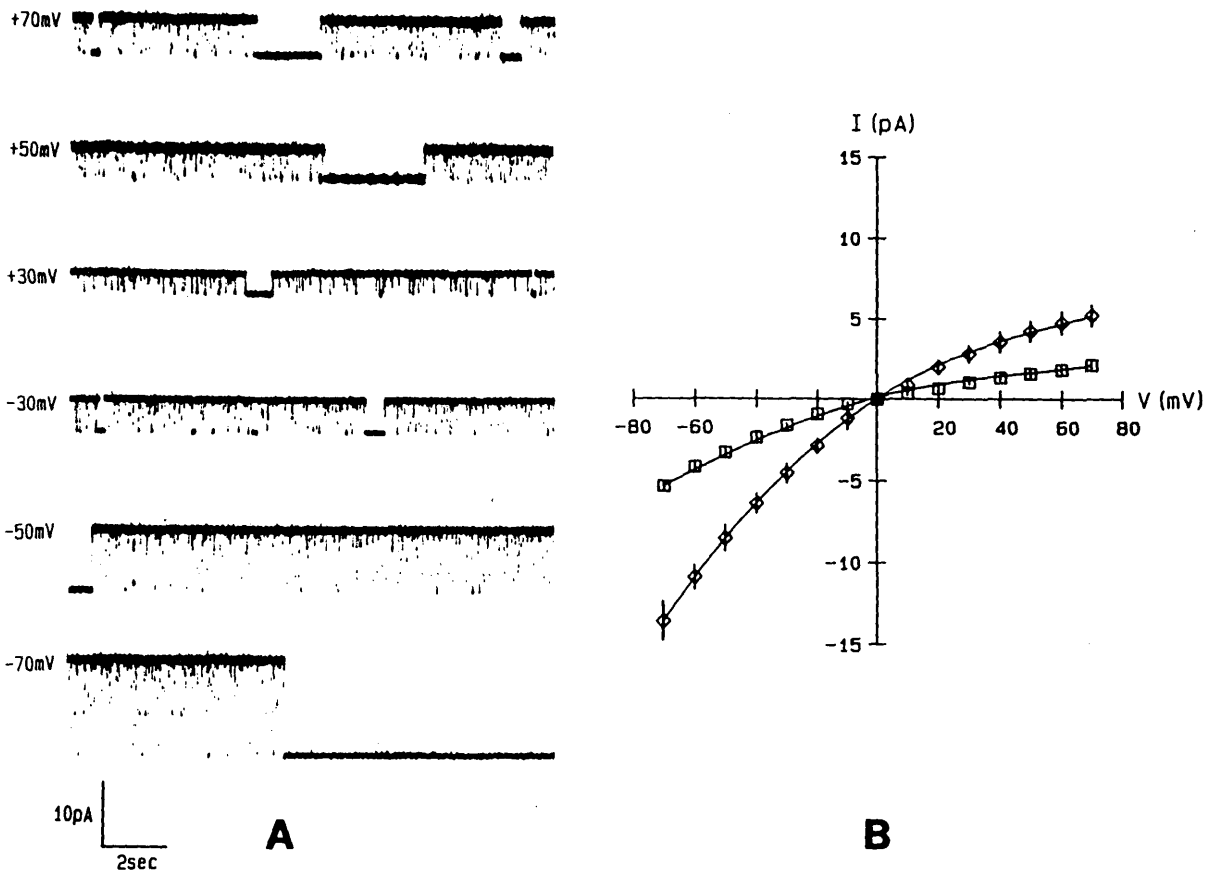


Fig. 2. (*A*) Platelet SM channel fluctuations at the holding potentials indicated on the left. 450 mM KCl, 5 mM HEPES/Tris, pH 7.2, *cis* and *trans*. The recording was low-pass filtered at 250 Hz. Traces at negative holding potentials have been inverted so that all channel openings are shown as upwards deflections. (*B*) Single-channel current-voltage relationship in symmetrical solutions of (□) 150 mM and (◇) 450 mM KCl, 5 mM HEPES/Tris, pH 7.2. Each point represents the mean ± SD of 12 separate determinations. Curves were drawn by eye

the added presence of Tris buffer ('standard' conditions), the apparent block is increased.

Anion *vs.* Cation Selectivity

Reversal potential measurements determined in the presence of asymmetric KCl solutions show that although the channel is preferentially selective for Cl^-, K^+ is also permeant.

Figure 5 (△) shows the single-channel current flow over a range of holding potentials with a 3 : 1 KCl gradient across the bilayer (450 mM KCl, 5 mM HEPES/Tris, pH 7.2 *cis* : 150 mM KCl, 5 mM HEPES/Tris, pH 7.2 *trans*). The measured reversal potential, +16 mV, deviates from that calculated from the Nernst equation for an ideally anion-selective channel under these conditions (i.e., +28 mV). The deviation from the Nernst potential does not vary significantly in size upon reversing the gradient across the bilayer. Figure 5 (▽) shows the single-channel current-voltage relationship with a 1 : 3 KCl gradient *cis* : *trans* (150 mM KCl *cis* : 450 mM KCl *trans*). The channel appears to show no significant asymmetry in cation/anion discrimination. Figure 5 (□) shows the current-voltage relationship for experiments carried out with an increased KCl gradient of 5 : 1 *cis* : *trans* (750 mM KCl *cis* : 150 mM KCl *trans*). There is a shift in the measured reversal potential to +22 mV. Under these conditions, the Nernst equation predicts a reversal potential of +41 mV for an ideally selective Cl^- channel. The results of all three reversal potential measurements are consistent with an anion/cation selectivity ratio of 4 : 1, as calculated from an appropriate version of the GHK voltage equation (*see* figure legend). The current measured in these experiments is therefore the resultant of the movement of both Cl^- and K^+ through the channel.

Relative Anion Permeabilities and Conductances

The relative permeabilities of various anions compared to Cl^- were estimated from reversal potential

measurements with 450 mM KCl in the *trans* chamber and either 450 mM KF, KBr, KI, KNO_3, KSCN, K-acetate or K-gluconate in the *cis* chamber. All solutions were buffered to pH 7.2 with 5 mM HEPES/Tris. Figure 6 shows three of the current-voltage curves obtained from these experiments. The measured reversal potential for F^- is negative (−20 mV), indicating that F^- is less permeant than Cl^-. The reversal potentials for Br^- and SCN^- are positive (+10 and +20 mV, respectively), indicating that they are accepted by the channel in preference to Cl^-.

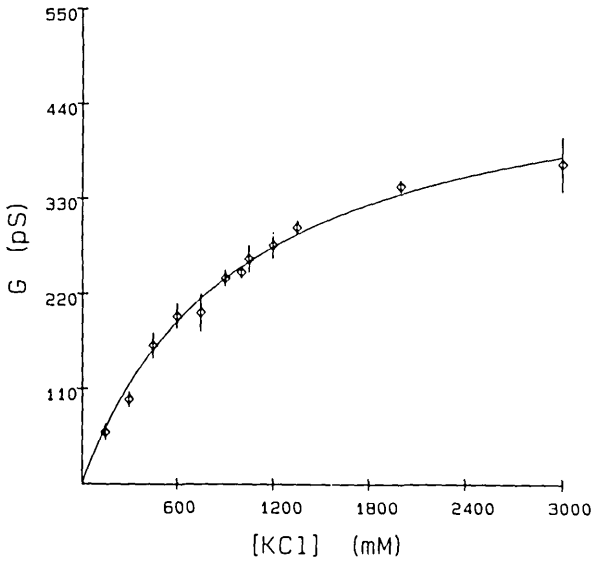


Fig. 3. Dependence of single channel conductance (G) on the KCl concentration. All values were measured at −40 mV and points represent the mean ± SD of 4 to 12 separate determinations at each concentration. The curve was drawn according to the equation $G/G_{max} = aK(aK + K_d)$, where G_{max} = 503 pS and K_d = 1008 mM

The Table summarizes the data from the anion permeability experiments in terms of permeability ratios. The sequence of relative anion permeabilities (in the presence of K^+) is as follows: $F^- <$ acetate$^-$ < gluconate$^-$ < $Cl^- < Br^- < I^- < NO_3^- <$ SCN^-.

The conductance at −40 mV of the above anions (except acetate) was determined in a separate series of experiments. The mean conductance values (± SD) are shown in the Table. Channels were bathed in symmetrical 450 mM KA (where A is the test anion), 5 mM HEPES/Tris, pH 7.2. Among the monovalent anions, nitrate has the highest conductance (198 ± 10 pS, n = 4) and gluconate the lowest (47 ± 4 pS, n = 3).

Cation Conductance

An inert, nonpermeant cation was sought to allow the measurement of anion current alone. An obvious candidate, tetraethylammonium, TEA^+, was

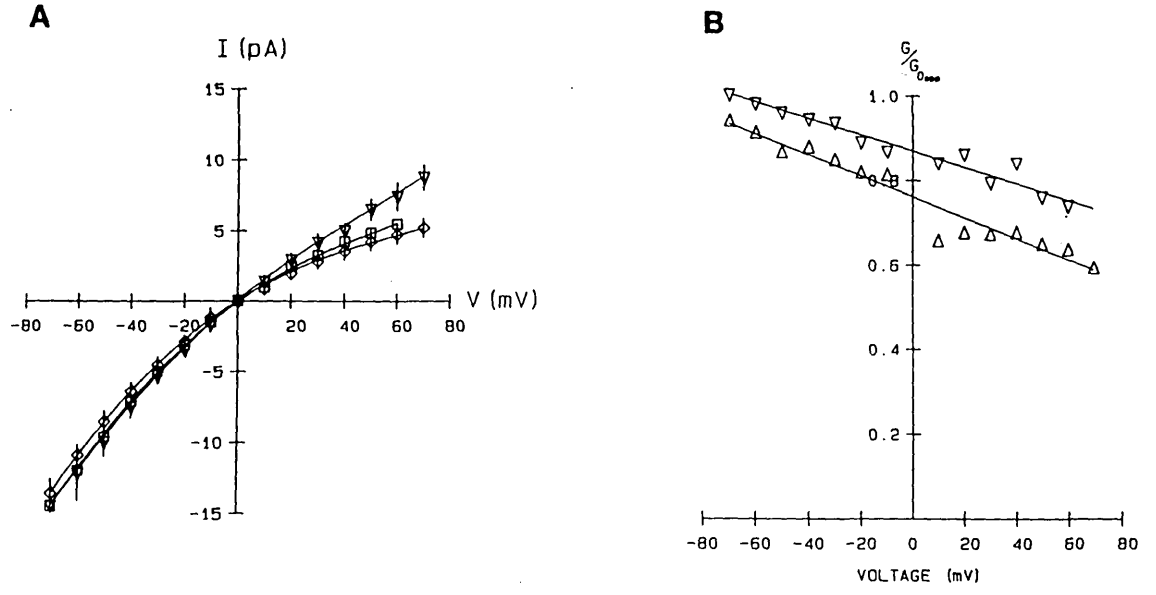


Fig. 4. The effect of HEPES/Tris buffers on single channel current. (*A*) Current-voltage relationships for single channels bathed in symmetrical 450 mM KCl and buffered as follows: (▽) 0.5 mM HEPES/KOH, pH 7.2 ('reduced HEPES'); (□) 5 mM HEPES/KOH, pH 7.2 ('no Tris'), or (◇) 5 mM HEPES/Tris, pH 7.2 ('standard' conditions, as for Fig. 2*B*). Each point represents the mean ± SD for four to 12 separate determinations. Curves were drawn by eye. (*B*) Relationship between $G/G_{\infty app}$ and voltage for the experiments shown in *A*. Experimental points are the ratios between mean conductances measured in the presence of (▽) 450 mM KCl, 5 mM HEPES/KOH, pH 7.2 ('no Tris'), or (△) 450 mM KCl, 5 mM HEPES/Tris, pH 7.2 ('standard' conditions). In both cases $G_{\infty app}$ values were measured in the presence of 450 mM KCl, 0.5 mM HEPES/KOH, pH 7.2 ('reduced HEPES'). Lines were drawn by eye

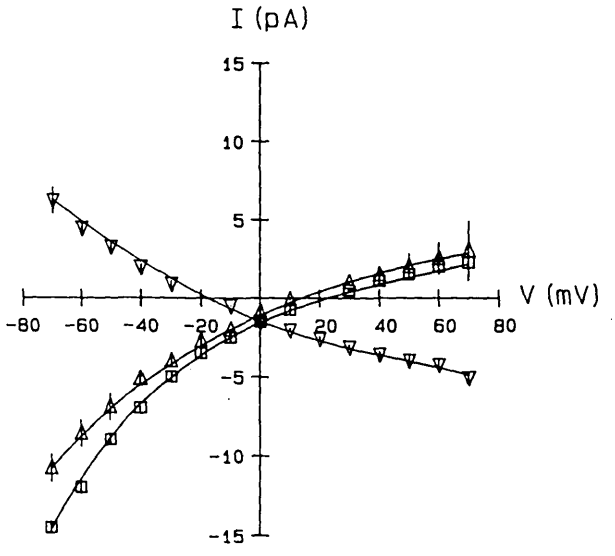


Fig. 5. Test for anion/cation selectivity. Single channel current-voltage relationships under the following conditions: [KCl] *cis*:[KCl] *trans*—(△) 450:150 mM; (▽) 150:450 mM; (□) 750:150 mM. All solutions were buffered with 5 mM HEPES/Tris to pH 7.2. Each point represents the mean ± SD for three to 10 separate determinations under each experimental condition. Curves were drawn by eye. The reversal potential, E_{rev} for a 3:1 KCl gradient (△) is measured as +16 mV and for a 5:1 KCl gradient (□) as +22 mV. The anion/cation selectivity ratio is calculated from $P_{Cl}/P_K = [(n.\exp(E_{rev}/k) - 1)/(n - \exp(E_{rev}/k))]$, where $k = RT/F$ and n is the *cis*:*trans* concentration ratio. P_{Cl}/P_K for these experiments is 4

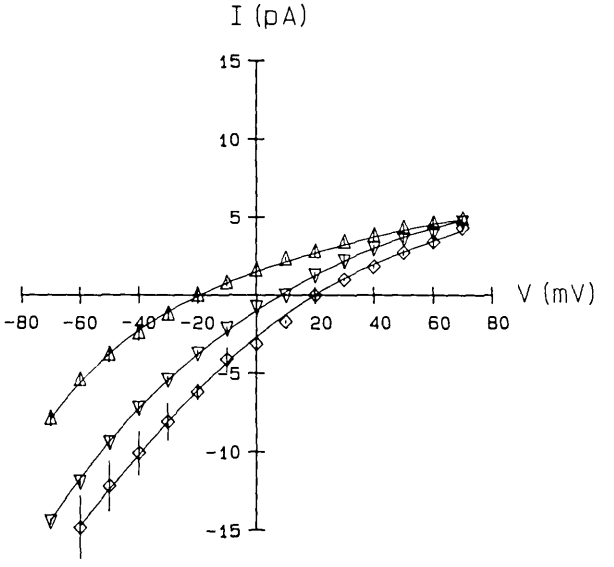


Fig. 6. Comparison of anion permeabilities. Single channel current-voltage relationships with 450 mM KCl in the *trans* chamber, and either (△) 450 mM KF, (▽) 450 mM KBr or (◇) 450 mM KSCN in the *cis* chamber. All solutions were buffered with 5 mM HEPES/Tris to pH 7.2. Each point represents the mean ± SD for five to eight separate determinations under each experimental condition. Curves were drawn by eye

Table. Reversal potential shifts, E_{rev}, are expressed with respect to control KCl solution[a]

Test anion	E_{rev} (mV)	$P_A/P_{Cl}(n)$	G (pS)	(n)
Fluoride	−20	0.32 (8)	77 ± 12	(4)
Acetate	−17	0.35 (5)	—	
Gluconate	−16	—[b] (10)	47 ± 4	(3)
Chloride	0	1.00 (−)	159 ± 20	(12)
Bromide	+10	1.58 (7)	175 ± 6	(4)
Iodide	+13	1.76 (4)	154 ± 20	(3)
Nitrate	+14	2.23 (8)	198 ± 10	(4)
Thiocyanate	+20	2.48 (5)	189 ± 12	(4)

[a] In all experiments the *trans* chamber contained the control 450 mM KCl solution; the *cis* chamber contained the K salt of the test anion, A, at the same concentration. E_{rev} represents mean values obtained from four to 10 experiments in each case. Permeability ratios are calculated from (Franciolini & Nonner, 1987); $E_{rev} = RT/F.\ln[(P_K a_K + P_{Cl} a_{Cl})]$, where a_K, a_A and a_{Cl} are the activities of K^+, A^- and Cl^-, respectively (taken from Robinson & Stokes, 1959). P_K/P_{Cl} is taken as 0.25 (*see* Fig. 5) and is considered to be independent of the test anion.

[b] No activity value was available for gluconate.

Single-channel conductance, G, at −40 mV for channels bathed in symmetrical 450 mM KA, 5 mM HEPES/Tris, pH 7.2, where A denotes the test anion. Mean conductance values (from 3–12 experiments) and standard deviations are shown.

tested but found to be permeant. Figure 7*A* shows the current-voltage relationships with a 3:1 KBr and a 3:1 TEABr gradient across the bilayer (*cis*, 450 mM KBr:*trans*, 150 mM KBr or *cis*, 450 mM TEABr:*trans*, 150 mM TEABr). From the reversal potential measurement in asymmetric KBr (+13 mV), the K:Br ratio is calculated as 1:3. In asymmetric TEABr, there is less apparent rectification and the current reverses at 0 mV, indicating that TEA^+ and Br^- are equally permeant. The single channel records shown in Fig. 7*B* illustrate an alteration in gating observed in asymmetric TEABr solutions compared with that observed in KBr. In TEABr the channel remains predominantly in the open state with only occasional brief closures.

Channel Block by DIDS, SITS and ATP

Agents which have been used as inhibitors of Cl^- transport proteins were applied to the SM channel; namely, DIDS and SITS (Cabantchik & Rothstein, 1972, 1974; Russell & Brodwick, 1979; Miller & White, 1984; Nelson, Tang & Palmer, 1984; Hanrahan, Alles & Lewis, 1985) and zinc (Woodbury & Miles, 1973; Franciolini & Nonner, 1987). Figure 8 shows current fluctuations from channels at holding potentials of −40 and +40 mV, recorded after symmetrical application of 100 μM DIDS or SITS.

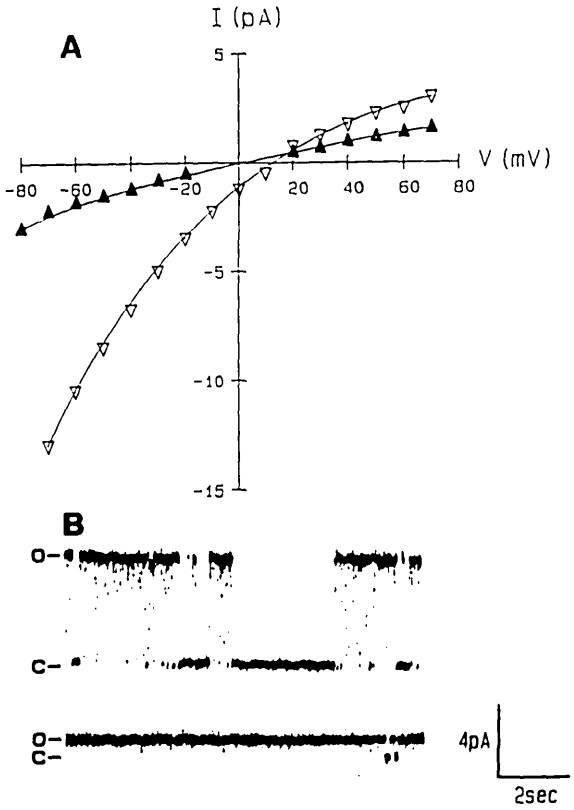


Fig. 7. (*A*) Single channel current-voltage relationships under the following conditions: *cis* : *trans*—(▽), 450 : 150 mM KBr; (▲) 450 : 150 mM TEABr. All solutions were buffered with 5 mM HEPES/Tris to pH 7.2. Each point represents the mean of three separate determinations. Sample standard deviations are contained within the symbols. Curves were drawn by eye. (*B*) Single-channel records from the above experiments at −40 mV in asymmetric KBr (upper trace) and TEABr (lower trace). Recordings are low-pass filtered at 250 Hz. An upwards deflection represents channel opening

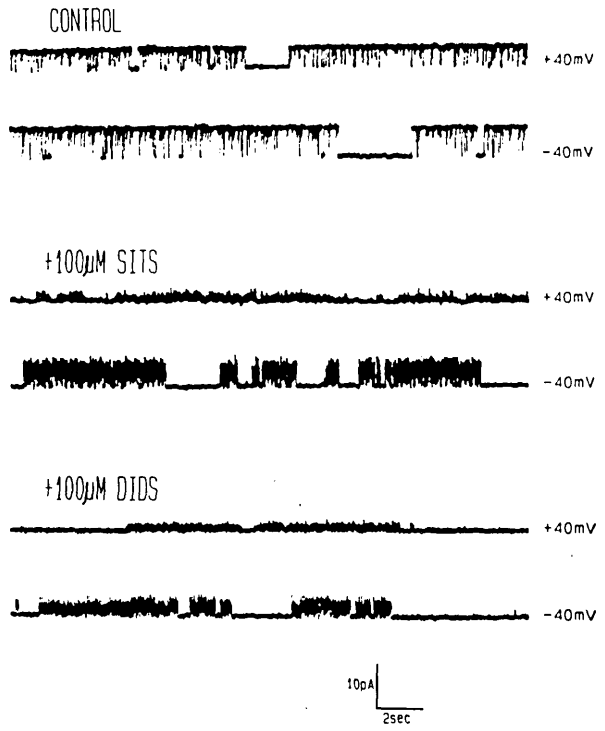


Fig. 8. The effect of DIDS and SITS on the platelet SM channel. All recordings were made in symmetrical 450 mM KCl, 5 mM HEPES/Tris, pH 7.2, with 100 μM SITS or 100 μM DIDS added symmetrically as shown. Current traces are shown low-pass filtered at 150 Hz at +40 and −40 mV. Traces at negative holding potentials have been inverted so that all channel openings are shown as upwards deflections

Openings at positive voltages are poorly resolved, and at negative voltages openings are noisy and burst durations appear to be shortened. At both positive and negative holding potentials the single channel conductance is reduced. The addition of up to 2 mM zinc symmetrically has no effect on the activity of the SM channel (*data not shown*).

The action of ATP on the SM channel was also investigated. Figure 9 shows the effect of 1, 3, and 5 mM ATP added to both *cis* and *trans* faces of a SM channel. In this case the rapid flickering block is seen only at negative holding potentials (−10 to −70 mV) and appears to increase as the ATP concentration is raised. No effect is seen at positive potentials (+10 to +70 mV). Thus ATP appears to be effective only from the *cis* face of the channel. The ATP blocking effect is reversed when ATP is removed by perfusion (*data not shown*).

Discussion

We report the basic characterization of a predominantly anion-selective channel found in the surface membrane of human platelets. The majority of fusion events incorporate a single active channel into the bilayer. Using the criterion of the direction of rectification of the current-voltage relationship in symmetrical KCl solutions, it is found that approximately 98% of insertions result in the channel being orientated in the same direction in the bilayer. No information is available concerning the initial orientation of vesicles formed following membrane separation and purification.

Channel activity occurs in characteristic bursts of openings (Fig. 1) often lasting several tens of seconds. Bursts are separated by long closed periods, and closed intervals between bursts lasting >5 min have been recorded. No subconductance states have been observed. A detailed analysis of the gating kinetics of this channel will be presented in a subsequent paper.

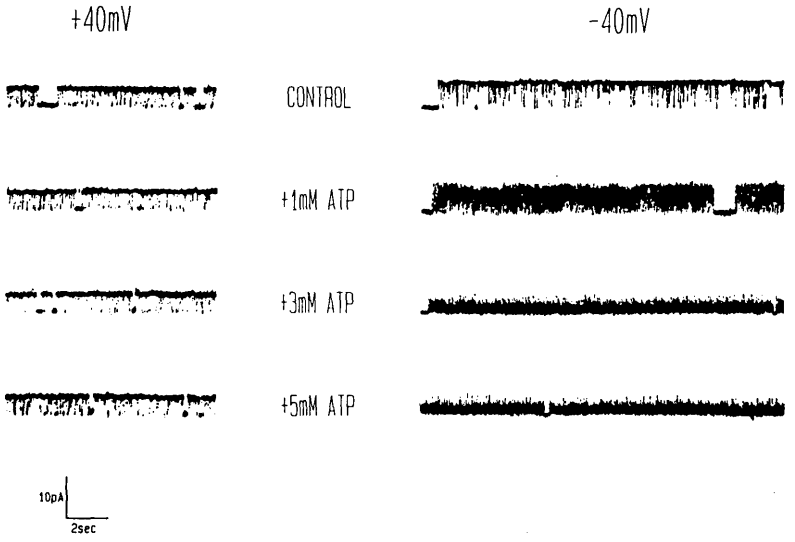


Fig. 9. The effect of ATP on the platelet SM channel. Current traces shown are from a single experiment in which ATP was added to both *cis* and *trans* faces of a channel bathed in symmetrical 450 mM KCl, 5 mM HEPES/Tris, pH 7.2, to give the final ATP concentrations indicated. Recordings are shown low-pass filtered at 150 Hz at +40 and −40 mV. Traces at −40 mV have been inverted so that all channel openings are shown as upwards deflections

Single Channel Rectification

We observe single channel current rectification under all ionic conditions applied to the channel, with more current flowing at negative holding potentials. This behavior was investigated by examining whether the presence of HEPES or Tris in our solutions was related to the degree of rectification (Fig. 4). It has been demonstrated by others that some anionic buffering compounds (including HEPES) may block chloride channels when applied in mM concentrations, e.g. in cultured *Drosophila* neurones (Yamamoto & Suzuki, 1987) and smooth muscle cells (Soejima & Kokubun, 1988). Tris is also known to compete for cationic binding sites in *Aplysia* neurones (Ascher, Marty & Neild, 1978).

From the results in Fig. 4, we surmise that the rectification observed in our experiments is caused, for the most part, by the asymmetric blocking of current flow. HEPES blocks in a voltage-dependent manner, mainly from the *trans* face of the channel (i.e., at positive voltages) with Tris buffer also blocking, though to a lesser degree and presumably mainly from the *cis* face.

Conductance and Selectivity

The SM channel has a relatively high conductance: approx. 160 pS in 450 mM KCl at −40 mV. With increasing KCl concentration, the single channel conductance increases to a saturating value of approx. 500 pS. The conductance-concentration relationship follows a simple rectangular hyperbola expected for Michaelis-Menten kinetics (Fig. 3). There is no deviation from this relationship at a conductance of three times the half-maximal conductance (approx. 1000 mM). Behavior of this type is typically, but not exclusively, found in channels that can be occupied by a single ion at a time (Läuger, 1973) and suggests the presence of a saturatable binding site within the channel. This is unlike the situation in VDAC, a large conductance nonselective channel in the mitochondrial outer membrane, where no saturation of conductance occurs at up to 4 M KCl (Colombini, 1986) and ions move through the channel under electrostatic influences rather than via ion-binding sites.

Reversal potential measurements in asymmetric KCl solutions indicate that both K^+ and Cl^- permeate the channel (Fig. 5). Several other 'anion' channels have been shown to have similar significant cation permeabilities. Blatz and Magleby (1985) found a small conductance anion channel in myotubules with a Cl : K permeability ratio of 5 : 1. Franciolini and Nonner (1987) measured a Cl : Na permeability ratio of 5 : 1 for a channel in hippocampal neurons. Woll et al. (1987) report an estimated Cl : Na ratio of 3.5 : 1 for a high conductance channel in skeletal muscle. The mechanism of ion permeation through channels of this type may be complex. Franciolini and Nonner (1987) have presented the only attempt to describe a possible mechanism. They postulate that anions and cations interact while passing through the hippocampal neuronal channel, and that cations will pass only when a permeant anion is present. This mechanism was tested in their experiments by replacing Cl^- with SO_4^{2-}, which is impermeant, and observing no cation current through the channel. We have no evidence for this sort of mechanism occurring in the platelet SM channel since all anions tested so far have been permeant, including SO_4^{2-} (*results not shown*). Cations as large as TEA^+ also pass through the SM channel

(Fig. 7), implying that the channel has a very large cross-sectional area, at least 37 Å^2 (Coronado & Miller, 1982). TEA^+ is found to be as permeant as Br^- from experiments in asymmetric TEABr (Fig. 7*A*), although the single channel conductance is considerably lower than in the presence of the same asymmetric concentrations of KBr. In TEABr the duration of channel openings is markedly increased (Fig. 7*B*). Similar low conductance and prolonged openings have been reported for Cs^+ conductance in the skeletal muscle sarcoplasmic reticulum K^+ channel (Cukierman et al., 1985).

Reversal potential measurements indicate that the relative permeability sequence for halide anions in the SM channel (*see* Table) corresponds to Eisenman's (1965) first halide anion sequence. The same sequence has been observed in Cl^- channels from the Schwann cell (Gray, Bevan & Ritchie, 1984), vascular smooth muscle (Soejima & Kokubun, 1988) and pulmonary epithelial cells (Schneider et al., 1985). The relative permeability sequence for all anions tested is approximately within the range of sequences described as lyotrophic (*see* Dani, Sanchez & Hille, 1983).

Channel Block by DIDS, SITS, and ATP

In addition to asymmetric block by HEPES acting from the *trans* face of the channel, we have observed block in SM channels by a number of other agents previously reported to block anion channels. The reactive disulfonic acid stilbenes (DIDS and SITS) are found to block from both sides of the channel when applied symmetrically (Fig. 8). These agents are known to block some Cl^- channels including the low conductance channels of *Torpedo* electroplax and rabbit urinary bladder (Miller & White, 1984; Hanrahan et al., 1985) and the large conductance channels of A6 epithelial cells and urinary bladder (Nelson et al., 1984; Hanrahan et al., 1985). Block in the SM channel is characterized by a series of small noisy openings at positive voltages and shortened bursts containing rapid flickering events at negative voltages. This behavior is unlike the reported action of these agents on other anion channels; for example, DIDS is seen to eliminate all channel openings in the *Torpedo* electroplax and rabbit urinary bladder channels (Miller & White, 1984; Hanrahan et al., 1985).

Zinc has been shown to block Cl^- currents in other preparations (Woodbury & Miles, 1973; Franciolini & Nonner, 1987). However, the SM channel is unaffected by the presence of up to 2 mM zinc applied to both *cis* and *trans* solutions.

The effect of ATP on the channel was investigated since Maruyama (1987) applied mM ATP to the pipette solution while patch clamping whole platelets to improve seal formation. No reference is made in the Maruyama paper to a Cl^- channel, and we considered the possibility that it may have been blocked in his experiments. ATP has recently been reported to induce a flickery channel block in a nonselective channel in neonatal rat central neurones (Ashford et al., 1988). The effect of ATP on our channel is shown in Fig. 9. Very fast flickering events are seen at negative voltages, though no effect is observed at positive voltages. ATP appears to be blocking from the *cis* face of the channel with the degree of block increasing as the ATP concentration is increased. A similar blocking effect is observed with ADP applied symmetrically to the channel (*results not shown*). This suggests that ATP and ADP may be acting as large impermeant anions, but only from one face of the channel. The presence of 3 mM ATP, together with the lower anion concentrations applied by Maruyama (1987) may explain the absence of the channel reported here from his patch recordings. If this is the case, it would imply that the *trans* side of our channel would face the platelet cytosol.

It should be noted that the blocking effects of SITS, DIDS and ATP were not observed in all applications to reconstituted SM anion channels. In some cases no effect on channel activity was found (*results not shown*), despite increasing the concentration of agent up to 10 mM. The blocking effect of SITS was observed in five out of eight applications; DIDS, three out of six and ATP, seven out of 10 applications. These observations may reflect some heterogeneity in the SM channel population, though in all other conduction properties studied (e.g., conductance and selectivity) channels that were sensitive or insensitive to these agents were indistinguishable.

The platelet surface membrane anion channel described here would appear to belong to an increasing class of 'anion' channels that also show a degree of cation permeability. As with other members of this class, the physiological role of the platelet SM channel remains to be established.

We would like to thank Prof. N. Crawford, Dr. N. Hack and Dr. K. Authi for much help and advice concerning the preparation of platelet membranes. We thank Mr. R. Montgomery for the design and assembly of the bilayer set-up. This work was supported by the Medical Research Council.

References

Ascher, P., Marty, A., Neild, T.O. 1978. Lifetime and elementary conductance of the channels mediating the excitatory effects of acetylcholine in *Aplysia* neurones. *J. Physiol. (London)* **278**:177–206

Ashford, M.L.J., Sturgess, N.C., Trout, N.J., Gardner, N.J., Hales, C.N. 1988. Adenosine-5'-triphosphate-sensitive ion channels in neonatal rat cultured central neurones. *Pfluegers Arch.* **412:**297–304

Blatz, A.L., Magleby, K.L. 1985. Single chloride-selective channels active at resting membrane potentials in cultured rat skeletal muscle. *Biophys. J.* **47:**119–123

Cabantchik, Z.I., Rothstein, A. 1972. The nature of the membrane sites controlling anion permeability of human red blood cells as determined by studies with disulfonic stilbene derivatives. *J. Membrane Biol.* **10:**311–330

Cabantchik, Z.I., Rothstein, A. 1974. Membrane proteins related to anion permeability of human red blood cells: I. Localization of disulfonic stilbene binding sites in proteins involved in permeation. *J. Membrane Biol.* **15:**207–226

Colombini, M. 1986. Voltage gating in VDAC. Towards a molecular mechanism. *In:* Ion Channel Reconstitution. C. Miller, editor. Plenum Press, New York

Coronado, R., Miller C. 1982. Conductance and block by organic cations in a K^+-selective channel from sarcoplasmic reticulum incorporated into planar phospholipid bilayers. *J. Gen. Physiol.* **79:**529–547

Cukierman, S., Yellen, G., Miller, C. 1985. The K^+ channel of sarcoplasmic reticulum. A new look at Cs^+ blockade. *Biophys. J.* **48:**477–484

Dani, J.A., Sanchez, J.A., Hille, B. 1983. Lyotrophic anions. Na channel gating and Ca electrode response. *J. Gen. Physiol.* **81:**255–281

Eisenman, G. 1965. Some elementary factors involved in specific ion permeation. *Proc. XXIII Int. Cong. Phys. Sci.* **87:**489–506

Franciolini, F., Nonner, W. 1987. Anion and cation permeability of a chloride channel in rat hippocampal neurones. *J. Gen. Physiol.* **90:**453–478

Gray, P.T.A., Bevan, S., Ritchie, J.M. 1984. High conductance anion-selective channels in rat cultured Schwann cells. *Proc. R. Soc. London B* **221:**395–409

Hanke, W. 1986. Incorporation of ion channels by fusion. *In:* Ion Channel Reconstitution. C. Miller, editor. Plenum Press, New York

Hanrahan, J.W., Alles, W.P., Lewis, S.A. 1985. Single anion-selective channels in basolateral membrane of a mammalian tight epithelium. *Proc. Natl. Acad. Sci. USA* **82:**7791–7795

Läuger, P. 1973. Ion transport through pores: A rate-theory analysis. *Biochim. Biophys. Acta* **311:**423–441

Maruyama, Y. 1987. A patch clamp study of mammalian platelets and their voltage-gated potassium current. *J. Physiol. (London)* **391:**467–485

Menashi, S., Weintroub, H., Crawford, N. 1981. Characterization of human platelet surface and intracellular membranes isolated by free flow electrophoresis. *J. Biol. Chem.* **256:**4095–4101

Miller, C. 1982. Open-state substructure of single chloride channels from *Torpedo* electroplax. *Phil. Trans. R. Soc. London B* **299:**401–411

Miller, C., White, M.M. 1984. Dimeric structure of single chloride channels from *Torpedo* electroplax. *Proc. Natl. Acad. Sci. USA* **81:**2772–2775

Mueller, P., Rudin, D.O. 1969. Bimolecular lipid membranes. Techniques of formation, study of electrical properties and induction of ionic gating phenomena. *In:* Laboratory Techniques in Membrane Biophysics. H. Passow and R. Stampfli, editors. pp. 141–156. Springer-Verlag, Berlin

Nelson, D.J., Tang, J.M., Palmer, L.G. 1984. Single channel recordings of apical membrane chloride conductance in A6 epithelial cells. *J. Membrane Biol.* **80:**81–89

Robinson, R.A., Stokes, R.H. 1959. Electrolyte Solutions. (2nd ed.) pp. 491–500. Butterworth, London

Russell, J.M., Brodwick, M.S. 1979. Properties of chloride transport in barnacle fibres. *J. Gen. Physiol.* **73:**343–368

Schneider, G.T., Cook, D.I., Gage, P.W., Young, J.A. 1985. Voltage sensitive, high conductance chloride channels in the luminal membrane of cultured pulmonary alveolar (type II) cells. *Pfluegers Arch.* **404:**354–357

Semba, C., Williams, A.J. 1986. Chloride channels in highly purified human platelet surface membranes. *J. Physiol. (London)* **373:**86P

Soejima, M., Kokubun, S. 1988. Single anion selective channel and its ion selectivity in vascular smooth muscle cell. *Pfluegers Arch.* **411:**304–311

Woll, K.H., Leibowitz, M.D., Neumcke, B., Hille, B. 1987. A high-conductance anion channel in adult amphibian skeletal muscle. *Pfluegers Arch.* **410:**632–640

Woodbury, J.W., Miles, P.R. 1973. Anion conductance of frog muscle membranes: One channel, two kinds of pH dependence. *J. Gen. Physiol.* **62:**324–353

Yamamoto, D., Suzuki, N. 1987. Blockage of chloride channels by HEPES buffer. *Proc. R. Soc. London B* **230:**93–100

Received 13 October 1988; revised 3 February 1989